Thesis/Dissertation Sheet

Surname/Family Name	:	**Yeola**
Given Name/s	:	**Avani**
Abbreviation for degree as give in the University calendar	:	**PhD**
Faculty	:	**Medicine**
School	:	**Prince of Wales Clinical School**
Thesis Title	:	**Generation of multipotent stem cells from primary human adipocytes for tissue repair**

Abstract 350 words maximum: (PLEASE TYPE)

Current trends in regenerative medicine for tissue repair focus on generating tissue specific stem cells. However, given the complexity of most tissues, the ideal stem cell would be the one that could undergo multilineage context-dependent differentiation to bring about holistic repair of the injured tissue.

In this thesis, I describe application of a vector and transcription factor-free method to reprogram human somatic cells into induced Multipotent Stem (iMS) cells utilizing the combination of 5'-Azacytidine (AZA) and recombinant human Platelet Derived Growth Factor-AB (rhPDGF-AB). I optimized xenofree conditions for this Demethylation Cytokine induced (DCi) reprogramming technique that yielded autologous iMS cells at high efficiency, from human adipocytes harvested from subjects aged 18-80 years. Human iMS cells display *in vitro* colony forming potential, serial re-plating, multi-lineage differentiation capacity and maintain a stable karyotype. They express CD73, CD90, CD105 and STRO-1 and lack expression of CD14, CD20, CD34 and CD45. Human iMS cells can be expanded long-term in autologous or allogeneic human serum containing medium. They have a transcriptional profile distinct to primary adipocytes, untreated or treated AdMSCs. IPA analysis revealed upregulation of embryonic stem cell core genes and activation of Epithelial-to-Mesenchymal Transition (EMT), PDGFR signalling and downstream JAK/STAT and PI3K/AKT/mTOR signalling in iMS cells when compared to primary adipocytes. Although iMS cells expressed pluripotency factors (OCT4, Nanog, SOX2 and SSEA4) they lacked spontaneous teratogenicity characteristic of pluripotent cells. When transplanted into injured intervertebral disc of NOD/SCID mice, human iMS cells were retained at transplant site for the duration of assessment (1 year) with no evidence of malignant transformation. iMS cells displayed *in vivo* plasticity and directly contributed to formation of new blood vessels, bone, cartilage and smooth muscle at the site of injury. To assess the specificity of cell plasticity, human iMS cells were also injected into cardiotoxin injured tibialis anterior muscle of SCID/beige mice. Donor iMS cells contributed to hCD56 expressing muscle satellite cells and hSpectrin expressing myofibres without heterotopic transformation or aberrant differentiation.

Taken together, these findings demonstrate feasibility of DCi reprogramming for generation of safe and therapeutically relevant autologous iMS cells and provide foundation to evaluate their tissue regenerative potential in controlled clinical trials.

FOR OFFICE USE ONLY Date of completion of requirements for Award:

Generating Multipotent Stem Cells from Primary Human Adipocytes for Tissue Repair

Avani Yeola

A thesis submitted in fulfiment of the requirements for the degree of

Doctor of Philosophy

UNSW
AUSTRALIA

Prince of Wales Clinical School

Faculty of Medicine

The University of New South Wales, Australia

June 2018

Abstract

Current trends in regenerative medicine for tissue repair focus on generating tissue-specific stem cells. However, given the complexity of most tissues, the ideal stem cell would be one that could undergo multilineage context-dependent differentiation to bring about holistic repair of the injured tissue.

This thesis describes application of a vector- and transcription factor-free method to reprogram human somatic cells into induced Multipotent Stem (iMS) cells utilizing the combination of 5-Azacytidine and recombinant human Platelet Derived Growth Factor-AB. I optimized xenofree conditions for this Demethylation Cytokine-induced (DCi) reprogramming technique that yielded autologous iMS cells at high efficiency from human adipocytes harvested from subjects aged 18-80 years. Human iMS cells display *in vitro* colony forming and serial re-plating ability, multilineage differentiation capacity and maintain a stable karyotype over several months. They express MSC markers but not markers of the blood lineage. iMS cells can be expanded long-term in medium containing autologous/allogeneic human serum. They have a transcriptional profile distinct to adipocytes or tissue-derived mesenchymal stem cells. IPA analysis revealed activation of genes associated with embryonic stem cells, EMT, PDGF signaling and downstream JAK/STAT, PI3K/AKT/mTOR pathways in iMS cells compared to adipocytes. Although iMS cells expressed pluripotency factors (OCT4, Nanog, SOX2 and SSEA4) they lacked spontaneous teratogenicity characteristic of pluripotent cells. When transplanted into injured intervertebral disc of NOD/SCID mice, human iMS cells were retained at transplant site for the duration of assessment (1 year) with no evidence of malignant

transformation. iMS cells displayed *in vivo* plasticity and directly contributed to formation of new blood vessels, bone, cartilage and smooth muscle at the site of injury. To assess the specificity of cell plasticity, human iMS cells were also injected into cardiotoxin injured tibialis anterior muscle of SCID/beige mice. Donor iMS cells contributed to hCD56 expressing muscle satellite cells and hSpectrin expressing myofibres without heterotopic transformation or aberrant differentiation.

Together these findings demonstrate the feasibility and utility of DCi reprogramming for generation of safe, therapeutically relevant autologous iMS cells, and provide a solid foundation to evaluate their tissue regenerative potential in controlled clinical trials.

Declarations

ORIGINALITY STATEMENT

‘I hereby declare that this submission is my own work and to the best of my knowledge it contains no materials previously published or written by another person, or substantial proportions of material which have been accepted for the award of any other degree or diploma at UNSW or any other educational institution, except where due acknowledgement is made in the thesis. Any contribution made to the research by others, with whom I have worked at UNSW or elsewhere, is explicitly acknowledged in the thesis. I also declare that the intellectual content of this thesis is the product of my own work, except to the extent that assistance from others in the project's design and conception or in style, presentation and linguistic expression is acknowledged.’

Signed .....

Date .....

Acknowledgements

First and foremost, I am dearly grateful to my family for all the unconditional love and support they have always had to offer. To my Mum, Anjali Yeola, thank you for everything that you do to make sure we get the best of all. To my Dad, Mohan Yeola, without whose immense faith in me, I simply would not have achieved what I have today. To my beloved Sister, Kimaya Yeola, who understands me better than no one else. And lastly, to my dear Husband, Omkar Damle, thank you for holding my hands on the toughest days, for cooking on long days, for all the sacrifices-big or small and for your absolute love and support. It is my honour to dedicate my PhD to all of you.

To John Pimanda, my primary PhD supervisor. A huge thank you for making me a part of your amazing group and for giving me an opportunity to work on one of the coolest projects in the lab. Thank you for your advice and guidance at every step of my PhD. You have not only taught me to do great science but have also prepared me to be more welcoming towards challenges. I am also thankful to you for reminding me how significant my research is and making me feel good about it in my lowest times.

To Vashe Chandrakanthan, my PhD supervisor too, thank you for playing the most important part in shaping up my project. Had it not been for your continuous encouragement and perseverance to not settle for anything but the best, I would not have acquired the technical skills that I didn't have at the beginning. Thank you for all the motivation that you have provided over the course of my PhD, it certainly has boosted my self-confidence.

My sincere gratitude also goes to Julie Thoms for revising my thesis. Your patience in reading my drafts is highly appreciated. Thanks to your critical comments, they made me think about my findings from a different angle. And most importantly, thank you for being such a good teacher and always having faith in me.

I am also thankful to all my friends and colleagues in the Pimanda group for the lively lab environment. I appreciate their support and funny stories that helped me get through long days at the lab. The interesting discussions over lunch have always helped me lighten up and get a fresh perspective on things. I am especially thankful to David Kang for teaching me some experimental techniques and to Prunella Ing for being ears whenever I needed someone to talk to.

My gratitude goes to the Australian Government, Department of Education for the Endeavour Postgraduate Research Scholarship. Thank you also to UNSW Australia Postgraduate Research Support Scheme and Prince of Wales Clinical School Travel grant as well as my supervisors for the funding which allowed me to present at international conferences.

And last but not the least, I am thankful to all the mice that had to be foregone during the process of this research. I have tried to make the most of your sacrifice and hope that this dissertation gives justice to your giving.

Publications

Chandrakanthan, V., **A. Yeola,** J. C. Kwan, R. A. Oliver, Q. Qiao, Y. C. Kang, P. Zarzour, D. Beck, L. Boelen, A. Unnikrishnan, J. E. Villanueva, A. C. Nunez, K. Knezevic, C. Palu, R. Nasrallah, M. Carnell, A. Macmillan, R. Whan, Y. Yu, P. Hardy, S. T. Grey, A. Gladbach, F. Delerue, L. Ittner, R. Mobbs, C. R. Walkley, L. E. Purton, R. L. Ward, J. W. Wong, L. B. Hesson, W. Walsh and J. E. Pimanda (2016). "PDGF-AB and 5-Azacytidine induce conversion of somatic cells into tissue-regenerative multipotent stem cells." *Proc Natl Acad Sci U S A* ***113****(16): E2306-2315.*

A. Yeola, R.A. Oliver, Y.Huang, Y.C. Kang, P.Hardy, M.Tursky, T.Hung C.Loo, C.Artuz, C.Lucas, P.Fortuna, E. Wolvetang, C. Power, D.Ma, J.McCaroll, M.Kavallaris, E.Hardeman, D.Beck, W. Walsh, R.Mobbs, V.Chandrakanthan and J.E. Pimanda. "Generating multipotent stem cells from primary human adipocytes for tissue repair." *Manuscript under preparation.*

Presentations

Yeola A, Oliver R, Huang Y, Kang Y, Hardy P, Tursky M, Hung TT, Loo C, Artuz C, Lucas C, Fortuna P, Wolvetang E, Power C, Ma D, McCaroll J, Kavallaris M, Hardeman E, Beck D, Walsh B, Mobbs R, Chandrakanthan V, Pimanda JE. *'Generating multipotent stem cells from primary human adipocytes for tissue repair'.* **International Society for Stem Cell Research Annual Meeting, Melbourne, VIC, Australia; June 2018.** Poster presentation.

Yeola A, Kang D, Oliver R, Hung TT, Tursky M, Artuz C, Fortuna P, hardy P, Power C, Ma D, Wolvetang E, Walsh B, Mobbs R, Chandrakanthan V, Pimanda JE. *'Generating multipotent stem cells from primary human adipocytes'.* **Prince of Wales Clinical School Postgraduate Research Seminar, Sydney, Australia; October 2017**. Finalist for best Poster Presentation.

Yeola A, Kang D, Oliver R, Hung TT, Tursky M, Artuz C, Fortuna P, hardy P, Power C, Ma D, Wolvetang E, Walsh B, Mobbs R, Chandrakanthan V, Pimanda JE. *'Generating multipotent stem cells from primary human adipocytes'.* **International Society for Stem Cell Research Annual Meeting, Boston, MA, USA; June 2017.** Poster presentation.

Yeola A, Kang D, Oliver R, Hung TT, Tursky M, Artuz C, Fortuna P, hardy P, Power C, Ma D, Wolvetang E, Walsh B, Mobbs R, Chandrakanthan V, Pimanda JE. *'Generating multipotent stem cells from primary human adipocytes'.* **Gordon Research Seminar and**

conference for Tissue Repair and Regeneration, New London, NH, USA; June 2017. Oral presentation.

Yeola A, Kang D, Oliver R, Hung TT, Tursky M, Artuz C, Fortuna P, hardy P, Power C, Ma D, Wolvetang E, Walsh B, Mobbs R, Chandrakanthan V, Pimanda JE. *'Generating multipotent stem cells from primary human adipocytes'*. **Spine Society of Australia 28th Annual Meeting, Tasmania, Australia; April 2017.** Oral presentation.

Yeola A, Kang D, Oliver R, Hung TT, Tursky M, Artuz C, Fortuna P, hardy P, Power C, Ma D, Wolvetang E, Walsh B, Mobbs R, Chandrakanthan V, Pimanda JE. *'Generating multipotent stem cells from primary human adipocytes'*. **The Victor Chang Cardiac Research Institute 17th International Symposium: From cardiovascular development to regenerative medicine, Sydney, Australia; November 2016.** Poster presentation.

Yeola A, Kang D, Oliver R, Hung TT, Tursky M, Artuz C, Fortuna P, hardy P, Power C, Ma D, Wolvetang E, Walsh B, Mobbs R, Chandrakanthan V, Pimanda JE. *'Generating multipotent stem cells from primary human adipocytes'*. **Prince of Wales Clinical School Postgraduate Research Seminar, Sydney, Australia; October 2016**. Award for best Oral presentation.

Yeola A, Mobbs R, Walsh B, Chandrakanthan V, Pimanda JE. *'Generating multipotent stem cells from primary human adipocytes'*.**43rd Annual Tow Research Awards Day, Sydney, Australia; November 2015.** Poster presentation.

Yeola A, Kang D, Oliver R, Hung TT, Tursky M, Artuz C, Fortuna P, hardy P, Power C, Ma D, Wolvetang E, Walsh B, Mobbs R, Chandrakanthan V, Pimanda JE. *'Generating multipotent stem cells from primary human adipocytes'*. **Australian Society for Stem Cell Research Annual Conference, Hunter Valley, Australia; November 2015**. Poster & Oral presentation, selected as Best of the Best poster.

Yeola A, Kang D, Oliver R, Walsh B, Mobbs R, Chandrakanthan V, Pimanda JE. *'Generating multipotent stem cells from primary human adipocytes'*. **Prince of Wales Clinical School Postgraduate Research Seminar, Sydney, Australia; October 2015**. Finalist for best Poster Presentation.

Yeola A, Mobbs R, Walsh B, Chandrakanthan V, Pimanda JE. *'Generating multipotent stem cells from primary human adipocytes'*. **Australian Society for Medical Research, Sydney, Australia; June 2015**. Finalist for best Poster Presentation.

Yeola A, Kang D, Oliver R, Walsh B, Mobbs R, Chandrakanthan V, Pimanda JE. *'Generating multipotent stem cells from primary human adipocytes'*. **Prince of Wales Clinical School Postgraduate Research Seminar, Sydney, Australia; October 2014**. Poster presentation.

List of Abbreviations

ACEC	Animal care & Ethics committee
AdMSCs	Adipose derived MSCs
AS	autologous serum
AZA	5-azacytidine
α-MEM	α-minimum essential medium
bFGF	basic fibroblast growth factor
BME	beta mercaptoethanol
BMP2	bone morphogenetic protein 2
BM-CFU-Fs	human bone marrow derived stromal cells
BRIL	Biological Resources Imaging Laboratory
BSA	bovine serum albumin
cm	Centimetre
cDNA	complementary deoxyribose nucleic acid
CD	cluster of differentiation
CD19	b-lymphocyte antigen
CD31	platelet endothelial cell adhesion molecule (PECAM-1), expressed on platelets, monocytes, neutrophils, endothelial cells
CD34	bell-cell adhesion factor expressed on early hematopoietic cells
CD44	homing cell adhesion molecule
CD45	common leucocyte antigen, hematopoietic marker
CD51	integrin alpha -5, expressed on platelets and osteogenic cells
CD73	ecto 5’ nucleotidase, marker of lymphocyte differentiation
CD90	thy1, expressed on stem cells and axons
CD105	endoglin, expressed on endothelial cells, fibroblasts and activated macrophages
CD146	melanoma cell adhesion molecule, used as marker for endothelial cell lineage
CFU-F	colony forming unit-fibroblast
CMV	cytomegalovirus
DAPI	4', 6-diamidino-2-phenylindole
DCi	demethylation cytokine induced
DDD	degenerative disc disease

DMEM	Dulbecco’s modified Eagle’s medium
DMSO	dimethyl sulfoxide
DNA	deoxyribose nucleic acid
ECM	extra cellular matrix
EDTA	ethylenediaminetetraacetic acid
EGF	epidermal growth factor
ESCs	embryonic stem cells
FACS	fluorescence-activated cell sorting
FCS	foetal calf serum
FDA	US Food and Drug Administration
FSC	forward scatter
FGF	fibroblast growth factor
GF	growth factor
GFP	green fluorescent protein
GSEA	gene set enrichment analysis
hr	Hour
H & E	heamatoxylin & eosin
HEK	human embryonic kidney
HGFA	hepatocyte growth factor A
hiCFU-Fs	human induced colony forming unit-fibroblast
HIV	human immunodeficiency virus
HLA DR	human leucocyte antigen, subtype DR
HREC	human research ethics committee
HRP	horseradish peroxidase
IFATS	International Federation for Adipose Therapeutics and Science
IGF	insulin-like growth factor
IHC	immunohistochemistry
iMS cell	induced multipotent stem cell
IP	Intraperitoneal
iPSCs	induced pluripotent stem cells
IRES	internal ribosomal entry site
ISCT	International Society of Cellular Therapy
KSR	knockout serum replacement
LB	Luria-Bertani
LTR	long terminal repeat

MET	mesenchymal to epithelial transition
mRNA	messenger RNA
miRNA	micro ribose nucleic acid
mg	Milligram
mL	Millilitre
MQ-water	milli-Q water
MSCs	mesenchymal stem cells
MSLCs	mesenchymal stem like cells
NA	numerical aperture
NEAA	non-essential amino acids
NSG	non-obese diabetic severe combined immunodeficiency mouse, γ
OCT	optimal cutting temperature
P	Passage
PBS	phosphate buffered saline
PDGF	platelet derived growth factor
PDGFR	platelet derived growth factor receptor
PFA	Paraformaldehyde
P/S	penicillin/streptomycin
PSC	pluripotent stem cell
RNA	ribose nucleic acid
ROCK	rho-associated, coiled-coil containing protein kinase
ROS	reactive oxygen species
rpm	revolutions per minute
RT	room temperature
SCID	severe combined immunodeficiency
SCNT	somatic cell nuclear transfer
SD	standard deviation
SEM	standard error of the mean
siRNA	small interfering RNA
shRNA	short hairpin RNA
SSC	side scatter
STRO1	stromal cell antigen, early MSC marker
TA	tibialis anterior
TB	terrific broth
TE	tris-EDTA

TGFβ	transforming growth factor β
TNF	tumour necrosis factor
µL	Microlitre
µm	Micrometre
µM	Micromolar
UNSW	University of New South Wales
UV	ultra violet
VCM	virus containing media
WT	wild type
% (v/v)	Percentage volume per volume
% (w/v)	Percentage weight per volume

Table of Contents

Abstract i
Declarations ii
Acknowledgements iv
Publications vi
Presentations vii
List of Abbreviations x
Table of Contents xiv
List of Tables xix
List of Figures xx
CHAPTER 1 Literature Review 1
1.1 Introduction 1
1.2 Intrinsic tissue repair mechanisms 2
1.3 Tissue resident stem/progenitor cells 8
1.4 Inadequacies of intrinsic tissue repair mechanisms 9
1.5 Conventional treatment alternatives for tissue repair and their limitations 10
1.6 Stem cell-based therapeutic options for tissue repair 13
1.6.1 Embryonic stem (ES) cells 13
1.6.1.1 Isolation and characterization of ES cells 13
1.6.1.2 Clinical applications of derivatives of human ES cells 14
1.6.1.3 Limitations associated with therapeutic use of human ES cells 15
1.6.2 Mesenchymal Stem Cells (MSCs) 16
1.6.2.1 Isolation and characterization of MSCs 16
1.6.2.2 MSCs for tissue repair 20
1.6.2.3 Limitations associated with application of MSCs for tissue repair 30
1.6.3 Reprogrammed cells 31
1.6.3.1 Somatic cell reprogramming 31
1.6.3.2 Different approaches for somatic cell reprogramming 36
1.6.3.3 By-products of induced pluripotency reprogramming 40
1.6.3.4 Therapeutic applications of iPS cells 42
1.6.3.5 Limitations of using iPS cells for tissue repair 43
1.7 Introduction to DCi reprogramming 47

1.7.1 The role of AZA in cell plasticity 48
1.7.2 The role of Platelet Derived Growth Factor (PDGF) in stem cell biology/regeneration 51
1.8 Thesis objectives 58
1.8.1 Hypotheses 59
1.8.2 Aims 59
CHAPTER 2 Materials and Methods 60
2.1 MATERIALS 60
2.1.1 Reagents 60
2.1.2 Antibodies 61
2.1.2.1 Primary antibodies 61
2.1.2.2 Secondary antibodies 62
2.1.3 Cytokines 63
2.1.4 Equipment 63
2.1.5 Kits 64
2.1.6 Buffers, Medium and Solutions 64
2.1.7 Media composition 64
2.1.8 Softwares 65
2.1.9 Statistical Analysis 65
2.2 METHODS 66
2.2.1 Tissue Culture Techniques 66
2.2.1.1 Cell Culture conditions 66
2.2.1.2 Trypsinization of adherent cells 66
2.2.1.3 Cryopreservation of cells 67
2.2.1.4 Thawing of cryopreserved cells 67
2.2.1.5 Counting cells 67
2.2.1.6 Primary adipocyte harvest and culture 68
2.2.2 Demethylation Cytokine induced (DCi) reprogramming of primary adipocytes 70
2.2.2.1. Foetal calf serum-supplemented medium 70
2.2.2.2. Autologous serum-supplemented medium 70
2.2.3 Live cell imaging 70
2.2.4 *In vitro* expansion of reprogrammed cells 71
2.2.5 *In vitro* characterization of reprogrammed cells 71
2.2.5.1 Colony forming unit-fibroblast (CFU-F) assay 71

2.2.5.2 Long term growth curve 72
2.2.5.3 *In vitro* differentiation 73
2.2.5.3.1 Osteogenic differentiation 73
2.2.5.3.2 Adipogenic differentiation 74
2.2.5.3.3 Chondrogenic differentiation 74
2.2.5.3.4 Endothelial differentiation 75
2.2.5.3.5 Myogenic (Smooth muscle) differentiation 75
2.2.5.4 Immunophenotyping 76
2.2.5.5 Karyotyping 78
2.2.6 Immunocytochemistry for pluripotency markers 78
2.2.7 *In vitro* teratoma assay 79
2.2.7.1 Assay setup 79
2.2.7.2 Assay maintenance 80
2.2.7.3 Endpoint studies 80
2.2.8 Sequencing/Transcriptomics 81
2.2.8.1 RNA extraction 81
2.2.8.2 Sequence alignment and expression quantification 82
2.2.8.3 Principal Component Analysis (PCA) 83
2.2.8.4 Pathway Analysis 83
2.2.8.5. Heatmaps 83
2.2.9 Lentiviral transduction 84
2.2.9.1 Bacterial transformation of plasmid DNA 84
2.2.9.2 Plasmid DNA extraction and quantification 84
2.2.9.3 Lentivirus mediated tagging of cells 84
2.2.9.4 Validation of transduction 89
2.2.10 Postero-lateral inter-lumbar vertebral injury model 91
2.2.10.1 Animal details 91
2.2.10.2 Study design and surgery details 91
2.2.10.3 Bioluminescence imaging (BLI) 94
2.2.10.4 Endpoint studies 94
2.2.11 Muscle injury study 96
2.2.11.1 Animal details 96
2.2.11.2 Tissue injury and cell transplantation 96
2.2.11.3 Endpoint studies 98
CHAPTER 3 Demethylation Cytokine induced (DCi) reprogramming of primary human adipocytes 100
3.1 Introduction 100
3.2 Results 101

3.2.1 DCi reprogramming can be extrapolated to primary human adipocytes 101
3.2.2 Primary human adipocytes cannot be reprogrammed in serum-free conditions 106
3.2.3 DCi reprogramming of primary human adipocytes in autologous serum-supplemented media. 109
3.2.4 *In vitro* characterization of reprogrammed human iMS cells 111
3.2.4.1 Colony forming unit-fibroblast (CFU-F) potential 111
3.2.4.2 Long-term growth curve 114
3.2.4.3 Immunophenotyping 121
3.2.4.4 Multilineage differentiation potential 123
3.2.4.5 Karyotyping 125
3.2.5 Dose optimization of DCi reprogramming factors 126
3.3 Chapter summary and discussion 130
CHAPTER 4 Molecular characterization and evaluation of pluripotency in human iMS cells 133
4.1 Introduction 133
4.2 Results 134
4.2.1 DCi reprogrammed AdMSCs share *in vitro* characteristics with iMS cells 134
4.2.2 Transcriptomic analysis of DCi reprogrammed cells 137
4.2.2.1 Principal Component Analysis (PCA) 137
4.2.2.2 IPA analysis 140
4.2.3 DCi reprogrammed cells re-express pluripotency factors 152
4.2.4 *In vitro* teratoma assay setup 154
4.2.5 iPS cells exhibit tri-germ layer plasticity 157
4.2.6 DCi reprogrammed iMS cells do not exhibit spontaneous *in vitro* tri-germ layer plasticity 159
4.2.7 DCi reprogrammed iMS cells do not display improved *in vitro* plasticity when co-cultured with iPS cells 162
4.3 Chapter summary and discussion 168
CHAPTER 5 Evaluation of *in vivo* safety and plasticity of human iMS cells 172
5.1 Introduction 172
5.2 Study design 173
5.3 Results 178
5.3.1 Donor cells are retained at the transplant site 178
5.3.2 Transplanted cells do not enter host circulation 181

5.3.3 Donor cells are maintained as undifferentiated cells at 3 months post-transplant 183
5.3.4 Transplanted cells exhibit context-dependent *in vivo* plasticity at 6 months post-surgery 186
5.4 Chapter summary and discussion 191
CHAPTER 6. Evaluation of tissue-specific repair potential of human iMS cells 195
6.1 Introduction 195
6.2 Study design 198
6.3 Results 200
6.3.1 CTX injury induces severe damage in the injected TA muscle 200
6.3.2 Donor cells are retained at the site of injury 202
6.3.3 Donor cells undergo directed differentiation to form satellite cells 206
6.3.4 DCi reprogrammed cells undergo better myogenic commitment and differentiation than untreated cells 209
6.3.5 Donor derived satellite cells contribute to formation of mature muscle fibres 212
6.4 Chapter summary and discussion 216
CHAPTER 7 Conclusions and future directions 222
7.1 DCi reprogramming, a novel technique to generate autologous, multipotent stem cells 222
7.2 *In vitro* characteristics/ insights from molecular work 224
7.3 Safety, efficacy and specificity of plasticity of iMS cells 225
Contributions 231
References 233
Appendix: Supplementary data 256

List of Tables

Table 1. 1 Summary of clinical trials registered for MSC-based treatment for musculoskeletal disorders 25
Table 1. 2 Comparison of different reprogramming approaches 39
Table 1. 3 Comparison of core features of ES cells, iPS cells and MSCs 46

Table 2. 1 Fluorophores used for detection of cell-surface markers 77
Table 2. 2 Description of plasmids used for lentiviral transfection 86
Table 2. 3 Study groups for postero-lateral inter-lumbar vertebral injury study 93
Table 2. 4 Study groups for skeletal muscle regeneration study 97

Table 3. 1 Experimental matrix depicting different combinations of DCi reprogramming factors tested for dose optimization. 127

Table 4. 1 Table depicting different combinations of test cells co-cultured with WT C2 iPS cells in different ratios 164

List of Figures

Figure 1. 1 Limb regeneration mechanism in salamanders 6
Figure 1. 2 Schematic representation of multipotency of MSCs 19
Figure 1. 3 Schematic depiction of cell fate changes on Waddington's epigenetic landscape during normal development and reprogramming 35
Figure 1. 4 Mode of action of AZA in demethylation 49
Figure 1. 5 PDGF signaling system 54

Figure 2. 1. Schematic of the lentiviral construct containing LUC and GFP 87
Figure 2. 2 Determination of replication competent virus in transduced target cell - supernatant. 90

Figure 3. 1 DCi reprogramming of primary human adipocytes in FCS-supplemented medium 104
Figure 3. 2 DCi reprogramming of primary human adipocytes in serum-free media 108
Figure 3. 3 DCi reprogramming of primary human adipocytes in autologous serum-supplemented medium 110
Figure 3. 4 Characterization of CFU-F capacity of iMS cells 112
Figure 3. 5 Comparison of DCi reprogramming efficiency in different conditions 113
Figure 3. 6 Characterization of serial replating ability of iMS cells 117
Figure 3. 7 Heterogeneity in morphology of iMS cells cultured in different expansion media 118
Figure 3. 8 Revived iMS cells propagated in serum-free medium or complete α-MEM supplemented with allogenic human serum 120
Figure 3. 9 Immunophenotyping of iMS cells for MSC-associated markers 122
Figure 3. 10 Characterization of multipotency of iMS cells 124
Figure 3. 11 Schematic for cell populations tested for genomic instability 125
Figure 3. 12 Dose optimization of DCi reprogramming factors across three different age groups. 129

Figure 4. 1 Derivation and *in vitro* characterization of Treated AdMSCs.....136
Figure 4. 2 DCi reprogrammed iMS cells have a distinct transcriptional profile.....139
Figure 4. 3 Canonical pathways and categories of diseases and functions enriched after DCi of primary human adipocytes, as derived from IPA.....142
Figure 4. 4 Unsupervised clustering analysis of differentially expressed genes across primary adipocytes v/s iMS cells.....148
Figure 4. 5 Canonical pathways and categories of diseases and functions enriched in the comparison of 'AdMSCs v/s iMS cells', as derived from IPA.....151
Figure 4. 6 DCi reprogrammed cells re-express pluripotency factors 153
Figure 4. 7 *In vitro* teratoma assay setup 156
Figure 4. 8 WT C2 iPS cells exhibit *in vitro* tri-germ layer plasticity.....158
Figure 4. 9 DCi reprogrammed iMS cells do not exhibit *in vitro* tri-germ layer plasticity 161
Figure 4. 10 iMS cells lack tri-germ layer plasticity even when co-cultured with iPS cells. 167

Figure 5. 1 In vitro validation of LeGO-iG2-Luc2-GFP transfection.....175
Figure 5. 2 Schematic representation of workflow for postero-lateral inter-lumbar vertebral injury model. 177
Figure 5. 3 Localization and survival of transplanted cells in the spine region.....180
Figure 5. 4 Evaluation of transplanted cells in host circulation. 182
Figure 5. 5 Tissue sections do not show any differences in gross architecture at 3 months post-transplant. 184
Figure 5. 6 Transplanted cells display are retained as undifferentiated cells at 3 months post-transplant. 185
Figure 5. 7 Tissue sections do not show any differences in gross architecture at 6 months post-transplant either. 187
Figure 5. 8 Transplanted cells display *in vivo* plasticity. 188
Figure 5. 9 Transplanted iMS cells display better in vivo plasticity.....190

Figure 6. 1 Schematic representation of workflow for CTX-induced skeletal muscle injury model 199
Figure 6. 2 CTX induces damage of muscle fibres.....201

Figure 6. 3 Retention of human cells in CTX-injured TA muscle.....204
Figure 6. 4 Transplanted iMS cells display better *in vivo* retention at the site of injury. 205
Figure 6. 5 Detection of donor-derived satellite cells within the injured muscle 208
Figure 6. 6 DCi reprogrammed cells exhibit better myogenic commitment and differentiation than untreated cells.....211
Figure 6. 7 Detection of human spectrin-positive myofibres in animals transplanted with human cells. 213
Figure 6. 8 Quantification of donor-derived human fibres in regenerating muscle sections. 215
Figure 6. 9 Schematic representation of proposed mechanism for donor cell contribution to myofibre regeneration 219

Figure 7. 1 Future directions for DCi reprogramming.....230

CHAPTER 1 Literature Review

1.1 Introduction

The adult human body is composed of a myriad of different cell types which are organized in an orderly fashion to form tissues and organs. A programmed sequence of events during embryogenesis drives the patterning and differentiation of embryonic stem (ES) cells leading to development of the complex structures that constitute the human body (Corson & Siggia, 2012). Harmonious interactions between individual components are necessary for the smooth functioning of the body as a biological unit. Tissue homeostasis is maintained by meticulous control of physiological processes at a cellular level within the context of the functioning biological unit. Any deviation from the balanced physiological state of the body occurring as a result of ageing, trauma, disease or congenital defects has direct implications at the cellular level (Biteau et al., 2011).

Tissue regeneration is the process by which damaged tissues and/or deficient cells are restored to a healthy functional state. Unlike lower order organisms such as the salamander, humans do not have the capacity to regrow lost or damaged appendages (Brockes & Kumar, 2005). The precise genetic and environmental causes underlying this loss of regeneration in mammals over millions of years of evolution remain poorly understood. In adult humans, tissue repair and regeneration processes are restricted to a few organs such as the liver, skin, blood, and gastrointestinal tract. Moreover, this repair potential diminishes with age. Additionally, the adult human body has limited capacity to repair damage, even in the tissues where tissue repair is possible (Sanchez Alvarado & Tsonis, 2006). In severe or chronic cases of tissue injury, the inherent tissue repair

mechanisms are often inefficient to combat the damage. For example, a myocardial infarcted adult human heart is unable to regenerate itself completely, instead the tissue repair mechanisms often culminate into undesirable scar tissue formation. Although this is a product of protective mechanisms executed by the body, it does not restore the organ to its original, functional state (Talman & Ruskoaho, 2016). This has dire consequences not only on the affected organ but also on the normal physiological functioning of the entire body.

Healing of damaged tissue is considered complete only when the differentiated, rejuvenated tissue integrates entirely with the neighbouring undamaged host tissue and its normal functioning is re-established. Regenerative medicine-based approaches to restore normal functionality of the affected tissues include treatment alternatives that involve replacing the damaged tissues with healthy tissues by means of therapeutic cell-based or engineered tissue-based alternatives (Mao & Mooney, 2015). Current trends in regenerative medicine focus on generating tissue specific stem cells to repair damaged tissues. However, given the complexity of most tissues, the ideal tissue regenerative stem cell would be the one that is sufficiently plastic to contribute to the repair of multiple tissue types in a context dependent manner.

1.2 Intrinsic tissue repair mechanisms

The limited tissue repair potential in humans is governed by discrete mechanisms that deal with normal wear and tear and minor injuries to some organs of the body. Intrinsic mechanisms of tissue repair include recruitment of adult stem and progenitor cells, de-differentiation or trans-differentiation of mature cells and rearrangement of pre-

existing tissues to allow integration of these renewed cells (Kang & Zheng, 2013). The replacement of worn or injured tissue depends on resident somatic stem cells that have self-renewal capacity as well as multipotency (Jopling et al., 2011). While the turnover of tissues such as cardiac muscle and neurons are quite limited; blood, skin, intestinal epithelium, skeletal muscle and bone are examples of tissues which are constantly regenerated or remodelled. The adult liver also retains significant regenerative capacity throughout life and is mainly attributed to the injury-induced proliferation of all its constituent mature cell populations, including hepatocytes (Michalopoulos et al. 1997). Indeed, the liver can renew its mass within two weeks after resection of almost two-thirds of all hepatic tissue (Taub, 2004). Among the different connective tissues of the human body, bone is unique in that it does not heal by scarring (Gerstenfeld et al., 2003).This is mainly attributed to its extensive vascular network that ensures a constant supply of nutrients, growth factors and hormones, thereby facilitating the process of regeneration. The functional balance between bone resorption and deposition by osteoclasts and osteoblasts respectively helps maintain the integrity of bone (Raggatt & Partridge, 2010). This retention of regenerative capacity, although limited, implies that some genetic programs associated with regeneration are still conserved.

The limited regenerative abilities in few tissues can also be attributed to specific features of the somatic stem cells. Cells that comprise tissues in a developing or adult organism possess a memory of their position relative to the different axes of the body plan. This epigenetically determined cellular property is known as ‘positional information’ and plays a crucial role in maintaining cell identity and the differentiation of cells in a context dependent manner (Bryant et al. 1981, Rinn et al. 2008). In humans, this positional information is retained throughout adulthood in some type of cells such as

fibroblasts (Bryant et al. 2002, Chang et al. 2002). Loss of positional information contributes to unregulated cell growth and malignant transformation (Ruiz I Altaba et al. 2007). Other than that, activation of immune responses following injury have been shown to facilitate skeletal muscle regeneration by stimulation of fibro-adipogenic progenitors in adults (Heredia et al., 2013). Similarly, injury-induced acute cardiac inflammation also drives angiogenesis and cardiomyocyte proliferation in mouse neonatal heart thereby facilitating its repair and regeneration (C. Han et al., 2015; Lavine et al., 2014). A recent study from Ritschka et al. reports the ability of senescent cells to induce plasticity and stemness in undamaged neighbouring cells and clearance of damaged or aged cells, thereby supporting tissue repair and homeostasis (Ritschka et al., 2017). Yet another recent report by Boya et.al. describes the role of basal autophagy in tissue repair and homeostasis where non-essential cellular components and damaged/senescent cells are cleared out whereas the tissue resident stem cells are prevented from undergoing senescence (Boya et al., 2018). However, not all tissues of the human body are equipped with as efficient a mechanism to counteract chronic or severe injuries.

In contrast to humans, lower order animals are endowed with far greater regenerative capacity, and this is mediated by mechanisms that are distinct to those found in higher order animals. For instance, the salamanders (amphibians of the order Caudata) regenerate their lost or wounded body parts by a unique mechanism independent of resident stem cells but which rather relies on the plasticity of differentiated cells (Brockes and Kumar 2005). In salamanders, mesenchymal tissues such as cartilage, muscle and connective tissue underlying the wound epidermis, lose their differentiated characteristics and adopt an undifferentiated, transient blastemal cell state (Wallace et al., 1981). Although the blastema is avascular, it is innervated (C. Mccusker et al., 2015). It is

essentially a mass composed of undifferentiated, regeneration-competent proliferative cells which undergo pattern formation and differentiation in response to resident cues to integrate and facilitate restoration of the tissue to its original, healthy state (Figure 1.1).

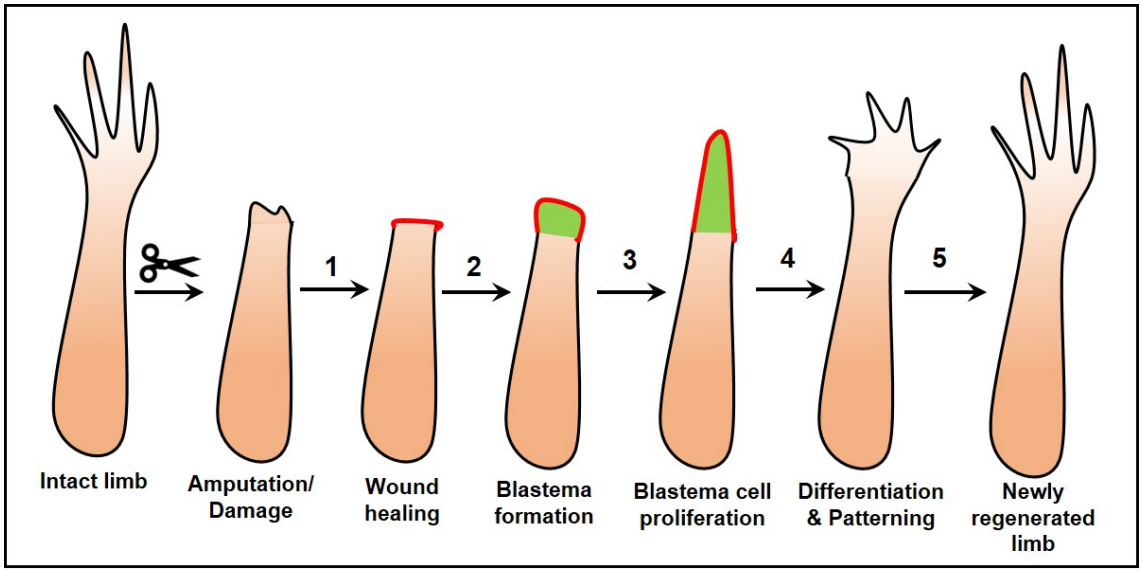

Figure 1. 1 Limb regeneration mechanism in salamanders

Amputation or damage to the salamander limb triggers the process of wound healing (1) which is followed by the cells underlying the wound epidermis to acquire a blastemal state (2). In response to resident cues, the blastemal cells undergo extensive proliferation (3), followed by differentiation and patterning, (4) to give rise to functional, regenerated limb (5). Adapted from (Whited & Tabin, 2009).

Indeed, growth factors such as the Fibroblast Growth Factors (FGFs) and Bone Morphogenetic Proteins (BMPs) released from the wound epidermis and nerve connections within the newly-formed blastema assist wound healing (Brockes & Kumar, 2005; A. Kumar et al., 2007). FGFs are master regulators of organogenesis and tissue homeostasis. Different isoforms of FGF ligands and their corresponding receptors are involved in repair of a range of tissues including lung, liver, bone, skeletal muscle, lens, etc. They bring about tissue repair by inducing cell proliferation within the blastema or regenerative bud, via wound angiogenesis, through paracrine effects on other progenitor cells, and regulation of cell differentiation (Maddaluno et al., 2017). BMPs are glycoproteins which are particularly involved in bone repair. They recruit osteoprogenitors to the fractured or damaged bone, and these osteoprogenitors then undergo differentiation to give rise to mature bone cells (Salazar et al., 2016). BMPs also play a role in adult lung tissue and intestinal repair by promoting proliferation of tissue resident stem cells in response to tissue damage. The tissue repair process is further facilitated by interactions between different components of the system such as extracellular matrix components, signaling mechanism and transportation system which together establish a microenvironment conducive to regeneration. Reorganization of newly formed tissues during regeneration is governed by patterning cues as well as self-organization of the progenitor cells formed within the blastema (Atabay et al., 2018). This epimorphic process of tissue repair and reorganization in lower order animals is well-orchestrated and involves regulated expression of homeotic genes which allow context-dependent formation of replacement tissues in accordance to the pre-determined body plan (Dolan et al., 2018). It would be a major biological feat if this unique regeneration mechanism in these animals could be replicated in mammalian cells. This would require somatic cells to lose their differentiated status in response to an injury and adopt a

blastemal cell state which could undergo further context-dependent multi-lineage differentiation for regeneration of the affected tissue.

1.3 Tissue resident stem/progenitor cells

In humans, an episode of injury triggers local and remote repair mechanisms in the form of signals communicated by the nervous system. Repair is mainly driven by a dedicated population of tissue resident stem and progenitor cells whose widespread presence in various tissues provides a bank of cells that can be recruited to heal tissues damaged by daily wear and tear (Chimenti et al., 2010; Jopling et al., 2010; Senyo et al., 2013). Numerous studies have identified populations of progenitor cells in injured tissues which may provide a source of cells to replenish and repair the damage (Brisby et al., 2013; Risbud et al., 2007). As these stem cells play an important role in maintaining proper tissue function, they need to be safeguarded from damage and/or loss as much as possible. These stem cells are maintained in a specialized microenvironment or niche, which provides spatial and temporal cues to support and co-ordinate their activities (Wagers, 2012). They have the ability to self-renew as well as differentiate into various distinct mature cell types, in response to physiological cues that demand cell replacement and repair. (Asahara et al., 1999; Passier & Mummery, 2003). As stem cells undergo commitment to a given lineage, their multipotency and capacity to self-renew gradually diminishes. While precursor stem cells are capable of unlimited division, progenitor cells that are derived from stem cells have a rather finite proliferative capacity. The potency of a progenitor cell is indeed influenced by its parent stem cell and interaction with the niche.

The stem/progenitor cells residing in tissues/organs (bone marrow, adipose tissue, skeletal muscle, gastrointestinal tract, etc.) or circulating in the blood are often maintained

in a quiescent state until they are activated by either a physiological need for additional cells to maintain tissues, or on sensing an abnormality in the healthy state of the tissue such as disease or injury (Tuan et al., 2003). In an event of tissue injury, specific growth factors and cytokines trigger recruitment of progenitor cells to mount a repair response. A dedicated transportation system comprised of vasculature or lymphatic vessels then helps mobilize these progenitor cells from their niche to sites of repair. A well-orchestrated repair response ensues with an increase in the pool of progenitor cells brought about by increased cell division facilitating faster recovery of the injured tissue (Hatzistergos et al., 2010; Wilson et al., 2008) The proliferation and differentiation of tissue resident cells in response to external cues facilitates replacement of damaged cells whereas their depletion or dysfunction results in aberrant tissue repair (Su et al., 2009; Wagers, 2012). Context dependent tissue repair by resident stem cells is further facilitated by retention of a position-specific molecular fingerprint within these cells that can be further relayed to bring about expression of region-specific genes (Rinn et al., 2006). Any perturbation to the signaling machinery, communication or transportation system would therefore negatively impact self-repair of the injured organ (C. D. Mccusker & Gardiner, 2013).

1.4 Inadequacies of intrinsic tissue repair mechanisms

Degenerative diseases, either acute or chronic, have a high impact on the affected individual as well as a socio-economic status of the health system. The intrinsic regenerative potential of human tissues is limited and diminishes with age (Colnot, 2011). In cases involving significant damage to a tissue, the repair response is often insufficient due to exhaustion of the local stem cell population. In order to improve the repair response, it is therefore necessary to either amplify or improve endogenous stem or

precursor cell population, or to recruit cells mobilized from remote sites to the site of injury. The inefficiency of the endogenous healing process is further compounded by the fact that repair mechanisms in humans are generally associated with the formation of collagen-rich car tissue, a product of the protective mechanisms exhibited by the body comprised mainly of fibroblasts (Bianco et al. 2013). The evolution of complex immune systems to provide better protection against infection could be one of the reasons why scarring overshadows the slow regeneration process post tissue injury (Gupta, 2016). This in turn causes the affected organ to be rendered dysfunctional. For example, irreversible scarring that occurs after an episode of myocardial infarction of the heart, not only impairs myocardial function but also increases its susceptibility to future events of infarction, infection and eventual organ failure. Although studies describing the use of anti-fibrogenic agents (e.g. TGFβ inhibitors) that effectively reduce the formation of scar tissue have been reported (Fukushima et al., 2001), these studies do not extend to multiple types of tissue injuries, and such treatment does not guarantee complete restoration of organ functionality. On this background, it is beneficial to understand if and how different treatment alternatives can be applied to restore normal functionality to both the affected tissue and the body as a whole.

1.5 Conventional treatment alternatives for tissue repair and their limitations

Surgery and medication have been the conventional treatment options for minor tissue injuries. For major injuries, organ transplantation or tissue grafting are the primary treatment alternatives. Conventional surgeries are often invasive and require complex post-operative care. Chronic tissue injuries such as osteoarthritis or muscle dystrophy often require multiple surgeries. In addition, the gap between supply of matched donor organs and their availability on demand continues to be high. In the past, the focus was

centred on growth factors to heal wounds and promote tissue regeneration (Falanga, 2005). These defined morphogens (administered externally or induced internally) help mobilize stem cells and facilitate their subsequent participation in tissue repair. For example, Wnt7a has been shown to promote the expansion of rodent satellite cells (Le Grand et al., 2009) and enhance muscle regeneration whereas Oncostatin M can cause dedifferentiation of cardiomyocytes into a more precursor-like cell state which can participate in cardiac remodelling (Kubin et al., 2011). BMP2 promotes osteogenesis from mesenchymal precursor cell populations and is in use in spinal fusion surgeries to promote bone healing (Lissenberg-Thunnissen et al., 2011). However, the use of recombinant growth factors as treatment options for tissue repair are also posed with certain shortcomings. For instance, the external administration of BMP2 for bone healing has undesirable effects in that it gives rise to ectopic bone formation and off-target effects on peripheral sensory neurons and the spinal cord (Carragee et al., 2011). Specific delivery of growth factors to the desired site of action is difficult and these highly active compounds are often prone to have effects on non-target cell types. Additionally, these compounds need to be delivered at high doses and in some cases, need to be administered in multiple rounds of treatment (Vogelin et al., 2000). Clinical translation of recombinant growth factors as therapeutic alternatives has therefore seen only limited success (Falanga, 2012).

The regenerative medicine field has also focussed on the use of tissue engineering and bioengineered skin constructs or artificial scaffolds like collagen (Glowacki & Mizuno, 2008). These porous constructs, which are seeded with cells, were expected to adapt to the wound environment and integrate to repair damaged tissues. However, these constructs were demonstrated to work in a pharmacological/tropic mode where the seeded

cells secrete pro-regenerative growth factors which activate the resident stem cell pool rather than themselves replacing the damaged tissues (Phillips et al., 2002). This process also becomes cumbersome and technically demanding when applied on a large scale. More importantly, the allogeneic transplantation of the bioengineered constructs runs a high risk of immune rejection by the recipient, and so requires parallel administration of immunosuppressants (Halloran, 2004). In some cases, the immunosuppression would be life-long leading to other complications and morbidities due to increased vulnerability to infections (Fishman, 2007). Additionally, currently available treatment options are primarily aimed at providing symptomatic pain relief and are associated with significantly adverse side effects. No treatment options have clearly shown to slow or reverse disease progression completely thereby impeding effective tissue repair.

There is a clear need to develop safe and efficient therapies in order to achieve context-dependent tissue repair. While many ongoing studies have explored and established novel tissue engineering strategies using scaffolds (synthetic and biological) in the presence of appropriate differentiation factors, the focus of this thesis is cell-based therapies for safe and effective tissue regeneration. Given that most adult tissues of the human body possess a small pool of resident stem/progenitor cells with limited regeneration potential, harvested and *ex vivo* expanded cells could serve as a significant input for cell-based therapy. The following sections will cover different cell populations that have been previously studied to assess their potential therapeutic benefits.

1.6 Stem cell-based therapeutic options for tissue repair

Stem cells are defined as clonogenic cells capable of both self-renewal and differentiation into multiple lineages (Weissman, 2000). Depending on their source and differentiation potential, stem cells are classified as totipotent stem cells (can give rise to tissues of all the germ layers and extraembryonic tissues), pluripotent stem cells (can give rise to tissues of all the germ layers, but not extraembryonic tissue or placenta) and adult stem cells (which are lineage restricted and can give rise to tissue-specific cells) (Blau et al., 2001). The following sections will cover detailed characteristics and the therapeutic relevance of different types of stem cells.

1.6.1 Embryonic stem (ES) cells

1.6.1.1 Isolation and characterization of ES cells

ES cells are pluripotent cells derived from the inner cell mass at the blastocyst stage in a developing embryo. Isolation of mouse ES cells was first reported in 1981 (Evans & Kaufman, 1981; Martin, 1981) and establishment of first human ES cell line in 1998 (Thomson et al., 1998). These cells display extensive proliferation potential and can differentiate into cells of all the three germ layers. Human ES cells are characterized by their expression of pluripotency associated markers; SSEA3, SSEA4, TRA-1-60, TRA-1-81, OCT4, NANOG and SOX2 (Brandenberger et al., 2004). ES cells are also characterized by high telomerase activity which helps in maintaining their long replicative lifespan (Thomson et al., 1998). While ES cells give rise to differentiated cells of specific lineages during normal development, they also generate the multipotent precursor cells that contribute to tissue homeostasis throughout normal life. ES cells

undergo division to self-renew and to produce daughter cells that are amenable to subsequent differentiation and migration (De Lucas et al., 2018; Garcia-Prat et al., 2017).

1.6.1.2 Clinical applications of derivatives of human ES cells

Since their initial discovery, there have been consistent efforts to harness the self-renewal capacity and multilineage differentiation potential of ES cells to combat acute and chronic tissue injuries (Lerou & Daley, 2005). ES cells cannot be transplanted in their undifferentiated form due to their inherent tumorigenicity (Ben-David & Benvenisty, 2011). Therefore, numerous studies on protocols devised for directed differentiation of human ES cells into desired cell types/tissue progenitors for subsequent therapeutic applications have been reported. For example, the application of human ES cell derivatives has been reported in treatment of full-thickness tendon injury (Cohen et al., 2010; Dale et al., 2018), cartilage defects in arthritic tissue (Olee et al., 2014), peripheral nerve injury (I. Jones et al., 2018), wound healing in diabetic mice (Kasap et al., 2017), ischemic tissue repair (Zhang et al., 2017), Type I diabetes (Maehr et al., 2009) and muscular dystrophy (Magli et al., 2016). Additionally, cell-free extracts from human ES cells have also been applied to generate differentiated cell populations which can then be used in a therapeutic context (J. Han & Sidhu, 2011).

Several clinical trials to determine the safety and efficacy of ES cell-derivatives in the treatment of a variety of disorders including macular degeneration (W. K. Song et al., 2015), muscular dystrophy, ischemia, non-ischemic dilated cardiomyopathy, and diabetes are currently underway. To date (12.04.2018), a total of 49 clinical studies at different study phases that involved human ES cells derivatives have been registered (Clinicaltrials.Gov, 2018).

1.6.1.3 Limitations associated with therapeutic use of human ES cells

Despite their promising potential, the therapeutic use of ES cells is largely limited due to the ethical considerations relating to their derivation, *ex vivo* maintenance and manipulation (Lenoir, 2000; Young, 2000). ES cell mediated therapy is therefore not an approved procedure in several countries (Lo & Parham, 2009; Reisman & Adams, 2014). The gap in knowledge with regards to the differentiation potential and proliferation rate of ES cells, poses a risk of teratoma or ectopic tissue formation as well as malignant transformation (J. Y. Li et al., 2008; Odorico et al., 2001). As a consequence, ES cells cannot be transplanted in their undifferentiated form due to their risk of inherent tumorigenicity, requiring their *ex vivo* differentiation to the appropriate lineage for the downstream application (Bongso et al., 2008). Furthermore, directed differentiation and controlled proliferation of ES cells is challenging and requires establishment of reproducible protocols for the cells to be applied in a therapeutic context. Prolonged culture of ES cells *in vitro* is also associated with the risk of introducing undesirable genetic and epigenetic changes as well as chromosomal instability (Draper et al., 2004; Mitalipova et al., 2005). Moreover, ES cell-derivatives also run the risk of immune rejection as they are applied allogeneically (Simonson et al., 2015). Altogether these shortcomings substantially limit the therapeutic application of ES cells.

1.6.2 Mesenchymal Stem Cells (MSCs)

1.6.2.1 Isolation and characterization of MSCs

Mesenchymal stem cells (MSCs) are an important type of tissue-resident, non-hematopoietic, adult stem cells involved in maintaining homeostasis across a wide range of human tissues (Caplan, 2010; Gronthos & Simmons, 1996). MSCs exhibit fibroblast-like morphology and were shown to grow in small colonies in plastic-adherent culture systems (Friedenstein et al., 1970) This attribute was first reported by Friedenstein and colleagues and was termed Colony Forming Unit-Fibroblast (CFU-F) (Friedenstein et al., 1976). MSCs are essentially a heterogeneous mix of progenitors that can self-renew, proliferate and differentiate into multiple mature cell types, including osteocytes, adipocytes and chondrocytes, both *in vitro* and *in vivo* (Barry & Murphy, 2004; Caplan & Bruder, 2001; Pittenger et al., 1999). Other than cells of the mesodermal lineage, MSCs can also differentiate into skeletal myocytes, cardiomyocytes, epithelial cells, endothelial cells and neurons from the ectodermal and endodermal lineages (Bianco et al., 2013; Bianco et al., 2008; Mannello, 2006).

MSCs, first isolated from the bone marrow constitute one of the well characterized stem cell populations (Pittenger et al., 1999). Subsequent studies have then reported their isolation from other tissues including dental pulp, adipose tissue, cartilage, skeletal muscle, skin, teeth, heart, gut, liver, ovarian epithelium, testis, umbilical cord and the perivascular niche of most organs (Crisan et al., 2008). While the MSC populations obtained from different sources resemble each other, they also exhibit some variation with respect to their differentiation potential and phenotype (Abdallah & Kassem, 2008; Baksh

et al., 2007; Kern et al., 2006). Their overall heterogeneity is further compounded as a result of phenotypic variance within a given population of MSCs (Bianco et al., 2013). Attempts to thoroughly understand MSC biology are further complicated by the absence of standardized protocols for isolation and expansion of cells, and by the phenotypic changes that occur during *in vitro* cultivation (Bara et al., 2014). In an effort towards defining standard criteria to define MSCs, the 'Mesenchymal and Tissue Stem Cell Committee' of the 'International Society for Cell Therapy (ISCT)' have formulated minimal criteria for definition as an MSC, which include: (a) Plastic adherence when cultured *in vitro*, (b) Presence of CD105, CD73, CD90 and absence of the hematopoietic markers namely CD45, CD34, CD14 or CD11b, CD79a or CD19 and HLA-DR surface molecules on 95% of the plastic adherent cells and (c) *in vitro* tri-lineage differentiation into osteocytes, adipocytes and chondrocytes (Dominici et al., 2006).

A cell population enriched for CFU-F cells can be isolated based on high expression of Stromal Cell Antigen (STRO-1), an antigen first reported as being expressed by a subpopulation of human bone marrow mononuclear cells (Gronthos et al., 1999). Recent reports have now shown that STRO-1 antibody binds to the cell surface protein heat shock cognate 70 (HSC70) (Fitter et al., 2017) which is involved in maintaining a stem cell phenotype (Liu et al., 2008). When cultured *in vitro*, the STRO-1+ cell population can form colonies and can be induced to differentiate into osteoblasts, adipocytes, chondrocytes, myoblasts, hematopoietic-supporting fibroblasts, and neural cells (Dennis et al., 2002). STRO-1 expression is down-regulated as MSCs form lineage committed or differentiated cells (Gronthos et al., 1999). However, STRO-1 cannot be used a sole marker for purifying MSCs, as some differentiated cell types such as Glycophorin A positive nucleated red cells and B lymphocytes co-express STRO-1

(Gronthos & Zannettino, 2008). Other perivascular markers such as CD106 and CD146 are therefore used in combination with STRO1 to increase the purity of clonogenic MSCs. Cells purified by applying this strategy exhibit a 5000-fold increase in CFU-F capacity as well as enhanced multipotency and homing over unfractionated cells. More importantly, the STRO-1+/CD106+/CD146+ population is devoid of any committed stromal cell elements, endothelial cells or hematopoietic stem or progenitor populations (Zannettino et al., 2008).

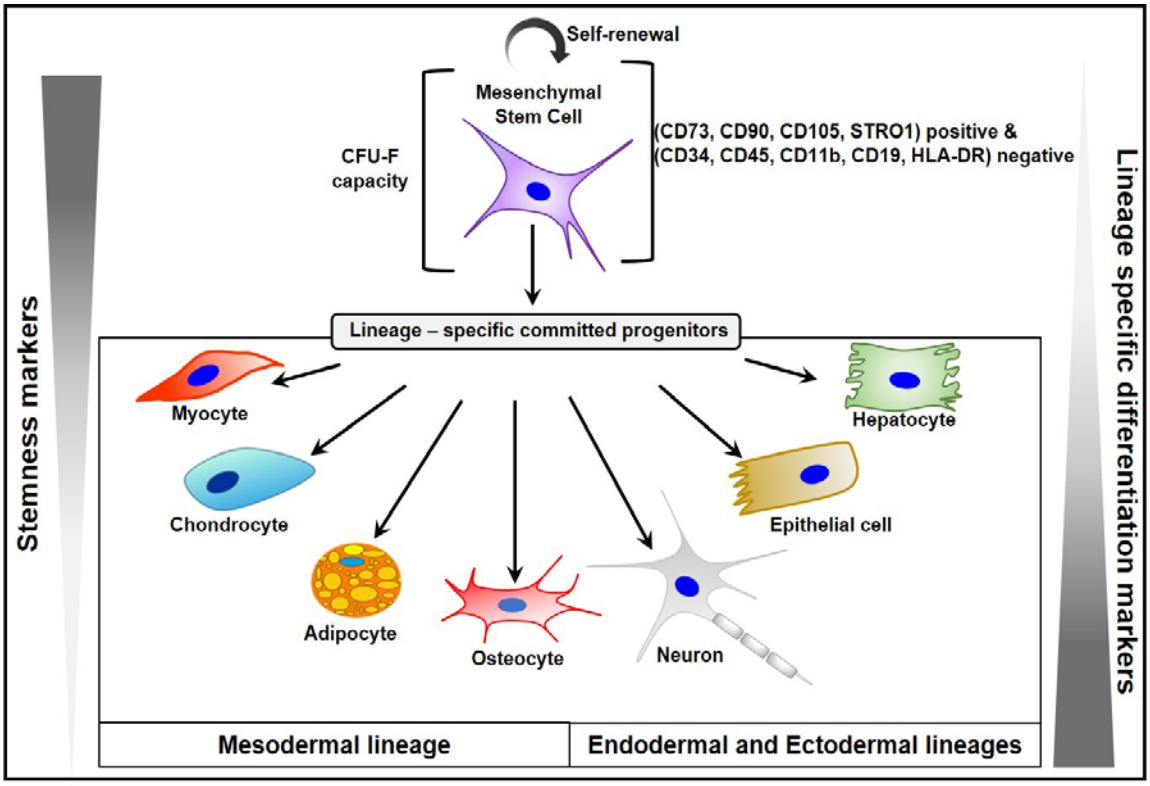

Figure 1. 2 Schematic representation of multipotency of MSCs

MSCs are characterized by their ability to self-renew, CFU-F potential and expression of CD73, CD90, CD105 and STRO1. MSCs can differentiate into lineage-specific committed progenitors which further differentiate primarily into mature cells of the mesodermal lineage like myocyte (muscle), chondrocyte (cartilage), adipocyte (fat), osteocyte (bone). They can also differentiate into the endodermal and ectodermal lineages like hepatocyte (liver), epithelial cell (skin) and neuron (nervous system). As MSCs undergo differentiation along a given lineage, the expression of markers associated with stemness is downregulated whereas the expression of lineage specific markers is upregulated.

1.6.2.2 MSCs for tissue repair

MSCs constitute attractive candidates for tissue regeneration as they can proliferate without losing their differentiation potential. MSCs can participate in tissue repair and regeneration, either directly, by differentiating into specific cell types, or indirectly via their trophic effects and secretory functions including anti-inflammatory activity and immune-modulatory effects (Carceller et al., 2015; Dave et al., 2015; Murphy et al., 2013; Uccelli et al., 2008; Wada et al., 2013). Moreover, MSCs prevent apoptosis in other cells and have low immunogenicity making them suitable for allogenic transplantation (Murphy et al., 2013). MSCs can also inhibit proliferation and cytotoxic activity of immune system cells, thereby alleviating the risk of graft-versus-host disease (M. Lee et al., 2014; Yagi et al., 2010). Their ability to secrete a variety of soluble mediators and respond to chemotactic signals facilitates their effective recruitment to injured tissues (Hwang et al., 2009). Adipose derived MSCs (AdMSCs) also help to inhibit scar proliferation by suppressing Transforming Growth Factor β (TGFβ)-induced myofibroblast activity (Yun et al., 2012). Additionally, MSCs are able to cross the blood-brain barrier thereby widening the scope of their therapeutic applicability (Simard & Rivest, 2004). Importantly, unlike embryonic ES cells or pluripotent stem cells (PSCs), the use of MSCs does not raise ethical concerns (Herberts et al., 2011). Moreover, MSCs can be harvested from autologous tissues thereby avoiding the risk of rejection that results from expression of the Major Histocompatibility Complex (MHC) in ES cells (Korbling & Estrov, 2003). The availability and versatility of MSCs therefore makes them suitable candidates for cell-based therapies for a wide range of clinical pathologies (Keating, 2012) leading to a recent proposal to rename them ‘Medicinal Signaling Cells’ (Caplan, 2017).

Several clinical trials to determine the safety and efficacy of MSCs in treatment of a variety of disorders including Crohn's disease, graft v/s. host disease, degenerative disc disease, cardiovascular disorders, diabetes, muscular dystrophy, spinal cord injury, osteoarthritis, etc. are currently underway. At the time of reporting (12.04.2018), a total of 825 clinical studies involving MSCs were registered at clinicaltrials.gov. Out of these, 136 studies involve the use of MSCs in therapies under the broad category of musculoskeletal diseases. MSC based therapy is also being applied to treat non-union fractures (Murphy et al., 2013) and other disorders like osteonecrosis (Gangji et al. 2004), cartilage injury (Haleem et al. 2010), osteoarthritis (Felson et al. 2006 (Y. H. Chang et al., 2016), etc.

The first clinical study of a MSC-based therapy for Degenerative Disc Disease (DDD) in humans was conducted in 2011. The pilot study involved injection of autologous, *in vitro* expanded MSCs into the degenerated lumbar discs of 10 patients. The study reported pain relief in 85% of patients 3 months after surgery and substantial improvements in lumbar and sciatic pain along with an improvement in the Oswestry Disability Index (ODI)[1]. At one year after treatment, the analgesic effect was more evident than the actual anatomical restoration of the damaged disc. The study outcomes were therefore attributed to the trophic effects of MSCs rather than their direct contribution towards repair (Orozco et al., 2011). Another clinical trial from Mesoblast Limited employed their highly purified and immunoselected proprietary allogenic Mesenchymal Precursor Cells (MPCs) for the treatment of lumbar back pain. This preliminary study (Mesoblast: MPC-06-ID Phase 2) involved injection of 6 or 18 million

[1] ODI is an index derived from Oswestry Low Back Pain Questionnaire used by clinicians and researchers to quantify disability for low back pain (Fairbank & Pynsent, 2000).

MPCs in a hyaluronic acid carrier into the nucleus pulposus of the degenerated lumbar disc of 100 patients. The completion of this Phase 2 study was reported in July 2015 with overall improvement in chronic low back pain and reduced need for additional surgical and non-surgical interventions in comparison to saline control or matrix control groups, at 12 months after surgery. 36-month results for this trial were released in March 2017 showing that single intra-discal injection of MPCs resulted in improvements in pain and function, that were durable for at least three years. Although injection with MPCs lead to an improvement in ODI and pain scores in patients, evidence regarding their direct contribution to disc repair was lacking (Mesoblastnews). Therefore, these data also point to the trophic effects of MSCs in tissue repair and leave room to critically investigate their fate on transplantation.

Positive results from another Phase I safety trial involving clinical application of allogenic MSCs obtained from human adipose tissue towards treatment of Osteoarthritis were reported in May 2017. This study, conducted by Regeneus Limited, involved intra-articular injection of their proprietary product, Progenza, in patients with knee osteoarthritis (Kuah et al., 2018). At 12 months post-injection, the cells were tolerated well, and no serious adverse events occurred. The Progenza treated joints did not show any further deterioration after injection and showed a statistically significant reduction in pain score (Western Ontario and McMaster Universities Arthritis Index (WOMAC))[2] when compared to the placebo group. The promising results of these trials form the foundation for future clinical trials, however precise evaluation of whether the injected cells facilitate tissue repair through tropic effects or direct contribution to tissue

[2] WOMAC is an index used by clinicians and researchers to quantify arthritis of different joints (Mcconnell et al., 2001)

regeneration is required before any such treatment enters mainstream use. Other completed clinical trials involving MSCs and/or their derivatives for treatment of musculoskeletal diseases are summarized in **Table 1.1**.

Table 1. 1 Summary of clinical trials registered for MSC-based treatment for musculoskeletal disorders

Study type	No.	Cell source	Administration route	Number of partici p-ants	Follow-up period (in months)	Phase	Condition or Disease addressed	Clinical trials.gov identifier	Results
Auto - logous	1	BM-MSCs	Intraarticular	12	24	I/II	Knee osteoarthritis	NCT01183728	Improvement in cartilage quality and algofunctional indices, Pain relief
	2	AdMSCs (RNL-JointStem)	Intraarticular	18	6	I/II	Degenerative arthritis	NCT01300598	Improvement in WOMAC score, Reduction in cartilage defects
	3	AdMSCs	Intrafemoral	15	24	N/A	Avascular necrosis of the femoral head	NCT01643655	No results posted
	4	BM-MSCs	Intraarticular	40	3	II	Knee osteoarthritis	NCT01504464	No results posted
	5	BM-MSCs	Placement in fusion bed	15	Not provided	I/II	Lumbar Intervertebral disc disease	NCT01513694	No results posted
	6	AdMSCs	Intraarticular	18	24	I/IIa	Knee osteoarthritis	NCT01809769	Improvement in pain, function and cartilage volume of the joint
	7	BM-MSCs	Intraarticular	10	12	I/II	Knee osteoarthritis	NCT01895413	No results posted

	8	BM-MSCs	Intraarticular	6	12	I	Full thickness articular cartilage defects	NCT00850187	No results posted
	9	BM-MSCs	Intraarticular	6	30	I	Ankle joint osteoarthritis	NCT01436058	Improvement in pain and function
	10	BM-MSCs	Intrafemoral	3	Not provided	II	Osteonecrosis of the femoral head	NCT01700920	No results posted
	11	BM-MSCs	Intraarticular	6	2	I	Hip osteoarthritis	NCT01499056	Improvement in pain and function
	12	BM-MSCs	Intracystal	6	12	I	Bone cyst	NCT01207193	No results posted
	13	BM-MSCs	Intraarticular	6	12	I	Knee osteoarthritis	NCT01207661	Improvement in pain and function
	14	BM-MSCs	At callus site	6	12	I	Leg Length Inequality	NCT01210950	No results posted
	15	BM-MSCs	Intraarticular	30	12	I/II	Knee osteoarthritis	NCT02123368	Improvement in pain scores, decreased joint damage
	16	Multiple	N/A	35	36	N/A	Knee osteoarthritis	NCT01879046	No results posted
	17	AdMSCs	Intraarticular	53	12	II	Knee osteoarthritis	NCT02162693	No results posted
	18	BM-MSCs	Intraarticular	13	12	II	Articular Cartilage Disorder of Knee	NCT02118519	Improved pain score and increased cartilage thickness
	19	UC-MSCs	Intraarticular	20	12	I	Articular cartilage defects of the knee	NCT02291926	No results posted
	20	BM-MSCs	Intraarticular	15	12	I/II	Articular Cartilage in Gonarthrosis	NCT01227694	No results posted
	21	AdMSCs (JointStem)	Intraarticular	24	6	II	Degenerative Arthritis	NCT02658344	No results posted

	22	BM-MSCs	Intraarticular	60	6	II/III	Knee Osteoarthritis by Rheumatoid Arthritis	NCT01873625	Improvement in pain scores, Reduction in reliability of drugs, Improvement in standing time
	23	BM-MSCs	N/A	18	6	I	Knee Osteoarthritis	NCT02468492	No results posted
	24	BM-MSCs	Intrafemoral	21	60	I	Osteonecrosis of the Femoral Head	NCT00821470	No results posted
	25	BM-MSCs	Intraarticular	25	12	I	Knee Osteoarthritis	NCT01931007	Pain reduction
	26	Osteoblastic cells	Intrafemoral	82	36	II	Osteonecrosis of the Femoral Head	NCT02890537	No results posted
	27	BM-MSCs	Intradiscal	80	24	N/A	Spondyloarthrosis, Spondylosis	NCT01603836	Results pending review
	28	BM-MSCs	Bone Marrow Transplant	50	60	I	Non-traumatic Osteonecrosis of the Femoral Head	NCT01544712	No results posted
	29	AdMSCs	Intraarticular	18	3	I	Osteoarthritis	NCT01585857	Improved pain score and function
	1	BM-MSCs	Intraarticular	30	12	I/II	Knee osteoarthritis	NCT01586312	Improvement in cartilage quality and algofunctional indices, Pain relief

Allo-geneic	2	UC-MSCs (CARTISTEM)	Intraarticular	12	12	I/II	Articular cartilage defects of the knee	NCT01733186	No results posted
	3	Pooled BM-MSCs (Stempeucel)	Intraarticular	60	24	II	Knee osteoarthritis	NCT01453738	Pain reduction
	4	BM-MSCs	Intradiscal	25	12	I/II	Degenerative disc disease	NCT01860417	Improvement in disc quality, pain relief
	5	Adult MSCs	Intraarticular	72	12	II	Knee osteoarthritis	NCT01448434	No results posted
	6	UC-MSCs (CARTISTEM)	Intraarticular	104	12	III	Knee Articular Cartilage Injury	NCT01041001	No results posted
	7	BM-MSCs	Bone Marrow Transplant	9	Not mentioned	N/A	Osteogenesis Imperfecta	NCT00187018	Marked growth acceleration
	8	BM-MSCs	Intravenous	120	6	N/A	Ankylosing Spondylitis	NCT01709656	No results posted
	9	AdMSCs	Intravenous	53	6	I/II	Rheumatoid Arthritis Aggravated	NCT01663116	No results posted
	10	BM-MSCs	Intraarticular	140	24	N/A	Degenerative osteoarthritis	NCT01413061	No results posted
	11	BM-MSCs	Bone Marrow Transplant	9	12	I	Osteogenesis Imperfecta	NCT00705120	No results posted
	12	BM-MSCs	Intradiscal	100	36	II	Degenerative disc disease	NCT01290367	No results posted
	13	BM-MSCs+Master graft granules	At fusion site	6	36	I/II	Degenerative disc disease	NCT00549913	No results posted

1.6.2.3 Limitations associated with application of MSCs for tissue repair

Despite their numerous advantages, the clinical use of MSCs has certain limitations. Although MSCs from fat or bone marrow are regularly injected into sites of injury, there is little objective evidence regarding their retention at site of transplant or direct contribution to new tissue formation (Bianco et al., 2013). MSCs vary in their abundance in different tissues and may require higher starting material depending on their subsequent application. For example, 5000 stem cells can be isolated from 1g of adipose tissue, which is 500 times more than the cells obtained from an equivalent amount of bone marrow (Hass et al., 2011; Pittenger et al., 1999; Zuk et al., 2002). Moreover, the resulting cells may have limited or variable ability to proliferate and differentiate into functional mesenchymal tissues owing to donor age and the effects of the prolonged culture required to expand the cells (Yao et al., 2016). Additionally, the regenerative potential of MSCs is a function of their source tissue. For instance, MSCs derived from the bone marrow have a higher propensity to form osteoblasts and chondrocytes (Jin et al., 2013) whereas those derived from the adipose tissue were shown to be more amenable towards formation of a capillary-like network (Freiman et al., 2016).

Owing to their ability to home to sites with an inflammatory microenvironment, MSCs are sometimes known to preferentially migrate towards tumour sites (Spaeth et al., 2008). They are also reported to stimulate tumorigenesis, metastasis and transformation into cancer cells. MSCs are involved in cancer pathogenesis through direct actions on cancer cells by release of paracrine factors that regulate tumour progression and metastasis. MSCs also stimulate neo-angiogenesis in the proliferating tumour by secreting angiogenic growth factors, thereby playing an indirect role in tumour growth (Gonzalez et al., 2017; H. Y. Lee & Hong, 2017).

The need for *ex vivo* expansion and lack of universal isolation protocols can also compromise the safe and effective therapeutic use of MSCs (Lim et al., 2014). Variability in source tissue, culture techniques, number and route of cell administration, and timing of cell delivery are other factors that contribute to the inconsistent outcomes of therapeutic application of MSCs (Daley & Scadden, 2008; Karp & Leng Teo, 2009; Le Blanc et al., 2008; Lin, 2002). In addition, MSCs have also been reported as the main cellular origins for fibrotic disease of various tissues (El Agha et al., 2017). More recently, Kramann et al. have shown that ablation of the mesenchymal stem cell (MSC)-like cell population from which myofibroblasts arise significantly ameliorates fibrosis and rescues organ function (Kramann et al., 2015). In the light of all these limitations, it is therefore beneficial to seek alternative options for cell-based therapy which still bear the beneficial characteristics of MSCs but circumvent the associated detrimental features.

1.6.3 Reprogrammed cells

1.6.3.1 Somatic cell reprogramming

Somatic cell reprogramming involves changing the fate of a terminally differentiated adult cell to a pluripotent/multipotent stem cell state (de-differentiation) or conversion from one cell type to another (trans-differentiation also known as direct lineage reprogramming). In the past, cellular differentiation was believed to be a unidirectional process where a pluripotent cell differentiates to form a lineage committed progenitor cell which then undergoes further differentiation leading to the formation of a mature, differentiated and fully functional cell. During development of a multicellular organism, a single totipotent zygote ultimately gives rise to multiple differentiated cell types with unique gene expression programs. The process was vividly depicted by a

pioneering embryologist, Conrad H. Waddington in his 'epigenetic landscape model' where he equates a cell to a ball rolling down from the top of a hill, as it proceeds through subsequent stages of differentiation. The ball rolls downwards under the influence of cell-signaling networks and crosses branching valleys that successively restrict developmental options leading to different cell types that can be formed. Eventually, a cell finds itself at the bottom of a valley in a stable, mature and terminally differentiated state (Waddington, 1957) (Figure 1.3A). Until the late 1950s it was largely believed that the potential of a cell diminishes over its course of development and generating a clone using an adult cell's nucleus would be essentially impossible. This general understanding was radically changed following the demonstration that the nucleus obtained from a frog's intestinal epithelial cell, when transplanted into an enucleated egg could generate a fully functional and fertile tadpole (Gurdon, 1962). More importantly, this discovery also paved the way for numerous cloning studies and raised the question of whether terminally differentiated cells could be reprogrammed to generate undifferentiated pluripotent stem cells which could be further re-differentiated into cells of all the three germ layers. This was addressed by the advent of several remarkable concepts including cell fusion (Evans & Kaufman, 1981) and 'Somatic Cell Nuclear Transfer (SCNT)' (Wilmut et al., 1997) which led to the successful creation of the first cloned animal, Dolly-the sheep (Loi et al., 1997). The process which involved transplantation of nuclei derived from cultured epithelial cells into enucleated oocytes opened doors for similar cloning studies to be carried out in other large animals (Keefer, 2015; Loi et al., 2013; Zhao et al., 2009).

Other studies reported that somatic cells could be epigenetically reprogrammed by fusion with nuclei of pluripotent stem cells such as ES cells (Cowan et al., 2005; Do & Scholer, 2004; Tada et al., 2001). These reprogrammed cells showed high levels of

expression of pluripotency-associated genes such as OCT4. Together these studies provided evidence of the underlying potential of pluripotent stem cells to induce pluripotency in somatic cells (Cowan et al., 2005). Subsequent studies have now demonstrated that mammalian cells are far more plastic than previously thought. While most fully differentiated cells do not divide further, some cell types do produce identical daughter cells, for example, adult pancreatic β cells divide to give rise to new β cells which are also fully differentiated (Dor et al., 2004). The seminal study by Takahashi and Yamanaka demonstrating the use of cell-type-specific transcription factors to change cell fates between developmentally distant cell types has transformed this paradigm (Takahashi & Yamanaka, 2006) (Figure 1.3B). In their pioneering study, they demonstrated generation of induced pluripotent stem (iPS) cells from adult fibroblasts by ectopic expression of the pluripotency associated transcription factors, namely; **O**CT4, **S**OX2, **K**LF4 and c**M**YC (OSKM). This study opened doors for wide scale adaptation and application of different cell reprogramming techniques to generate the desired cell-types suitable for downstream therapeutic purposes. The following section will cover different approaches used for somatic cell reprogramming.

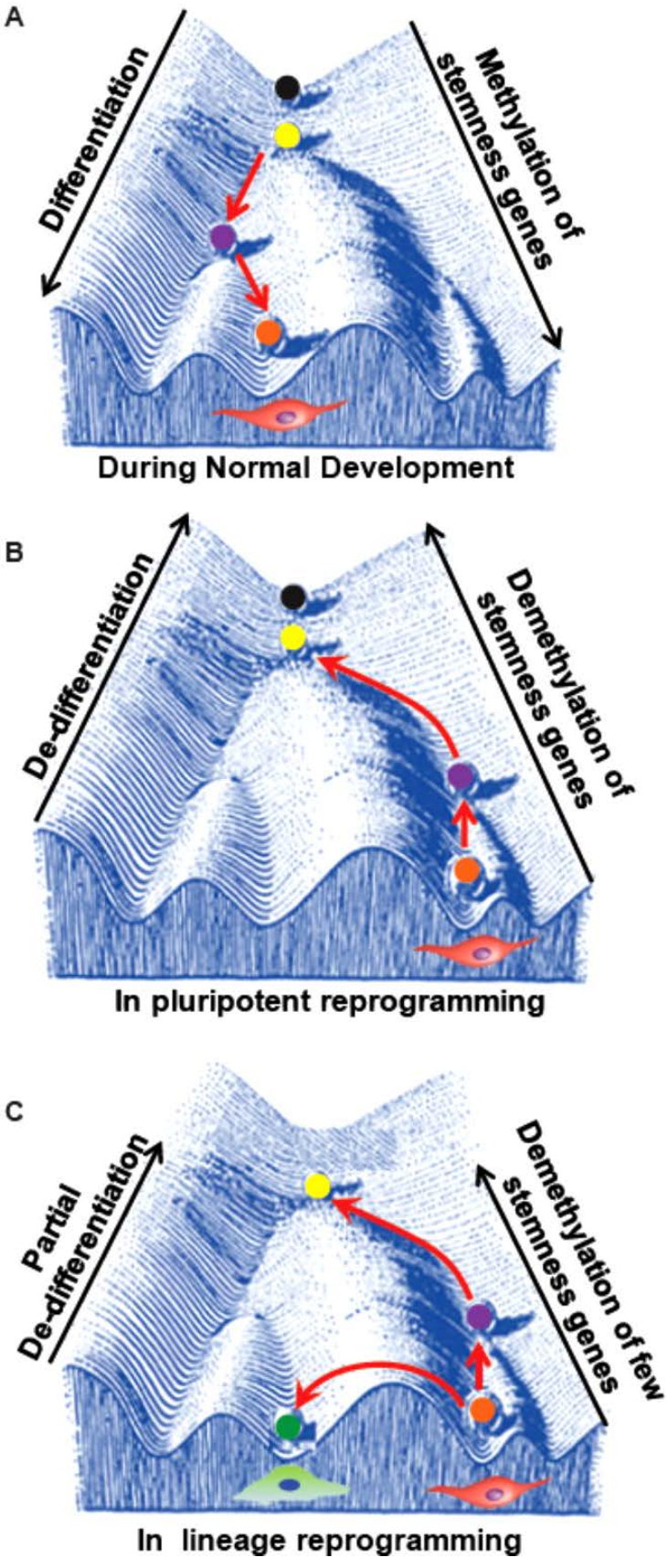
A
Differentiation
Methylation of stemness genes
During Normal Development
B
De-differentiation
Demethylation of stemness genes
In pluripotent reprogramming
C
Partial De-differentiation
Demethylation of few stemness genes
In lineage reprogramming

Figure 1. 3 Schematic depiction of cell fate changes on Waddington's epigenetic landscape during normal development and reprogramming

(A) In normal development, a pluripotent cell, such as an embryonic stem cell (black ball), rolls down bifurcating valleys, which represent all possible developmental paths. The cell makes a series of choices and differentiates into a lineage committed cell (yellow ball), progenitor cell (purple ball) and finally a differentiated, mature cell (orange ball) at the bottom of the valley, under the force of gravity. As a cell matures, stemness genes undergo methylation and are silenced. (B) Recent evidence has shown that seemingly energetically unfavourable reverse processes can be brought about. During pluripotent reprogramming, the entire developmental process is reversed, and a differentiated cell (orange ball) is returned to its completely undifferentiated, pluripotent state (black ball). This is represented by the ball (cell) rolling from the bottom of the valley backward all the way to the apex of the landscape. Pluripotent reprogramming is associated with demethylation and subsequent re-activation of stemness genes. (C) Lineage reprogramming includes partial de-differentiation where a mature cell (orange ball) reverts its cell state only to a progenitor (purple ball) or lineage committed cell state (yellow ball) and trans-differentiation where the mature cell (orange ball) converts directly to another mature cell (green ball) and could be seen as the ball being pushed sideways over a ridge. Lineage reprogramming involves demethylation/re-activation of only few stemness genes (Adapted from, Geo and Alwin 1956, (Q. Zhou et al., 2008).

1.6.3.2 Different approaches for somatic cell reprogramming

Somatic cell reprogramming strategies can be classified into pluripotent reprogramming and lineage reprogramming. Pluripotent reprogramming involves the total fate reversal of a completely differentiated cell to an embryonic stem cell like state. It involves removal of all or nearly all of the epigenetic marks that are laid down during development. This strategy can be applied to reprogram a wide variety of cells including fibroblasts, hepatocytes, stomach cells, neurons, etc. (J. B. Kim et al., 2008; Nakagawa et al., 2008; Takahashi et al., 2007). In contrast, lineage reprogramming involves direct conversion of one specialized cell type to another without undergoing complete de-differentiation to the pluripotent state (Figure 1.3C) (J. Xu et al., 2015).

Since its inception, various studies to improve the efficiency of reprogramming have been reported. Although the oncogenic factor cMYC helps in increasing efficiency of reprogramming to pluripotency, it is not absolutely essential to bring about cell fate reversal (Nakagawa et al., 2008). Later, Xu and colleagues reported in an independent study that removal of C-myc from the reprogramming cocktail significantly enhances the efficiency of reprogramming (Xu et al., 2013). In 2009, Ichida and colleagues were successful in finding substitutes for two of the OSKM factors and found that the a single chemical molecule named ‘RepSox’ in combination with Oct 4 and Klf 4 could still bring about the generation of iPSCs from somatic cells (Ichida et al., 2009). A decade since the original study outlining somatic cell reprogramming, efforts to improve the efficiency of the technique have been consistent. Additional studies demonstrating ways to improve reprogramming efficiency include the role of inflammatory cytokine interleukin-6 (IL-6), application of a microfluidic environment to bring about a 50-fold increase in efficiency over traditional reprogramming through delivery of synthetic mRNAs encoding

transcription factors or by exposure to ionizing radiation (Chiche et al., 2017; S. B. Lee et al., 2017; Luni et al., 2016)

Although the iPS cell generation method is advantageous in generating an expanded pool of precursors, their clinical utility is restricted due to the use of viral vectors, low reprogramming efficiency, and the need for *ex vivo* differentiation (Yamanaka, 2009). In an attempt to address some of these limitations, adenoviruses were used to supply cDNAs encoding for reprogramming factors thereby proving that genomic integration is not required for cells to be turned back to their pluripotent state (Stadtfeld et al., 2008). Zhou and Fusaki then reported the use of adenoviruses (W. Zhou & Freed, 2009) or Sendai viruses (Fusaki et al., 2009) for the delivery of these cDNAs to reprogram human fibroblasts. Improving further, Kim et al. demonstrated generation of iPS cells by direct delivery of reprogramming factors that can cross the cell membrane (D. Kim et al., 2009). Alternate reprogramming strategies which facilitate reprogramming by non-coding RNA (Loewer et al., 2010) micro RNA (Kogut et al., 2018; Sul et al., 2012), different small molecule compounds (Hou et al., 2013) and antibodies (Blanchard et al., 2017) have also been reported. Another study reported a substantial reduction in reprogramming efficiency as a consequence of the double knock down of the transcription factors Foxd1 and Foxo1 during OSKM mediated reprogramming (Koga et al., 2014). Investigators have also demonstrated improvement in reprogramming efficiency by inhibition of chromatin modifiers that are involved in maintenance of the somatic cell state or substantial increase in the duration of OSKM induction (from 2 weeks to 20 weeks) (Cheloufi et al., 2015; Gafni et al., 2013).

Another advancement in the arena of transcription factor induced reprogramming to pluripotency describe the generation of a novel cell-type called the ‘F-class cells’. These cells were obtained from murine fibroblasts after a high fold and persistent expression of the OSKM factors (Tonge et al., 2014). The F-class cells are termed as such because of the fuzzy borders of their colonies and they are strikingly different from the iPS cells at multiple levels. They exhibit increased expression of genes associated with cell-fate commitment rather than those associated with a pluripotent stem cell fate. Additionally, the F-class trajectory is not associated with demethylation of the ES cell-associated loci, which is common in iPS cell reprogramming (Hussein et al., 2014). Many researchers believe that F-class cells could serve as better candidates for cell-based therapy compared to iPS cells, given their high proliferation rates and great resemblance to MSCs (Vidal et al., 2015).

Table 1. 2 Comparison of different reprogramming approaches

	Technique	Advantages	Limitations	References
Pluripotent Reprogramming	Fusion with ES cells	Simplicity, Not immunogenic, oocyte independent	Ethical concerns, Generates tetraploid hybrids, Low efficiency	(Blau et al., 1983)
	SCNT	Ensures complete epigenetic reprogramming, made cloning possible	Teratogenicity, Low reprogramming efficiency. Technically challenging, Immunogenic, Dependence on oocytes	(Gurdon, 1962; Wilmut et al., 1997)
	OSKM mediated	No ethical concerns, Applicable to any type of somatic cell, Generates pluripotent cells	Teratogenicity, genetic and epigenetic aberrations, low reprogramming efficiency ~0.01%, random integration of oncogenic factors, need for ex vivo differentiation, slow kinetics	(Takahashi et al., 2007; Takahashi & Yamanaka, 2006)
	RNA mediated	Highly specific, Transient expression of RNA	RNA may require prior modifications to prevent degradation, multiple rounds of administration, Efficiency ~1%	(Warren et al., 2010)
	Small molecules mediated	Cell permeable, non-immunogenic, easily administered, reversible effects	Incomplete reprogramming, Multiple rounds of administration	(W. Li et al., 2013; Zhu et al., 2006)
Lineage reprogramming	ES cell extract mediated	Relatively simpler	Incomplete reprogramming, Low efficiency, may need ex vivo conditioning or differentiation, Dependence on embryos	(J. Han & Sidhu, 2011; Rajasingh et al., 2008)
	Lineage specific TF mediated	High efficiency	Generates cells with limited potency, Difficult to delineate specific TFs that can be applied for reprogramming	(Davis et al., 1987; Ieda et al., 2010)
	Small molecules mediated	Rapid and dose dependent modulation	Requires rigorous screening to delineate right combination	(X. Li et al., 2015)

SCNT: Somatic Cell Nuclear Transfer; ES cells: Embryonic Stem cells; OSKM: **O**CT4, **S**OX2, **K**LF4, c**M**yc; TF: Transcription Factor

1.6.3.3 By-products of induced pluripotency reprogramming

Transformation of cells from a terminally-differentiated cell state to a pluripotent stem cell state is accompanied by extensive genome-wide chromatin remodeling. Maintenance of pluripotency requires an interplay of transcriptional regulators, epigenetic modifiers and extracellular signaling pathways. The transformation of cell fate to a pluripotent state therefore induces wide-scale changes not only at the genetic level but also at the epigenetic level (Buganim et al., 2012; Maherali et al., 2007). These modifications are important for effective cell reprogramming in ways similar to that known in normal embryonic development as they regulate the access to, and expression of, stage-specific genes (P. A. Jones & Taylor, 1980; Mikkelsen et al., 2008).

Chromatin resetting at the genetic level involves reactivation of embryonic genes that are functional during normal embryonic development (Tanaka, 2003). There is accumulated evidence to suggest that somatic cell reprogramming is a multistep process with two predominant waves of changes in gene expression including an early wave of enhanced cell proliferation along with mesenchymal to epithelial transition and a late wave which is characterized by reactivation of pluripotency genes (Polo et al., 2012). This second wave involves specific upregulation of genes associated with pluripotency (e.g. Oct4, Sox2, Klf-4, c-Myc, Nanog, Tra-1-81, SSEA-4, etc.) and concomitant downregulation of genes which are characteristic of the respective terminally differentiated cell state (e.g. pparγ2 for adipocytes, runx2 for osteocytes and sox9 for chondrocytes). Additionally, there is upregulation of telomerase enzyme activity and gain of immortality (Maherali et al., 2007).

At the epigenetic level, histone modifying enzymes function in a well-orchestrated fashion either to maintain the chromatin architecture representative of the somatic cell state or assist in establishment of pluripotency as per the phase of reprogramming (Apostolou & Hochedlinger, 2013). The modulation of epigenetic regulators such as DNA dioxygenases, histone deacetylases, H3K36 demethylase, H3K27 demethylase and H3K9 demethylases greatly influences the efficiency and kinetics of reprogramming towards the iPS cell state (Mikkelsen et al., 2008). Additionally, the later stage of reprogramming in female cells is associated with erasure of inactive X chromosome-heterochromatin marks resulting in X-chromosome re-activation (Pasque et al., 2014; Payer et al., 2013). During reprogramming, as the somatic cell moves towards acquisition of pluripotency, the reprogramming factors also bring about rearrangements in the overall chromatin architecture which are further maintained by the Mediator and Cohesin complexes which are both known to orchestrate long-range chromatin interactions (Kagey et al., 2010). In summary, in the early stages of reprogramming, the four reprogramming factors (OSKM) bring about epigenetic changes in somatic cells and push them to an intermediate or partially reprogrammed state which is characterized by establishment of histone marks associated with pluripotency (Egli et al., 2008). Changes in DNA methylation profiles and transcriptional activation of pluripotency associated genes then occur at later stages of reprogramming (Polo et al. 2012).

1.6.3.4 Therapeutic applications of iPS cells

iPS cells have gained considerable attention as a promising cell population for regenerative therapies as they overcome the ethical limitations associated with ES cells. Moreover, they can be generated from any source tissues, thereby widening the scope of their applications (Takahashi & Yamanaka, 2013). For any cell population to be applied therapeutically, it is imperative that its safety, specificity and efficacy be critically evaluated. Since iPS cells bear the inherent risk of tumour formation, they require prior *ex vivo* differentiation before they can be therapeutically applied.

Numerous studies attempting to determine the therapeutic safety and efficacy of iPS cell-derivatives have emerged recently. Several clinical trials applying iPS cells and their derivatives in treatment of a variety of disorders including macular degeneration, graft v/s host disease, neurological disorders, solid tumors, diabetes, anemia, etc. are currently ongoing. At the date of writing (19.03.2018), a total of 30 clinical studies recruiting patients for treatment of various disorders with derivatives of iPS cells have been registered (Clinicaltrials.Gov, 2018)

In 2013, a pioneering clinical trial led by Masayo Takahashi at the RIKEN center in Japan was initiated to test the safety and feasibility of transplanting autologous iPS cell derivatives for treatment of neovascular age-related macular degeneration. A sheet of retinal pigmented epithelium (RPE) cells was derived from patient-specific iPS cells. The generated RPE cells were deemed safe by genomic testing and remained intact for one year after autologous transplant without causing any adverse events. The recipient's vision did not show any evidence of the decline which is commonly associated with macular degeneration (Mandai et al., 2017). However, RPE cells prepared in the same

way from another patient were found to contain genetic abnormalities, and hence never underwent transplantation. The focus then shifted to banked allogenic iPS cells generated from a donor's skin cells for generation of RPE. These allogenic RPE cells were transplanted into a patient (in his 70s) with age-related macular degeneration. However, the first serious adverse event possibly arising due to the technique of transplantation was reported in January 2018 in a Japanese press release (Thejapantimes, 2018). This incident required removal of the pre-retinal membrane as medication with steroids and anti-vascular endothelial growth factor did not improve the symptoms. The scientific as well as non-scientific community remains curious regarding the eventual outcome of this trial.

1.6.3.5 Limitations of using iPS cells for tissue repair

Generation of integration-free iPS cells from a starting population of somatic cells continues to be a challenge for most reprogramming techniques. Random integration of the reprogramming factors into the genome of recipient cells may still cause deleterious mutations and thereby compromise the therapeutic application of the generated reprogrammed cells. Additionally, over-expression of OCT4 has been reported to exert oncogenic effects on somatic cells (Hochedlinger et al., 2005). Despite numerous modifications, the original protocol to induce pluripotency is not full-proof in that it selects for mutations in the parental cell population and introduces new mutations during reprogramming (Hussein et al., 2014). The generated iPS cells are highly dynamic and can undergo rapid transitions to other cell states which respond differently to reprogramming interventions. The expression level and stoichiometry of reprogramming factors is another aspect that influences the efficiency of reprogramming (Carey et al., 2011). This generates a heterogeneous cell population and is associated with undesirable outcomes including mutagenesis and low reprogramming efficiency. These techniques

also have the drawbacks of incomplete reprogramming and therefore require meticulous screening to obtain a pure population of completely reprogrammed cells. In addition, optimal efficiency of some reprogramming approaches can only be attained when the reprogramming factors are administered in multiple rounds. iPS cells are not suitable for direct transplantation due to their inherent propensity to form tumors or ectopic tissues at the graft site (Yamanaka & Blau, 2010). The reprogrammed iPS cells also need to undergo *ex vivo* expansion and differentiation before they are transplanted into the host. This runs the risk of introduction of karyotypic changes in the cells over prolonged *in vitro* culture. Collectively, these limitations associated with iPS cells have led to a shift in focus from complete reprogramming (to a pluripotent stem cell state) to partial reprogramming (de-differentiation towards progenitor/multipotent stem like cell of a specific tissue lineage) or trans-differentiation to another somatic cell state by using defined transcription factors. Different transcription factor combinations have been widely applied for the *in vitro* or *in vivo* induction of specific cell types such as insulin-producing cells (Q. Zhou et al., 2008), neuronal cells (Vierbuchen et al., 2010), hematopoietic stem and progenitor cells (C. F. Pereira et al., 2013; Riddell et al., 2014; Sandler et al., 2014), cardiomyocytes (Fu et al., 2013; Ieda et al., 2010) and hepatocytes (Huang et al., 2011; Sekiya & Suzuki, 2011).

Despite numerous attempts to generate tissue-specific cells for repair, the inability of engrafted cell populations to integrate into the host environment remains a key obstacle. Moreover, most of these techniques require vector-based gene transfer and have low reprogramming efficiency. In addition, most structural tissues are a complex mix of different types of cells and require therapeutic cells that can undergo context dependent differentiation into multiple lineages. The increasing need of regenerative medicine

based therapeutic options for treatment of difficult to cure diseases demands development/establishment of novel cell sources. Complete physical and functional restoration of the damaged tissue/organ continues to be a major unmet need in the clinic. This further emphasizes the need for alternative cell populations and development of newer reprogramming techniques which circumvent the above constraints and at the same time have higher reprogramming efficiency. The ideal tissue regenerative stem cell would be the one that combines the advantages of ES cells, iPS cells and MSCs (summarized in Table 1.4) and would be sufficiently plastic to contribute to the repair of multiple tissue types in a context dependent manner without the risk of tumour formation.

Table 1. 3 Comparison of core features of ES cells, iPS cells and MSCs

	Feature	ES cells	iPS cells	MSCs
General features	Can be obtained from any source tissue	No	Yes	Yes
	Invasive cell collection procedure	Yes	No	Yes, sometimes
***In vitro* characteristics**	Long-term self-renewal	Yes	Yes	Yes
	Trans-germ layer multipotency	Yes	Yes	Yes
	Pluripotent cell-molecular signature	Yes	Yes	No
	Chromosomal instability	Yes	Yes	No
***In vivo* characteristics**	Tumorigenicity	Yes	Yes	No
	In vivo plasticity	Yes	Yes	No
	Ethical concerns	Yes	No	No
	Direct contribution to tissue repair and regeneration	Yes	Yes	No

Comparison of different therapeutically relevant cell populations. Features desired in the ideal regenerative cell population are highlighted in yellow.

1.7 Introduction to DCi reprogramming

Given the numerous limitations associated with therapeutic application of MSCs and iPS cells, it is necessary to develop cell-based therapeutic alternatives that possess all the beneficial properties of stem cells but do not bear the inadequacies associated with currently available options for cell-therapy. In 2016, our group published a novel, vector and transcription factor-free method to reprogram murine somatic cells into induced multipotent stem (iMS) cells by combined treatment with 5'-azacitidine (AZA) and platelet derived growth factor (PDGF)-AB (Chandrakanthan et al., 2016). This method is termed Demethylation Cytokine induced (DCi) reprogramming. Murine iMS cells display certain resemblances to MSCs in that they have *in vitro* CFU-F potential, multilineage differentiation capacity, and the ability to self-renew. Treatment with DCi reprogramming factors did not induce any karyotypic changes on the murine somatic cells. Moreover, DCi reprogrammed cells also re-expressed pluripotency associated genes and displayed a distinct transcriptional profile compared to the untreated cells or corresponding MSCs. At the molecular level, DCi reprogramming required signaling through PDGFRa for cell-fate conversion and was associated with synergistic activation of the JAK/STAT and JNK/c-JUN pathways. When transplanted syngeneically in an injured tissue, murine iMS cells are retained at the site of transplantation and display context-dependent *in vivo* plasticity. Most importantly, the iMS cells contribute directly to tissue regeneration without scar formation or malignant transformation. No adverse events including teratoma formation were reported in this study.

1.7.1 The role of AZA in cell plasticity

Azacytidine (AZA) is a chemical analogue of the pyrimidine nucleoside cytidine, a component of nucleic acids (Figure 1.4A) (Krawczyk et al., 2013). Following cellular uptake, AZA gets incorporated into DNA as well as RNA (Issa & Kantarjian, 2009). AZA has been shown to demethylate DNA both globally and at specific gene loci. DNA methylation/demethylation is one of the epigenetic mechanisms that regulate gene expression. When administered in low doses, AZA that is incorporated into replicating DNA forms adducts with DNA methyltransferase (DNMTs) through covalent links and creates genome-wide protein-DNA crosslinks. This further results in the depletion of soluble methyltransferase levels available within the cell for DNA methylation and therefore results into subsequent demethylation of DNA (Figure 1.4B) (Stresemann & Lyko, 2008). This in turn leads to replication dependent global demethylation and reactivation of silent genes (Figure 1.4) (Silverman & Mufti, 2005). However, a high dose of AZA can result in direct cytotoxicity in abnormal hematopoietic cells in the bone marrow through its rapid incorporation into DNA and RNA (Christman, 2002; P. A. Jones & Taylor, 1980). This inhibits DNA methylation and in turn activates tumour suppressor genes, eventually leading to cell death (Christman, 2002; Stresemann & Lyko, 2008; Taylor & Jones, 1979). Drug therapies which use AZA harness this property in the treatment of myelodysplasia, chronic myelomonocytic leukemia and acute myeloid leukemia (Stone, 2009). In addition, AZA has also been shown to induce increased transcription of the TET2 gene accompanied by transient upregulation of pluripotency marker expression and changes in histone modifications (Manzoni et al., 2016).

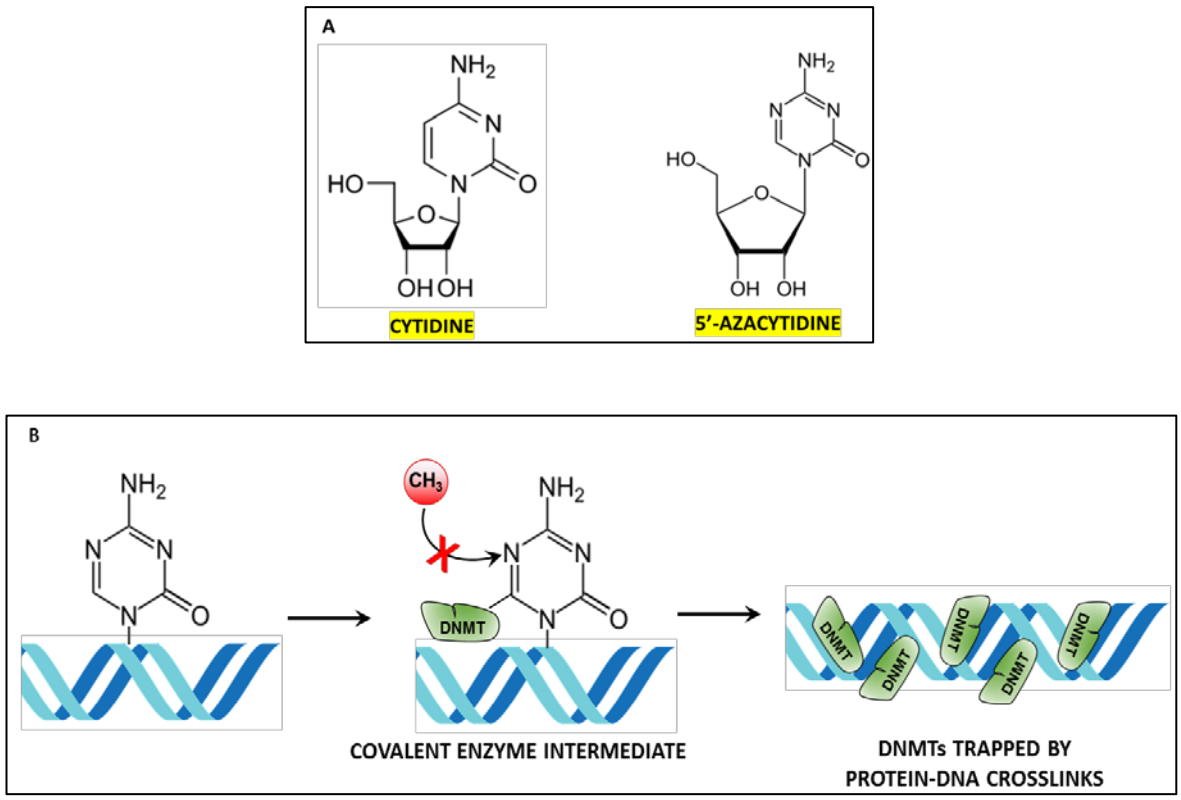

Figure 1. 4 Mode of action of AZA in demethylation

(A) AZA is a chemical analog of cytidine nucleoside. (B) AZA forms covalent links with DNMT, creating genome-wide protein-DNA crosslinks. This further results in the depletion of soluble methyltransferase levels within the cell in turn causing replication dependent global demethylation and reactivation of silenced/repressed genes. (Adapted from (Selvaraj et al., 2010; Silverman & Mufti, 2005).

During embryonic development, as cells differentiate and become more specialized, their early transcriptional plasticity and multilineage developmental potential is gradually restricted by epigenetic silencing of pluripotency associated genes (Hemberger et al., 2009). While cellular lineage restriction is unidirectional *in vivo*, epigenetic silencing can be overturned as demonstrated by somatic cell reprogramming. AZA, as an epigenetic modifier has been shown to increase the efficiency of somatic cell reprogramming to iPS cells (De Carvalho et al., 2010). Treatment with AZA renders previously non-inducible cell types responsive to reprogramming. (Blau et al., 1983). AZA induced DNA hypomethylation causes reactivation of imprinted genes in mouse embryonic fibroblasts (El Kharroubi et al., 2001). Treatment of partially reprogrammed cell lines with AZA or reduction of DNA methyltransferase expression by siRNA or shRNA induces a rapid and stable transition from partially to fully reprogrammed iPS cells (Mikkelsen et al., 2008). In another study, the pre-treatment of human foetal fibroblasts with AZA and a histone deacetylase inhibitor in conjunction with human embryonic stem cell extract has also been shown to improve the efficiency of somatic cell reprogramming (J. Han et al., 2010).

Multiple studies demonstrating the effects of AZA in cell-fate modification of one somatic cell to another have also been reported. Exposure of MSCs to AZA alters their *in vitro* multipotency possibly by changing their responsiveness to specific differentiating agents (Rosca & Burlacu, 2011). AZA is also a commonly used reagent to promote differentiation of adult stem cells such as bone marrow derived MSCs and endogenous cardiac progenitor cells into beating cardiomyocytes (Chong et al., 2011; Fukuda, 2002; Makino et al., 1999; Rajasingh et al., 2011). AZA-induced epigenetic reprogramming of endothelial progenitor cells confers improved plasticity and the ability to bring about

ischemic myocardial repair (Thal et al., 2012). Moreover, AZA has been shown to mediate transdifferentiation of human dermal fibroblasts into insulin producing islet-like cells (Katz et al., 2013) or to lead to re-expression of regulatory genes and thereby facilitate production of stable mesodermal lineages from fibroblasts *in vitro.* (Pennarossa et al., 2013). Enhanced cellular plasticity and transdifferentiation of AdMSCs into myoblast-like cells after treatment with AZA in an optimal myogenetic matrix has also been reported (Tan et al., 2015). A more recent report demonstrates the use of AZA in differentiation of human AdMSCs into cardiomyocytes when cultured within a fibrin scaffold (Bagheri-Hosseinabadi et al., 2018). AZA treated MSCs displayed *in vivo* plasticity into cardiomyocyte-like cells when transplanted into infarcted rat hearts (J. Y. Li et al., 2018). Additionally, MSCs show improved immunomodulation and migration potential following treatment with AZA (S. Lee et al., 2015). Collectively, AZA by itself or when used in conjunction with other factors can augment cell-fate changes in terminally differentiated cells by epigenetic modifications and subsequent regulation of cell-stage-specific gene expression.

1.7.2 The role of Platelet Derived Growth Factor (PDGF) in stem cell biology/regeneration

PDGF is one of the major growth factors in the human body and plays a significant role in cell growth and division. During early developmental stages, it acts as a mitogen and drives the proliferation and migration of undifferentiated MSCs and progenitor cells (Heldin, Wasteson, et al., 1985). While it is predominantly synthesized, stored, and secreted by activated platelets, other cells such as endothelial cells, smooth muscle cells and activated macrophages are also known to secrete PDGF.

The PDGF signaling system consists of four glycoprotein ligands namely PDGF-A, PDGF-B, PDGF-C and PDGF-D and two receptors namely PDGFRα and PDGFRβ (Figure 1.5A). All the ligands are inactive in their monomeric forms but are rendered functionally active on forming disulphide-linked dimers. Although all homodimeric forms of the ligands are functional, the only heterodimer that can activate the downstream signaling pathway is the one comprised of ligands PDGF-A and PDGF-B (Heldin & Westermark, 1990).The PDGF receptor is a tyrosine kinase cell surface receptor and exists as two distinct but structurally-related subtypes, namely PDGFRα and PDGFRβ (Demoulin & Essaghir, 2014). PGFR homodimer and/or heterodimer formation is a function of the PDGFR expression profile within a given cell population (Andrae et al., 2008). PDGF-AA, PDGF-BB, PDGF-AB and PDGF-CC dimers bind to PDGFRα whereas the PDGF-AB, PDGF-BB and PDGF-CC dimers have a comparatively greater affinity to bind to PDGFRβ. The PDGF ligands bind to the extracellular domain of PDGFR and leading to receptor dimerization (Figure 1.6A) (Seifert et al., 1989). Receptor dimerization triggers subsequent autophosphorylation of specific tyrosine residues present on the cytosolic domain of the receptor which in turn activates the PI3K/Akt and PI3K/PLC signaling pathway or ROS-mediated activation of the STAT3 pathway. The downstream effects of these pathways include regulation of gene expression, cell cycle regulation as well as cell migration and proliferation (Figure 1.5B) (Ball et al., 2007).

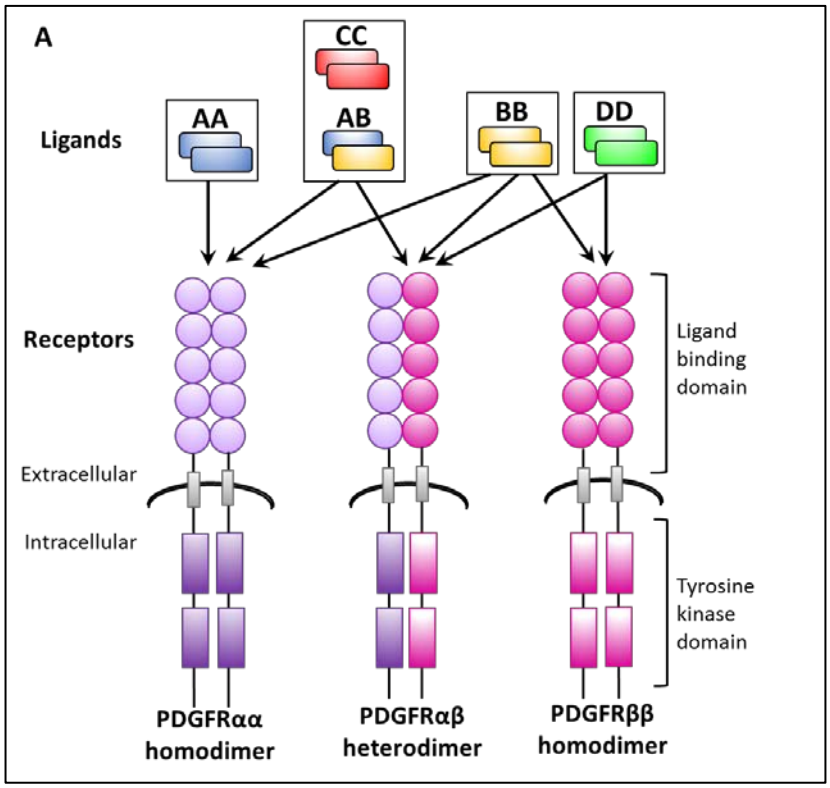
A
Ligands
CC
AA
AB
BB
DD
Receptors
Ligand binding domain
Extracellular
Intracellular
Tyrosine kinase domain
PDGFRαα homodimer
PDGFRαβ heterodimer
PDGFRββ homodimer

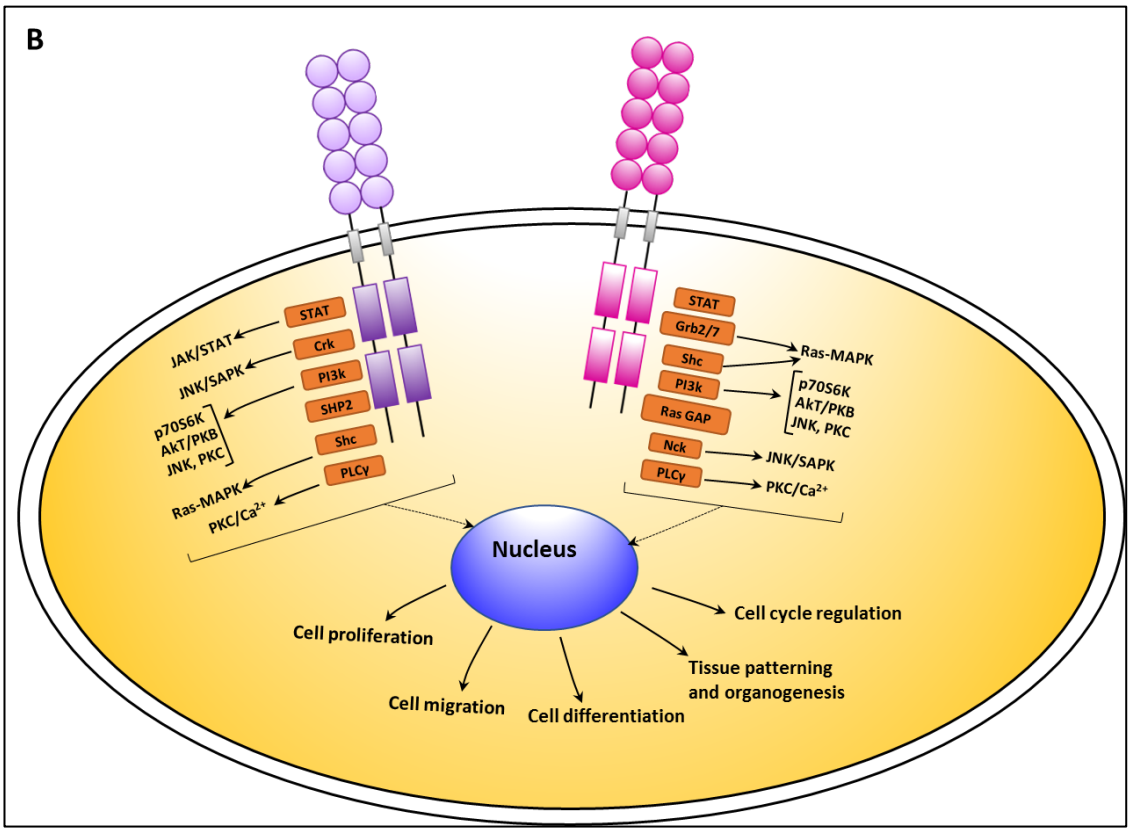
B
STAT
Crk
PI3k
SHP2
Shc
PLCγ
JAK/STAT
JNK/SAPK
p70S6K
AkT/PKB
JNK, PKC
Ras-MAPK
PKC/Ca2+
STAT
Grb2/7
Shc
PI3k
Ras GAP
Nck
PLCγ
Ras-MAPK
p70S6K
AkT/PKB
JNK, PKC
JNK/SAPK
PKC/Ca2+
Nucleus
Cell proliferation
Cell migration
Cell differentiation
Cell cycle regulation
Tissue patterning and organogenesis

Figure 1. 5 PDGF signaling system

(A) PDGF ligand dimers are represented by their constituent subunits, for example, AA is a PDGFA homodimer whereas AB is a heterodimer comprised of PDGFA and PDGFB. All PDGF receptors have an extracellular ligand binding domain comprised of five immunoglobulin rings and cytoplasmic tyrosine kinase binding domain. Arrows indicate binding interactions between ligands and receptors. (B) PDGF ligand binding causes receptor dimerization which in turn triggers autophosphorylation of tyrosine residues in the cytoplasmic domain. Subsequently, docking sites for signaling proteins and adaptors that initiate multiple downstream signal transduction pathways like Ras-MAPK (mitogen activated protein kinase), PI3K (phosphatidylinositol 3-kinase), PLCγ (phospholipase C γ). Together these pathways are involved in different cellular mechanisms including proliferation, migration, differentiation, cell cycle regulation as well as tissue patterning and homeostasis. Adapted from (Bergsten et al., 2001; Hoch & Soriano, 2003; Larochelle et al., 2001).

PDGFs are one of the growth factors that influence the self-renewal and differentiation abilities of MSCs (Leo & Grande, 2006). PDGFs exert their mitogenic effects on MSCs by permitting them to skip the G1 cell cycle checkpoint (G. Song et al., 2005). This in turn enhances the abilities of MSCs to proliferate and differentiate as well as encourages their homing, migration and engraftment to sites of tissue injury or neoplasia (Andrae et al., 2008; Hoch & Soriano, 2003). These effects are implemented by causing elevated expression of MSC-specific intracellular and cell-surface markers. For instance, MSCs exhibit higher CD44 expression and have improved adhesive and migratory abilities following stimulation with PDGF (Zhu et al., 2006). PDGF-BB, when supplemented with TGF-β and FGF, promotes the growth of pericytes in serum-free culture (Ng et al., 2008). MSCs have a high PDGFRα: PDGFRβ ratio and inhibition of the PDGFRα signaling negatively affects the self-renewal of MSCs in culture. Notably, MSCs treated with PDGFβ inhibitors display upregulated expression of the pluripotency associated genes Oct4 and Nanog and possess higher levels of multipotency (Ball et al., 2012). A study elucidating the response of MSCs to chemotactic stimuli has shown that PDGF-AB and IGF-1 serve as better chemoattractants for MSCs compared to other chemokines. Additionally, the sensitivity of MSCs to chemokines can be further improved with the use of inflammatory cytokines like TNF (Ponte et al., 2007).

From a therapeutic point of view, PDGFs have been demonstrated to play a role in tissue regeneration, wound healing and angiogenesis (Gehmert et al., 2011; Hutton et al., 2013; Raghavan et al., 2012). PDGF signaling is a potent inducer of fibroblast migration which is required for effective blastema (regenerative bud) formation during axolotl digit tip regeneration (Currie et al., 2016). PDGF-AA secreted by dedifferentiated schwann cell precursors within the wounded mammalian distal digit (amputated distal to

the nail bed) can also promote expansion of the blastema and subsequent digit regeneration (Johnston et al., 2016). In another report, a distinct transcriptional variant of Pdgfra generated by fibro-adipogenic progenitors, which codes for a protein isoform with a truncated kinase domain, has been shown to play a significant role in maintaining the balance between muscle regeneration and fibrosis (Mueller et al., 2016). Injury-induced secretion of PDGF-BB has been implicated in epicardial cell functions and coronary vessel formation during zebrafish heart regeneration (J. Kim et al., 2010). A recent study also reports the potential of PDGF-BB to enhance skeletal muscle regeneration through activation of satellite cell proliferation and migration, thereby exerting a protective role in muscular dystrophies (Pinol-Jurado et al., 2017). On the other hand, inhibition of PDGFR signaling, which causes inactivation of the Ras/MAPK pathway, has been shown to suppress cardiac regeneration in wild-type zebrafish (Missinato et al., 2018).

PDGFs facilitate bone regeneration by stimulating proliferation of BM-MSCs and driving their subsequent differentiation into osteoblasts via activation of the BMP-Smad1/5/8-Runx2/Osterix pathway (Caplan & Correa, 2011; A. Li et al., 2014). PDGFs in combination with other growth factors also improve healing capacity of the affected bone by chemotactic attraction and subsequent activation of macrophages which are required for clearance of cellular debris and damaged cells (Shah et al., 2014). PDGF along with other cytokines secreted by MSCs seeded on damaged cartilaginous endplates has also been shown to promote intervertebral disc regeneration through extracellular matrix remodelling (C. L. Pereira et al., 2016). In the context of tissue engineering, PDGF immobilized on nanofibers have also been shown to enhance proliferation and tenogenic[3] differentiation of AdMSCs in a gradient-dependent manner (Madhurakkat Perikamana et

[3] Tenogenic differentiation: Generation of tendon tissue/tenocytes

al., 2018) PDGFRβ-enriched MSCs exhibit enhanced chemotactic migration and engraftment in wound injury and promote angiogenesis as well as wound healing (Wang et al., 2018). Additionally, disruption of PDGFR or Fibronectin (an extracellular matrix molecule) causes the conversion of MSCs from spindle-shaped contractile cells to rounded E-cadherin-rich cells. These newly formed cells exhibit enhanced expression of markers which are characteristic of pluripotency, mesendoderm, and endoderm, and demonstrate angiogenic behaviour *in vivo*. This observation provides supporting evidence to the idea that MSCs can be effectively reprogrammed by stalling natural mesenchymal signals (Ball et al., 2014).

In summary, PDGFs play a significant role in facilitating tissue repair mechanisms. However, there have been very limited studies to date examining the effects of PDGFs in the induction of somatic cell reprogramming for safe and efficient generation of therapeutically relevant cell populations. Therefore, there is significant potential in harnessing the described mitogenic, chemotactic and angiogenic properties of the PDGF ligand. Given that the cell fate of somatic cells can be modified by exposure to exogenic factors, studying the combined effect of PDGF in combination with another pertinent epigenetic modifier i.e. AZA to induce reprogramming of primary human somatic cells will be the focus of this thesis.

1.8 Thesis objectives

Despite the advent of novel cell reprogramming techniques, there has been limited success in generation of an autologous, safe and efficient cell-based therapeutic alternative that possesses the advantages of pluripotent stem cells and MSCs but does not carry the risk of tumorigenicity. Additionally, it is important to ensure that tissue regeneration through transplanted cells does not occur at the cost of malignant transformation or host rejection. Any extrinsic attempt at tissue regeneration in the form of regenerative therapies therefore requires careful consideration to the basic biology of tissue development and organisation. Although multiple clinical studies employing MSCs for tissue repair have been documented, fundamental evidence on their primary, functional contribution to bring about *in vivo* tissue regeneration is limited.

Given its numerous merits (described earlier in **1.7**), DCi reprogramming has promise over current cell reprogramming approaches. Therefore, it is of value to understand whether the technique can be extended to human cells for generation of tissue regenerative multipotent stem cells. Therefore, the overall goal of this study is to adapt DCi reprogramming to transform human somatic cells into multipotent stem cells and explore their safety and efficacy at the *in vivo* level. Indeed, the outcome of these studies would form the backbone for future clinical studies in human subjects affected with acute or chronic tissue injuries.

1.8.1 Hypotheses

1. Primary human somatic cells can be converted to human induced multipotent stem (iMS) cells using a DCi reprogramming approach.

2. DCi reprogrammed human iMS cells can contribute directly to tissue repair and regeneration without undergoing malignant transformation or ectopic tissue formation.

1.8.2 Aims

The specific aims of this study are:

1. To apply and optimise the DCi reprogramming approach for conversion of primary human adipocytes into human iMS cells (Chapter 3).

2. To characterise the reprogrammed human iMS cells at the molecular level and evaluate their pluripotency *in vitro* (Chapter 4).

3. To evaluate *in vivo* safety and plasticity of human iMS cells in a generic tissue injury model (Chapter 5).

4. To investigate the tissue repair potential of human iMS cells in the context of a tissue-specific injury (Chapter 6).

CHAPTER 2 Materials and Methods

2.1 MATERIALS

2.1.1 Reagents

Reagent	Catalogue Number	Supplier
5'- Azacytidine	3842	Tocris Biosciences
Alizarin red	A3757	Sigma Aldrich
Alcian blue	A5268	Sigma Aldrich
Beta (β)-Glycerophosphate	G9891	Sigma Aldrich
Bovine Serum Albumin	A2153	Sigma Aldrich
Collagenase Type I	C2674	Sigma Aldrich
Crystal violet	C6158	Sigma Aldrich
DAPI	422801	BioLegend
D-Luciferin	122799	Perkin Elmer
Dimethyl sulfoxide (DMSO)	D2650	Sigma Aldrich
Dexamethasone	D4902	Sigma Aldrich
DNAse	79254	Qiagen
Donkey serum	D9663	Sigma Aldrich
Dulbecco's modified Eagle's medium (DMEM)	11995-065	Thermofisher Scientific
Dulbecco's modified Eagle's medium/ Ham's F-12 (DMEM/F-12)	D6421	Sigma Aldrich
Dulbecco's Phosphate Buffered Saline (PBS), calcium and magnesium free	14190250	Thermofisher Scientific
Abolute Ethanol (analytical grade)	AJA214	Univar
EDTA-Sodium salt	E5134-1kg	Sigma Aldrich
Foetal Calf Serum (FCS)	NZFBS-25	Scientifix
Formaldehyde	PIE28906	Thermofisher Scientific
Gelatin	G1890	Sigma Aldrich
Glycerol	M1753	Sigma Aldrich
HEPES	15630080	Thermofisher Scientific
Iso-butyl-3-methyl xanthine (IBMX)	I5879	Sigma Aldrich
Indomethacin	I7378	Sigma Aldrich
Insulin	I9278	Sigma Aldrich
Isopropyl alcohol	PT076	Univar
Insulin-transferrin-selenium (ITS)	I3146	Sigma Aldrich

Knockout Serum Replacement	10828028	Thermofisher Scientific
L-ascorbate-2-phosphate	A8960	Sigma Aldrich
L-glutamine	25030081	Thermofisher Scientific
Lipofectamine	11668-019	Life Technologies
Matrigel	356237	Corning
Methylcellulose	M7027	Sigma Aldrich
Non-Essential Amino Acid (NEAA)	11140050	Thermofisher Scientific
OCT	4583	Tissue-Tek
Oil Red 'O'	O1391	Sigma Aldrich
Oncostatin M	130-093-844	Miltenyi Biotec
Paraformaldehyde (16%)	15710	Electron Microscopy Sciences
Penicillin/Streptopmycin (P/S) (10,000 U/mL)	10378-016	Thermofisher Scientific
Poly-L-Lysine solution	P4832	Sigma Aldrich
ProLong Diamond anti-fade solution	P36961	Molecular Probes
Qiazol	79306	Qiagen
ROCK inhibitor	72302	Stem Cell Technologies
Sodium pyruvate	11360070	Sigma Aldrich
Streptomycin (5mg/mL)	15140	Thermofisher Scientific
Stem MACS Expansion Medium	130-104-182	Miltenyi Biotec
Trypan blue	T8154	Sigma Aldrich
TrypLE Express™	12604-013	Thermofisher Scientific
Trypsin-EDTA	15090-046	Life Technologies
Xylene	AJA576	Univar

2.1.2 Antibodies

2.1.2.1 Primary antibodies

Name	Dilution	Catalogue number	Supplier
Anti-STRO-1 antibody supernatant	1:50	-	From Prof. Stan Gronthos (Gronthos et al., 1999)
Anti-Myosin Heavy Chain (MHC)	1:50	621202	BioLegend
Anti-α smooth muscle actin (αSMA)-Cy3 conjugate	1:400	C6198	Sigma Aldrich

Anti-CD31	1:100	303102	BioLegend
Anti-PDGFRβ	1:100	136002	BioLegend
Anti-OCT4	1:50	653701	Australian Biosearch
Anti-SOX2	1:50	656102	Australian Biosearch
Anti-Nanog	1:50	674201	Australian Biosearch
Anti-SSEA4	1:50	330401	Australian Biosearch
Anti-GFP-Alexa fluor 488 conjugate	1:250	A21311	Molecular Probes
Anti-BMP2	1:100	sc-6895	Santacruz Biotechnology
Anti-SOX9	1:150	sc-17341	Santacruz Biotechnology
Anti-Lamin A/C	1:100	MA3-1000	ThermoFisher Scientific
Anti-Laminin	1:100	L9393	ThermoFisher Scientific
Anti-CD56	1:50	MA5-11563	ThermoFisher Scientific
Anti-Spectrin	1:60	NCL-SPEC1	Novacastra (Leica)

2.1.2.2 Secondary antibodies

Name	Dilution	Catalogue number	Supplier
Donkey anti-Mouse IgG Secondary antibody, Alexa Fluor 488 conjugate	1:300	A21202	ThermoFisher Scientific
Rabbit anti-Mouse IgG Secondary antibody, Alexa Fluor 555 conjugate	1:400	A21427	ThermoFisher Scientific
Donkey anti-Rabbit IgG Secondary antibody, Alexa Fluor 568 conjugate	1:300	A31572	ThermoFisher Scientific
Donkey anti-Mouse IgG Secondary antibody, Alexa Fluor 594 conjugate	1:400	A21203	ThermoFisher Scientific
Chicken anti-Mouse IgG Secondary antibody, Alexa Fluor 647 conjugate	1:400	A21463	ThermoFisher Scientific

2.1.3 Cytokines

Name	Catalogue number	Supplier
Fibroblast like Growth Factor 2 (FGF2)	130-093-839	Miltenyi Biotec
Vascular Endothelial Growth Factor A (VEGF-A)	493-MV	R&D Systems
Platelet Derived Growth Factor-AB (PDGF-AB)	130-103-442	Miltenyi Biotec
Platelet Derived Growth Factor-BB (PDGF-BB)	130-103-442	Miltenyi Biotec
Transforming Growth Factor-beta1 (TGF-β1)	130-095-067	Miltenyi Biotec
ROCK inhibitor	Y-27632	Stem Cell Technologies

2.1.4 Equipment

Equipment	Supplier
Centrifuges	Beckman Coulter Allegra, X-15R
Class II biological safety cabinet	Email Westinghouse, 1687-2340/612-2
Cryo freezing container, Mr Frosty	Thermofisher Scientific
Cryotome	Thermo Shandon
Cryovials	CRYO.S, 122263
Cell culture dishes, plates and flasks	Nunc
DNA/RNA LoBind collection tube	Eppendorf, 0030108051
EDTA Vacutainer	BD Biosciences
Fluorescent Activated Cell Sorter (FACS)	LSR Fortessa
Forceps, Scissors, Scalpels	Fine Science Tools
Freezers (4, -30 and -80 degrees)	Sanyo, Nuline
GentleMACS Octodissociator	Miltenyi Biotec
Glassware	Crown Boroglass
Glass slides (for immunostaining)	Millipore
Haemocytometer	Boeco
Incubators for cell culture	Sanyo, MCO-19A1C
Magnetic stirrer	IKA-CMAG-M57
Micropipettes	Gilson
Bright field microscope	Olympus, CKX41
Confocal microscope	Zeiss LSM 780
Mr Frosty™	Thermofisher Scientific, 35050-061
NanoDrop spectrophotometer	Thermofisher Scientific, ND-1000
IVIS Spectrum CT Imaging System	Perkin Elmer, 128201
Vacutainer Blood Collection tube	BD, 367954
Water Bath	Grant, GD100

2.1.5 Kits

Name	Catalogue number	Supplier
MSC Phenotyping kit, human	130-095-198	Miltenyi Biotec
StemMACS MSC Expansion kit XF	130-104-182	Miltenyi Biotec
NucleoBond® Xtra Midi kit	740410	Macherey-Nagel
RNeasy Mini Kit	74104	Qiagen

2.1.6 Buffers, Medium and Solutions

Name	Catalogue number	Supplier
Red cell lysis buffer	11814389001	Sigma
Alpha MEM	12571	Life Technologies
OptiMEM	31985-070	Life Technologies
DMEM-HG	11965092	Life Technologies
DMEM-LG	11885084	Life Technologies
DMEM-F12	D6421	Life Technologies
FCS	FBS-500S	Scientifix

2.1.7 Media composition

Name	Basal medium	Serum (FCS/Autologous /Allogenic)	Antibiotics	Other supplements
Complete MSC medium	Alpha MEM	20%	100 units/mL P/S	2mM L-Glutamine
Adipocyte Culture medium	DMEM – High Glucose	10%	100 units/mL P/S	2mM L-Glutamine
Serum-free MSC Expansion medium	Stem-MACS MSC Expansion kit	-	100 units/mL P/S	10% Xenofree supplement, 2mM L-Glutamine

2.1.8 Softwares

1. Live cell imaging, Fixed cells data analysis software: Fiji (Image J)
2. Flow cytometry data analysis: FlowJo X software version 4.0 (TreeStar, Oregon, USA).
3. Sequence Alignment: STAR version 2.5.0b.
4. Quantification of gene expression levels: Htseq version 0.9.
5. BLI Data analysis software: Living Image version 5.0.
6. Normalization of RNA Seq data: EdgeR: R statistical analysos software version 3.3.3.
7. Pathway analysis: Ingenuity Pathway Analysis Suite (IPA 12402621, Qiagen, Redwood city), Core Analysis tool.
8. Hierarchical clustering of gene expression data: Partek Genomics Suite version 6.6.
9. Inveon Micro CT data analysis software: Inveon Research Workplace [IRW], Siemens Medical Solutions, Knoxville, Tennessee.
10. Figure and Schematic making: Adobe Illustrator.
11. Graph plotting: Graph pad Prism 7.
12. Statistical Analysis: Microsoft Excel 2016.

2.1.9 Statistical Analysis

Data analysis was carried out using Microsoft Excel 2007 and GraphPad Prism version 7. Data points are reported as mean ± SD or mean ± SEM from at least three samples or as reported in figure legends. Statistical significance of $P \leq 0.05$ (*), $P \leq 0.005$ (**) or $P \leq 0.0005$ (***) was determined by one-tailed Student's T-test.

2.2 METHODS

2.2.1 Tissue Culture Techniques

2.2.1.1 Cell Culture conditions

All cell culture procedures were conducted in a confined sterile environment[4] using aseptic techniques in a Class II biological safety cabinet. Human cells cultured for expansion were maintained in Sanyo $C0_2$ incubators, at 37˚C, 5% CO_2 in a humidified environment. A Beckman Coulter Allegra, X-15R centrifuge was used for centrifugation of cell suspensions during expansions.

2.2.1.2 Trypsinization of adherent cells

TrypLE Express ™ was used to detach adherent cells from the surface of tissue culture flasks. Culture medium was aspirated, and cells were first washed once with pre-warmed PBS and then dissociated by treatment with 1mL of TrypLE Express™ for 5 minutes[5] at 37˚C to enable the enzymatic digestion of proteins which bound the cultured cells to the tissue culture flasks. Cells were dislodged by gentle tapping of the flask. The enzymatic activity was then neutralized by addition of 2mL of complete α-MEM medium supplemented with 20% FCS, 1% L-glutamine and 1% P/S. The cell suspension was then centrifuged at 300g for 5 minutes at 4˚C. The supernatant was aspirated, and the cell pellet resuspended in 1-2 mL of culture medium to produce a single cell suspension for subculturing or cryopreservation as required.

[4] All procedures carried out at room temperature referred to a standard air-conditioned PC2 laboratory with temperature at 20-25°C.
[5] Over incubation with trypsin can have adverse effects on cell recovery and viability.

2.2.1.3 Cryopreservation of cells

Cells were cryopreserved in complete α-MEM containing 20% FCS, 1% L-glutamine, 1% P/S and 10% (v/v) DMSO. Just prior to freezing, DMSO was added dropwise to a final concentration of 10% (v/v) to ˜1x10^6 cells resuspended in complete α-MEM in 2 mL pre-labelled cryovials. The cryovials were preserved in a Mr Frosty^{TM}, placed into a -80°C freezer overnight. The Mr Frosty^{TM} freezer allows gradual cooling of the cells at an optimum rate of 1°C per minute. The cryovials were subsequently transferred to the liquid nitrogen vapour phase tank for long term storage at -196°C.

2.2.1.4 Thawing of cryopreserved cells

Cryovials retrieved from liquid nitrogen (-196°C) were transported in dry ice and thawed in a 37°C water bath until a small core of ice remained. The thawed cell suspensions were transferred drop-wise into a 14 mL polypropylene tube containing 10mL of pre-warmed appropriate growth medium. The cells were centrifuged at 300g for 5 min at 4°C. To eliminate any residual DMSO, the cell pellets were washed twice in complete medium before being finally resuspended in 1-2 mL of appropriate growth medium and plated further as required.

2.2.1.5 Counting cells

Cell counts were determined using the Trypan Blue exclusion method. Harvested cells were resuspended in 1-2 mL of appropriate medium. 10 µL of this cell suspension was then mixed with an equal volume of 0.4% (w/v) Trypan blue dye (Sigma) and used for counting on the Neubauer's improved Haemocytometer. Trypan blue can only enter through the disrupted membranes of dead cells, staining them blue. Live cells are left unstained (Strober, 2001). To obtain an accurate cell count, at least 100 cells over four

squares of the haemocytometer were counted. The following equation was used to calculate cell density:

$$\text{Total cells/mL (Density)} = \frac{\text{Total cells counted x Dilution factor}}{\text{Number of squares counted}} \text{ x 10,000 cells/mL}$$

2.2.1.6 Primary adipocyte harvest and culture

All tissue specimens were obtained with informed consent and prior approval from the Prince of Wales Hospital Human Research & Ethics Committee (HREC 14/119) from patients undergoing surgery (microdiscectomy, spinal fusion or disc arthroplasty). All tissue processing was done using aseptic techniques in the sterile environment of a biosafety cabinet. 4-5 gm of subcutaneous fat was used for isolation of cells. The tissue was stored in normal saline supplemented with Penicillin/Streptomycin (P/S) antibiotics and processed as soon as possible post-harvest. The tissue specimen was rinsed in PBS then cleaned using scalpels and forceps to get rid of any blood, soft-connective or cauterized tissue and debris[6]. The cleaned tissue was then gently minced with scalpels in 1-2 mL of 0.2% Collagenase I (to aid the digestion process).

The homogenized tissue was transferred to a 50 mL container and 15 mL of 0.2% Collagenase I added before incubating at 37˚C with shaking at 60 rpm for 40 minutes to facilitate enzyme-mediated digestion. During incubation, the container was swirled intermittently to allow efficient exposure of the enzyme to the majority of the tissue. The

[6] Minimise the number of washes to reduce loss of source adipocytes.

digested tissue was filtered through a 40 µm strainer before being inactivated with 100% serum. The cell suspension was then spun at 300g for 5 min at 4˚C, which caused the suspension to separate into three distinct layers. Primary adipocytes were located in the upper layer, the stromal vascular fraction (SVF) which contains the adipose derived MSCs (AdMSCs) pelleted to the bottom, with buffer supernatant in between.

A differential plating method as described previously in Fernyhough et al. (2004) was used to obtain pure cultures of primary adipocytes and AdMSCs. One component of this involved seeding of the buoyant primary adipocytes in 35 mm dishes in adipocyte culture medium in a ceiling culture setup[7] . This arrangement allows the attachment of unilocular adipocytes to the cell culture dish surface over prolonged time in culture. Primary adipocytes cultured in this way were left undisturbed for 8-10 days before being subjected to DCi reprogramming.

The second component of the differential plating method is used for AdMSCs that can firmly adhere to the culture dish. The SVF pellet obtained after spinning the homogenized cell-suspension was seeded in complete MSC medium in T25 flasks for culturing AdMSCs. AdMSCs were washed 2 days following seeding to deplete dead and non-adherent cells. Fresh complete MSC medium[8] was added every 3-4 days until the cells reached 70% confluence following which they were routinely passaged at a density of 5000 cells per T25 flask.

[7] Covered in detail in Chapter 3.
[8] Complete MSC medium contained either with 20% FCS or autologous or allogenic human serum as per experimental requirements.

2.2.2 Demethylation Cytokine induced (DCi) reprogramming of primary adipocytes

2.2.2.1. Foetal calf serum-supplemented medium

Terminally differentiated unilocular adipocytes were subjected to DCi reprogramming in complete MSC medium supplemented with 10 µM AZA and 200ng/mL rhPDGF-AB for 2 days, then changed to complete MSC medium supplemented with 200ng/mL rhPDGF-AB as described in (Chandrakanthan et al., 2016). The medium was changed every 3-4 days. Cellular conversion was recorded by microscopic examination and live cell imaging during the course of reprogramming. After 25 days, the reprogrammed iMS cells were trypsinized and seeded at a density of 5000 cells per T25 flask and passaged as for AdMCS (section 2.2.1.6).

2.2.2.2. Autologous serum-supplemented medium

For some experiments, bovine serum in the medium was replaced with patient derived autologous serum. A maximum of 200 mL of patient blood was collected in EDTA vacutainers for serum separation at the time of tissue harvest. The vacutainers were then spun at 3500rpm for 10 mins at room temperature to allow separation of serum from the red cells. This serum was used in lieu of FCS at the same concentration of 20% and maintaining the dose of AZA at 10 µM and rhPDGF-AB at 200ng/mL.

2.2.3 Live cell imaging

Phase contrast images of live cells were captured using an IncuCyte microscope (Essen Bioscience) with 10x (0.25 NA) objective or a Nikon Ti-E microscope with a 20x objective (0.45 NA). Images were captured every 30mins for a period of 8 days starting

from Day 2 after exposure to the reprogramming factors. 12-bit images were acquired with a 1280x1024 pixel array and analysed using ImageJ.

2.2.4 *In vitro* expansion of reprogrammed cells

Reprogrammed iMS cells can be expanded *in vitro* owing to their ability to self-renew. To understand the optimal conditions for *in vitro* expansion, the cells were cultured in the following three conditions:

Condition 1	Condition 2	Condition 3
Stem MACS MSC Expansion medium	Complete MSC medium +/- autologous serum	Complete MSC medium +/- allogenic serum

Control AdMSCs and iMS cells cultured in the above-mentioned conditions were monitored for long term growth and the readings recorded as cumulative cell number, calculated at each passage. This experiment was done for three biological replicates or as mentioned in individual 'Results' sections.

2.2.5 *In vitro* characterization of reprogrammed cells

To evaluate the characteristics of reprogrammed iMS cells in comparison to control MSCs, the following *in vitro* characterization assays were undertaken.

2.2.5.1 Colony forming unit-fibroblast (CFU-F) assay

Under appropriate culture conditions, MSCs give rise to colonies of fibroblastoid cells. Each colony is derived from a single cell, termed as colony forming unit–fibroblast (CFU-F) (Friedenstein et al., 1970). A colony is defined as a group of adherent cells

clustered together. Control AdMSCs and iMS cells were seeded at densities of 200, 300 or 400 cells per 35 mm dish and cultured in complete MSC medium. Medium was changed the next day to deplete dead cells and subsequently every 3-4 days. The cells were seen to aggregate and form colonies after around 8 days in culture. At the end of 2 weeks, the cells were fixed in 4% PFA and washed twice in PBS for 15 minutes each. The cells were then stained with 0.5% (w/v) Crystal violet made in 80% ethanol for 30 minutes to 1 hour, depending on the density of colonies. Dishes were then washed, air dried, and scanned at 600dpi resolution.

MSCs are known to form micro (5-24 cells; <2mm), small (≥ 25 cells; 2-4mm) and large (>4mm) colonies, however Chandrakanthan et al. have shown that the serial replating ability in murine iMS cells is restricted to large colonies (Chandrakanthan et al., 2016). Individual large colonies were counted by visual examination under a phase contrast microscope. The dish with the highest number of distinguishable colonies was documented to have the optimal cell seeding density. This cell seeding density was then used in comparing the DCi reprogramming efficiency in different conditions or for comparing the CFU-F efficiency of different cell populations under study.

2.2.5.2 Long term growth curve

Control AdMSCs and iMS cells were cultured in expansion medium[9] to assess their ability to proliferate *in vitro* over an extended period of time. At 70% confluence, the cells were trypsinized and re-seeded at 5000 cells per T25 flask. When passaging, the

[5] Expansion medium was Stem MACS MSC expansion medium without any supplements for serum-free expansion or complete α-MEM supplemented either with 20% FCS or autologous or allogenic human serum as per experimental requirements.

total viable cell count was calculated as in **1.2.1.5** and the corresponding cumulative cell count was determined as follows:

$$\text{Cumulative cell count at } P_n = \frac{\text{Total cell count at } P_{(n-1)}}{\text{Seeding density x Cell count at } P_n}$$

A comparative analysis was done by plotting a graph of expansion time (in days) v/s common logarithm of cumulative cell count at each passage using Graph Pad Prism software.

2.2.5.3 *In vitro* differentiation

The *in vitro* plasticity of control Ad-MSCs and reprogrammed iMS cells was determined by inducing the cells to undergo differentiation into various cell types when cultured in a medium supplemented with the respective growth factors. The differentiation protocols were adapted from (Medvinsky et al., 2008). Prior to induction, early passage (P3) AdMSCs and iMS cells were seeded at $2x10^4$ cells/well in a 6-well plate and cultured in MSC medium until they reached confluence. During this period, medium was changed every 3-4 days.

2.2.5.3.1 Osteogenic differentiation

Well-adhered, confluent cells were switched to osteogenic medium containing Alpha MEM (Life Technologies), 10% FCS, 100 μg/mL penicillin and 250 ng/mL streptomycin, 200 mM L-Glutamine, 0.1 μM dexamethasone (Sigma-Aldrich), 10 mM β-glycerophosphate. (Sigma-Aldrich), 200 μM L-ascorbic acid 2-phosphate (Sigma-Aldrich) for 21 days. The cells were then fixed in 4% PFA and was stained for calcium

deposition and extracellular matrix with freshly prepared 1% NH_4^+ buffered (pH 4.1-4.3) Alizarin Red S solution to determine osteogenesis.

2.2.5.3.2 Adipogenic differentiation

Well-adhered, confluent cells were switched to DMEM-HG (Life Technologies, 11965092), containing 10% FCS, 100 µg/mL penicillin and 250 ng/mL streptomycin, 200 mM L-Glutamine and 0.5 mM methyl-3-isobutyl methylxantine (Sigma-Aldrich), 1 µM dexamethasone (Sigma-Aldrich), 6 µg/mL insulin (Sigma-Aldrich), 100 µM indomethacin (Sigma -Aldrich) for 7-10 days with medium changes every 3-4 days. Intracellular lipid droplets, which could be observed using light microscopy, were used to follow differentiation. The cells were then fixed in 4% PFA and stained with Oil Red O that stains lipid droplets to determine adipogenesis.

2.2.5.3.3 Chondrogenic differentiation

Well-adhered, confluent cells were cultured in serum-free DMEM-HG, 100 µg/mL penicillin and 250 ng/mL streptomycin, 200 mM L-Glutamine, 50 µg/mL insulin-transferrin selenium (ITS) acid mix (BD Biosciences), 0.2 mM L-ascorbic acid 2-phosphate (Sigma-Aldrich), 1mM sodium pyruvate, 0.1 µM dexamethasone (Sigma-Aldrich), 40 µg/mL Proline (Sigma-Aldrich) and 10 ng/mL transforming growth factor β3 (TGF-β3; R and D Systems), and the medium was changed every 4 days. After 28 days in culture, differentiated cells were stained for sulfated proteoglycans with 1% Alcian blue to determine chondrogenesis.

2.2.5.3.4 Endothelial differentiation

Cells were cultured in MSC medium on chambered glass slides pre-coated with 0.1% gelatin. Once confluent, the cells were induced with DMEM-LG (Life Technologies, 11885084) supplemented with 2% FCS, 100 μg/mL penicillin, 250 ng/mL streptomycin, 200 mM L-Glutamine, 10ng/mL Vascular Endothelial Growth Factor (VEGF) and 10^{-8}M dexamethasone, with medium changes every 3-4 days. After 14 days, cells were fixed in 4% PFA and immunostained for CD31, Platelet derived growth factor receptor β (PDGFRβ) and nuclear stain DAPI as detailed below in **2.2.5.3.1.**

2.2.5.3.5 Myogenic (Smooth muscle) differentiation

Cells were cultured in MSC medium on chambered glass slides pre-coated with 0.1% gelatin. Once confluent, the cells were induced with DMEM-HG supplemented with 5% FCS, 100 μg/mL penicillin, 250 ng/mL streptomycin, 200 mM L-Glutamine and 50 ng/mL recombinant human platelet derived growth factor BB (rhPDGF-BB) (Miltenyi Biotec), with medium changes every 3-4 days. After 14 days, cells were fixed in 4% PFA and immunostained for smooth muscle myosin heavy chain (MYH1), alpha-smooth muscle actin (α-SMA) and nuclear stain DAPI as detailed in **2.2.5.3.1.**

2.2.5.3.5 Immunocytochemistry for validation of differentiation

At the end of differentiation, cells were washed with PBS (Invitrogen) for 10 minutes. The cells were then fixed with 4% PFA (v/v) (ProsciTec) in PBS for 15-20 minutes and then permeabilized with 0.2% Tween-20 (v/v) in PBS for 15 minutes at room temperature (RT). The cells were washed once with PBS and then blocked with 10%

donkey serum (v/v) in PBS for 1hr at RT to minimise non-specific antibody binding. Blocked cells were incubated overnight at 4°C with primary antibodies diluted in 2% bovine serum albumin (BSA) (w/v) in PBS, washed, then stained with secondary antibodies in 2% BSA for one hour at 4°C. Nuclear staining was done with DAPI for 10-15 minutes at RT. Slides were mounted with Prolong-diamond mounting medium (Invitrogen). Images were taken using a L780 LSM Zeiss confocal microscope.

2.2.5.4 Immunophenotyping

The identity of reprogrammed cells was analysed based on cell-surface marker expression using an MSC phenotyping kit (Miltenyi Biotec). According to the International Society for Cellular Therapy (ISCT) guidelines, for cells to be deemed as MSCs they should have high expression of the cell surface markers CD73, CD90 and CD105 while lacking any expression of CD14 and the hematopoietic markers CD34 and CD45 (Dominici et al., 2006). Cells at P1/P2, cultured in complete MSC medium were used for phenotyping. Cells were first trypsinized and harvested as detailed in **1.2.1.2.** The cells were then labelled according to the manufacturer's instructions and assessed by Flow cytometry for expression of cell surface markers. Flow analysis was performed using a LSR Fortessa X20 cell analyser with FacsDiva^{TM} software (BD Biosciences, version 6.1.3). Compensation was adjusted manually using cells stained with single fluorophores. Isotype stained control was used to set the gates. Compensated data was exported for analysis using Flowjo software (Tree Star Inc., version 10.0.7).

Table 2. 1 Fluorophores used for detection of cell-surface markers

Cell surface marker tested	Conjugated fluorophore	Channel used for analysis
CD73	Allophycocyanin (APC)	670_14
CD90	Fluorescein Isothiocyanate (FITC)	530_30
CD105	Phycoerythrin (PE)	582_15
CD34/45	Peridinin Chlorophyll Protein (Per-CP)	710_50

2.2.5.5 Karyotyping

Untreated and AZA/rhPDGF-AB treated AdMSCs and corresponding iMS cells were obtained as described in sections **2.2.1.6**. and **2.2.2.2.** and were expanded *in vitro* as described in **2.2.4.** in medium supplemented with autologous serum. P0, P3 and P5 of all the three cell-types from three age-matched patients were sent for conventional pangenomic G-banded karyotyping to Cytolabs, WA, Australia.

2.2.6 Immunocytochemistry for pluripotency markers

Expression of pluripotency-associated markers in cultured cells was evaluated as described in (Briggs et al., 2013). Briefly, C2 iPS cell colonies grown in conditioned medium for 3 days were washed with PBS for 10 mins and fixed in 4% PFA (v/v) (ProsciTec) in PBS for 20 mins at RT. The cells were washed twice with PBS for 15 minutes each time, covered in PBS and stored at 4°C until stained.

Day 1: Fixed cells were permeabilized in 0.02% Tween-20 in PBS for 30 minutes at RT then blocked for 1 hour with 10% donkey serum (v/v) in 2%BSA/ 0.02% NaN_3, then incubated at 4°C overnight in the dark with primary antibodies (against OCT4, NANOG, SOX2 and SSEA-4) diluted in 2% BSA/0.02%NaN_3 (Refer Table **2.1.2** for exact dilutions and catalogue numbers of antibodies used).

Day 2: After washing, cells were stained with species and isotype matched Alexa-Fluor conjugated secondary antibodies (1:400, Invitrogen) for 1–2 hours at 4°C. Nuclei were stained with Hoechst or 4, 6-diamidino-2-phenylindole (DAPI) (1:500, Sigma-Aldrich) for 20 minutes, and the slides were mounted with Prolong Diamond anti-fade mounting medium (Invitrogen and was to cure overnight.

Day 3: The slides were imaged on Carl Zeiss LSM L780 confocal microscope using a 20X/0.8NA objective.

2.2.7 *In vitro* teratoma assay

To evaluate the multilineage plasticity of human iMS cells, a novel *in vitro* assay mimicking the *in vivo* soft tissue environment was set up as described in (Whitworth, Frith, et al., 2014; Whitworth, Ovchinnikov, et al., 2014).

2.2.7.1 Assay setup

Day 1:

I. Coating: Pre-cooled Corning costar ultra-low attachment multiwell 24 well plates™ were layered with 2-3 mm of 9.5% methylcellulose prepared in KSR medium. The plates were placed in a standard incubator for 2 hours to allow gelling of the methylcellulose.

II. Cell seeding: GFP-tagged cells (AdMSCs, treated AdMSCs and human iMS cells) and C2 iPS cells in culture were harvested, reconstituted in injection buffer and counted. In each well, a total of $2.5x10^6$ cells were seeded with 20% matrigel and 10 µM ROCK inhibitor (RI). The plates were spun at 350g for 5 minutes at 20 degrees and 500 uL of medium (KSR+RI) was added in each well to prevent cell apoptosis. The plates were then incubated at 37°C overnight to allow aggregation of spin Embryoid Bodies (EBs).

Day 2:

Medium top-up: The cells were supplemented with 400 µL KSR medium (without RI)/well and incubated at 37°C overnight for further settling of the cells.

Day 3:

Medium change: The medium was replaced with fresh 600 µL KSR medium/well and cells incubated at 37°C overnight.

Day 4:

Methylcellulose re-layering: Medium from each of the wells was discarded, ensuring no traces of liquid were left behind. Cells in each well were then overlayed with 2-3mm thick 9.5% methylcellulose. The plates were placed in a standard incubator for at least an hour to allow gelling[10] of the methylcellulose before being topped with 600 µL KSR medium/well.

2.2.7.2 Assay maintenance

The cells were maintained for a total of 8 weeks with medium changes every alternate day (500 µL KSR medium/well).

2.2.7.3 Endpoint studies

On completion of the assay, individual EBs were harvested and any traces of methylcellulose were washed off with PBS followed by fixation in 4% PFA for 30 mins. The fixed EBs were then embedded in OCT or paraffin and sectioned in 20 µm slices, with 3-4 sections mounted per slide. The sections were then used for IF staining and confocal imaging.

2.2.7.3.1 IF staining and confocal imaging of cryosections

For immunostaining, frozen slides were rehydrated in PBS for 30 mins at RT. Samples were permeabilized in 0.02% Tween-20 (v/v) in PBS for 15 mins and then blocked with 10% donkey serum in PBS for 60 mins at RT. Primary antibodies were diluted in 2% BSA in PBS and slides were incubated at 4°C overnight. On the following day, stained slides were washed with PBS and then incubated with diluted secondary

[10] A pipette tip or fine needle can be used to confirm gelling.

antibodies in 2% BSA in PBS for 60 mins (please refer to **Table 2.1.2**. for the specific dilutions of each antibody). Slides were washed twice with PBS and nuclei were stained with 1:500 diluted DAPI in PBS. Stained slides were mounted in ProLong Diamond anti-fade solution™ and the slides were left to cure overnight in dark at RT. On the following day, coverslip edges were sealed with a transparent nail polish and confocal images were taken using Carl Zeiss LSM 780 under a 20X/0.8NA magnification air objective.

2.2.8 Sequencing/Transcriptomics

2.2.8.1 RNA extraction

For expression analysis, mRNA was extracted using the RNeasy Mini kit (Qiagen, 217004) according to manufacturer's instructions. Briefly, harvested cells were washed twice in PBS, lysed in 700 µL lysis buffer (supplied) with 143 mM β-mercaptoethanol and vortexed for 1 min. Lysates were stored at -80°C prior to RNA extraction. For extraction, all centrifugation occurred at 10000 g at room temperature. Lysate was mixed with 350 µL chloroform (Sigma, 288306) and loaded onto the RNeasy spin columns with a 2 mL collection tube and centrifuged for 15 secs. Columns were washed with 350 µL wash buffer (supplied) and centrifuged for 15 secs then incubated with 30 Kunitz units[11] of DNase (Qiagen, 79254) for 15 min at room temperature, followed by the addition of 350 µL wash buffer and 15 secs centrifugation. Columns were washed twice with 500 µL ethanol buffer (supplied) with a 15 sec and a 2 min centrifugation, respectively. RNA was eluted with 30 µL RNase-free water and centrifuged for 1 min into DNA/RNA LoBind

[11] One Kunitz unit is defined as the amount of DNase I that causes an increase in A_{260} of 0.001 per minute per mL at 25°C, pH 5.0, with highly polymerised DNA as the substrate (Kunitz, 1950).

collection tubes (Eppendorf, 0030108051) and the quality and quantity were assessed using a Nanodrop spectrophotometer. Measurements are documented in **Table S1**.

2.2.8.2 Sequence alignment and expression quantification

TruSeq cDNA libraries were generated from 200ng total input RNA using Illumina's simplified sample prep kit by Novogene Bioinformatics Technology Co. Ltd. (Tianjin, China) following manufacturer's instructions. Briefly, mRNA is first purified using polyA selection from total RNA, then chemically fragmented and converted into single-stranded cDNA using random hexamer priming. The second strand is then generated to create double-stranded cDNA. For TruSeq library construction, blunt-end DNA fragments are generated from double-stranded cDNA using a combination of fill-in reactions and exonuclease activity. An 'A'-base is then added to the blunt ends of each strand, preparing them for ligation to the sequencing adaptors. Each adapter contains a 'T'-base overhang on 3'-end providing a complementary overhang for ligating the adapter to the 'A'-tailed fragmented DNA. The final products are sequenced on the HiSeqXten analyser by Novogene Bioinformatics Technology CO. Ltd. (Tianjin, China) using standard protocol.

The sequencing reads were aligned to the human genome assembly hg19 using the software package STAR 2.5.0b with standard parameters (Dobin et al., 2013). The numbers of total and mapped reads for each dataset are listed in **Table S2**. Gene expression levels were quantified using htseq v0.9 (Anders et al., 2015) and normalised using the software package EdgeR in the R statistical analysis software v3.3.3 (Mccarthy et al., 2012; Robinson et al., 2010).

2.2.8.3 Principal Component Analysis (PCA)

Genome-wide expression profiles were analysed using principle component analysis (PCA) (Diffner et al., 2013; Ringner, 2008). The PCA algorithm is a dimension reduction technique that identifies directions (called principle components) along which gene expression measures are most variant. The principle components are linear combinations of the original gene expression measures and allow to visualise genome-wide expression profiles in two or more dimensions.

2.2.8.4 Pathway Analysis

The list of significantly differentially expressed genes across the 'primary adipocytes v/s iMS cells' comparison was first filtered for transcriptional regulators. The core analysis tool within the Ingenuity® Pathway Analysis suite (IPA® version 12402621, QIAGEN Redwood City, www.qiagen.com/ingenuity) was used to identify pathways that are significantly overrepresented. Enriched pathways were identified with corrected p-values using the built-in analysis.

2.2.8.5. Heatmaps

Hierarchical clustering with average linkage and Euclidean distance was performed in Partek Genomics Suite 6.6.

2.2.9 Lentiviral transduction

2.2.9.1 Bacterial transformation of plasmid DNA

Plasmids for lentivirus generation were propagated in STBL2 bacterial cells (Invitrogen) according to the manufacturer's directions.

2.2.9.2 Plasmid DNA extraction and quantification

Lentiviral plasmids in STBL2 bacteria were grown overnight in Terrific broth (Invitrogen) at 30ºC. Plasmid DNA was isolated using a NucleoBond® Xtra Midi kit (Machery-Nagel, 740410) according to the manufacturer's instructions. Plasmid DNA was quantified using a Nanodrop spectrophotometer.

2.2.9.3 Lentivirus mediated tagging of cells

The replication incompetent lentiviruses (Naldini et al. 1996) used in this project are derived from Human Immmunodeficiency Virus (HIV). All lentiviral work was carried out with approval from the UNSW Gene Technology Research Committee (NLRD 13-25). HEK293T cells were used to package replication incompetent lentiviral particles to facilitate stable expression of GFP and luciferase in target. A day prior to transfection, HEK293T cells were seeded at 1.5 x 10^6 cells per T25 flask. The leGO-iG2-luc2 lentiviral vector and packaging plasmids were added together in the amounts described in Table 2.2 to OptiMEM to give a final volume of 500 µL and incubated at RT for 5 mins.

Meanwhile, Lipofectamine 2000 reagent (Life technologies,) was diluted with Opti-MEM (12 µL Lipofectamine 2000/488 µL Opti-MEM). This was followed by a gentle drop-wise addition of the DNA to the Lipofectamine-Opti-MEM mix for a 20-

minute room temperature incubation to allow formation of the lipid-DNA complexes. As a negative control, a mock condition without the plasmids was also included.

Culture medium were removed from pre-seeded HEK293T cells and replaced with 4 mL Opti-MEM containing 10% FBS and antibiotics. The DNA/Lipofectamine transfection mix was then added to the cells drop-wise, and the flask rocked back and forth to ensure even coverage. The cells were incubated overnight (<16 hr) in a 5% CO_2 humidified tissue culture incubator at 37°C. The transfection mix was replaced with fresh DMEM with 10% FBS on the following morning to allow cells to recover and changed in the evening to 5 mL of the complete α-MEM with 20% cells for transduction of target cells on the following day.

Post overnight incubation, 90-100% producer HEK293T cells were positive for GFP expression. The virus conditioned medium (VCM) was collected from the producer 293T cells and was replaced with 5 mL DMEM with 10% FBS and antibiotics, before returning the cells back to the incubator for a second viral harvest the following day. The collected VCM was centrifuged at 1200 rpm for 7 mins at 4^{o}C then filtered through a 0.45 um low protein binding polyvinylidene fluoride (PVDF) and stored on ice until needed.

Table 2. 2 Description of plasmids used for lentiviral transfection

Plasmid	Description	Amount (in µg)	Reference
KGP. 1R (gag/pol)	Form the viral core structure, RNA genome binding proteins and nucleoprotein core complex	6	(Hanawa et al., 2005)
RT (rev)	Encodes for the reverse transcriptase enzyme	2	(Hanawa et al., 2002)
VSV-G (env)	Encodes for the envelope proteins	2	(Hanawa et al., 2002)
pLeGO-iG2-Luc2	Lentiviral plasmid expressing luciferase and GFP	10	(Weber et al., 2008)

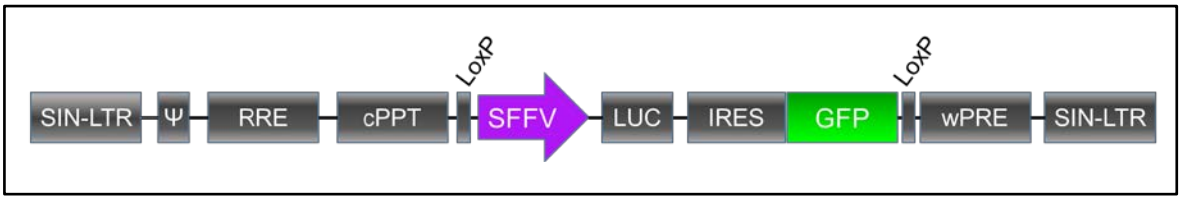

Figure 2. 1. Schematic of the lentiviral construct containing LUC and GFP

A HIV-1 based lentiviral vector carrying the transgene encoding for firefly luciferase (LUC) and GFP. An internal ribosome entry site (IRES) sequence allows GFP and LUC to be transcribed under the control of spleen focus-forming virus (SFFV) promoter/enhancer.

2.2.9.3.1 Transduction

Target cells seeded in T25 flasks were used for transduction. For efficient lentiviral transduction, it is recommended that the target cells (AdMSCs/treated AdMSCs/iMS cells in this case) be 75-80% confluent. Immediately prior to transduction, polybrene was added to the filtered VCM (described above) at a final concentration of 8µg/mL. Medium was aspirated from flasks seeded with the target cells and 4.5 mL of the VCM/Polybrene mix was added to each flask[12]. The cells were incubated overnight at 37˚C in a 5% CO_2 incubator to allow viral uptake by the target cells. A second round of transduction was performed on the following day.

After each round of transduction (and before the PBS washes), an aliquot of the medium supernatant was also collected to later check for presence of replication competent virus. On the morning following second round of transduction, cells were washed thrice in PBS and harvested. They were then counted and replated at 20,000 cells/T75 flask in complete α-MEM for additional expansion. Medium was changed every 3-4 days until the cells were ready to be passaged on reaching 70-80% confluence. After expansion, cells were harvested and counted, and transduction efficiency was assessed by flow cytometry analysis of GFP expression.

[12] A small aliquot (0.5 mL) of the VCM used for each round of transduction was stored to be used later to transfect HEK293T cells (positive control for the replication competence test).

2.2.9.4 Validation of transduction

Flow cytometry was used for the simultaneous multiparametric analysis of cells, including cell size and granularity and GFP expression. Cells were centrifuged at 300g for 5 mins at 4°C. The obtained cell pellet was resuspended in a minimum of 200 μL cold FACS fixative (2%FCS, 1% formaldehyde made in PBS) and stored at 4°C for at least 16 hours prior to acquisition. Data from cells were acquired on the LSR Fortessa™ flow cytometry system (BD Biosciences) at the flow cytometry facility in UNSW's Biological Resources Imaging Laboratory (BRIL) using FacsDiva™ software (BD Biosciences, version 6.1.3) for 10000 – 30000 events/sample. The acquired data was then analysed using Flowjo software (Tree Star Inc., version 10.0.7).

To ensure the transduced cells were devoid of any replication competent virus, the medium supernatant collected from these cells (described in **2.2.8.3.1**) was tested for viral particles able to infect HEK293T cells. Aliquots of VCM were used as positive controls. Untransduced HEK293T cells served as negative controls. HEK293T cells transfected with medium supernatant collected from target cells were negative for GFP expression. This confirmed the absence of replication competent virus within the transduced cells (Figure 2.2). Target cells that were negative for replication competent lentivirus and ≥90% GFP positive were used for subsequent experiments.

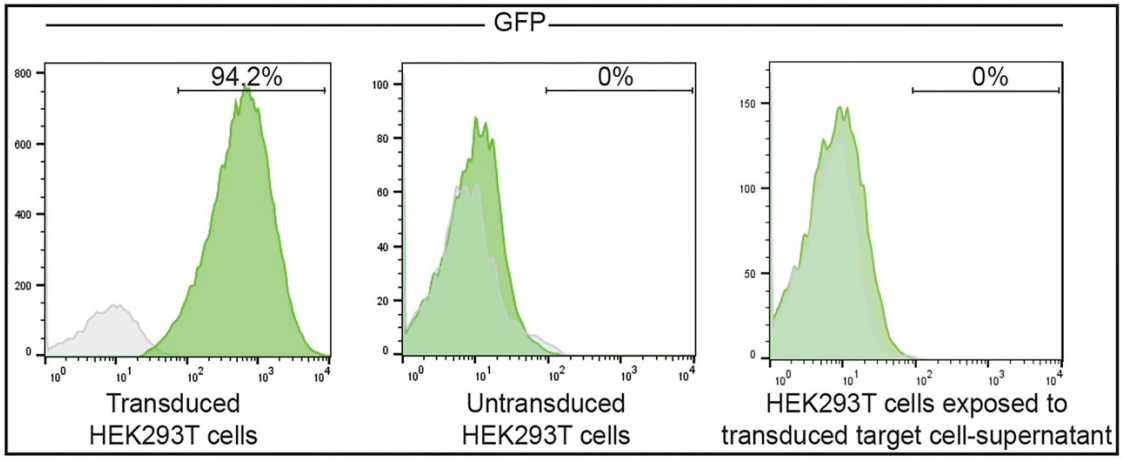

Figure 2. 2 Determination of replication competent virus in transduced target cell - supernatant.

Representative flow cytometry histograms showing HEK293T cells transduced with live virus with positive GFP expression whereas the untransduced HEK293T cells and HEK293T cells exposed to supernatant from transduced target cells with absence in GFP expression.

2.2.10 Postero-lateral inter-lumbar vertebral injury model

2.2.10.1 Animal details

3-4-month-old female NSG mice (Jackson Laboratories, Strain 005557) were used for the study. These mice carry two mutations i.e. severe combined immunodeficiency and a complete null allele of the Interleukin 2 (IL2) receptor common gamma chain, rendering them deficient in B, T and Natural Killer (NK) cells. All animals were purchased from Australian BioResources (ABR, Sydney) and housed in the Biological Resource Centre at the Lowy Cancer Research Centre, University of New South Wales (UNSW). Mice were fed *ab libitum* and housed in adherence to institutional guidelines and all experiments were approved by the University of New South Wales Animal Care & Ethics Committee (ACEC number :15/131A).

2.2.10.2 Study design and surgery details

Primary adipocytes were isolated from patient-derived subcutaneous fat as described in **2.2.1.6.** and were subjected to DCi reprogramming in autologous serum supplemented medium as described in **2.2.2.B.** The reprogrammed iMS cells, control AdMSCs and treated AdMSCs were subjected to lentiviral LeGO iG2-luc2 transduction as described in **2.2.9.3.** GFP tagged cells were expanded *in vitro* to achieve the cell number required for transplantation, as described in **2.2.7.**

A day prior to transplantation, the cells were harvested and counted. $1x10^6$ cells in up to 30 µL were seeded onto 1mm x 1mm collagen sponges. The sponges were placed into an ultra-low adherent 6 well plate and 1 mL of MSC medium was added to each of the wells and incubated overnight at 37˚C. On the day of surgery, cell-embedded sponges

were bilaterally implanted into the posterior-lateral lumbar spine region (L4-L5) in recipient mice. The study groups are shown in **Table 2.2.3.**

All cell transplants were performed by a single orthopaedic surgeon (Prof. Bill Walsh, Surgical and Orthopaedic Research Lab, Sydney, Australia). Animals were anesthetized using isoflurane (5% for induction, 2-3% for maintenance), then posterior midline incisions were made over the caudal portion of the lumbar spine and two separate fascial incisions were made 4 mm bilaterally from the midline. A blunt muscle splitting technique was used lateral to the facet joints to expose the transverse processes of L4 and L5 lumbar spines. The processes were then decorticated using a scalpel. Next, collagen sponges embedded with cells were implanted between the transverse processes bilaterally into the para-spinal muscle bed. Finally, the fasciae and skin were each closed using a simple continuous technique with Ligaclip Multiple Clip Applier (Ethicon) and betadine was applied at the suture site to prevent any infections. Post-surgery, the mice were monitored every day for a week and then three times a week until endpoint. In instances of delayed wound closure, the incisions were re-clipped.

Table 2. 3 Study groups for postero-lateral inter-lumbar vertebral injury study

Endpoint	Group I (AdMSCs)	Group II (treated AdMSCs)	Group III (iMS cells)	Group IV (Sham-sponges only, no cells)
Total number of animals	8	8	8	6
3 months	2	2	2	2
6 months	3	3	3	2
1 year	3	3	3	2

2.2.10.3 Bioluminescence imaging (BLI)

In vivo detection of luciferase expressing cells was done by non-invasive BLI. The mice were periodically imaged for bioluminescence on the IVIS Spectrum CT (Perkin Elmer) using the Living Image 5.0 acquisition software (Perkin Elmer) on days 1, 3, 7 and 14, and then every second week. On the day of scan, mice were weighed and were intraperitoneally injected with 150mg/kg of D-luciferin (15mg/ mL reconstituted in PBS) before being anaesthetized. The mice were then imaged on the IVIS Spectrum CT imaging station with 'Auto' settings for a total of 30 mins post luciferin injection. During sequential scans, the animals are checked at regular intervals for any signs of discomfort. Luciferase-expressing cells (those transfected with LeGO-iG2-luc2) metabolize the substrate luciferin in an ATP-dependent mechanism, thereby producing luminescence, the average intensity of which is recorded in photons/sec/cm^2/sr, during the scans. The scanned images are then analysed using the Living Image 5.0 software to evaluate changes in signal intensity which is a direct function of the number of luciferase-expressing cells present in the animal.

2.2.10.4 Endpoint studies

2.2.10.4.1 Micro-CT: On reaching the defined endpoint, mice were euthanized humanely by CO_2 inhalation[13]. The spine-allograft complex including the pelvis was then harvested from the thoracic to caudal vertebral region; care was taken not to disturb the transplant site. The lumbar spine-allograft complex was scanned using Micro-CT (Siemens Inveon Micro-CT System, Siemens Medical Solutions, Erlangen, Germany). Image analysis software (Inveon Research Workplace (IRW), Siemens Medical

[13] For euthanasia, cervical dislocation was not used in order to alleviate chances of disturbing the spine near the transplantation site.

Solutions, Knoxville, Tennessee) was used for reconstruction, visualization and analysis of the spinal fusion.

2.2.10.4.2 Tissue fixation, cryo-sectioning, IF staining and imaging: The spine specimens were fixed in 4% PFA for 48 hours. Fixed tissues were washed twice in PBS and then dehydrated in two steps, firstly in a 7% sucrose solution followed by 15% sucrose solution overnight at 4ºC. Dehydrated tissues were washed in PBS for 48 hrs at RT, with fresh PBS added every 12 hrs. The tissues were subsequently decalcified in 17% Na-EDTA for 48 hrs at RT. The tissues were then embedded in paraffin or OCT compound (Tissue-Tek) and transferred into cryo-moulds. OCT embedded sections were snap frozen on dry ice and stored at -80°C. The samples were sent to Biospecimen Preparation Laboratory at UNSW for sectioning on cryotome at a thickness of 30µm, with one section per slide. The sectioned slides were stored at -80°C and retrieved as required for immunofluorescence and histology analysis. Frozen tissue sections were used for IF staining with antibodies against pan-laminin, hlamin A/C, hCD56, hSpectrin and nuclear stain DAPI followed by confocal imaging as described earlier in **2.2.7.3.1**.

2.2.10.4.3 Image analysis: The total number of transplanted cells (GFP positive cells) in the host tissue were quantified using NIH Image J software. The images were filtered and adjusted for threshold and were used for manual counting of the total number of GFP positive donor cells incorporated within host tissues. Three to five serial sections were analysed per spine specimen for each of the 5 biological replicates. The proportion of transplanted cells integrated with the host tissues was expressed as percentage of double-positive (GFP and lineage specific marker) cells in the total number of cells expressing the lineage specific marker alone.

2.2.11 Muscle injury study

2.2.11.1 Animal details

Three to four-month-old female SCID/Beige mice (Charles River Laboratories, Strain code:250) were used for this study. All animals were obtained from Prof. Maria Kavallaris, Children's Cancer Institute Australia, UNSW and were housed in the Biological Resource Centre at the Lowy Cancer Research Centre, University of New South Wales (UNSW). Mice were fed and housed in adherence with institutional guidelines and all experiments were approved by the University of New South Wales Animal Care & Ethics Committee (ACEC number :17/30B).

2.2.11.2 Tissue injury and cell transplantation

Mice were anesthetized with isoflurane inhalation and placed in a prone position. The left Tibialis Anterior (TA) muscle region was sterilized with 70% ethanol and shaved using a disposable scalpel. Approximately 70 µL of cardiotoxin (10 µM) was injected into the TA muscle using a 31G needle. The needle was inserted at a shallow angle to the belly of the TA muscle and was withdrawn as the toxin was dispensed to ensure diffuse muscular injury. On the following day, *in vitro* expanded cells (as per study groups indicated in **Table 2.4**) in 70 µL of 50% matrigel in PBS were injected directly into these pre-injured muscles. The contralateral TA muscle served as an uninjured control.

Table 2. 4 Study groups for skeletal muscle regeneration study

Endpoint	Group I (AdMSCs)	Group II (treated AdMSCs)	Group III (iMS cells)	Group IV (Sham-vehicle only, no cells)
Total number of animals	5	5	5	4
1 week	1	1	1	1
2 weeks	2	2	2	1
4 weeks	2	2	2	2

2.2.11.3 Endpoint studies

On reaching the study endpoints of 1, 2 or 4 weeks, animals from each group were euthanized by cervical dislocation and their TA muscles were harvested. The animal was then placed in prone position and the skin around the TA muscle regions was sterilized with 70% ethanol. Using scissors, the skin was removed from the ankle to the knee. The distal TA tendon was then identified, and thin-tip tweezers were inserted below it. The TA muscle was then separated from the underlying muscles by gently sliding the tweezers along the muscle length. The TA tendon was cut and gently pulled up to the knee following edge of the muscle and another cut was made below the knee to obtain intact TA muscle. The harvested muscles were fixed and sectioned following the protocol described in **2.2.9.3.**

Cryosections were then sent to the collaborating Surgical and Orthopaedic Research Lab (SORL, UNSW, Sydney, Australia) for routine Haematoxylin & Eosin (H&E) staining. Immunohistochemistry was also conducted to evaluate the contribution of transplanted cells to regeneration of injured skeletal muscle. Specific anti-human antibodies including hLamin A/C and hSpectrin were used to selectively mark human nuclei and lamina of human muscle fibres respectively.

2.2.11.3.1. Quantification of donor human cells retained within injured muscles:

Tile scans of five serial 20 µm cryosections, stained with hLamin A/C antibody, pan-laminin and DAPI were used for quantification by confocal microscopy. Negative and positive control slides were used to set the upper and lower limits of laser powers on each channel of the Zeiss LSM 780 confocal microscope. The percentage of hLamin A/C A/C positive nuclei was then counted manually using ImageJ software. Within each section, 4-5 individual regions were counted for the number of hLamin A/C positive and

negative nuclei. Values calculated using three to five cryosections from each experimental group were expressed as mean ± SD. Differences between experimental groups were analysed by one-tailed Student's T-test.

2.2.11.3.1.1 Quantification of donor-derived satellite cells within regenerating muscles: For this quantification, muscle sections were stained for pan-laminin which marks the basal lamina of all (human/mouse) muscle fibres, hCD56 which specifically marks satellite cells only of human origin, and DAPI. The abundance of donor derived satellite cells at each of the endpoints (one, two or four weeks) was expressed as the % hCD56 positive cells (average ± SD) out of the total number of cells located on the periphery of muscle fibres. Differences between experimental groups were analysed using a one-tailed Student's T-Test.

2.2.11.3.1.2 Quantification of donor-derived muscle fibres: For this quantification, muscle sections were stained for pan-laminin which marks the basal lamina of all (human/mouse) muscle fibres, hSpectrin which specifically marks muscle fibres only of human descent, and DAPI. The frequency of donor derived muscle fibres at the last endpoint of four weeks was expressed as the % of fibres co-stained with laminin and hSpectrin (average ± SD) out of the total number of counted muscle fibres (800-1000 in each section). Differences between experimental groups were determined using a one-tailed Student's T-test.

CHAPTER 3 Demethylation Cytokine induced (DCi) reprogramming of primary human adipocytes

3.1 Introduction

Terminally differentiated murine cells can be reverted to a plastic, proliferative cell-state by Demethylation Cytokine induced (DCi) reprogramming using a combination of 5-Azacytidine (AZA) and Platelet Derived Growth Factor-AB (PDGF-AB) (Chandrakanthan et al., 2016). AZA is a nucleoside analogue that is used clinically to treat pre-leukemic and leukemic blood disorders (Silverman & Mufti, 2005). AZA demethylates DNA (P. A. Jones & Taylor, 1980) and acts as an inducer of cell plasticity (Taylor & Jones, 1979). AZA is also applied in protocols for *in vitro* transdifferentiation (Kaur et al., 2014; Locklin et al., 1998; Makino et al., 1999; Nixon & Green, 1984; Pennarossa et al., 2013; Tan et al., 2015). More importantly, it is also used to convert partially reprogrammed induced pluripotent stem (iPS) cells to fully reprogrammed iPS cells (Mikkelsen et al., 2008). PDGF-AB is known to be a mitogen as well as cell survival factor (Heldin, Betsholtz, et al., 1985; Heldin & Westermark, 1990; Hoch & Soriano, 2003).

When combined with PDGF-AB, AZA induces cell plasticity in terminally differentiated cells, leading to reprogramming and acquisition of proliferative capacity. Extensive *in vitro* and *in vivo* characterizations of DCi reprogrammed murine induced Multipotent Stem (iMS) cells have demonstrated their properties of continued self-

renewal, plasticity and non-tumorigenic abilities (Chandrakanthan et al., 2016). The DCi method of cell dedifferentiation is advantageous over other cell reprogramming methods in that it is viral vector-free as well as transcription factor-free and involves only transient exposure of the target somatic cells to reprogramming agents. Murine iMS cells thus generated have also been reported to mediate tissue repair in a context dependent manner without undergoing malignant transformation or ectopic tissue formation (Chandrakanthan et al., 2016).

Given the numerous merits of DCi reprogramming, and its potential as a therapy, we investigated whether the technique could be applied to human cells. This chapter will cover optimization of the DCi reprogramming method for primary human somatic cells, followed by detailed *in vitro* characterization of reprogrammed human iMS cells including CFU-F assay, long-term growth measurement, assessment of *in vitro* differentiation potential, molecular immunophenotyping and karyotyping.

3.2 Results

3.2.1 DCi reprogramming can be extrapolated to primary human adipocytes

To investigate whether DCi reprogramming can be applied to human cells, I first set out to apply the DCi reprogramming protocol for murine cells to human primary somatic cells. Given its ease of availability and harvest, subcutaneous fat was used as the source of mature primary adipocytes as the starting population for reprogramming. Fat harvested from five patients undergoing surgery was digested with collagenase and then homogenized to obtain a single cell suspension. A differential plating method (Fernyhough et al., 2004) was used to ensure a pure starting population of terminally differentiated adipocytes as well as adipose derived MSCs (AdMSCs) is obtained. This

plating method allows attachment of unilocular adipocytes to the surface of cell culture dish over the extended period of 10 days in ceiling culture as described in **2.2.1.6.**

The original DCi reprogramming protocol for murine cells (Chandrakanthan et al., 2016) was applied to human primary adipocytes substituting (200 ng/mL) recombinant mouse PDGF-AB (r**m**PDGF-AB) with (200 ng/mL) recombinant human PDGF-AB (r**h**PDGF-AB) in the reprogramming medium. The duration of reprogramming had to be extended beyond the 12 days used in the mouse protocol as no cell conversion was observed by then (Figure S1). Exposure to (10 µM) AZA however was still restricted for the first 2 days of reprogramming regimen, with media changes every 3-4 days as described in **2.2.2.** Adipocytes subjected to reprogramming underwent clear morphological changes. By day 25, a proportion of adipocytes exposed to the reprogramming medium had lost their fat globules and acquired stromal cell morphology, suggesting cell conversion (Figure 3.1A-B). On the other hand, the untreated adipocytes or adipocytes exposed to AZA or rhPDGF-AB alone did not undergo cell conversion but were merely maintained as dormant terminally differentiated adipocytes (Figure S2). This highlights the need to use AZA in combination with rhPDGF-AB for induction of cell reprogramming.

The cells were then subjected to *in vitro* characterization. Adipocytes treated with Foetal Calf Serum (FCS)-supplemented reprogramming medium demonstrated large colony CFU-F potential, although lower than that of corresponding primary human adipose derived MSCs (AdMSCs); whereas untreated cells and cells treated with rhPDGF-AB or AZA alone did not form any colonies (Figure 3.1C). The reprogrammed cells also displayed long-term growth (Figure 3.1D) and trilineage differentiation

potential (Figure 3.1E). Therefore, DCi reprogrammed cells shared key features with AdMSCs and will henceforth be referred to as human induced Multipotent Stem (iMS) cells.

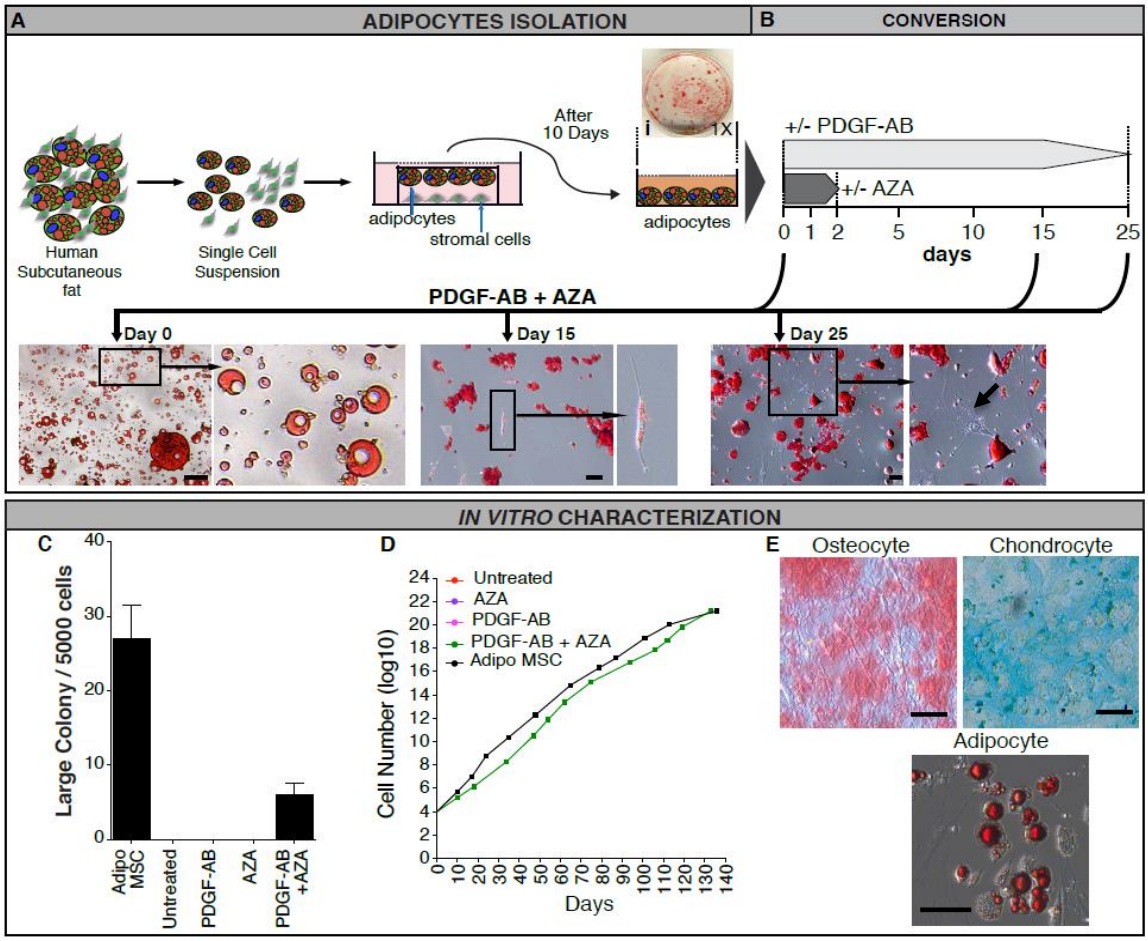

Figure 3. 1 DCi reprogramming of primary human adipocytes in FCS-supplemented medium

(A) Schematic outline of steps followed to harvest and isolate subcutaneous mature adipocytes. The photographs show Oil Red 'O' staining of unilocular mature adipocytes attached to a petri dish. (B) Schematic outline of treatments at selected time points used to evaluate the morphology of adipocytes in reprogramming medium (rhPDGF-AB+AZA) showing a single stromal-like cell (black arrows) by day 25. (C) Large colony forming units-fibroblast activity of adipose derived MSCs, untreated and AZA or rhPDGF-AB or rhPDGF-AB+AZA treated adipocytes. (D) Growth curves of Adipo MSC (AdMSCs), untreated and AZA or rhPDGF-AB+AZA treated adipocytes (Mean, n=5).

(E) rhPDGF-AB+AZA treated adipocytes can be differentiated into osteocytes (Alizarin Red), chondrocytes (Alcian Blue) and adipocytes (Oil Red ‘O’). Standard Deviation bars = SD between independent experiments. Scale bar = 30µm.

3.2.2 Primary human adipocytes cannot be reprogrammed in serum-free conditions

Foetal Calf Serum (FCS) remains to date the primary source of growth supplements as well as bioactive compounds for cell attachment and long-term *in vitro* expansion of stem cells (Kume et al., 2006). However, FCS carries the risk of pathogen contamination or transmission of xenogeneic proteins and can have undesirable effects in clinical applications (Mannello & Tonti, 2007). Batch-to-batch variations in FCS have also been reported to undermine the efficacy of *in vitro* cultures. Moreover, therapeutic use of stem/reprogrammed cells in humans necessitates their culture and expansion be carried out in xeno-free conditions which have minute, or no, biological components derived from non-human sources.

To address this issue, the FCS-supplemented reprogramming medium used above was substituted with serum-free medium (Stem MACS^{TM} MSC Expansion kit XF, Miltenyi Biotec). The dose of reprogramming cocktail was maintained at 10µM AZA, 200 ng/mL rhPDGF-AB and this experiment was done on samples obtained from three patients. Primary human adipocytes were found to be refractive to DCi reprogramming in these serum-free conditions and did not undergo cell conversion. Treated adipocytes did not show any morphological changes upon exposure to DCi reprogramming factors (Figure 3.2A-B) as opposed to that seen in FCS-supplemented conditions (Figure 3.1A-B). Unlike reprogramming in FCS-supplemented medium (Figure 3.1B), no stromal cells or CFU-Fs were present at the end of reprogramming regimen in serum-free medium (Figure 3.2B-C)[14]. These findings show that serum components are required to release

[14] Compare with Figure 3.1B-C.

the mature somatic cells from their terminally differentiated state and allow them to acquire an undifferentiated, progenitor-like cell state.

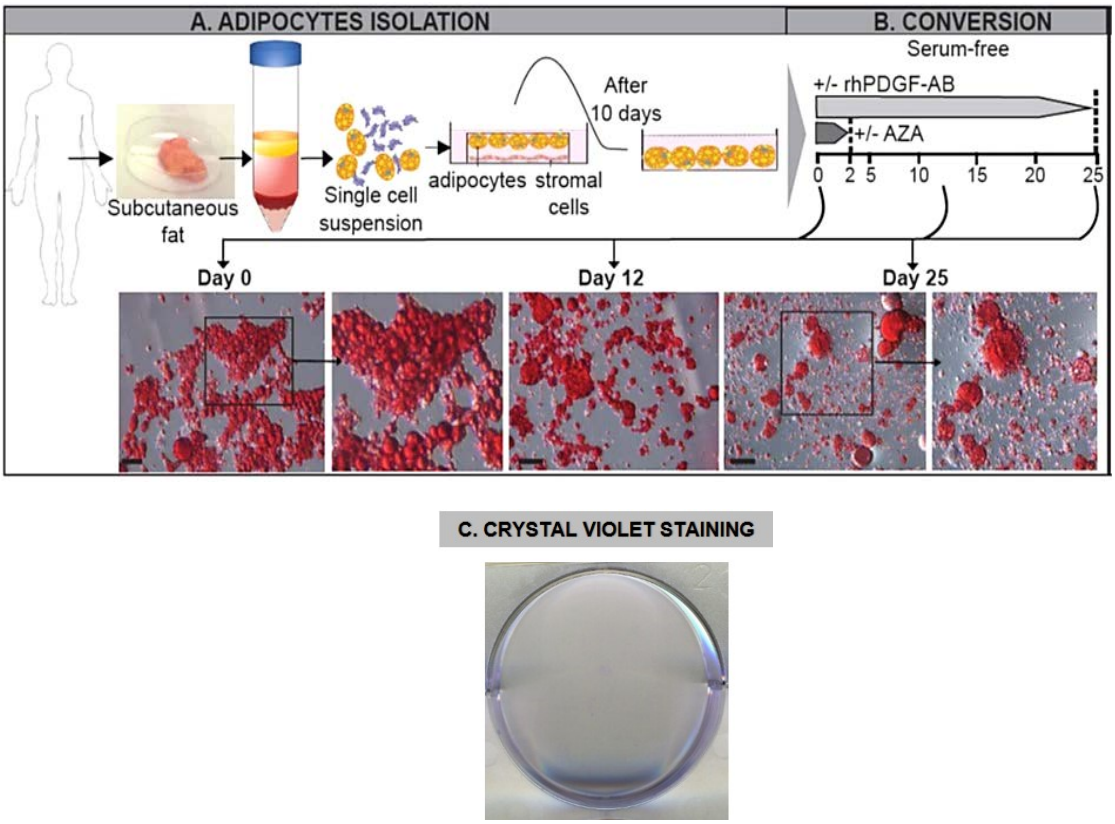

Figure 3. 2 DCi reprogramming of primary human adipocytes in serum-free media

(A) Schematic outline of steps followed to harvest and isolate subcutaneous mature adipocytes. (B) Schematic outline of treatments at selected time points used to evaluate the morphology of adipocytes in serum-free reprogramming medium (rhPDGF-AB+AZA). The photographs show Oil Red 'O' staining of attached, non-reprogrammed adipocytes at selected timepoints. (C) Crystal violet staining on primary adipocytes treated with rhPDGF-AB+AZA in serum-free reprogramming media for 25 days showing absence of CFU-Fs.

3.2.3 DCi reprogramming of primary human adipocytes in autologous serum-supplemented media.

Having identified the need for serum components for cell conversion while maintaining xeno-free conditions for DCi reprogramming, I sought to replace FCS in the DCi reprogramming medium with autologous serum (AS). In this experiment, adipocytes obtained from five patients were exposed to DCi reprogramming factors in medium containing 20% autologous serum (AS). Mature, unilocular adipocytes were found to be responsive to DCi reprogramming in AS-supplemented media, and changes in morphology with concomitant loss of fat droplets from the adipocytes were evident at different timepoints during reprogramming (Figure 3.3B, also see Figure S3 for adipocytes exposed to AS-supplemented medium containing AZA or rhPDGF-AB alone). This cell conversion was also recorded in real time by continuous live-imaging of adipocytes treated with rhPDGF-AB + AZA in AS-supplemented medium as per the setup described in **2.2.6.** By day 25, a proportion of adipocytes had eventually acquired a stromal cell morphology, in ways similar to that observed in FCS-supplemented DCi reprogramming[15]. The converted cells also gained motility and proliferative abilities thereby attesting conversion from a terminally differentiated cell state to a de-differentiated, self-renewing cell state (Movie S1).

[15] Compare Figure 3.3B with Figure 3.1B

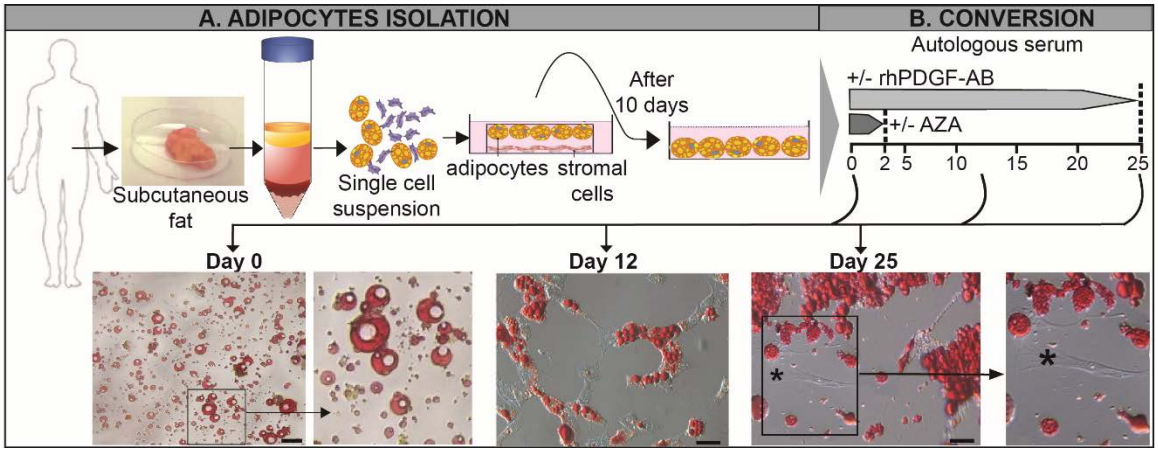

Figure 3. 3 DCi reprogramming of primary human adipocytes in autologous serum-supplemented medium

(A) Schematic outline of steps followed to harvest and isolate mature adipocytes from human subcutaneous fat tissue. (B) Schematic outline of treatments at selected time points used to evaluate the morphology of adipocytes in 20% AS-supplemented reprogramming medium (rhPDGF-AB+AZA). * shows reprogrammed cell at day 25 in reprogramming.

3.2.4 *In vitro* characterization of reprogrammed human iMS cells

The reprogrammed human iMS cells were then subjected to detailed *in vitro* characterization to determine whether they possess MSC-like features. The ability to self-renew was assayed by long-term growth assays whereas plastic-adherence was tested using CFU-F assays. Immunophenotyping and multi-lineage differentiation assays were conducted to evaluate expression of MSC-associated markers and *in vitro* plasticity respectively.

3.2.4.1 Colony forming unit-fibroblast (CFU-F) potential

The reprogrammed cells were first assessed for their colony forming potential. For the CFU-F assay, AdMSCs and iMS cells at P1 were seeded at a density of 400 cells/35mm dish and cultured for 2 weeks in standard tissue culture conditions. Cultured cells were then fixed with 4% PFA and stained in crystal violet solution as detailed in **2.2.4.1.** The colony morphology of iMS cells was comparable to that of control AdMSCs (Figure 3.4). Notably, adipocytes treated with AS-supplemented reprogramming media demonstrated CFU-F potential at levels higher than that of adipocytes treated with FCS-supplemented reprogramming medium. These data suggest that primary adipocytes undergo improved cell conversion when reprogrammed in the presence of human serum as compared to FCS (Figure 3.5).

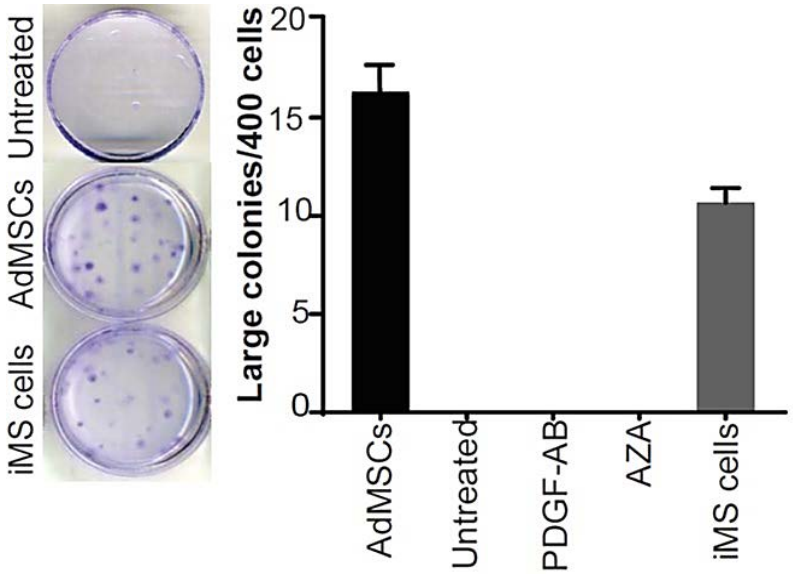

Figure 3. 4 Characterization of CFU-F capacity of iMS cells

Large colony forming units-fibroblast (CFU-F) activity of AdMSCs, untreated and rhPDGF-AB or AZA or rhPDGF-AB+AZA treated adipocytes (iMS cells) (n=3; Mean±SD).

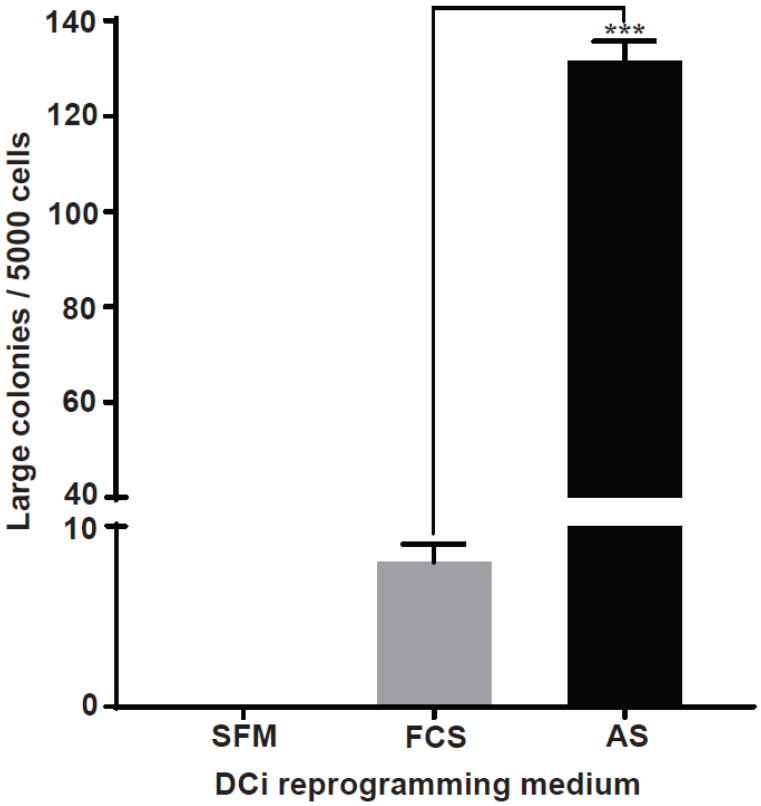

Figure 3. 5 Comparison of DCi reprogramming efficiency in different conditions

Large CFU-F activity of iMS reprogrammed in serum-free medium v/s reprogramming medium supplemented with FCS or AS (Mean±SD; n=3) (*** $p \leq 0.0005$ using T-test).

3.2.4.2 Long-term growth curve

I then examined the serial replating ability of human iMS cells in long-term growth assays. Expansion of MSCs in animal serum-free conditions has earlier been reported (Escobedo-Lucea et al., 2013; I. Muller et al., 2006). In order to test if freshly harvested AdMSCs and iMS cells[16] could also be maintained for long-term in serum-free conditions, they were cultured from P0 in serum-free medium without additional growth factors or cytokines. The cells were harvested on reaching 80% confluence and reseeded at a density of 5000 cells per T25 flask at each passage. At each passage, the total viable cell count and cumulative cell count was calculated as detailed in **2.2.1.5.** Long term growth curves for each of the cells in expansion were plotted as shown in Figure 3.6A. Each curve represents the mean of three independent experiments. Similar to AdMSCs, iMS cells could be serially passaged without reprogramming factors in serum-free medium for around 120 days, after which the cultures showed signs of reduced proliferation rates. At around 180 days in culture, the cumulative cell number plateaued in both iMS cell and AdMSCs. This observation will be explored further in subsequent sections. The reduction in proliferation of iMS cells was also accompanied by morphological changes. iMS cells cultured long term in serum-free medium exhibited a flattened cell morphology with increase in cell size and overall reduction in size of the large colonies. This observation was consistent with aging associated senescence that is typical of primary cultures (Figure 3.7**,** top panel).

Given the self-renewal ability of stem cells, they should be able to proliferate indefinitely under standard culture conditions. More importantly, clinical application of

[16] AdMSCs and iMS cells from three patients were used for this assay.

iMS cells would require their unobstructed proliferation thereby maintaining the cell number adequate to exert their therapeutic effects. Modifications in cell maintenance medium were tested to understand whether the phenomenon of plateaued cell growth could be rescued. Serum-free medium was replaced with human-serum supplemented medium, to test its ability to support long-term maintenance of iMS cells *in vitro.* Indeed, freshly harvested AdMSCs and iMS cells (n=2) were cultured from P0 in complete α-MEM medium containing 20% AS without any additional growth factors. iMS cells could be maintained for longer than 120 days and did not show plateauing in AS-supplemented maintenance medium. This suggests that AS is instrumental in providing certain components that supports long-term self-renewal of iMS cells (Figure 3.6B).

While AS might be beneficial for expansion of iMS cells for subsequent therapeutic applications, limited availability of the patient's own blood poses a major restriction. Therefore, allogenic human serum was tested for its ability to support continual *in vitro* maintenance of iMS cells. In order to circumvent age-associated variations in serum composition that might in turn affect cell expansion, allogeneic serum was obtained from donors of the same age group as that of the patients[17] included in this experiment. iMS cells maintained in allogenic human-serum supplemented media could also be steadily proliferated for almost 140 days without any reduction in cell growth rate. Due to limited availability of AS, expansion of control AdMSCs was tested only in medium supplemented with allogenic human serum and not autologous serum (Figure 3.6B).

The presence of (20%) autologous/allogenic human serum in expansion media averted the phenomenon of exhausted cell growth. This highlights the need for serum

[17] Patient-derived adipose tissue used as a source of adipocytes to generate iMS cells.

components for better maintenance of stemness in iMS cells. This was also supported by unchanged morphology of cells even in later passages (Figure 3.7, middle and bottom panels).

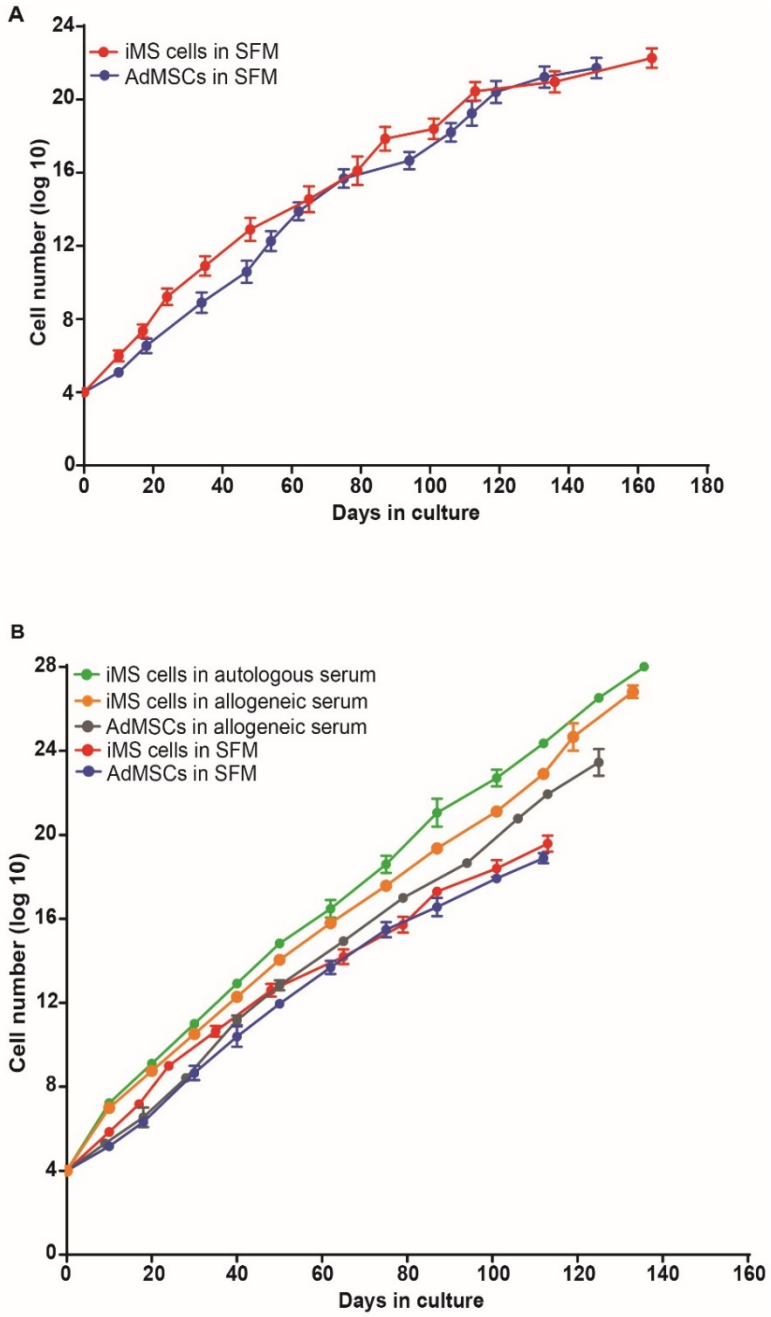

Figure 3. 6 Characterization of serial replating ability of iMS cells

(A) Long-term growth curves of AdMSCs and iMS cells that were harvested at P0 and propagated in serum-free media (n=3, Mean ±SD), (B) iMS cells at P0 propagated in serum-free media, or complete α-MEM supplemented with autologous or allogenic human serum and AdMSCs at P0 propagated in serum-free media or complete α-MEM supplemented with allogenic human serum (n=3, Mean ±SD).

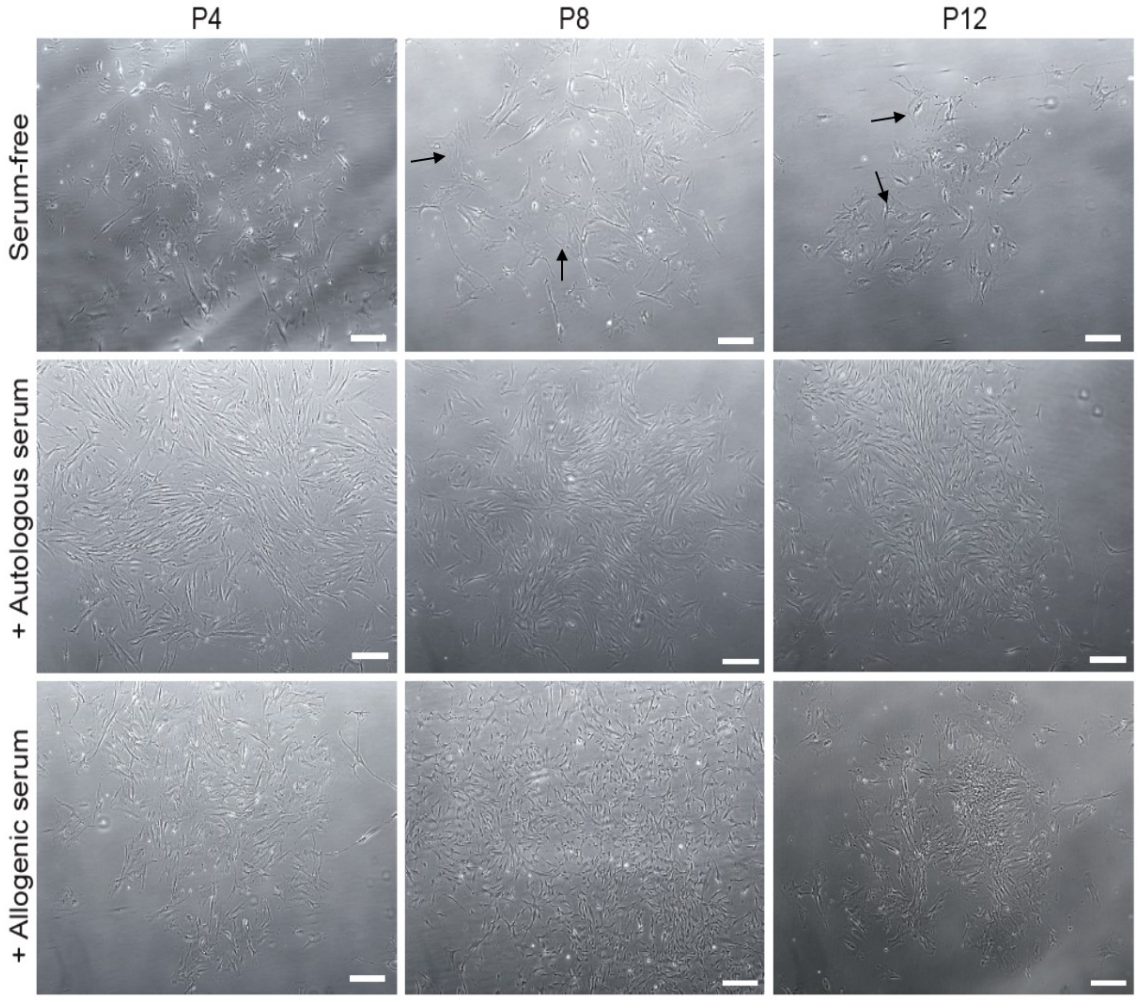

Figure 3. 7 Heterogeneity in morphology of iMS cells cultured in different expansion media

DCi reprogrammed iMS cells expanded in serum-free media and media supplemented with autologous or allogenic serum. Cells expanded in serum-free media exhibit flattened cell morphology (black arrows) and is accompanied with reduction in colony size at later passages (P8, P12). iMS cells however maintain the cell morphology and proliferative vigour across late passages when expanded in media supplemented with autologous or allogenic human serum. Images were taken just before harvesting the cells for subsequent passaging, using the 4x objective of a standard inverted microscope and a Nikon D3100 camera. (Scale bar, 5µm).

Clinical application of stem cells requires maintenance of their cell integrity and viability over long-term storage. Moreover, generation of a cell number adequate for therapeutic purposes requires extensive *in vitro* expansion of these stored cells. In order to test whether frozen iMS cells could be revived in media supplemented with human serum, early passage (P3) iMS cells (n=3) were revived as per the standard protocol described in **2.2.1.4.** The revived cells were tested for their long-term growth potential in serum-free expansion medium v/s allogenic human-serum supplemented medium. Similar to freshly reprogrammed cells, freeze-thawed iMS cells could be maintained for longer in human-serum supplemented medium compared to that in serum-free medium. (Figure 3.8).

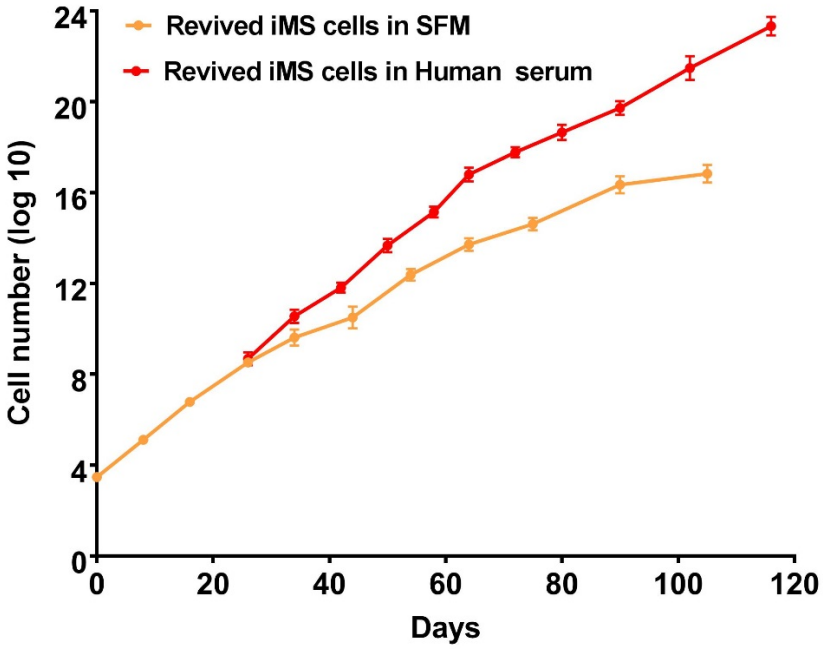

Figure 3. 8 Revived iMS cells propagated in serum-free medium or complete α-MEM supplemented with allogenic human serum

(n=3, Mean ± SD)

3.2.4.3 Immunophenotyping

iMS cells were next characterized with respect to their expression of cell surface markers using the MSC phenotyping kit™ (Miltenyi Biotec) as detailed in **2.2.7.** The phenotyping kit includes antibodies to stain CD73, CD90, CD105 and CD34/45 as per set guidelines of International Society of Cellular Therapy (ISCT) (Dominici et al., 2006). Moreover, STRO-1 was included as an additional marker for characterization of cells, given its high specificity for clonogenic stromal cell progenitors (Gronthos et al., 1999).

Flow cytometry profiles of AdMSCs and iMS cells were analysed using FlowJo software and plotted as shown in Figure 3.9A. iMS cells demonstrated expression of MSC-specific markers including CD73, CD90, CD105 and STRO1 at levels and frequencies comparable with that expressed on patient-matched AdMSCs. These observations were consistent across samples derived from three different individuals (Figure 3.9B).

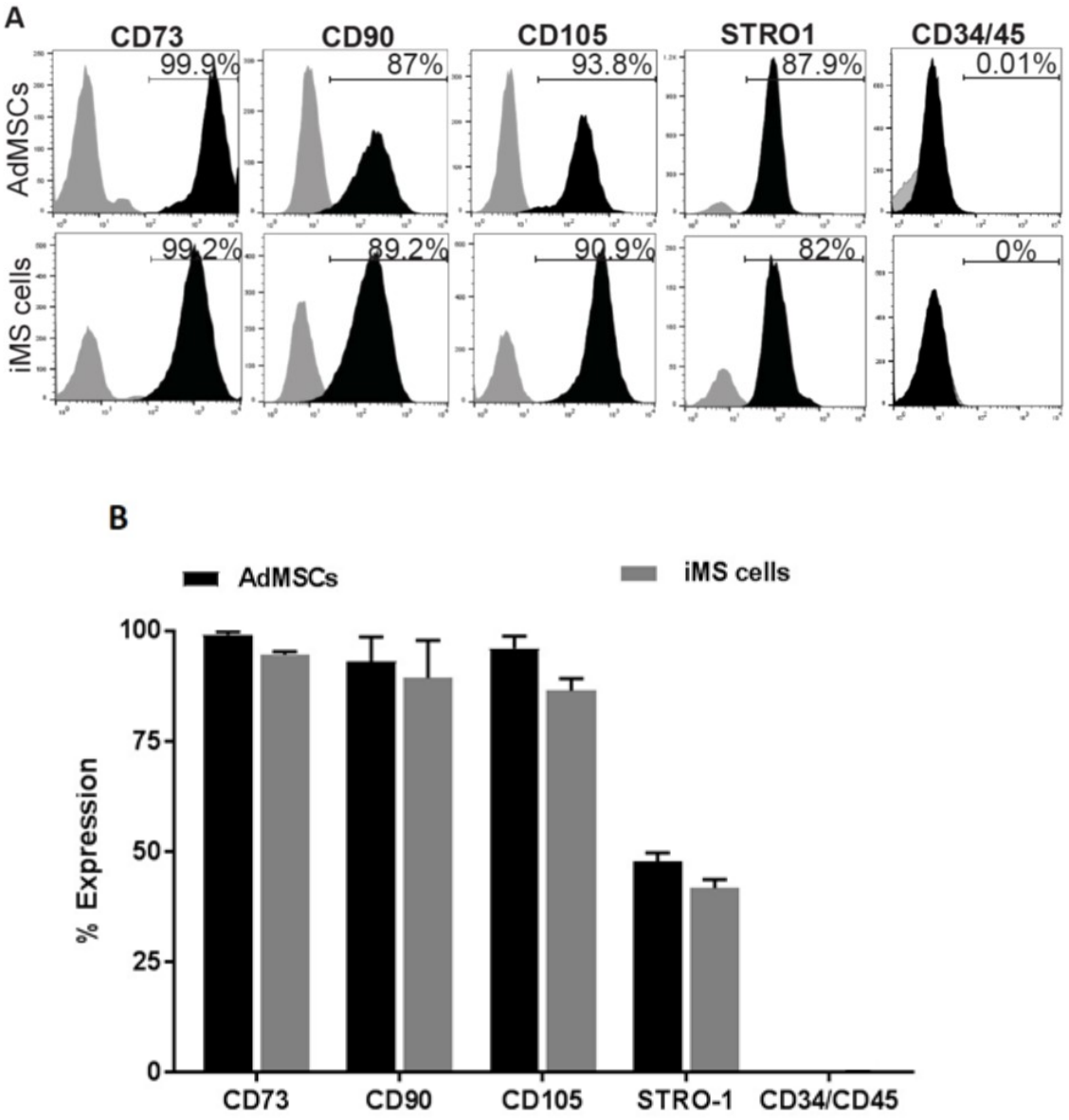

Figure 3. 9 Immunophenotyping of iMS cells for MSC-associated markers

(A) Representative flow cytometry profiles of AdMSCs and adipocytes reprogrammed to iMS cells. The MSC-associated markers CD73, CD90, CD105 or STRO1 are expressed on iMS cells at levels and frequencies comparable with that expressed on passage-matched AdMSCs. (B) % expression of MSC-associated markers in AdMSCs and iMS cells from three different individuals (n=3, Mean±SD).

3.2.4.4 Multilineage differentiation potential

Nextly, iMS cells were characterized with respect to their *in vitro* multi-lineage differentiation potential. Cells at early passages were seeded at high density in differentiation media composed of various growth factors and chemical components required to foster lineage-specific differentiation, as detailed in **2.2.4.3**. As shown in Figure 3.10, both AdMSCs and iMS cells could be re-differentiated towards adipogenic (lipid accumulation in cytoplasm, as stained with Oil Red 'O'), osteogenic (mineral deposition, as stained by Alizarin Red), chondrogenic (sulphated proteocglycan deposition, as stained by Alcian Blue), myogenic (smooth muscle fibres, as stained by αSMA and MYH) as well as endothelial (CD31 stained cells) lineages. However, when cultured in the matrigel tube formation assay, iMS cells but not AdMSCs showed differentiation into $PDGFRB^+$ pericytes enveloping $CD31^+$ endothelial cells. iMS cells not induced for the above differentiations stained negative for the respective differentiation markers (Figure S4).

In summary, DCi reprogrammed iMS cells are plastic adherent in standard tissue culture conditions, possess long-term self-renewal ability, strongly express MSC-associated markers and demonstrate *in vitro* multi-lineage differentiation potential; thereby satisfying the minimal criteria defined by ISCT for them to be deemed as MSCs (Dominici et al., 2006).

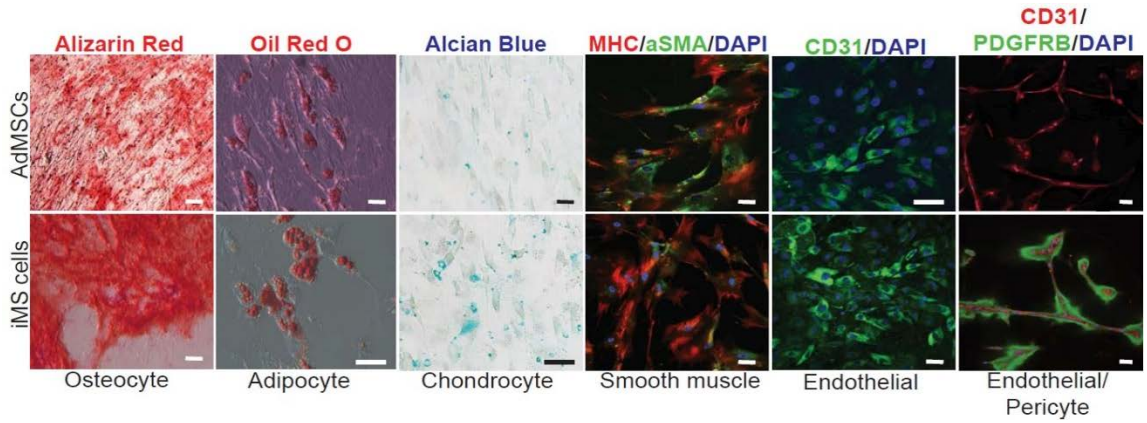

Figure 3. 10 Characterization of multipotency of iMS cells

Representative images showing rhPDGF-AB+AZA treated adipocytes can be differentiated into osteocytes (Alizarin Red), adipocytes (Oil Red 'O'), chondrocytes (Alcian Blue), smooth muscle (Myosin heavy Chain (MHC)/α Smooth Muscle Actin (αSMA)), endothelial (CD31) cells, matrigel tube formation for AdMSCs (upper panel; endothelial cells only) and iMS cells (lower panel; endothelial cells and pericytes). (n=3, Scale bar = 20µm).

3.2.4.5 Karyotyping

Figure 3. 11 Schematic for cell populations tested for genomic instability

Determination of genomic integrity is an important step towards assessing the suitability of reprogrammed cells for preclinical studies. To determine the safety of PDGF-AB/AZA treatment on cells, cytogenetic stability of the DCi reprogrammed primary adipocytes and patient-matched untreated AdMSCs was assessed. Pre-clinical testing however requires cells in large numbers thereby necessitating the *in vitro* expansion of freshly harvested and reprogrammed cells. Genomic instability arising from long-term culture is a potential concern with stem cells (Bochkov et al., 2007). It is hence imperative to test the *in vitro* expanded derivatives for their genomic stability before their transplantation in donor organisms. Therefore, along with P0; P3 and P5 cells from three age-matched patients were subjected to conventional pangenomic G-banded karyotyping as depicted above (tested at Cytolabs, WA, Australia).

The majority of cells examined from all the three patients displayed a normal 46, XX or 46, XY karyotype. No major karyotypic differences were observed across different passages of individual cell types. The genomic stability of reprogrammed iMS cells was also confirmed by the absence of any major structural or numerical alterations in the

chromosomes. This data suggests that DCi reprogramming does not induce frequent karyotypic abnormalities thereby attesting to the safety of this cell conversion technique.

3.2.5 Dose optimization of DCi reprogramming factors

Autologous serum can support DCi reprogramming better than FCS (Figure 3.5). I therefore hypothesized that DCi reprogramming factors at doses different than that applied in FCS-supplemented reprogramming media might be required to improve the efficiency and yield of this cell conversion technique. To determine the optimal dose of DCi reprogramming factors across patients from different age groups, nine different combinations of these reprogramming factors were tested on primary adipocytes obtained from three patients in each age group as depicted shown in Table 3.1.

Table 3. 1 Experimental matrix depicting different combinations of DCi reprogramming factors tested for dose optimization.

	Group I (≤45 years of age)			Group II (46-65 years of age)			Group III (≥66 years of age)		
	AZA (in µM)			AZA (in µM)			AZA (in µM)		
PDGF-AB (in ng/mL)	5	10	20	5	10	20	5	10	20
100									
200									
400									

Grid showing different tested combinations of AZA and rhPDGF-AB to reprogram primary adipocytes harvested from adipose tissues of three patients belonging to different age-groups, namely ≤45 years of age, 46-65 years of age and ≥66 years of age.

Harvested primary adipocytes were seeded in ceiling culture for 10 days before being subjected to DCi reprogramming in AS-supplemented media for a total of 25 days as described in section **3.2.3.** Reprogrammed cells formed CFU-Fs in culture and these were counted as a readout for effective cell conversion. The total number of CFU-Fs were normalized to 9 mL of adipocyte suspension seeded for reprogramming. The average number of colonies (mean ± SD) obtained in each reprogramming condition were plotted as shown in Graph 3.12A. While the combination of 5µM AZA and 400 ng/mL rh PDGF-AB yielded the highest number of colonies for reprogrammed adipocytes derived from patients younger than 45 years and older than 65 years, the combination of 5µM AZA and 200 ng/mL rh PDGF-AB yielded maximum colonies for reprogrammed adipocytes of patients aged between 46-65 years.

iMS cells reprogrammed in each of the nine different combinations were harvested and subsequently expanded in serum-free conditions to further assess their *in vitro* proliferative abilities. Cells reprogrammed in the dose that proliferated for the longest period of time in serum-free culture[18] was determined as the optimal dose of DCi reprogramming factors. Out of all the tested combinations, adipocytes reprogrammed in the dose of **5 µM AZA and 400 ng/mL rhPDGF-AB** showed the best long-term *in vitro* proliferation capacity across all age groups (Figure 3.12B).

[18] Although this expansion was done in serum-free medium, the cells that plateaued at later stages could be rejuvenated and cultured in proliferative phase when supplemented with human serum, similar to data shown in Figure 3.8.

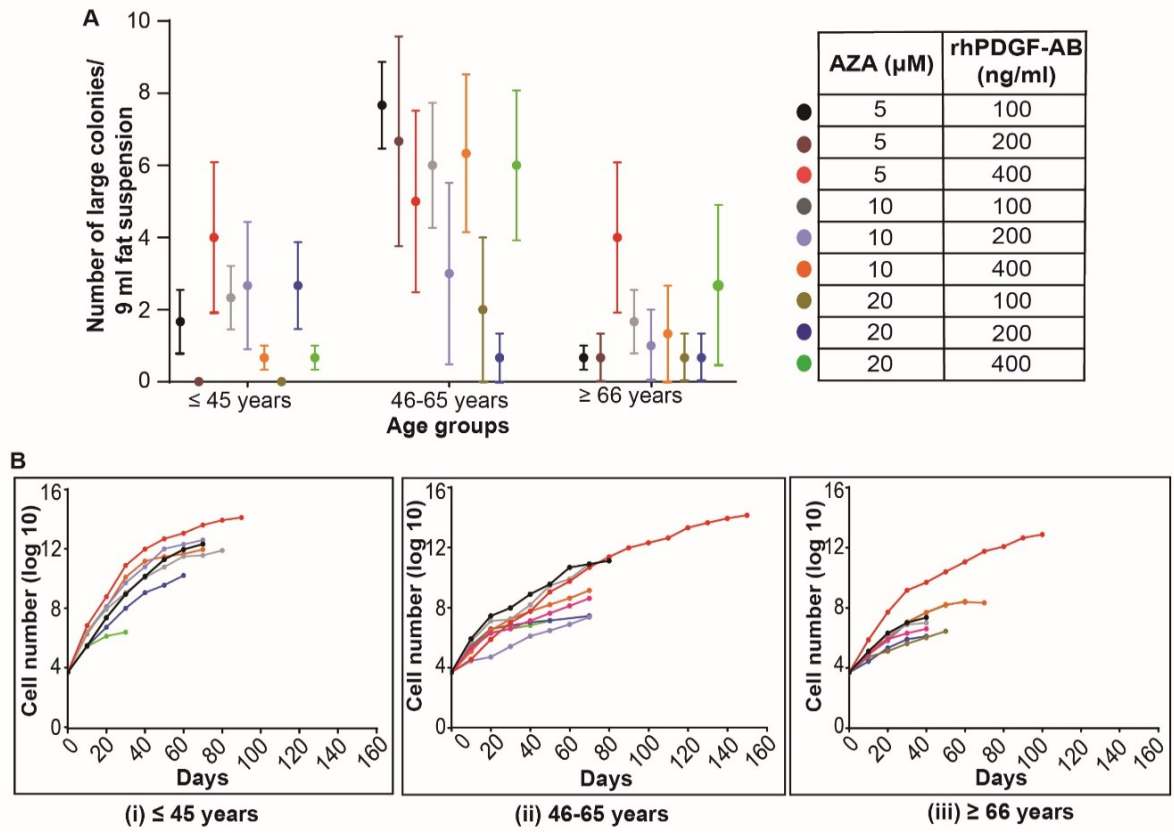

Figure 3. 12 Dose optimization of DCi reprogramming factors across three different age groups.

(A) 9 mL of homogenized adipocyte suspension from individual patient-derived fat tissue (n=3 for each age group) was seeded and subjected to DCi reprogramming in AS-supplemented conditions. Quantification of CFU-F colonies from primary adipocytes cultured in AS-supplemented media with nine different combinations of AZA and rhPDGF-AB. (B) Long-term serum-free expansion of cells reprogrammed (with each of the nine different DCi reprogramming factors-combinations) from adipocytes obtained from patients of 3 different age-groups; (i) ≤45 years, (ii) 46-65 years, (iii) ≥66 years (Mean; n=3).

3.3 Chapter summary and discussion

This chapter describes the application and optimisation of DCi reprogramming to human somatic cells. Terminally differentiated primary human adipocytes can be converted to iMS cells using the combined action of rhPDGF-AB and AZA in foetal calf or autologous serum supplemented conditions (described in Sections **3.2.1** and **3.2.3**). However, somatic cells were unresponsive to AZA or rhPDGF-AB in the absence of serum and did not undergo reprogramming (Section 3.2.2). This finding emphasizes the need to combine AZA and rhPDGF-AB in the presence of serum components to achieve the desired acquisition of a proliferative, multipotent, progenitor-like cell state. The exact serum components needed for cell conversion are unknown and will require further detailed investigation. It is possible that AZA plays a role in demethylation and re-activation of pluripotency associated genes in somatic cells thereby facilitating de-differentiation, whereas PDGF-AB helps to maintain this de-differentiated cell state and subsequent propagation of cells in culture. The exact molecular mechanism underlying this phenomenon also needs further understanding.

Primary adipocytes were found to be refractive to DCi reprogramming in serum-free conditions (**Section 3.2.2**). This observation underscores the role of serum in providing the necessary nutrients, protease inhibitors as well as growth and attachment factors that aid in de-differentiation and proliferation of an otherwise latent somatic cell population. Human serum-supplemented medium promoted better DCi reprogramming of primary human adipocytes over FCS-supplemented medium (Figure 3.5), thereby emphasizing the efficiency of xenofree conditions.

The dose of DCi reprogramming factors was optimized at 5µM AZA and 400ng/mL rh-PDGF-AB and can be applied to reprogram primary adipocytes from individuals across a wide age range. While this protocol was tested on primary human adipocytes, it could potentially be extended to reprogram other somatic cells that might be suitable as per the intended downstream applications.

DCi reprogrammed iMS cells are plastic-adherent and display CFU-F ability, serial re-plating ability, multi-lineage differentiation potential and express MSC associated markers, in adherence to the ISCT minimal criteria for MSC definition (Dominici et al., 2006). iMS cells also express STRO-1 which typically marks clonogenic stromal cell progenitors (Gronthos et al., 1999; Zannettino et al., 2008) (as shown in **Section 3.2.4**).

Under appropriate cell culture conditions, iMS cells could be maintained for almost five months *in vitro* before they showed signs of exhausted cell proliferation. Although iMS cells showed plateauing with respect to cell growth at late passages in serum-free media, this phenomenon could be rescued with the use of autologous or allogeneic human serum supplementation in the expansion media (Figure 3.6). This presence of human serum in the media supported maintenance of stemness and indefinite *in vitro* proliferation of iMS cells. Therefore, under appropriate culture conditions, iMS cells retain their self-renewal potential over long-term culture. These observations could be mainly attributed to the need of serum components that are essential for *in vitro* cell attachment, unhindered proliferation and for protection against aging associated cell senescence. Our results are comparable to previous reports describing the expansion of MSCs in human serum-supplemented media (Le Blanc et al., 2007; Stute et al., 2004). Autologous serum maybe limited but the capacity of allogenic human serum to maintain iMS cell expansion (Figure 3.6B) opens a path for expanding cells for clinical

applications without exposing them to cross species contamination. It is also important to note that ideally for clinical applications, iMS cells would be transplanted directly following cell conversion without *ex vivo* expansion. The expectation being that these cells will proliferate on demand *in vivo* where autologous serum factors would not be limited.

iMS cells are similar to MSCs in many aspects. However, certain *in vitro* characteristics also highlight the superiority of iMS cells over AdMSCs with respect to their differentiation potential and long-term proliferative capacity (Figure 3.6, 3.10). These observations suggest that there may be bigger differences between AdMSCs and iMS cells that are not obvious at the *in vitro* level. The following chapters will focus on deciphering these differences at the molecular as well as *in vivo* level.

Taken together, DCi reprogramming is a novel cell conversion technique that can be used to generate autologous iMS cells from a starting population of somatic cells. Moreover, iMS cells and their *in vitro* expanded derivatives display genomic stability as demonstrated by conventional karyotyping. As a vector and transcription factor-free method, DCi reprograming has promise as a tool to generate autologous multipotent stem cells. However, progressing this technique to the clinic requires extensive evaluation of the safety and efficacy of iMS cells. The next chapter will focus on molecular characterization and evaluation of pluripotency in iMS cells.

CHAPTER 4 Molecular characterization and evaluation of pluripotency in human iMS cells

4.1 Introduction

Stem cells are broadly classified based on their features of self-renewal and developmental potency. Unlike MSCs, pluripotent stem cells are self-renewing cells that can naturally differentiate into representative cells of all the three germ layers, namely endoderm, mesoderm and ectoderm but not the extra-embryonic membranes or trophoblast layers of the placenta (De Los Angeles et al., 2015). Human embryonic stem (ES) cells obtained from the inner cell mass in the blastocyst of a developing embryo are pluripotent in nature (Evans & Kaufman, 1981; Thomson et al., 1998). Induced pluripotent stem (iPS) cells generated by de-differentiation of somatic cells by different cell reprogramming techniques constitute another example of pluripotent stem cells (Takahashi et al., 2007; Takahashi & Yamanaka, 2006). Their ability to undergo spontaneous multilineage differentiation opens doors for widescale application of these pluripotent cells in diverse contexts for understanding developmental and regeneration mechanisms as well as models for drug testing. Given this background, we set out to determine where iMS cells sit within the pluripotency landscape. This chapter will focus on characterizing human iMS cells to elucidate their molecular identity and pluripotency.

Based on our previous observations regarding DCi reprogrammed adipocytes (i.e. iMS cells), we hypothesized that AdMSCs that are exposed to DCi reprogramming factors might be distinct to untreated AdMSCs. This chapter will therefore first cover the

effects of DCi reprogramming factors on AdMSCs and their detailed *in vitro* characterization with respect to colony forming ability, immunophenotyping for MSC-associated markers and differentiation into mesodermal derivatives. This will be followed by molecular characterization of iMS cells in comparison to other cell populations. The concluding section of this chapter will cover detailed characterization of DCi reprogrammed cells[19] with respect to expression of pluripotency markers and evaluation of their tri-germ layer plasticity as tested in a novel *in vitro* teratoma assay.

4.2 Results

4.2.1 DCi reprogrammed AdMSCs share *in vitro* characteristics with iMS cells

We first set out with DCi reprogramming of AdMSCs. Briefly, AdMSCs were isolated from patient-derived adipose tissue (n=3) and treated with 5μM AZA and 400ng/ml rhPDGF-AB as per the optimized protocol described in **3.2.5.** DCi reprogrammed AdMSCs will hereafter be referred to as 'treated AdMSCs' (Figure 4.1A-B).

Prior to their use in subsequent assays, treated AdMSCs were subjected to detailed *in vitro* characterization. Treated AdMSCs were found to be comparable to iMS cells in that they displayed CFU-F potential (Figure 4.1C (i)), expressed MSC-associated markers (Figure 4.1C (ii)) and could be differentiated into osteocytes, adipocytes, chondrocytes, smooth muscle, endothelial cells as well as pericytes (Figure 4.1C (iii)). From our earlier observations, although iMS cells shared certain features with AdMSCs, notably AdMSCs displayed limited *in vitro* plasticity and could not be differentiated into pericytes when

[19] Corresponding patient and passage-matched AdMSCs were also included as one of the test cell populations.

cultured in their respective differentiation media (as described in section **3.2.4D,** Figure 3.10). The greater plasticity of iMS cells and treated AdMSCs was also suggestive of greater differences between AdMSCs and warranted further investigation. From this chapter onwards, I have incorporated treated AdMSCs along with iMS cells in a series of *in vitro* and *in vivo* functional assays when evaluating distinguishing features between DCi reprogrammed cells and AdMSCs. Having shown that exposure of DCi reprogramming factors on primary adipocytes generates a population of phenotypically and functionally different iMS cells (Refer to Section **3.2.4**), I next sought to understand the molecular differences of these cell populations.

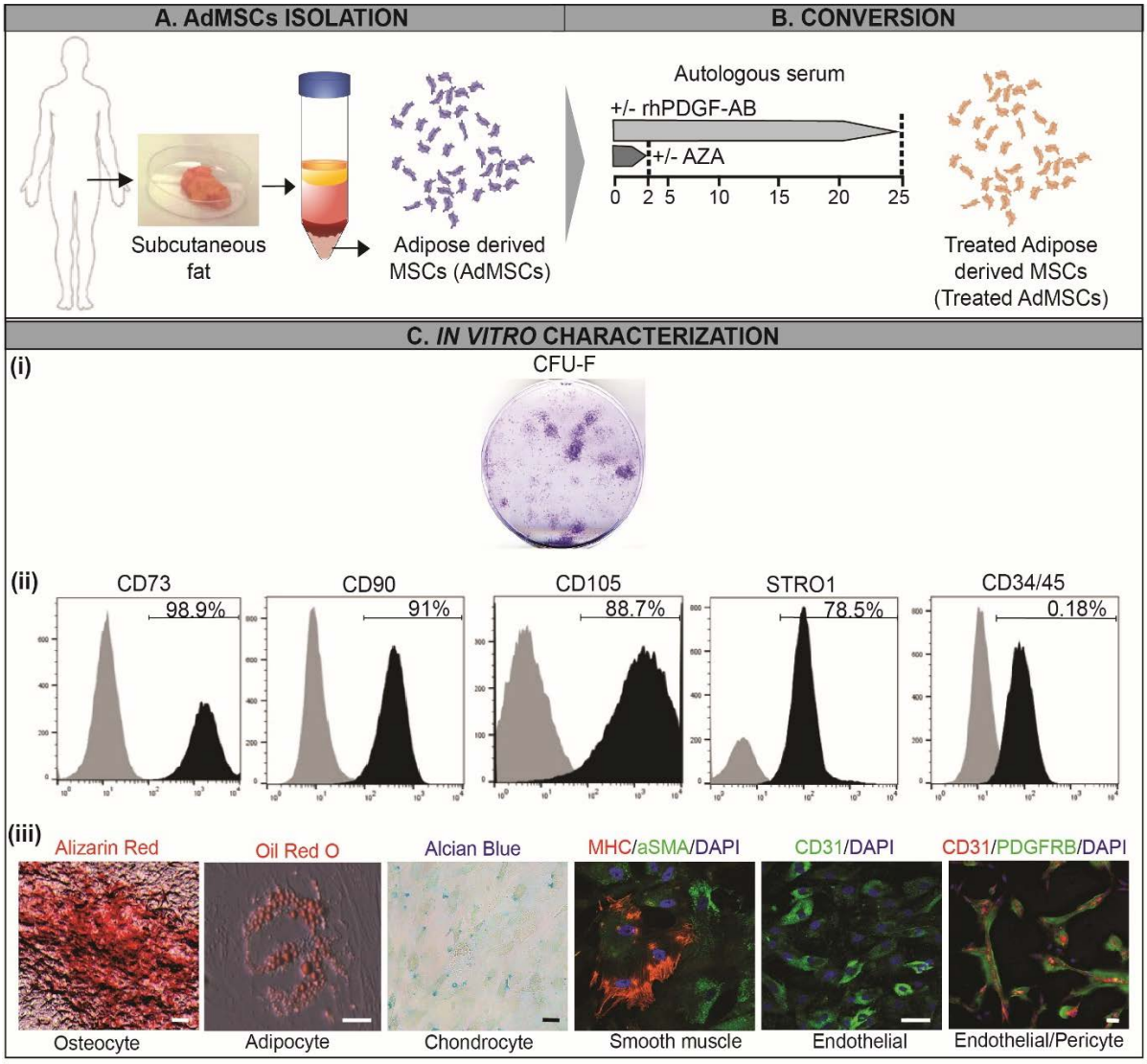

Figure 4. 1 Derivation and *in vitro* characterization of Treated AdMSCs

(A) Schematic representing isolation of AdMSCs and (B) their conversion to 'treated AdMSCs' by DCi reprogramming. (C) Treated AdMSCs display (i) CFU-F ability, (ii) express MSC-associated markers and (iii) can be re-differentiated into osteocytes (Alizarin Red), adipocytes (Oil Red 'O'), chondrocytes (Alcian Blue), smooth muscle cells (MYH/αSMA), endothelial cells (CD31) and pericytes (CD31/PDGFRβ). (Scale bar, 20µm).

4.2.2 Transcriptomic analysis of DCi reprogrammed cells

To evaluate the molecular identity of DCi reprogrammed cells we next performed transcriptomic analysis on cell populations before and after exposure to the DCi reprogramming cocktail. Primary adipocytes and corresponding iMS cells as well as AdMSCs and corresponding treated AdMSCs from three patients were included for this experiment. High quality RNA (260/280 ~2.0, Table S1) was extracted and shipped for sequencing to Novogene Company Limited (Hong Kong, China). Genome-wide expression analysis (RNA sequencing) was conducted on the above-mentioned cell populations. High alignment (96.9-98.4% mapped reads) of the sequence reads to the human genome (UCSC genome assembly hg19) confirmed the data quality (Table S2).

4.2.2.1 Principal Component Analysis (PCA)

Genome-wide expression profiles were analysed using principle component analysis (PCA) (Diffner et al., 2013; Ringner, 2008) to visualise the relationship between the transcriptomes of each of the cell populations. The PCA algorithm is a dimension reduction technique that identifies directions (called principle components) along which gene expression measures are most variant. The principle components are linear combinations of the original gene expression measures and allow to visualise genome-wide expression profiles in two or more dimensions. Of all the determined PCs, PC1 explains the most variance, followed by PC2, PC3, etc. The data from our analysis are projected to PC1 and PC2, PCs that explain the highest variance. DCi reprogrammed iMS cells (purple dots in Figure 4.2) and treated AdMSCs (green dots in Figure 4.2) clustered together with AdMSCs (yellow dots in Figure 4.2) and were well separated from

corresponding primary adipocytes which formed a second cluster (orange dots in Figure 4.2).

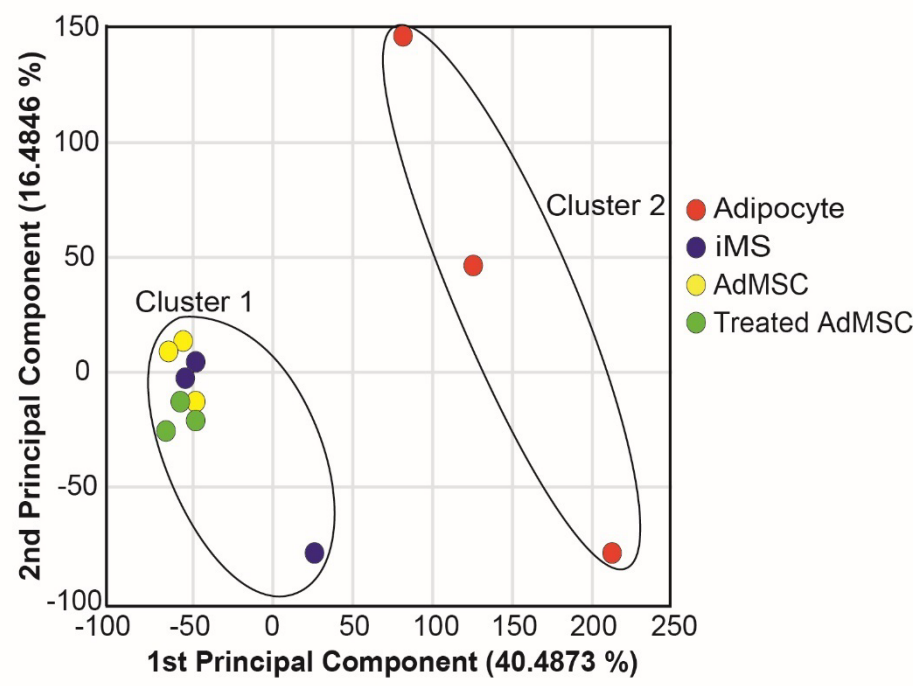

Figure 4. 2 DCi reprogrammed iMS cells have a distinct transcriptional profile.

Two-dimensional PCA plots of transcriptomes (n=3 patients) of all primary adipocytes (orange dots), iMS cells (purple dots), AdMSCs (yellow dots) and treated AdMSCs (green dots).

4.2.2.2 IPA analysis

4.2.2.2.1 Primary adipocytes v/s iMS cells

To gain insights into the molecular processes underlying DCi reprogramming, we then compared gene expression between 'primary adipocytes and reprogrammed iMS cells' and 'AdMSCs and treated AdMSCs'. This analysis identified a large number (5021) of differentially expressed (DE) genes, as compared to 344 DE genes in the comparison of AdMSC vs iMS cells. We next used Qiagen's Ingenuity Pathway Analysis (IPA) software to understand which canonical pathways and diseases and functions were most affected by the DCi process. The entire DE gene list was too extensive for direct analysis using IPA. Using the knowledge that modulation of master transcriptional regulators is a fundamental requirement for reprogramming to iPS cells (Heng et al., 2010; Vierbuchen & Wernig, 2012), we reasoned that changes in transcriptional regulation might also be of key importance in the DCi reprogramming process. Therefore, from the complete list of differentially expressed genes between iMS cells and primary adipocytes we only used 'transcriptional regulators' for subsequent analysis. This focussed gene list was uploaded into IPA software for core analysis, and then overlaid with the global molecular network within the Ingenuity Pathway Knowledge Base (IPKB).

The top enriched categories of canonical pathways with a *p*-value less than 0.05 are plotted in Figure 4.3A. Wnt/β catenin signaling and the Adipogenesis pathway were the top two canonical pathways significantly changed across the comparison of primary adipocytes v/s iMS cells. Wnt/β catenin signaling is known to play a role in ES cell renewal and somatic cell reprogramming (Miki et al., 2011). As a sign of DCi reprogramming-induced de-differentiation of primary adipocytes to a progenitor/stem

cell state, we therefore expected Wnt/β catenin signaling to be activated whereas adipogenesis to be repressed in iMS cells. In addition, TGF-β signaling, Notch signaling, BMP signaling, JAK-STAT signaling, regulation of the EMT pathway and pathways related to embryonic stem cell pluripotency also differed between adipocytes and iMS cells. Full details of the categories of canonical pathways which differed are listed in Supplementary Table S3. The IPA software also includes curated lists of genes associated with specific cellular functions and disease states. The top enriched diseases and functions with a *p*-value less than 0.05 were plotted (Figure 4.3B). This analysis indicated that cellular functions related to cell cycle, cellular movement, and cellular, embryonic and organismal development were significantly changed in iMS cells compared to adipocytes. All categories of diseases and functions and their associated genes are also listed in Supplementary Table S3.

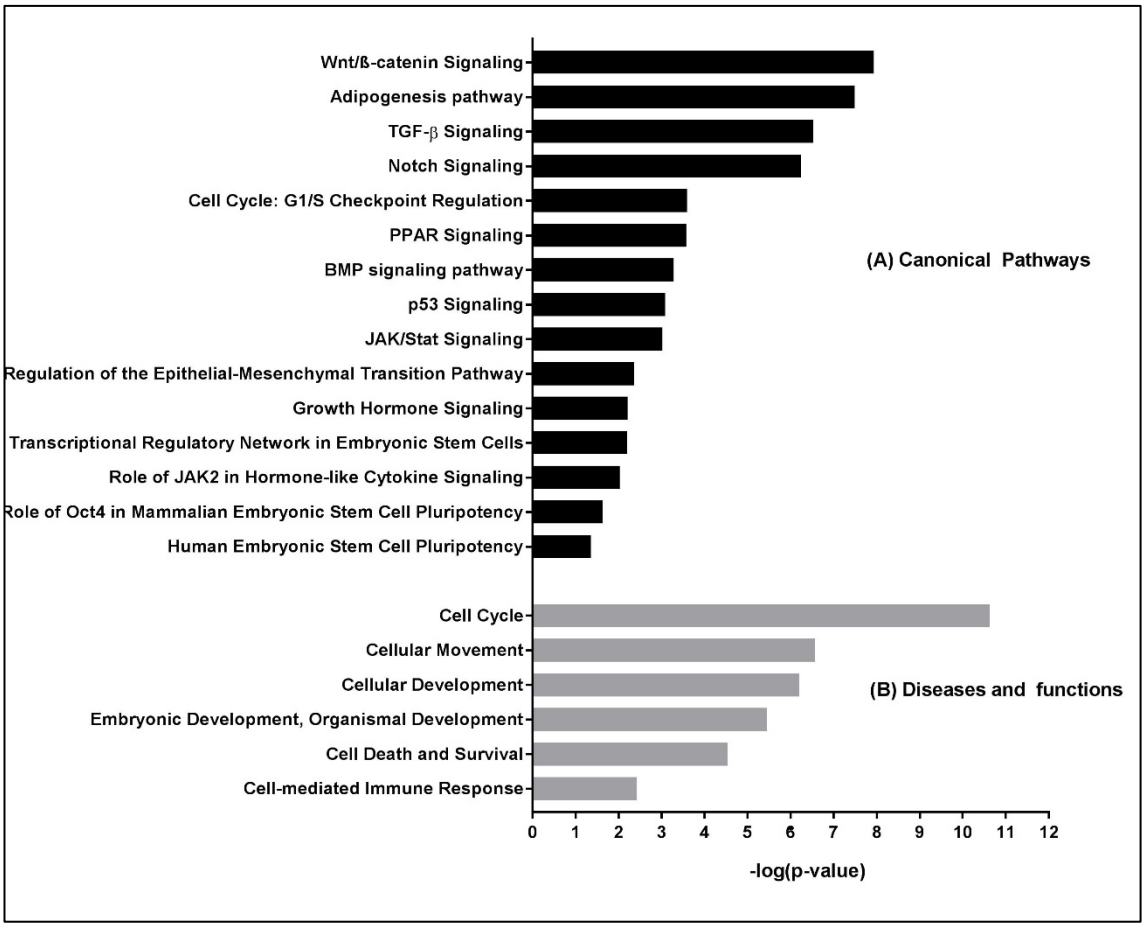

Figure 4. 3 Canonical pathways and categories of diseases and functions enriched after DCi of primary human adipocytes, as derived from IPA.

Canonical pathways were selected following IPA 'Core Analysis' and filtered for *p*-value ≤ 0.05.

Since iMS cells are the result of reprogramming somatic cells, we hypothesized that genes associated with the terminally differentially state (in this case adipocytes) should be downregulated in iMS cells, whereas genes associated with a progenitor/ stem cell state should be upregulated. We therefore focussed on genes involved in the adipogenesis pathway (MSigDB HALLMARK_ADIPOGENESIS, contributed by Arthur Liberzon, Broad Institute) and ES cell core genes (MSigDB WONG_EMBRYONIC_STEM_CELL_CORE, (Wong et al., 2008)). In order to visualise gene expression patterns, normalised fragments per kilobase of transcript per million mapped reads (FPKM) were used to create an unsupervised clustering heat map comparing iMS cells to primary adipocytes. As expected, we observed that DE genes associated with adipogenesis were downregulated (blue) in iMS cells (Figure 4.4A) whereas DE genes from the ES cell core set were upregulated (red) in iMS cells (Figure 4.4B).

During embryogenesis, one of the fundamental processes regulated by OCT4 is the epithelial-to-mesenchymal transition (Saunders & Mcclay, 2014). OCT4 is also the master regulator of pluripotency and self-renewal (Kellner 2010). Therefore, somatic cell reprogramming is expected to bring about reactivation of OCT4 and other genes associated with pluripotency. This hypothesis will be tested in detail in the following sections. The epithelial-to-Mesenchymal Transition (EMT) pathway is also associated with the epigenetic reprogramming process (Skrypek et al., 2017). Interestingly, our results also showed enrichment of EMT pathway (Gene set: HALLMARK_EMT_PATHWAY, contributed by Arthur Lizerbon, Broad Institute) in DCi reprogrammed iMS cells when compared to primary adipocytes (Figure 4.4C). Moreover, genes associated with Wnt/β catenin signaling (Gene set: HALLMARK_WNT/β_CATENIN_PATHWAY, contributed by Arthur Lizerbon, Broad

Institute) were seen to be upregulated in iMS cells as compared to primary adipocytes (Figure 4.4D). This observation was in accordance with earlier report describing activation of this pathway in somatic cell reprogramming and form maintenance of ES cell self-renewal (Miki et al., 2011), thereby validating induced cell fate conversion as a consequence of DCi reprogramming. To gain further mechanistic insights into the reprogramming process, we selected gene sets known to be important for other relevant pathways such as PPAR signaling (KEGG_PPAR_SIGNALING_PATHWAY), TGFβ signaling (KEGG_TGF_BETA_SIGNALING_PATHWAY), allograft rejection (HALLMARK_ALLOGRAFT_REJECTION, contributed by Arthur Liberzon, Broad Institute), JAK-STAT signaling (KEGG_JAK_STAT_SIGNALING_PATHWAY), PDGF signaling (BIOCARTA_PDGF_PATHWAY) and PI3K-AKT-mTOR signaling (HALLMARK_PI3K_AKT_MTOR_SIGNALING, contributed by Arthur Lizerbon, Broad Institute), and analysed the relative expression of genes from these sets in primary adipocytes compared to iMS cells. In parallel with adipogenesis, genes associated with PPAR signaling (Figure S5A), TGFβ signaling (Figure S5B) and allograft rejection mechanism (Figure S5C) were downregulated in iMS cells whereas genes associated with JAK-STAT signaling (Figure S5D), PDGF signaling (Figure S5E) and PI3K-AKT-mTOR pathway (Figure S5F) were upregulated in iMS cells. Therefore, suppression of genes associated with differentiated state (adipocytes) with concomitant activation of genes associated with progenitor/stem like cell state in iMS cells confirms cell fate conversion consequent to exposure to DCi reprogramming factors. Since the list of DE genes was filtered for transcriptional regulators, our data also supports their role in cell reprogramming and conforms with other reports (Heng et al., 2010; Vierbuchen & Wernig, 2012). In summary, although DCi reprogramming involves use of an epigenetic modifier and a cytokine, the eventual effects involve modulation of transcriptional

regulators. The precise extent and interlink between epigenetic and genetic modifications induced by DCi reprogramming however requires detailed investigation and is beyond the scope of this thesis.

A. Adipogenesis

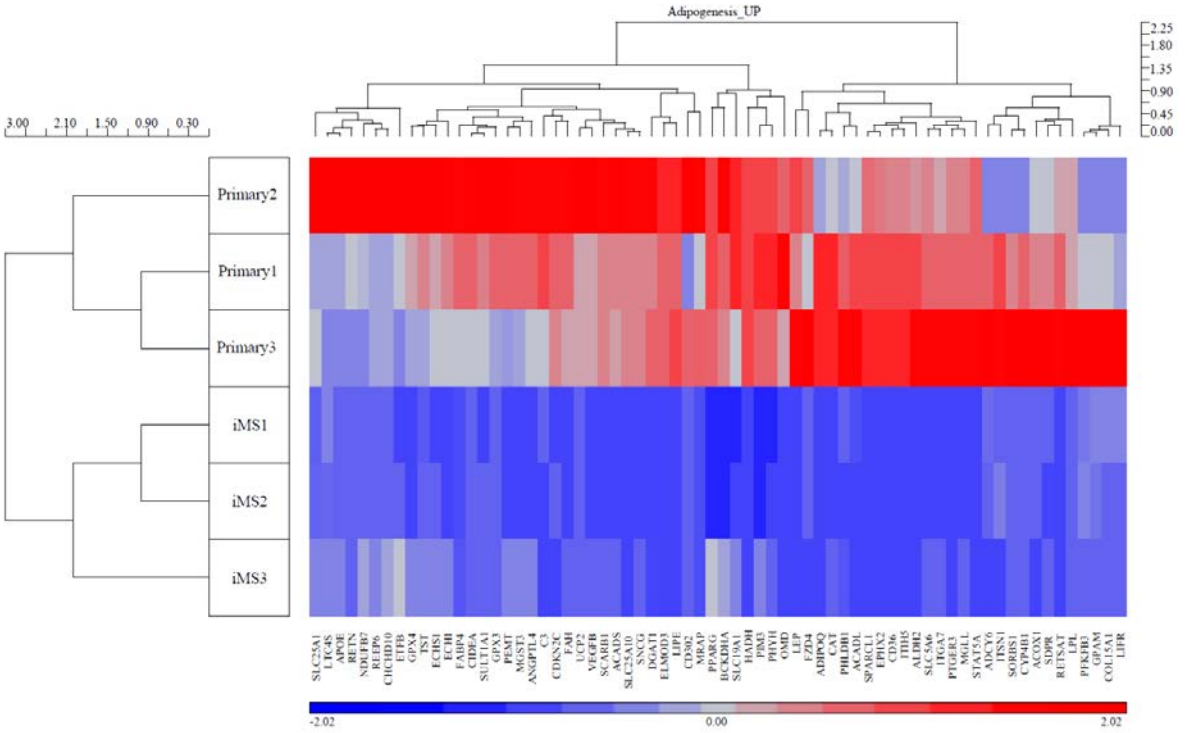

B. ES cell core genes

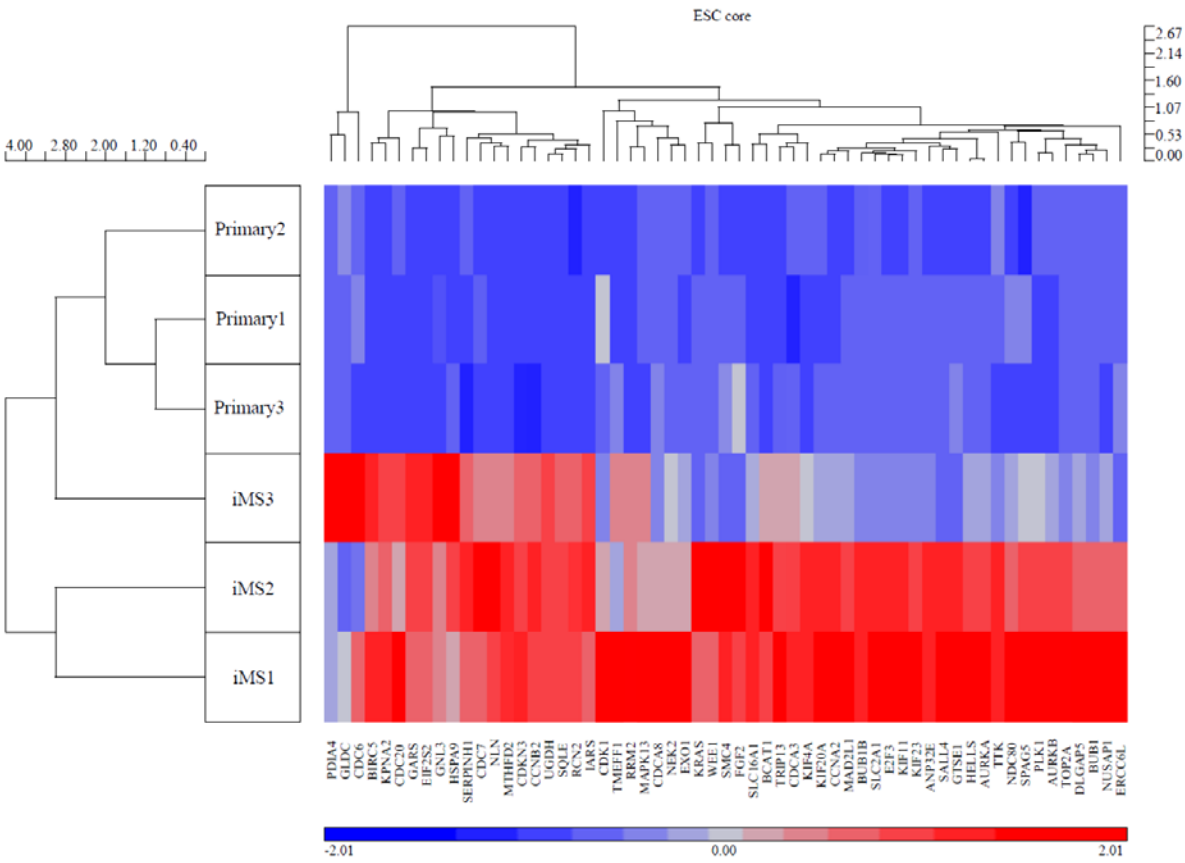

C. Epithelial-to-Mesenchymal transition (EMT) pathway

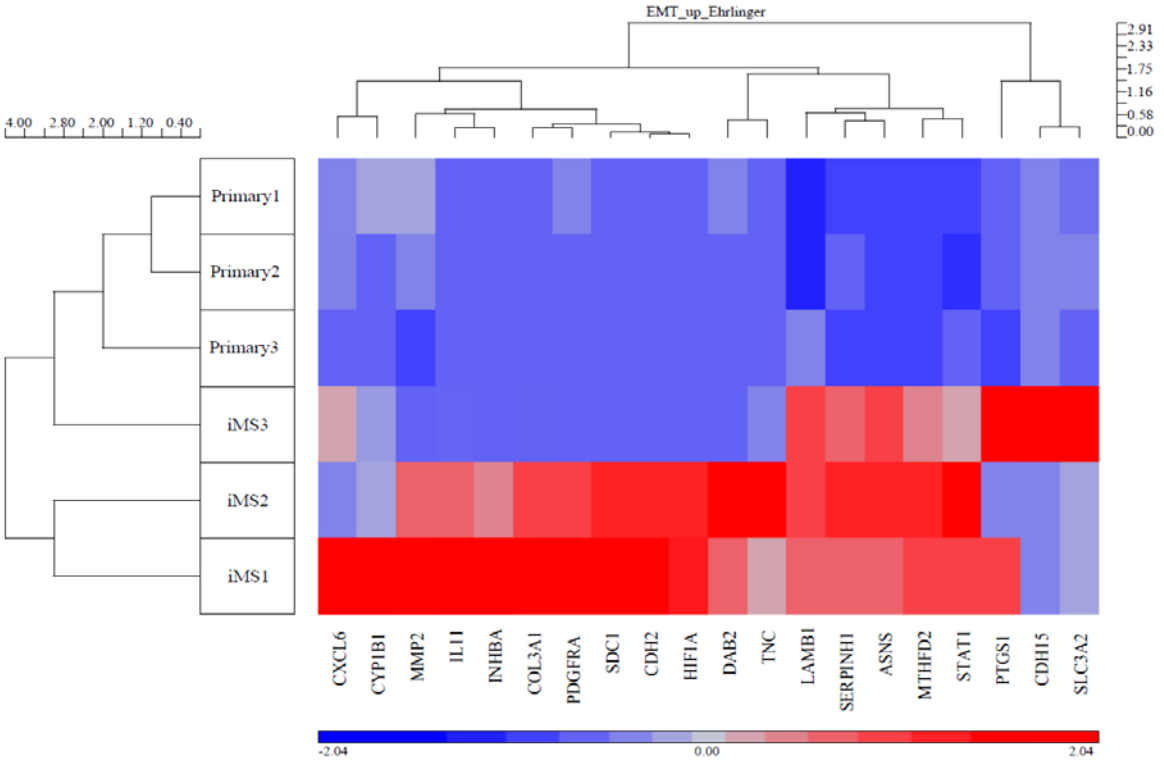

D. Wnt/β Catenin pathway

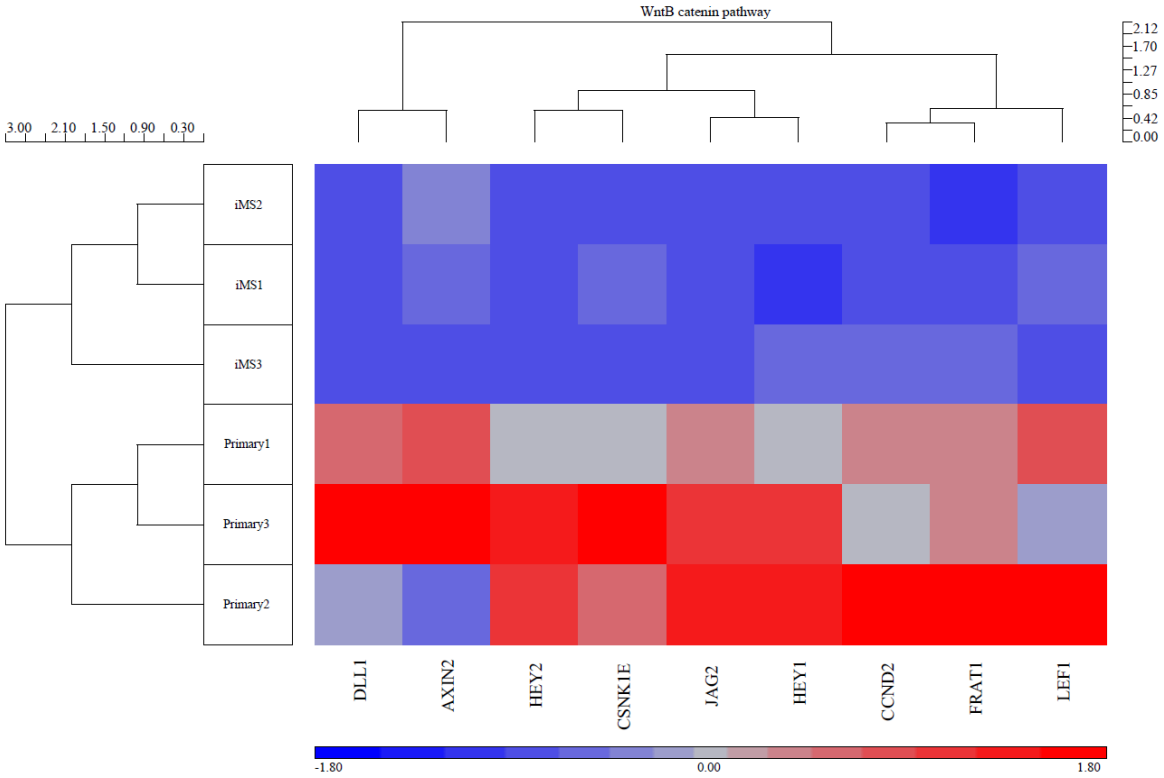

Figure 4. 4 Unsupervised clustering analysis of differentially expressed genes across primary adipocytes v/s iMS cells.

The results of triplicate RNA-seq data for each of the cell populations were analysed using Partek to generate the hierarchical clustering map for genes associated with (A) Adipogenesis, (B) ES cell core, (C) EMT pathway and (D) Wnt/β Catenin pathway**.**

4.2.2.2.2 AdMSCs v/s iMS cells

Having characterised some of the molecular changes that occur during the reprogramming process, we then set out to understand how iMS cells differ from AdMSCs. Although iMS cells have similar features to AdMSCs isolated directly from adipose tissue, we observed phenotypic differences between these cells in our previous analyses (eg with respect to *in vitro* proliferation and multilineage differentiation potential as described in Section **3.2.4**). We therefore performed a differential expression analysis comparing iMS cells to AdMSCs, and as described previously the differentially expressed genes were uploaded to IPA software for core analysis and then overlaid with the global molecular network within IPKB. In this case, there were only 344 DE genes, so all DE genes were used for the subsequent IPA analysis.

Among the canonical pathways that were significantly enriched in the 'AdMSCs v/s iMS cells' comparison were the Th1 and Th2 activation pathway, the G-protein coupled receptor signaling pathway, signaling by Rho family GTPases, Notch signaling, and pathways related to ES cell pluripotency (Figure 4.5A). Importantly, some of these pathways, such as the STAT3 pathway and calcium signaling, are known to be downstream of PDGF signaling, suggesting that these changes are directly due to the DCi reprogramming procedure. All categories of canonical pathways where differences were observed, and their associated genes, are listed in Supplementary Table S4. In addition, the top enriched diseases and functions with a *p*-value less than 0.05 were plotted (Figure 4.5B). This analysis indicated that diseases and cellular functions related to cell morphology, cell death and survival, cellular growth and proliferation as well as cellular development were seen to be significantly enriched. All categories of diseases and functions and their associated genes are also listed in Supplementary Table S4.

Taken together, these data provide some insight on the characteristics of DCi reprogrammed iMS cells which distinguish them from tissue-derived AdMSCs. For example, enrichment of pathways including GPCR signaling, Notch signaling and EMT pathway provides some hints on the altered cellular processes, however these findings need to be explored further to get a better understanding of the induced changes. Furthermore, enrichment of 'allograft rejection mechanisms' and 'GvHD' associated genes in iMS cells in comparison to AdMSCs is suggestive of improved immunosuppression. Overall, this transcriptomic analysis provides important understanding into the molecular differences between different cell populations tested. Our findings are consistent with the hypothesis that exposure to DCi reprogramming factors resets the transcriptional networks related to cell-fate and cell-growth kinetics and allows reactivation of the pluripotency program. The following sections will therefore aim to further validate these findings using *in vitro* characterization and functional assays.

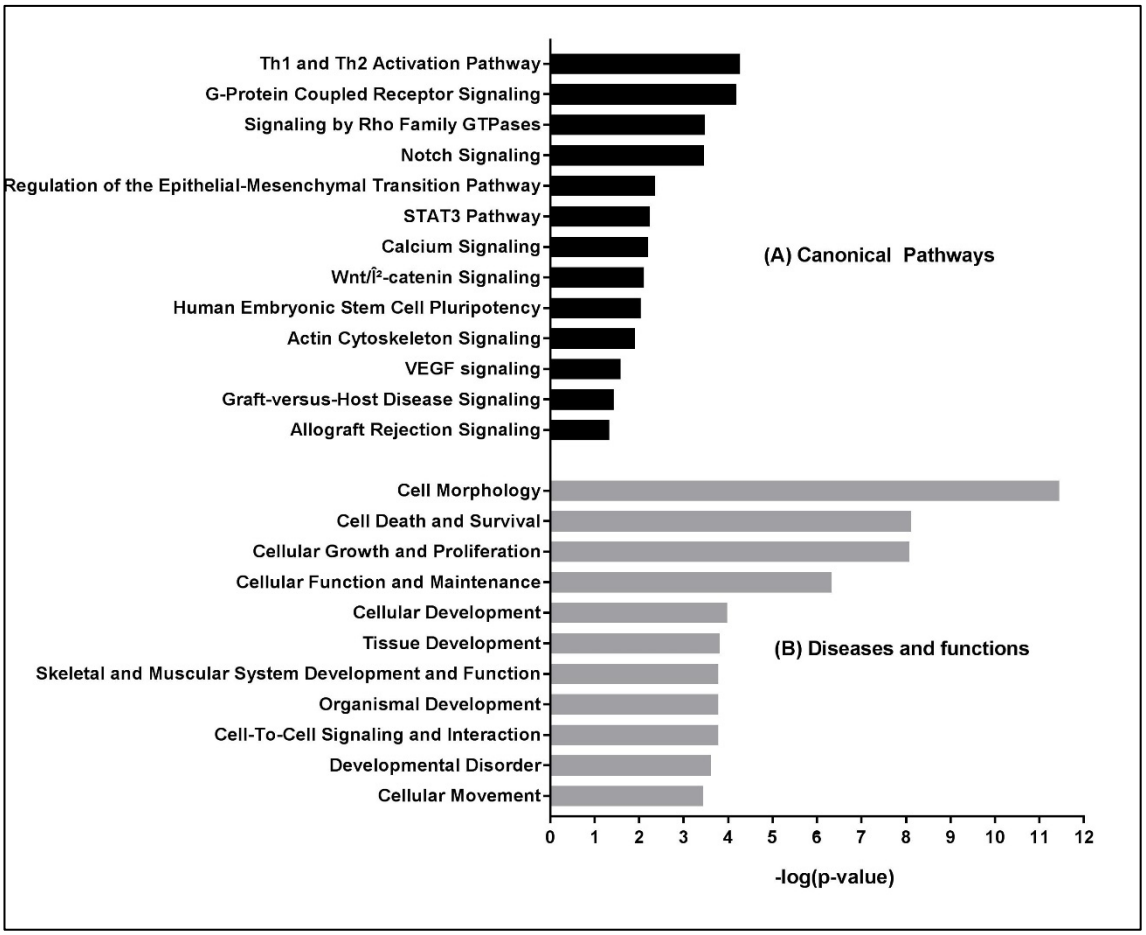

Figure 4. 5 Canonical pathways and categories of diseases and functions enriched in the comparison of 'AdMSCs v/s iMS cells', as derived from IPA.

Canonical pathways were selected following IPA 'Core Analysis' and filtered for p value ≤ 0.05.

4.2.3 DCi reprogrammed cells re-express pluripotency factors

We next attempted to validate our findings at the functional level. Preliminary results from our molecular analysis show upregulation of ES cell core genes which are a signature of pluripotency. In this section, I compared DCi reprogrammed iMS cells with pluripotent stem cells to get a better understanding of the features of DCi reprogrammed cells and more importantly understand the extent of induced de-differentiation. Numerous studies characterizing pluripotent stem cells at the molecular and functional level have been reported. Human pluripotent stem cells are known to express certain early developmental nuclear transcription factors including OCT4, Nanog, SOX2; keratan sulfate antigens TRA-1-60 and TRA-1-81 as well as the glycolipid antigens SSEA-3 and SSEA-4 (Boyer et al., 2005; De Los Angeles et al., 2015; Silva et al., 2009). A preliminary test for pluripotency characterization therefore includes evaluation of pluripotent cell marker expression at the molecular level.

WT C2 iPS cells originally obtained by episomal reprogramming of human fibroblasts (Briggs et al., 2013), (kindly provided by Prof. David Ma, St. Vincent's Clinic, Sydney, NSW, Australia) expressing OCT4, Nanog, SOX2 and SSEA4 served as positive controls for this assay. Patient-matched AdMSCs, treated AdMSCs and iMS cells were assayed for expression of these markers. The transcription factors OCT4, Nanog and SOX2 were expressed in treated AdMSCs and iMS cells in frequencies ranging from 0.25-3.5%. However, the glycolipid antigen SSEA4 was expressed in around 80% of the rhPDGF-AB/AZA treated cells. Notably, these markers were not detected in pre-treatment AdMSCs (Figure 4.6). This observation suggests that rhPDGF-AB/AZA treatment converts primary lineage committed cells into cells that are less differentiated than MSCs.

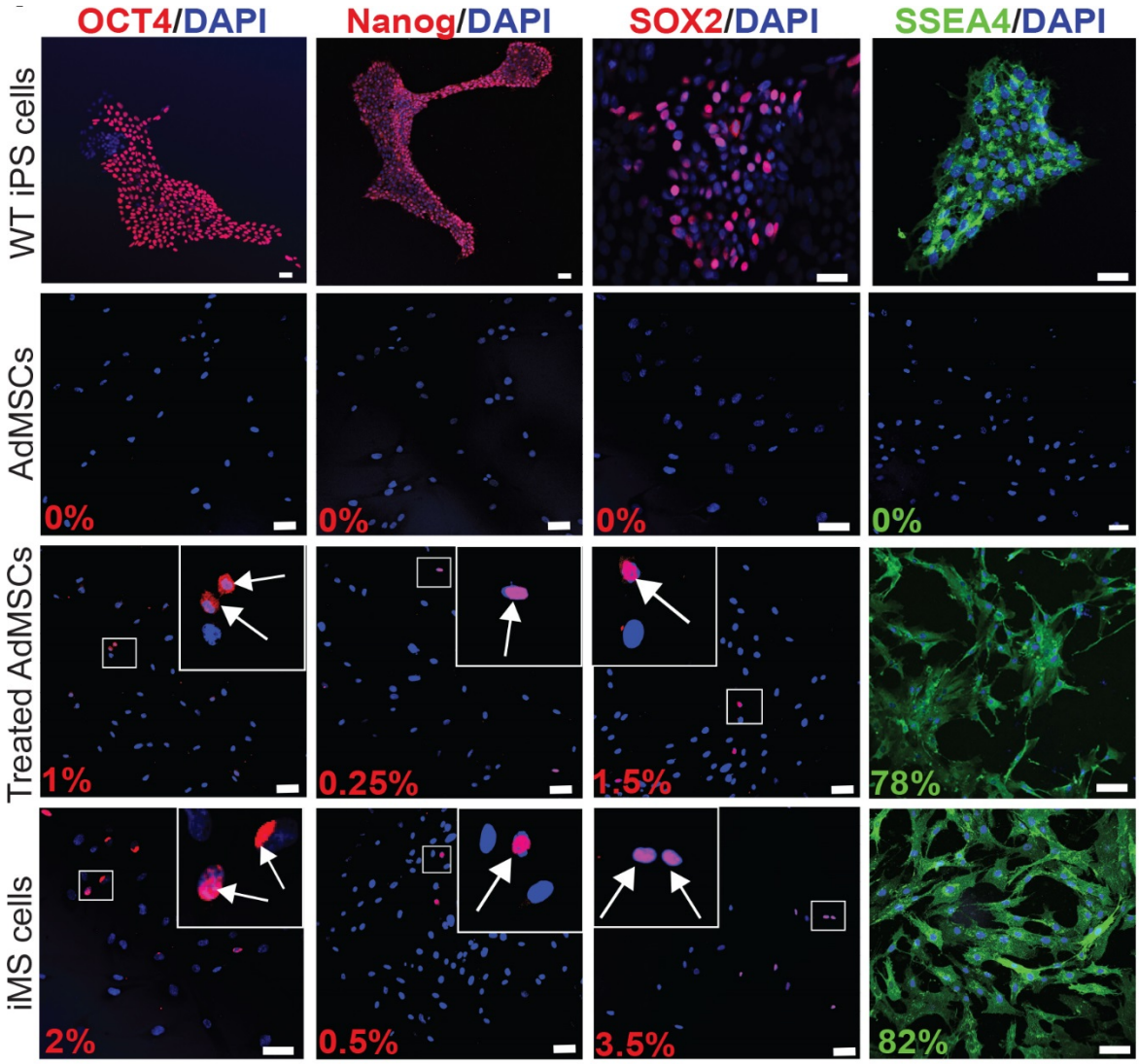

Figure 4. 6 DCi reprogrammed cells re-express pluripotency factors

Confocal images of immunofluorescent staining of WT iPS cells, pre-treatment AdMSCs, rhPDGF-AB/AZA-treated AdMSCs and iMS cells showing OCT4, Nanog, SOX2 and SSEA4 expression. Dual staining of DAPI and specific marker in treated AdMSCs and iMS cells is shown by white arrows and the percentages of cells expressing these stains are listed. (Scaled bar, 20 μm).

4.2.4 *In vitro* teratoma assay setup

Having shown that DCi reprogrammed iMS cells are pluripotent with respect to expression of pluripotency genes, we next asked whether they have the capacity to form teratomas and differentiate into cells of all the three embryonic germ layers thereby fulfilling another criterion of pluripotency. Testing the capacity to differentiate into tissues of all the three primordial germ layers can be done at *the in vivo* or *in vitro* level. Murine pluripotent cells are tested for their ability to contribute towards formation of chimeric embryo and potentially an entire organism. Human pluripotent cells cannot be tested in this way and are instead tested in a surrogate *in vivo* teratoma assay. This *in vivo* test involves injecting undifferentiated test cells into adult severe combined immunodeficient (SCID) mice. The functional read out of this test is formation of a benign teratoma at the site of injection that consists of multiple tissues differentiated from all the three primordial germ layers (Marti et al., 2013). The *in vivo* teratoma formation assay is the gold standard assay for pluripotency characterization (Daley et al., 2009; De Los Angeles et al., 2015), however it has certain limitations. This laborious *in vivo* assay requires animals and is time and cost consuming. Practical application of this assay is further jeopardized because of poor survival of the xenotransplanted cells in immunodeficient mice or failure to form *in vivo* teratomas in some cases (F. J. Muller et al., 2010). Collectively, all these factors warrant substitution of the *in vivo* teratoma assay with alternate assays.

An alternative *in vitro* assay designed by Masuda et al. involves development of teratomas from ESCs and iPS cells in a special culture technique (Masuda et al., 2012). This assay is based on their previously established organ culture system which includes culture of iPS cells/MSCs for a week on isolated fetal rat metanephrons, which acts as a

scaffold and provides the growth factors required for differentiation of the stem cells being assayed (Yokoo et al., 2006). The application of this assay is however limited due to the need of bona fide tissues from rat foetus and the technical complications associated with its isolation. These factors have in turn necessitated the development of other *in vitro* alternatives for assessment of tri-germ layer plasticity of stem cells. The following section describes the setup of a novel, surrogate *in vitro* teratoma assay adopted from the original method described for characterization of canine and equine iPS cells (Whitworth, Frith, et al., 2014; Whitworth, Ovchinnikov, et al., 2014).

The *in vitro* teratoma assay is carried out in low adherent 24 well cell-culture plates and involves the test cells being sandwiched in between two layers of methylcellulose gel to mimic the *in vivo* soft tissue microenvironment. On the first day, the plates are first layered with 2-3 mm of 9.5% methylcellulose gel. Once the gel is solidified, *in vitro* expanded cells are seeded at a density of 250,000 cells/well, making sure that the cells are concentrated in the centre of the well. The cells are provided with Knockout Serum Replacement (KSR) medium with rock inhibitor to alleviate any chances of cell-apoptosis. After 24 hours of incubation, each of the wells are topped with KSR medium alone. The cells gradually clump together forming dense aggregates. On the following day, the medium is completely removed and another layer of 2-3mm thick 9.5% methylcellulose is added on top of the cells. The gel is allowed to solidify following which the cells are replenished with fresh KSR medium. The cells are maintained for an extended period of 8 weeks in KSR medium without any supplementary growth or differentiation factors (Figure 4.7). Medium is changed every alternate day to ensure viability of the growing cell aggregates. The ability of test cells to undergo spontaneous multi-germ layer differentiation is evaluated by histology and immunocytochemistry on the *in vitro* teratomas (embryoid bodies) harvested at the assay endpoints.

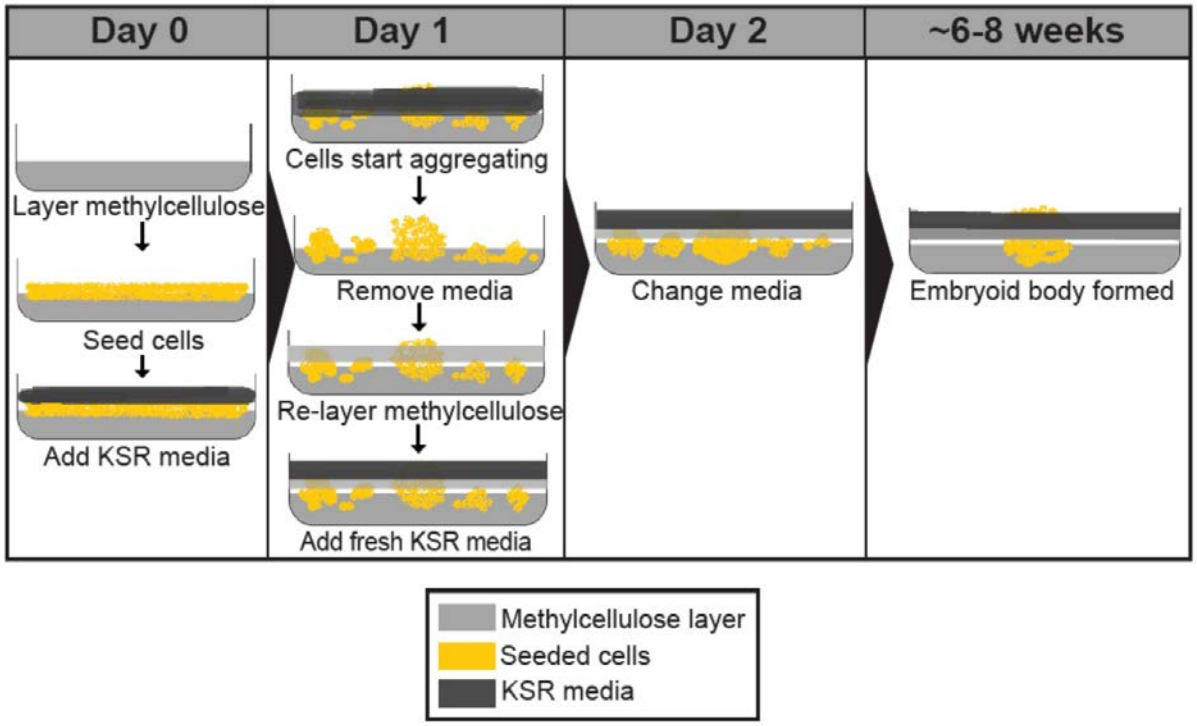

Figure 4. 7 *In vitro* teratoma assay setup

Schematic representation of steps involved in setting up the *in vitro* teratoma assay applying the original method described in Whitworth et al. (Whitworth, Frith, et al., 2014; Whitworth, Ovchinnikov, et al., 2014).

4.2.5 iPS cells exhibit tri-germ layer plasticity

In vitro expanded WT C2 iPS cells were used as positive controls for the above described *in vitro* teratoma assay. iPS cells were seeded at a density of $2.5x10^5$cells/well (n=15) in the above setup. At the end of eight weeks, the aggregated embryoid bodies were harvested and characterized by histology and immunocytochemistry for differentiation markers. Owing to their pluripotent nature, these iPS cells were able to proliferate and differentiate to form *in vitro* teratomas composed of derivatives of all three germ layers; namely squamous epithelium of endodermal origin, mature chondrocytes of mesodermal origin, and pigmented neuroepithelium of ectodermal origins. The E-Cadherin (E-CAD) stained endodermal columnar epithelial cells (Figure 4.8a) displayed distinct basal nuclei with clear secretion vacuoles (Figure 4.8b). Mature chondrocytes, as stained with the cartilage marker, SOX9 (Figure 4.8c) showed characteristic round and regular structures with holes and dark blue nuclei (Figure 4.8d). Cells positive for ectoderm marker, Tuj1 (Figure 4.8e) had round nuclei and thin cytoplasmic elongations (Figure 4.8f). These data confirm that the control WT C2 iPS cells display *in vitro* tri-germ layer plasticity.

The above findings validate feasibility of application of this *in vitro* teratoma assay and will be next applied on test cell populations. Having optimized the protocol on positive controls, I then moved on to evaluation of spontaneous *in vitro* differentiation potential in the test cell populations.

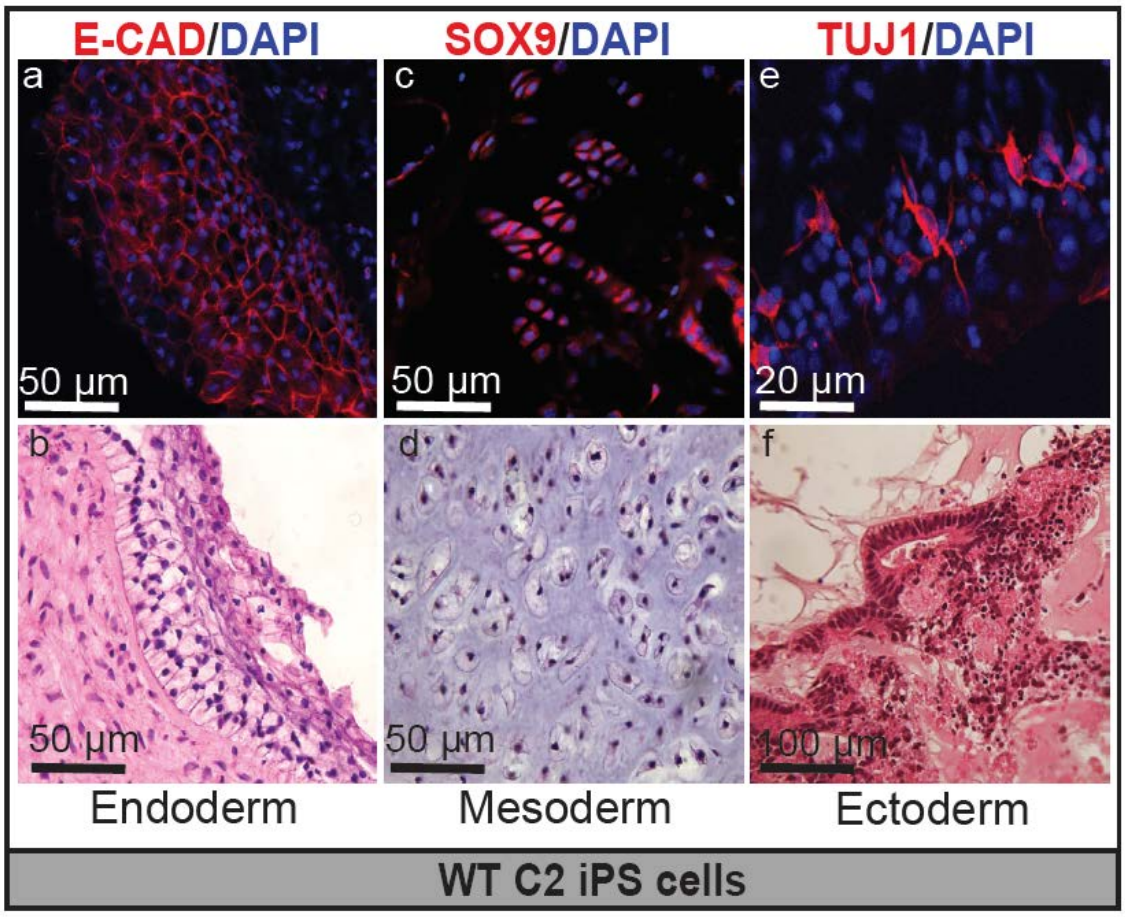

Figure 4. 8 WT C2 iPS cells exhibit *in vitro* tri-germ layer plasticity

H&E staining and immunofluorescence detection of the three germ layers in embryoid bodies generated from the WT C2 iPSC line. *Differentiation to endoderm* (squamous epithelium): E-CAD (red) marker with DAPI in blue (a) and H & E staining (b) *Differentiation to mesoderm* (cartilage): SOX9 (red) marker with DAPI in blue (c) and H & E staining (d) *Differentiation to ectoderm* (pigmented neuroepithelium): TUJ1(red) marker with DAPI in blue (e) and H & E staining (f) Image information: (a,c,e) taken on Optical Microscope Leica DMIL; (b,d,f) taken on Confocal Microscope Zeiss LSM 780. (Scale bars: as depicted).

4.2.6 DCi reprogrammed iMS cells do not exhibit spontaneous *in vitro* tri-germ layer plasticity

The translational objective of this project is to apply DCi reprogrammed iMS cells for *in vivo* tissue repair and regeneration purposes. Spontaneous teratogenicity, which leads to context-independent differentiation into cells of multiple lineages, is an undesirable feature for cells intended for therapeutic applications. To evaluate their spontaneous tri-germ layer plasticity, the *in vitro* teratoma assay was performed on AdMSCs, treated AdMSCs, and iMS cells obtained from DCi reprogramming of mature primary adipocytes. All three test populations were patient-matched and taken at early passages (P1/P2). Briefly, $2.5x10^5$ cells were seeded per well and sandwiched between two layers of 9.5% methylcellulose as outlined in **4.2.4.** The cells were cultured in KSR medium without any supplementary growth or differentiation factors. The assay was carried out for a total of eight weeks with medium changes every alternate day.

The seeded cells formed dense aggregates and continued to grow and proliferate in culture as evident from increase in size of the cell aggregates throughout the assay. This observation was similar to that seen in case of positive control WT C2 iPS cells. At the end of the assay, the cell aggregates (putative *in vitro* teratomas) were harvested, fixed and cryo-sectioned for histological analysis as described in **2.2.7.3.** H & E staining was first conducted on the sections to determine spontaneous differentiation through morphological changes. Although all the test cell populations continued to thrive, none of them could give rise to differentiated cells in this setting. In each of the three test cell populations, the cell aggregates contained only undifferentiated stromal-like cells, likely of the mesodermal origin (Figure 4.9). The absence of endodermal and ectodermal

lineage-derived cells in the cell aggregates indicates limited potency of untreated and treated AdMSCs as well as iMS cells in this test environment. All these cell populations therefore lack spontaneous *in vitro* tri-germ layer plasticity as determined in this *in vitro* teratoma assay.

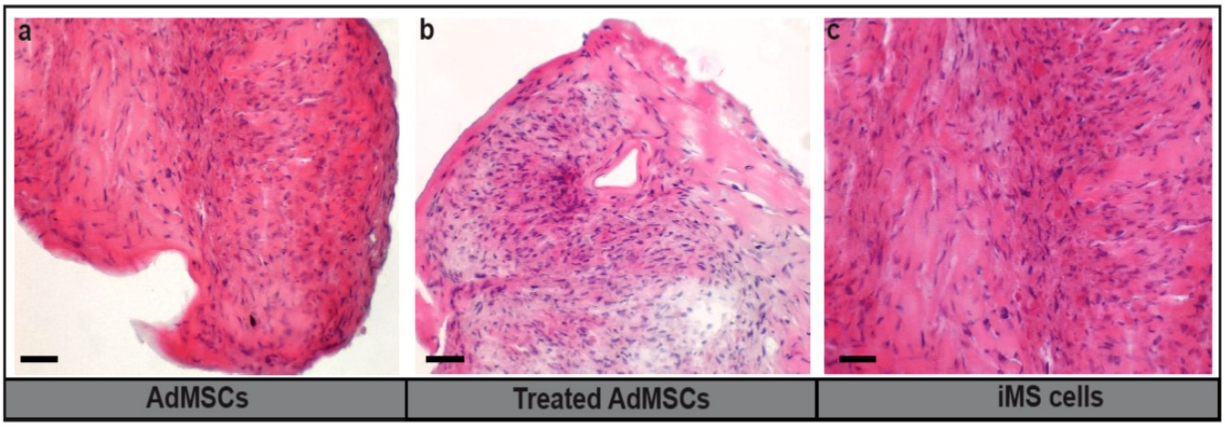

Figure 4. 9 DCi reprogrammed iMS cells do not exhibit *in vitro* tri-germ layer plasticity

H&E staining for sections of *in vitro* teratomas obtained from (a)AdMSCs, (b) Treated AdMSCs and (c) iMS cells cultured individually in the *in vitro* teratoma assay. (Scale bars, 100 µm).

4.2.7 DCi reprogrammed iMS cells do not display improved *in vitro* plasticity when co-cultured with iPS cells

Pluripotency can be induced by co-culture with pluripotent ES cells (Cowan et al., 2005). Additionally, DCi reprogrammed murine iMS cells when co-transplanted with murine ES cells showed contribution to tissues of the ectodermal, mesodermal as well as endodermal lineages *in vivo* (Chandrakanthan et al., 2016). We therefore hypothesized that iMS cells would gain features of pluripotency when co-cultured in an instructive environment provided by pluripotent stem cells. To evaluate their tri-germ layer plasticity in the presence of other pluripotent cells, the *in vitro* teratoma assay was therefore performed on patient and passage-matched AdMSCs, treated AdMSCs and iMS cells co-cultured with WT C2 iPS cells[20]. In order to enable distinction between the iPS cells and test cells in the co-culture system, all the three types of cells i.e. AdMSCs, treated AdMSCs and iMS cells were first transduced with a lentiviral vector carrying a double reporter construct, LeGO-iG2-Luc2, (obtained from Kristoffer Weber-Riecken, University Medical Centre Hamburg, Germany) expressing green fluorescent protein (GFP) and luciferase, all under the control of a common CMV promoter, as detailed in **2.2.9** and in Figure S6 (for vector map). The GFP tagged test cells could therefore be distinguished from control WT C2 iPS cells.

On the first day of assay setup, test cells mixed with WT C2 iPS cells in different ratios as depicted in Table 4.1. The mixed cells were then seeded at a density of $2.5x10^5$ per well as per the protocol described in **2.2.7.1.** The co-cultures were maintained in the *in vitro* teratoma assay for a total duration of eight weeks, with medium changes on alternate days. Cell aggregates formed at the end of the assay from each of the conditions

[20] This experiment was conducted in replicate with test cell populations obtained from two different individuals with WT C2 iPS cells being the same in each case.

were carefully harvested and processed as described in **2.2.7.3.** and subjected to H & E staining.

Table 4. 1 Table depicting different combinations of test cells co-cultured with WT C2 iPS cells in different ratios

Co-culture of	iPS cells:AdMSCs	iPS cells:treated AdMSCs	iPS cells: iMS cells
Condition 1	1:1	1:1	1:1
Condition 2	3:1	3:1	3:1
Condition 3	5:1	5:1	5:1
Condition 4	1:3	1:3	1:3
Condition 5	1:5	1:5	1:5

Grid showing combinations of WT C2 iPS cells and test cell populations i.e. AdMSCs, treated AdMSCs and iMS cells co-cultured in different ratios[21] and cultured in the *in vitro* teratoma assay. All combinations were tested in triplicate.

[21] The total seeding density was kept constant at $2.5x10^5$ cells/well.

Imaging of these H & E stained sections revealed patches of necrotic cells in each of the conditions tested for all three types of co-cultures. This was evident from presence of disintegrated nuclei (Figure S7). This observation held true for all the different cell populations tested (Figure 4.10). Morphological evaluation showed the presence of mostly degenerated structures as opposed to intact cells seen in individual cultures of control WT C2 iPS cells (compare Figure 4.10 to Figure 4.9).

The above data is suggestive of an adverse effect of culturing together cells from different sources which might have occurred as a result of the test cell populations responding inappropriately to cues from the iPS cells. Since the WT C2 iPS cells and AdMSCs/treated AdMSCs or iMS cells were obtained from different individuals, the observed degeneration could be a result of immune reactivity and merits further investigation. There is also the possibility that the medium composition is not suitable for long-term culture of MSCs or iMS cells when combined together with iPS cells. Competition for space and nutrients in the co-cultures could be another factor that might have influenced the inability of the cells to undergo differentiation. Moreover, in this assay, we only tested one cell seeding density of $2.5x10^5$ cells/well. It might be beneficial to understand the effects of seeding cells at higher or lower densities. Additionally, the assay can be further refined to include rotating bioreactors similar to that reported in (Distefano et al., 2018) which would facilitate better interaction between the two cell populations in co-culture. These rotating conditions would also ensure effective exposure of nutrients provided in the culture medium to all the cells of the developing spherical embryoid body.

Based on our existing data we are unable to definitively conclude whether human iMS cells are pluripotent by the definition of teratoma formation. We have earlier shown

that mixtures of murine ES cells and murine iMS survive together and form *in vivo* teratomas comprised of cells of all the three germ layers (Chandrakanthan et al., 2016). Traditional *in vivo* teratoma assays will be required to resolve whether these murine observations can be replicated in the human setting.

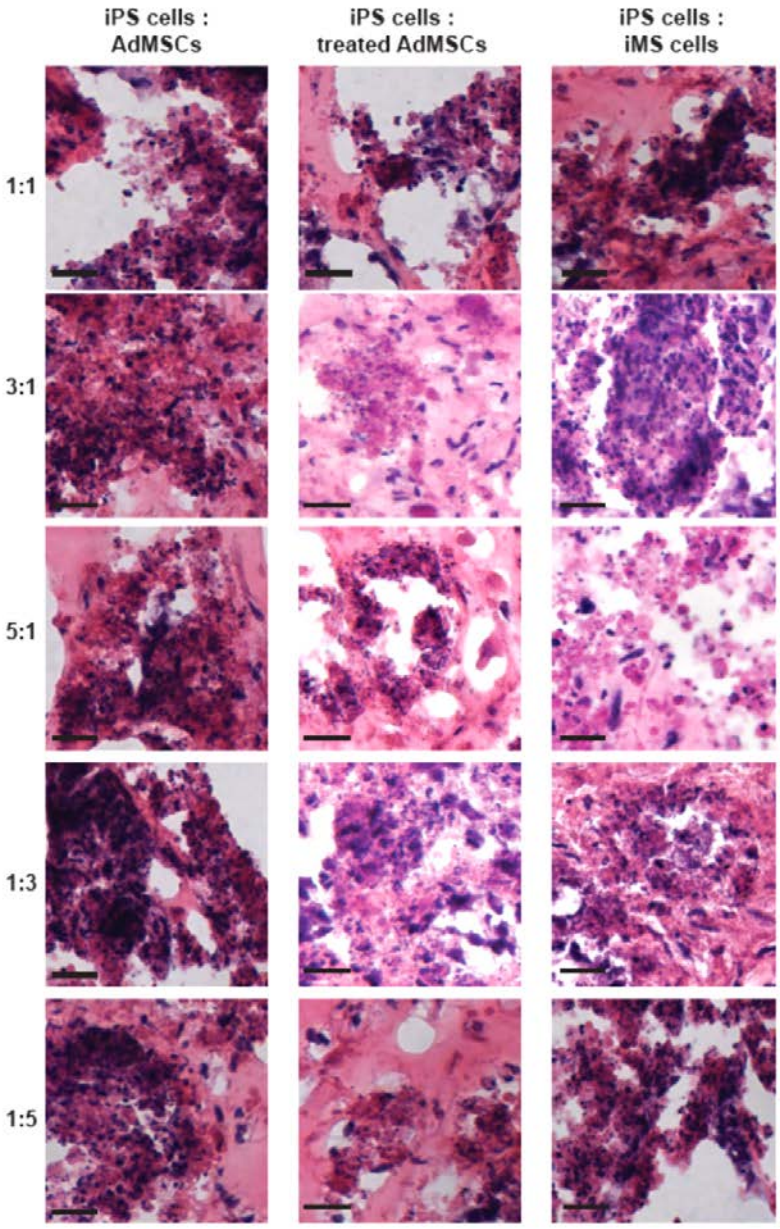

Figure 4. 10 iMS cells lack tri-germ layer plasticity even when co-cultured with iPS cells.

Representative H & E stained sections of *in vitro* teratomas obtained from co-cultures of iPS cells with AdMSCs, treated AdMSCs and iMS cells. No distinct differentiated cells could be detected in any of the co-cultures in any of the five different ratios tested. Necrotic cells with disintegrated nuclei could be seen in each of the co-cultures. (Scale bar, 100 µm).

4.3 Chapter summary and discussion

This chapter covers characterization of DCi reprogrammed cells at the molecular level and attempts to evaluate their pluripotency at the *in vitro* level. The aim of these investigations was to understand the effect of DCi reprogrammed cells from the transcriptomic perspective and the degree of de-differentiation or cell fate reversal induced by exposure to AZA and rhPDGF-AB in somatic cells.

When compared to the starting population of primary adipocytes, DCi reprogrammed iMS cells showed downregulation of adipogenesis pathway and PPAR signaling (Figure 4.4, S5). A simultaneous upregulation of ES core genes, the EMT pathway as well as pluripotency genes (Figure 4.4, S5) further substantiated bona fide cell fate reversal, as a consequence of exposure to DCi reprogramming. The significant activation of cell cycle functions, cellular movement and overall embryonic and organismal development (Figure 4.3) also explain the gain in cell survival and proliferation capacity in iMS cells which was lacking in pre-treatment adipocytes. Moreover, DCi reprogramming also resulted in downregulation of genes associated with TGFβ signaling and the allograft rejection mechanism, and upregulation of genes associated with PDGF signaling, JAK-STAT signaling and PI3K-AKT-mTOR signaling in iMS cells (Figure 4.3 and Figure S5). TGFβ is a master regulator of fibrosis (Meng et al., 2016), and its downregulation in iMS cells accompanied by suppression of genes associated with the allograft rejection mechanism support the application of iMS cells at the *in vivo* level, in that they would likely be well-tolerated upon xenogeneic transplantation. While PDGF signaling has been implicated in tissue remodelling and cellular differentiation (Hoch & Soriano, 2003), JAK-STAT signaling mediates cell survival in response to tissue stress (La Fortezza et al., 2016) and PI3K-AKT-mTOR

signaling has been implicated in tissue maintenance and repair(Chen et al., 2013; Peiris et al., 2016). Taken together, these findings suggest that the generated iMS cells acquire enhanced proliferative and regenerative potential as a result of DCi reprogramming.

Comparison of 'AdMSCs v/s iMS cells' revealed enrichment of the immune related Th1 and Th2 activation and IL-17A signaling pathways along with Notch signaling (Figure 4.5). Earlier reports have shown that IL-17A-induced MSCs are superior modulators of immune functions (Sivanathan et al., 2015) and tissue repair mechanisms can be promoted by modulation of the immune system (Julier et al., 2017). Other pathways such as the STAT3 pathway and Calcium signaling are downstream pathways of the PDGF signaling circuitry (Hoch & Soriano, 2003). Indeed, significant enrichment of these pathways with parallel involvement of cell growth, proliferation and migration processes (Figure 4.5) provide some reasons underlying the enhanced potency of iMS cells in comparison to AdMSCs. All these features in turn highlight the molecular differences between iMS cells and AdMSCs. However, a better understanding of the involved gene networks and upstream regulators would aid in acquiring a deeper understanding of the transcriptomic changes induced by DCi reprogramming. Insights gained from these studies could also be used to better modulate the cell conversion process and achieve higher reprogramming efficiency.

Our functional validation study, which demonstrated expression of the pluripotency associated markers, OCT4, Nanog, SOX2 and SSEA4 in iMS cells, also distinguishes AdMSCs and iMS cells from untreated AdMSCs (Figure 4.6). Unlike WT iPS cells, untreated or treated AdMSCs and iMS cells did not undergo spontaneous differentiation when assessed by the *in vitro* teratoma assay (Compare Figure 4.8 to Figure 4.9). Microenvironment plays an influential role in determining the differentiation

fate of the cells in culture. This assay was tested with only one type of gel/matrix i.e. methylcellulose and only at a single strength (9.5%) (as described in **4.2.4**, Figure 4.7). Previous studies have reported that stiffness of extracellular matrix can directly influence the fate of cultured stem/stromal cells (Talele et al., 2015). Additionally, the *in vitro* teratoma assay involved culturing cells in KSR medium without any supplementary cytokines or growth factors. Although control iPS cells could thrive and differentiate into cells representative of all the three germ layers in this setting (Figure 4.8), these culture conditions were not conducive for differentiation of any of the test cell populations (Figure 4.9). This observation justifies the lack of developmental potency in MSCs which is inherent in ES cells and is acquired in iPS cells. It also indicates that untreated and treated AdMSCs, as well as iMS cells, rely on external cues (from culture medium or microenvironment) in order to fully manifest their multilineage differentiation potential. Notably, none of the test cell populations when cultured by themselves underwent cell death or apoptosis (Figure 4.9). This observation also provides an implication towards the potential role of serum-based growth/differentiation factors for causing lineage commitment in the test cell populations. The KSR culture medium of the *in vitro* teratoma assay lacked these nutrients thereby hampering differentiation of the test cell populations. This in turn substantiates the inability of test cell populations to undergo spontaneous multi-lineage differentiation *in vitro*.

Preliminary results from the above *in vitro* teratoma study suggest that DCi reprogrammed iMS cells could be safely used for *in vivo* transplantation studies. However, a comprehensive understanding of the spontaneous teratoma formation capacity of stem cells is required in order to assess the potential risks of using such cells in a clinical setting. It is hence important to evaluate and validate pluripotency by the gold standard *in vivo* teratoma formation assay (Nelakanti et al., 2015).

In summary, these data show that rhPDGF-AB/AZA treatment converts primary lineage-committed cells into cells that have molecular and phenotypic features different than MSCs. DCi reprogrammed cells are also distinct from pluripotent cells in that they cannot form spontaneous *in vitro* teratomas, at least in our *in vitro* assay, and display low expression of pluripotency associated factors. It will be interesting to know if, and in what respect, these differences are manifested at the *in vivo* level. More importantly, it would be worthwhile to assess whether DCi reprogramming confers iMS cells with improved *in vivo* plasticity and tissue repair potential compared to naturally occurring MSCs. These questions will be addressed in subsequent chapters.

CHAPTER 5 Evaluation of *in vivo* safety and plasticity of human iMS cells

5.1 Introduction

MSCs have been touted as an attractive source for cell therapy to treat degenerative disorders owing to their attributes of plasticity, self-renewal potential and immunomodulation (Horie et al., 2012; N. K. Lee et al., 2017). However, there is little objective evidence that they are retained at the site of injection or that they directly contribute to new tissue formation (Bianco et al., 2013). For clinical application, the transplanted cells must be maintained in an *in vivo* environment of tissue loss and should subsequently undergo context-dependent differentiation in order to bring about reconstitution of the damaged tissues. However, the ability of stem cells to undergo proliferation and differentiation in the presence of appropriate stimuli also risks malignant transformation and ectopic tissue formation *in vivo* (Herberts et al., 2011). This chapter will thus focus on investigating the *in vivo* safety and efficacy of human iMS cells to survive and integrate into injured recipient mouse tissues.

In the previous chapters, I have detailed *in vitro* characteristics of reprogrammed human iMS cells, and their similarities and differences in relation to corresponding tissue resident AdMSCs. Compared with AdMSCs, DCi reprogrammed iMS cells (described in **3.5**) and treated AdMSCs (described in **4.3.1**) displayed improved capacity to differentiate into cells of multiple lineages when cultured *in vitro* in respective induction media. Additionally, AdMSCs did not display any features of pluripotency at the *in vitro* level whereas iMS cells and treated AdMSCs expressed pluripotency associated markers (described in **4.3.2**). Based on these differences, we hypothesized that treated AdMSCs

might behave differently to AdMSCs *in vivo* with respect to their retention and differentiation efficiency. The following experiments include treated AdMSCs as another test cell population along with corresponding iMS cells.

5.2 Study design

To evaluate the *in vivo* safety and efficacy of reprogrammed human iMS cells, a generic postero-lateral inter-lumbar vertebral disc injury model in immunodeficient NOD/SCID/Gamma (NSG) mice was used. In mammals, the articular cartilage lacks the capacity to repair itself following damage and hence poses an interesting target for developing new repair strategies. Moreover, the cartilage tissue is immune-privileged (Sun et al., 2013), and does not elicit an inflammatory immune response on encountering foreign cells, thereby providing a favourable environment for testing the behaviour of xenogeneic iMS cells.

iMS cells obtained after DCi reprogramming of patient-derived adipocytes, along with corresponding patient-matched AdMSCs and treated AdMSCs were used for this *in vivo* study. To enable *in vivo* tracking of the transplanted cells and their differentiated forms, all cell types i.e. AdMSCs, treated AdMSCs and reprogrammed iMS cells were transduced with a lentiviral vector carrying a double reporter construct, LeGO-iG2-Luc2, (obtained from Kristoffer Weber-Riecken, University Medical Centre Hamburg, Germany) expressing green fluorescent protein (GFP) and luciferase, all under the control of a common CMV promoter, as detailed in **2.2.7** and Figure S5 (for vector map). Luciferase expression of the transduced cells was first validated *in vitro*. iG2-Luc2 transduced AdMSCs, treated AdMSCs and iMS cells were seeded in standard 96-well tissue culture plates at serial densities ranging from 20000 to 156 cells/well. BLI signal was measured on the following day after addition of D-luciferin substrate (150µg/mL) to

each of the wells. A positive correlation was observed between BLI signal intensity and cell seeding density (Figure 5.1).

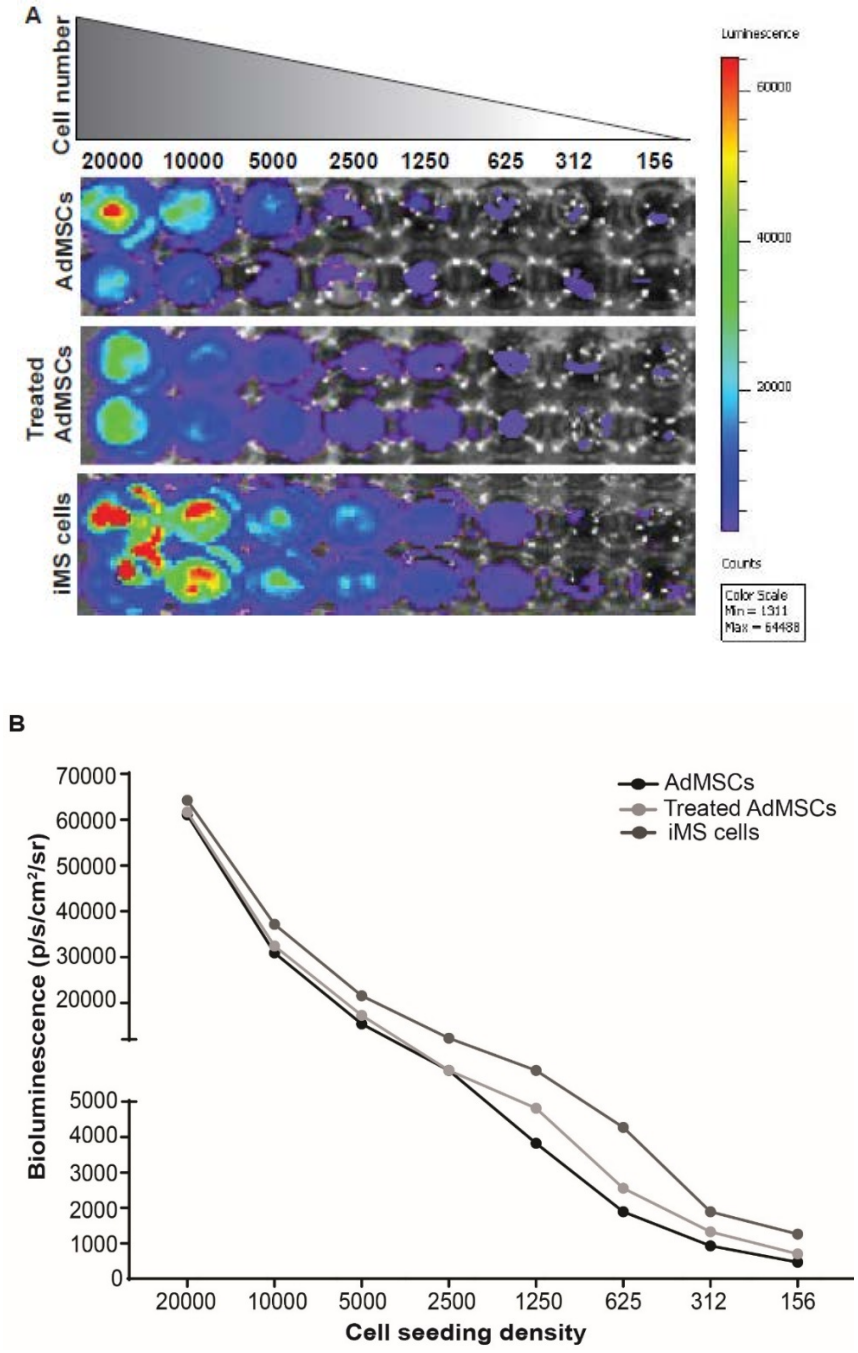

Figure 5. 1 In vitro validation of LeGO-iG2-Luc2-GFP transfection.

(A) Photograph showing bioluminescence of AdMSCs, treated AdMSCs and iMS cells that were plated at densities of 20000, 10000, 5000, 2500, 1250, 625, 312 and 156 cells/well, from left to right. (B) Quantification of the bioluminescence in (A) (photons/sec/cm^2/sr) showing that the signal intensity decreased with reduction in cell number (n=2, Mean±SD).

The transduced cells were then expanded *in vitro* to obtain a cell number sufficient for transplantation at a density of $1x10^6$/side of the spine of host animal. A day prior to the surgery, AdMSCs, treated AdMSCs and reprogrammed human iMS cells were loaded onto biodegradable Helistat^{TM} collagen sponges. On the day of surgery, cells were transplanted into the postero-lateral gutters adjacent to the decorticated lumbar (L4-L5) vertebrae of immunodeficient female NSG mice (n=8 in each cell-type group) (Figure 5.2). In this process, surrounding connective tissue, muscle and bone were also damaged as previously detailed in (Rao et al., 2007) and described in **2.2.11.**

Transplantation of stably transduced cells permitted non-invasive monitoring of cell survival *in vivo* using bioluminescence imaging (BLI). 24 hours after transplantation, the mice were intraperitoneally injected with D-luciferin (150mg/kg body weight) and were assessed for bioluminescence. In order to track the transplanted cells, periodic BLI was done every 2 weeks for the next 3 months, and monthly thereafter for a total of 6 months or 1 year, depending on the study endpoint. Engraftment of transplanted cells and their contribution to different tissues was evaluated by immunostaining for GFP along with co-expression of lineage specific markers.

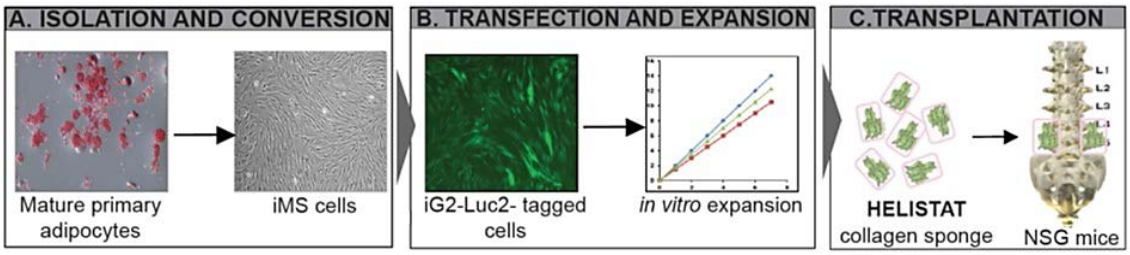

Figure 5. 2 Schematic representation of workflow for postero-lateral inter-lumbar vertebral injury model.

(A) Schematic depicting mature primary adipocytes isolated from patient-derived adipose tissue that were subjected to DCi reprogramming to obtain iMS cells. (B) Reprogrammed iMS cells[22] were transfected with lentiviral LeGO-iG2-Luc2 vector and expanded *in vitro* to generate cell numbers adequate for transplantation. (C) Schematic showing cells loaded onto biodegradable Helistat^{TM} collagen sponges and their transplantation into the decorticated postero-lateral gutters of L4-L5 vertebra in NSG mice.

[22] Along with reprogrammed iMS cells, different study groups included transplantation with AdMSCs or treated AdMSCs (not shown in schematic).

5.3 Results

5.3.1 Donor cells are retained at the transplant site

Transfection with LeGO-iG2-Luc2 vector also allowed *in vivo* tracking of transplanted human cells. Periodic BLI was conducted on each of the recipient mice (of all the study groups) to evaluate cellular persistence at the transplant site as described in **2.2.11.3.** Retention of the BLI signal at the transplant site was recorded over an extended period of 1 year showing robust long-term survival of the integrated human cells in the host spine region. Instances of cell migration and ectopic tissue formation were ruled out as no unexpected BLI signal was detected in any of the animals (Figure 5.3A).

Quantitative bioluminescence intensity was recorded to be the highest at 7 days post-transplant, which I interpret as time taken for the human cells to acclimatize and begin proliferating in a foreign, injured environment. After 7 days, the signal decreased steadily in animals from all the groups. This could be explained by gradual clearance of a proportion of transplanted cells that do not survive in the host tissue environment but retention of those competent cells that could possibly differentiate to eventually undergo effective integration into the host tissues. At 12 months post-surgery, the BLI signal was still found to be localized at the site of transplant suggesting effective engraftment of the transplanted cells (Figure 5.3). An approximate number of cells retained at the transplant site at 1 year can be back-calculated based on our *in vitro* validation (Figure 5.1) and can be estimated to be around $1x10^5$ AdMSCs, $1.7x10^5$ treated AdMSCs and $2.5x10^5$ iMS cells.

Therapeutic application of a given donor cell population requires its long-term maintenance at the site of transplantation. Detection of luciferase expression at the site of injection after 1 year of implantation confirmed that the human cells survived and

maintained vascular connection with host tissue over long-term. The transplanted cells did not home to distant, non-target sites either as established by localization of bioluminescence within the site of injection. This observation was true for all the three study groups i.e. AdMSCs, treated AdMSCs and iMS cells (Figure 5.3A). After 1 year, there was no evidence of tumorigenicity or marked inflammation in any of the animals emphasizing the safety of transplanted cells for clinical purposes. However, detailed evaluation of *ex vivo* luciferase expression in individual organs harvested from the animals is necessary to validate these findings.

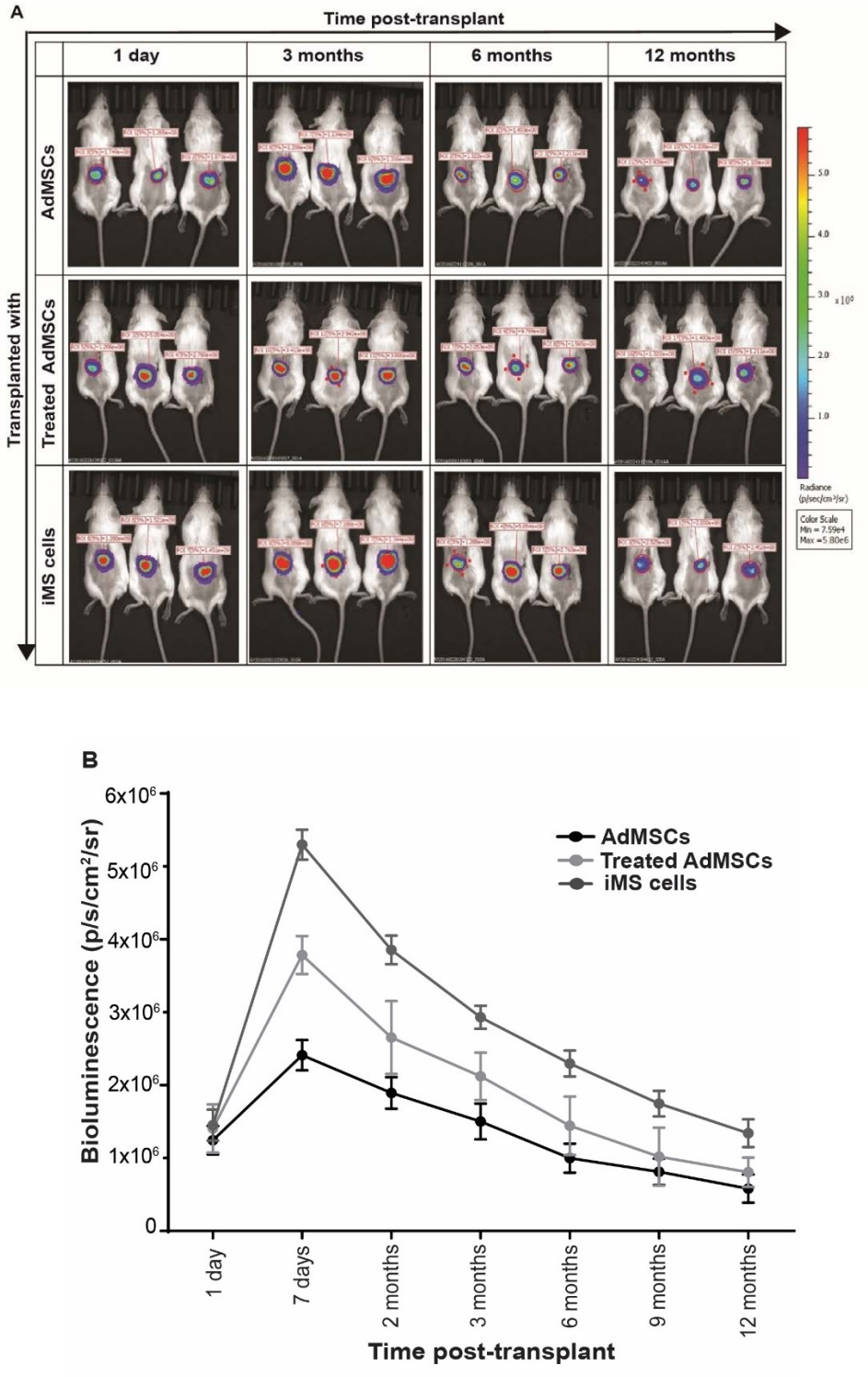

Figure 5. 3 Localization and survival of transplanted cells in the spine region

(A) Scans of periodic BLI showing persistence of transplanted cells at injection site within the recipient mice from 1 day to 12 months post-surgery. (B) Quantification of BLI signal intensity in spine region at successive time-points after surgery. (n=3; Mean ± SD).

5.3.2 Transplanted cells do not enter host circulation

For efficient integration of transplanted cells into the host tissues, retention of viable cells at the transplant site is vital. LeGO-iG2-Luc2 transfection imparts terminal GFP expression on the recipient cells. To understand if transplanted human cells had entered host circulation, mouse peripheral blood (collected at 3, 6 and 12 months post-surgery) was checked for presence of GFP positive cells by flow cytometry. Absence of GFP positive human cells in circulation indicated retention at the injury site. This observation held true for all the three study groups (Figure 5.4).

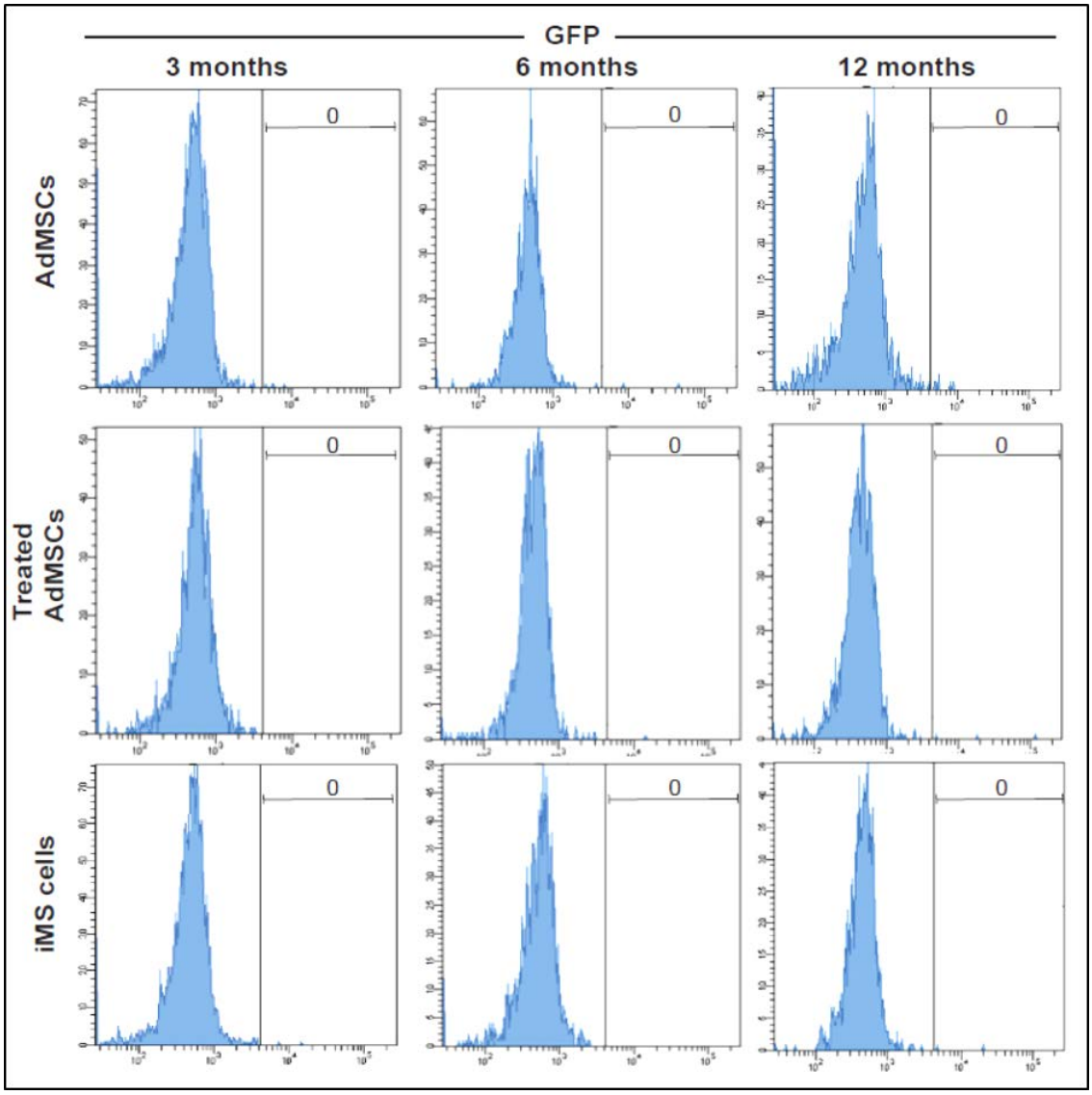

Figure 5. 4 Evaluation of transplanted cells in host circulation.

Representative flow cytometry profiles of peripheral blood collected at 3, 6 and 12 months post-surgery from recipient mice (n=2 for 3 months endpoint, n=3 for 6 and 12 months endpoint) transplanted with AdMSCs, treated AdMSCs and iMS cells, tested for GFP expression. No GFP positive human cells were detected in any of the animals at any time point tested.

5.3.3 Donor cells are maintained as undifferentiated cells at 3 months post-transplant

As the human cells were retained at the injection site within the decorticated, injured spine; our next step was to confirm the efficacy of these transplanted cells and their ability to undergo *in situ* differentiation. On reaching the first endpoint of 3 months, animals (n=2 from each study group) were humanely sacrificed by euthanization. Spine sections were harvested by aseptic techniques and fixed in 4% PFA. 20 µm serial sections of decalcified, paraffin/OCT embedded spines were used for immunohistochemistry and confocal microscopy as described in **2.2.11.4.**

H & E staining on the cross-sections did not reveal any differences in gross tissue architecture across animals transplanted with AdMSCs, treated AdMSCs or iMS cells (Figure 5.5). Immunofluorescence studies on these cross-sections demonstrated the presence of GFP positive donor cells retained at the transplant site. These cells were viable and were maintained as morphologically undifferentiated cells. Double immunofluorescent staining of GFP expressing cells with markers specific for blood vessel, bone, skeletal muscle or cartilage further confirmed the absence of differentiated cells of the mesodermal lineage (Figure 5.6). These findings suggest that the human cells, though sustained at the transplant site, are not responsive to cues presented by the murine host environment to differentiate into mature specialized cells within 3 months of transplant. This could be attributed to the existing species barrier between the donor cells and recipient tissues. However, the retention of bioluminescence beyond 3 months (Figure 5.3) encouraged us to continue the experiment and evaluate the behaviour of donor cells at the next endpoint.

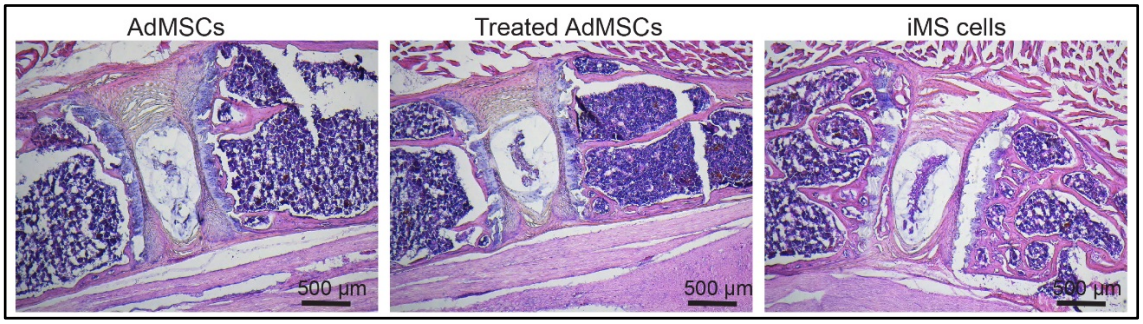

Figure 5. 5 Tissue sections do not show any differences in gross architecture at 3 months post-transplant.

Representative images of H & E stained tissue sections harvested at 3 months after transplantation with AdMSCs, treated AdMSCs or iMS cells. Overall, no major structural differences could be deciphered between different tissue sections (Scale bars. 500 µm).

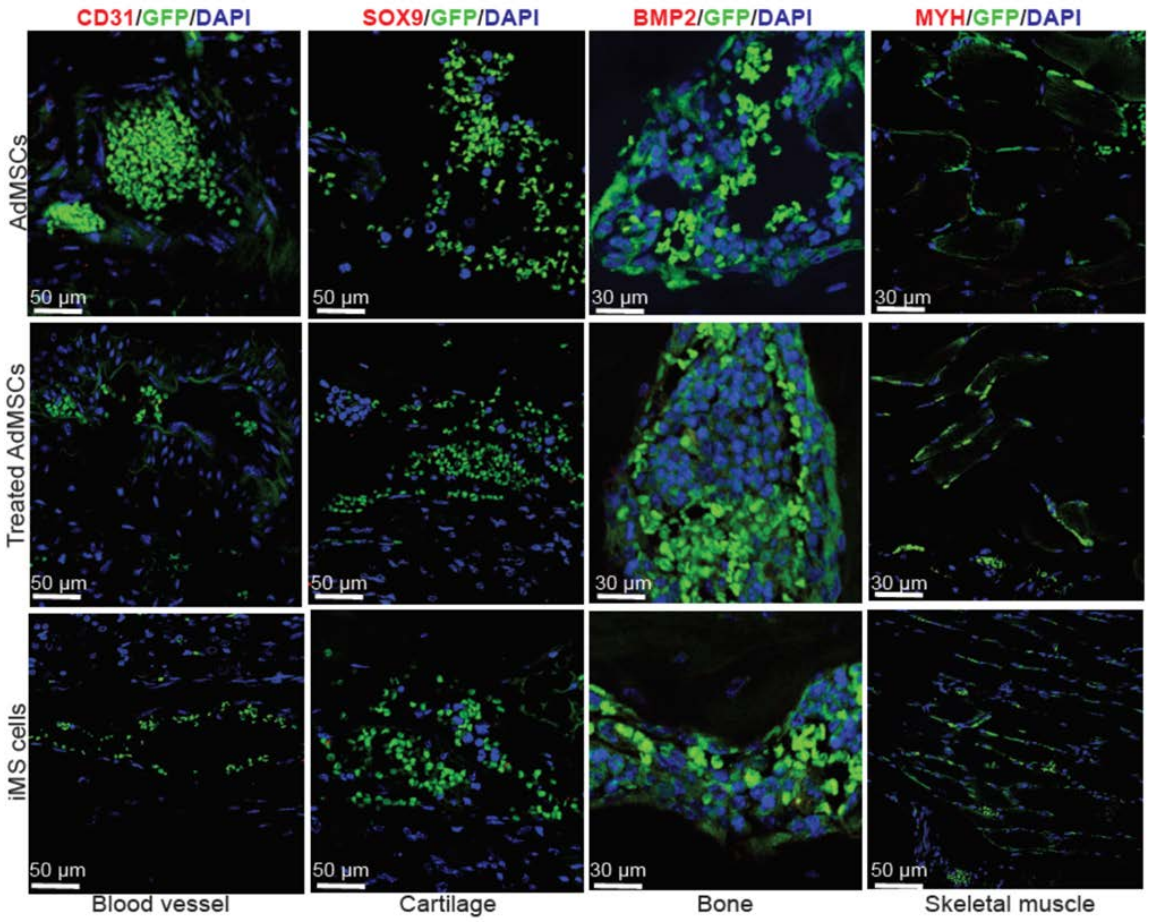

Figure 5. 6 Transplanted cells display are retained as undifferentiated cells at 3 months post-transplant.

Representative confocal images of tissue sections harvested at 3 months after transplantation with AdMSCs, treated AdMSCs or iMS cells, showing undifferentiated donor cells (GFP positive) without any contribution to blood vessel, cartilage, bone and skeletal muscle as indicated by absence of staining[23] for anti-human CD31, SOX9, BMP2 and MYH respectively (Scale bars, 30µm or 50µm as depicted).

[23] All primary and secondary antibodies used here are in routine use and work under identical experimental conditions when the target antigen is present.

5.3.4 Transplanted cells exhibit context-dependent *in vivo* plasticity at 6 months post-surgery

On reaching the next study endpoint of 6 months, animals (n=3 from each study group) were humanely sacrificed by euthanization. Spine sections were harvested by aseptic techniques and subjected to microCT for radiological evidence of new tissue formation. The spines were then fixed in 4% PFA. 20 µm serial sections of decalcified, paraffin/OCT embedded spines were used for immunohistochemistry and confocal microscopy as described in **2.2.11.4.**

H & E staining on the cross-sections did not reveal any differences in gross tissue architecture across tissues transplanted with AdMSCs, treated AdMSCs or iMS cells. There was no evidence of new tissue or ectopic bone formation in any of the spines (in any of the study groups) as visualized from microCT scans on the IRW software as well as H & E staining (Figure 5.7). This could be because the tissue injury model employed here involves only a minor manual disruption of the lumbar vertebra and is possibly beyond the detection limits of microCT (Figure S7). Immunofluorescence studies on these cross-sections demonstrated engraftment of transplanted GFP positive cells within the host tissues. Double immunofluorescent staining revealed integration of GFP expressing human cells which also expressed lineage markers characteristic of endothelial cells (CD31 positive, located within the blood vessel walls), chondrocytes (SOX9 positive), bone cells (BMP2 positive) and skeletal muscle cells (MYH positive). Similar findings were obtained in case of tissue sections obtained from animals transplanted with AdMSCs and treated AdMSCs. There were no qualitative differences between the test cell populations with respect to their integration and plasticity (Figure 5.8), so I next evaluated quantitative differences between the different groups.

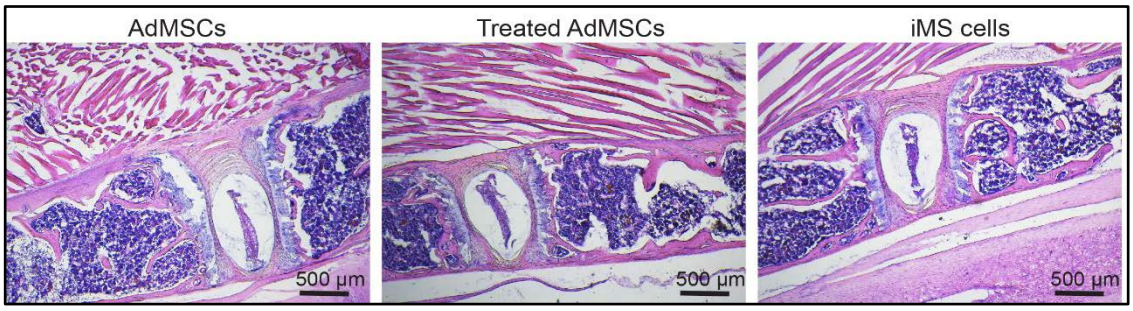

Figure 5. 7 Tissue sections do not show any differences in gross architecture at 6 months post-transplant either.

Representative images of H & E stained tissue sections harvested at 6 months after transplantation with AdMSCs, treated AdMSCs or iMS cells. Overall, no major structural differences could be deciphered between different tissue sections (Scale bars. 500 µm).

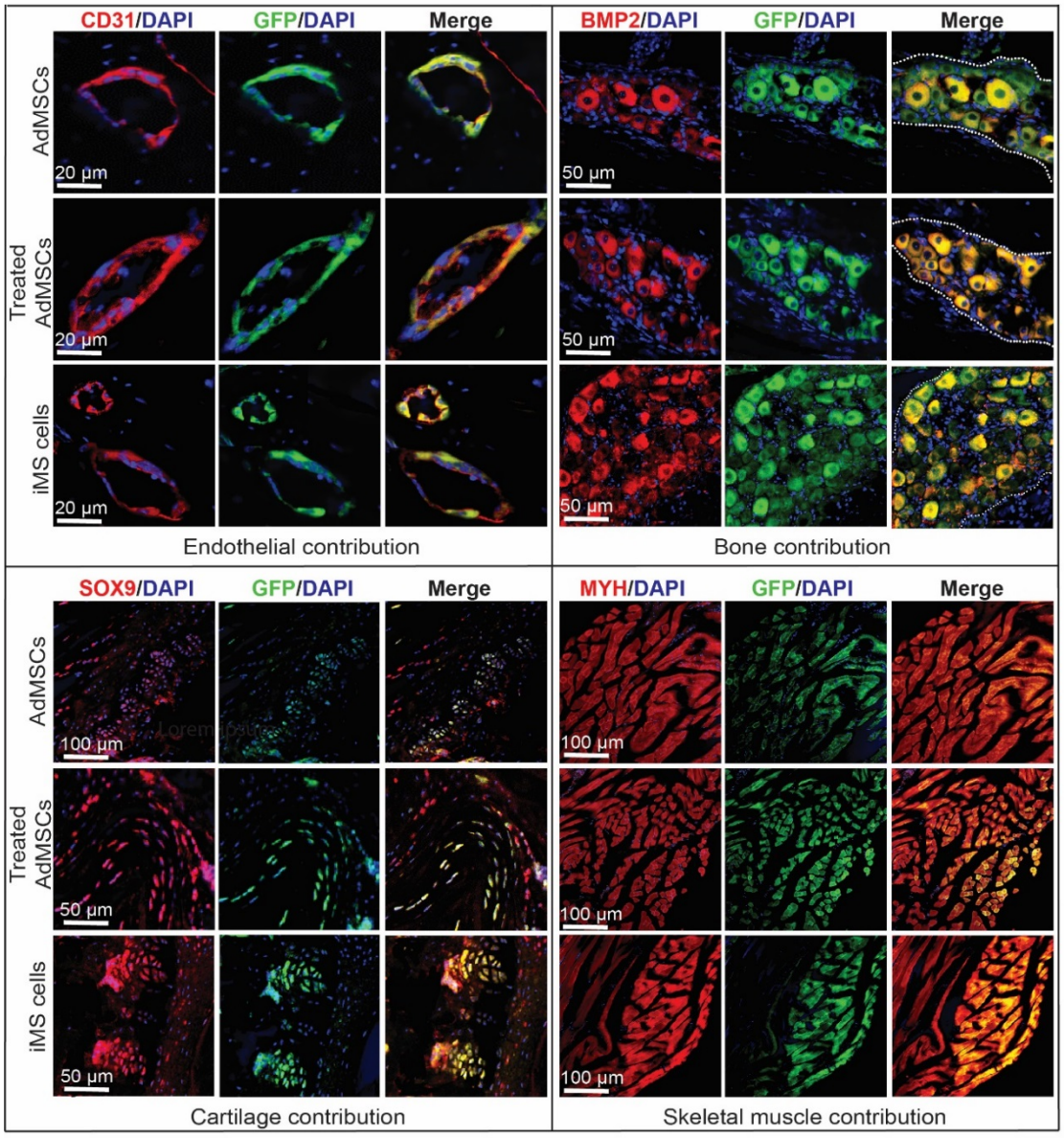

Figure 5. 8 Transplanted cells display *in vivo* plasticity.

Representative confocal images of tissue sections harvested 6 months from animals (n=3) after transplantation with AdMSCs, treated AdMSCs or iMS cells, showing donor cell contribution to blood vessels (CD31), cartilage (SOX9), bone (BMP2) and skeletal muscle (MYH) as indicated by co-staining[24] with GFP (Scale bars, 20µm, 50µm or 100µm as depicted).

[24] Using the same primary and secondary antibodies at same dilution as used for staining sections at 3 months endpoint (Figure 5.5).

Tile scans of five serial 20 µm cryosections, stained with anti-human antibodies for lineage specific markers were used for quantification by confocal microscopy. Untreated (sham) samples and vehicle control samples that consisted of non-injected spines stained negative for GFP (Figure S8). Negative and positive control slides were used to set the upper and lower limits of laser powers on each channel of the Zeiss LSM 780 confocal microscope. The percentage of GFP positive cells was then calculated manually using ImageJ software. The extent of angiogenesis, chondrogenesis, osteogenesis or myogenesis by reprogrammed human iMS cells in the injected area was determined by quantifying the number of double positive cells stained with GFP and respective lineage specific marker. Within each section, 4-5 individual regions comprised of differentiated tissues were counted for the number of GFP positive and GFP negative cells. The abundance of each differentiated lineage was expressed as the % of total GFP positive cells (average ± SD), plotted for each type of differentiated tissue. Values calculated using five different cryosections of each of the three samples per experimental group were expressed as mean ± SD. Differences between experimental groups consisting of 3-4 samples each were analysed using Student's T-test. Quantification of GFP positive blood vessels, bone, cartilage and skeletal muscle fibres showed significant differences between the experimental groups. Although AdMSCs also displayed *in vivo* plasticity and contribution to regenerating host tissues, treated AdMSCs and iMS cells showed a significantly higher level of *in vivo* multi-lineage differentiation capacity (Figure 5.9). This could possibly be a result of exposure to DCi reprogramming factors.

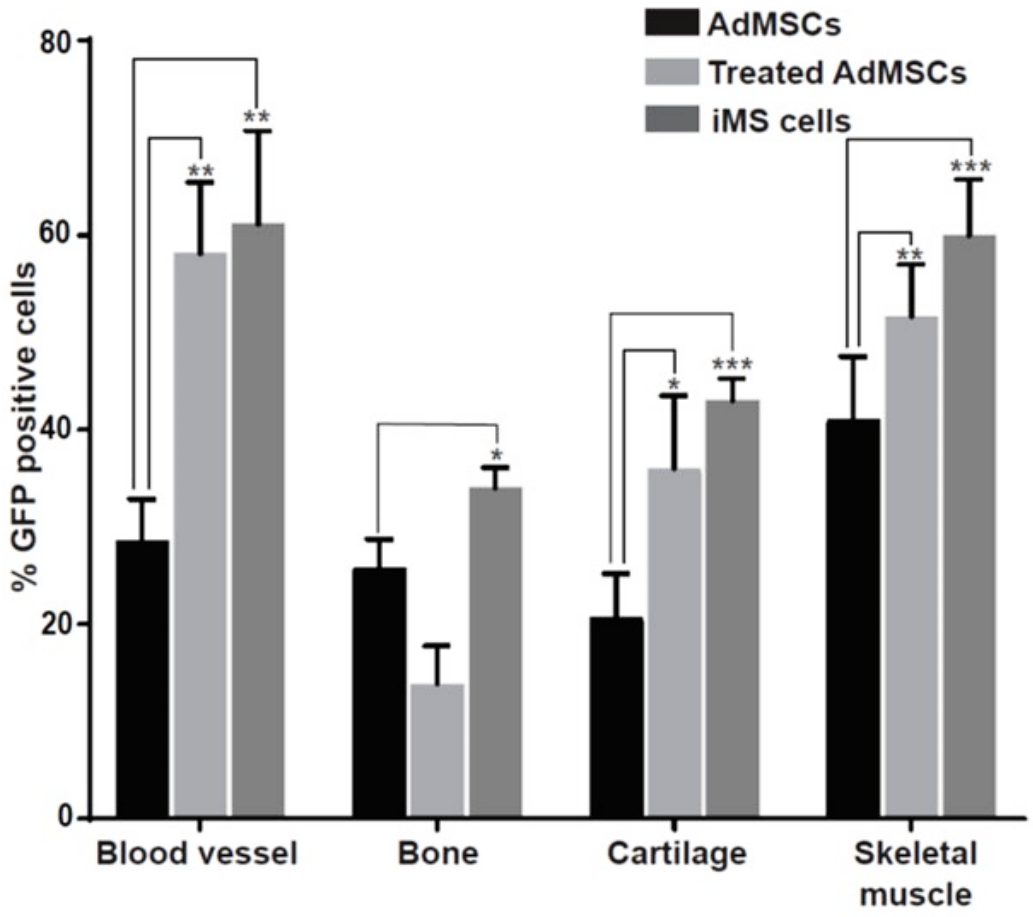

Figure 5. 9 Transplanted iMS cells display better *in vivo* plasticity

Graph showing donor cell contribution to blood vessel, bone, cartilage and skeletal muscle tissues of the host at six months post-transplant, calculated as the number of cells double positive for GFP and corresponding lineage specific marker. Bars represent the average number of donor derived cells for each cell types. Error bars, SD between individual sections (n=3). (*P≤0.05, **P≤0.005, ***P≤0.0005, Student's T-test).

5.4 Chapter summary and discussion

This chapter describes the long-term survival and tissue contribution of iMS cells in an immunodeficient mouse model of postero-lateral inter-lumbar vertebral injury. Delivery, localization and engraftment along with survival of the transplanted cells in host tissues were tracked for up to 1 year using serial optical BLI. The gradual decrease in bioluminescence after reaching its peak at 7 days post-transplant could be attributed to clearance of non-engrafted cells. This study involved cell transplantation only at a single dose of $1x10^6$ cells/injury site. It would be valuable to understand if change in this cell number influences their persistence and tissue contribution at the site of injury. Apart from that, this injury model includes a very small physical lesion to the host tissues. It would be of value to understand how iMS cells behave when transplanted in the context of a more severe or chronic injury such as osteoarthritis or musculoskeletal damage. Although NSG mice modelling inter-vertebral disc injury constitutes a practical model for studying *in vivo* safety and efficacy of human cells because of its cost-effectiveness, handling and small size; they do not mimic the actual scenario in immunocompetent healthy animals. Studies in large animal models e.g. sheep or pigs would also help to better simulate the degenerative process in humans.

MSCs are known to play a role in tissue repair and regeneration due to their abilities to self-renew and modulate host immune defences as well as their potential to undergo context-dependent differentiation into multiple cell types (Mannello, 2006; Miguelez-Rivera et al., 2017; Teixeira et al., 2017). Numerous studies reporting the transplantation of MSCs to treat intervertebral disc degeneration have been reported (Centeno et al., 2017; H. Kumar et al., 2017; Sakai et al., 2006). MSCs are also known for their ability to overcome allogenic rejection (Ryan et al., 2005) and inhibit the

fibrogenic process (Leung et al., 2014). However, whether they themselves participate in direct repair and formation of new tissue or influence tissue healing by indirect, trophic mechanisms lacks clarity.

In our study, undifferentiated donor cells were detected within the recipient tissues harvested at the first endpoint of 3 months. This observation is suggestive of a competitive environment presented by the injury-induced activation of host precursor cells. There is also the possibility that the paracrine effect of transplanted cells might have led to recruitment of endogenous MSCs and other cells to the injury site. Furthermore, such cells might be more receptive to intrinsic differentiation signals than the xenogeneic donor human cells.

At the next study-endpoint of 6 months, we identified engrafted human cells that had undergone differentiation as identified by co-expression of GFP and human lineage-specific markers. This observation indicated long term maintenance of their stem cell properties. The transplanted human cells underwent controlled, context-dependent differentiation and contributed to formation of blood vessel, bone, cartilage and skeletal muscle within the injured host-tissue microenvironment. Notably, morphological evaluation did not reveal aberrant differentiation of the transplanted cells, which has earlier been reported as a potential risk associated with therapeutic use of MSCs (Breitbach et al., 2007; Vadala et al., 2012). Given the mesodermal origin of the source adipocytes used for generation of DCi reprogrammed iMS cells used for this study, we restricted staining of the spine sections only for differentiation markers of the mesodermal lineages. It might however be worthwhile to understand if the iMS cells possess further potency to differentiate into cells of other lineages.

These findings emphasise the responsiveness of transplanted human cells in an injured (xenogeneic, species-unmatched) host tissue environment. The trophic effects of endogenous host stem or differentiated cells may have influenced homing and recruitment of the transplanted cells triggering the molecular signals required for adherence and eventual differentiation. This premise however needs detailed investigation.

Although AdMSCs also exhibited *in vivo* plasticity, treated AdMSCs and iMS cells displayed it at a significantly higher level. Exposure to DCi reprogramming factors might have been responsible for imparting this enhanced *in vivo* differentiation capacity. AZA, a component of the DCi reprogramming cocktail is previously reported to induce cell plasticity (P. A. Jones & Taylor, 1980) and for conversion of partially reprogrammed cells to completely reprogrammed cells (Mikkelsen et al., 2008). This hypothesis however needs systematic investigation. Our findings do however demonstrate efficient *in vivo* context-dependent plasticity of xeno-transplanted, DCi reprogrammed human cells within a damaged murine tissue. The transplanted cells are recruited along with the host's endogenous stem cells to regenerate the damaged tissue. The pleiotropic autocrine or paracrine immunomodulatory effects exerted by the transplanted cells themselves may have also played a role in supporting their retention, extracellular matrix deposition and subsequent engraftment within host tissues. However, more rigorous studies understanding the influence of catabolic and inflammatory environment during injury are necessary to elucidate the specific mechanisms underlying the observed *in vivo* plasticity of DCi reprogrammed cells.

There were no instances of ectopic tissue or spontaneous tumour formation as confirmed by absence of unexpected tissue growth monitored over the period of 1 year. Over this long-term period, the xenogeneic cells persisted within the injured murine tissues but did not migrate into other distant organs, as shown by localization of the BLI

signal at the transplant site. This was further substantiated by absence of GFP positive human cells in the host circulation. These findings suggest a chemotactic environment presented by the regenerating tissue that resulted in sustained homing of the transplanted cells. The transplanted human cells were responsive to inherent cues and underwent context-dependent differentiation within this niche. It is also important to note that the cells did not undergo malignant transformation which would have been observed as an anomalous increase in bioluminescence signal during periodic imaging. This ability of human iMS cells to survive in the hostile environment of damaged tissue without displaying any spontaneous tumorigenicity is promising for their potential therapeutic applications.

The few MSC-based therapeutic alternatives which currently exist need to undergo *ex vivo* differentiation or conditioning prior to transplant to enhance their self-renewal and survival capacity (Vu et al., 2016). Unlike these cell types, iMS cells do not require *ex vivo* induction for them to be able to demonstrate their *in vivo* effects. This also alleviates the risk of inducing cellular alterations including modifications in the expression patterns of genes as well as cell-surface markers. These findings thus emphasize the feasibility of using iMS cells as an alternative source of mesenchymal cells for basic applications and for preclinical studies in tissue repair. However, there exists a strong need for future investigations to explore differences associated with use of non-species-matched cells in understanding tissue-specific regeneration mechanisms.

The data described in this chapter elucidate the *in vivo* context-dependent plasticity and long-term safety of transplanted cells. However, it does not provide clear evidence for direct tissue repair potential of DCi reprogrammed human iMS cells. The following chapter will therefore focus on understanding the tissue regenerative behaviour of iMS cells in the context of a specific tissue-injury model.

CHAPTER 6. Evaluation of tissue-specific repair potential of human iMS cells

6.1 Introduction

In the previous chapter I described the long-term *in vivo* safety and plasticity of DCi reprogrammed human iMS cells in the context of a generic tissue injury model. iMS cells were shown to integrate within injured host tissues and contributed towards formation of multiple tissues, in response to resident cues (described in 5.3.4). Following on from these findings, we next sought to assess the specificity of iMS cell plasticity in order to determine whether these cells can contribute to direct repair of an injury to a specific cell/tissue-type.

Skeletal muscle is one of the most regenerative adult tissues in humans (Carlson, 1973). The normal process of skeletal muscle repair following acute injury is comprised of an initial degenerative phase followed by a regenerative phase. In the degenerative phase, disruption of the myofibre sarcolemma triggers extensive muscle necrosis which leads to infiltration of mononucleated inflammatory cells and activation of quiescent endogenous satellite cells. This occurs as early as 6 hours after injury. Macrophages continue to infiltrate the injured tissue for about four days post injury in order to phagocytose the cellular debris generated as a result of muscle necrosis. The repair or regenerative phase is characterised by proliferation and differentiation of myogenic cells. These myogenic cells then differentiate and fuse to existing damaged myofibres or to one

another to form a new myotube (Garry et al., 2016). The regenerating myofibres formed at this stage are characterised by their centrally located myonuclei. Subsequently, the fibres undergo maturation to increase in size and are organized together into muscle bundles. At this stage, the myonuclei move towards the periphery of the muscle fibre, marking completion of the regeneration process (Charge & Rudnicki, 2004).

Acute-injury-induced skeletal muscle regeneration is a powerful system to study tissue-specific regeneration. The regenerative capacity within the adult skeletal muscle arises primarily from satellite cells (SCs) (N. C. Chang & Rudnicki, 2014; Giordani et al., 2018). This otherwise quiescent population of SCs is activated by an episode of injury or trauma. Human SCs however have limited self-renewal potency and are also known to decrease in number with age (Day et al., 2010). The decline in regenerative capacity of SCs is also responsible for age-associated loss of muscle mass due to compromised muscle maintenance and repair (Chakkalakal et al., 2012). On the other hand, inherited disorders such as muscular dystrophies are associated with progressive muscle damage which induces continuous cycles of muscle degeneration and regeneration. This in turn pushes the host SCs into recurrent rounds of activation, proliferation and differentiation eventually leading to exhaustion of the SC pool (Blau et al., 1983).

Given the limited availability of SCs in degenerating muscles, cell-based therapy is a promising strategy for treatment of adult-onset muscular dystrophies and age or accident related muscle loss. For sustained treatment alternatives, the ideal repair cell population should have proliferative as well as regenerative potential. The applied cells should not only be able to contribute to myofibre formation but also reconstitute a functional stem cell pool. Studies demonstrating engraftment of transplanted myoblasts from wild-type donors into host skeletal muscle have earlier been reported (Huard et al., 1994). However, these cells have limitations due to their low viability, inadequate

disbursement from injection sites and immune rejection owing to their allogenic nature. Gene therapy using recombinant adeno-associated vectors for delivery and expression of transgenes to direct differentiation of stem cells to the desired phenotype has recently gained attention (Koo et al., 2014). This however faces the limitation of *ex vivo* expansion prior to application. Moreover, for therapeutic applications, inducing differentiation without the need for introduction of transgenes is preferred (Peault et al., 2007).

An alternative strategy to circumvent these constraints is to isolate and transplant SCs. *In vitro* expanded allogenic SCs have been used to restore dystrophic and age-associated muscle loss in animal models (Montarras et al., 2005). However, these transplanted SCs are rapidly lost with progression of muscle degeneration. Moreover, *in vitro* expansion of SCs is shown to significantly reduce their engraftment capacity thereby compromising their therapeutic potential. These limitations are further compounded by heterogeneity in satellite cells depending on their isolation technique and culture conditions (Cornelison, 2008). Given these inadequacies, it is preferable to generate an autologous stem cell population which is capable of undergoing lineage-specific differentiation to repair the damaged muscles along with reconstitution of a pool of viable stem cells.

As reported in the previous chapters, DCi reprogrammed human iMS cells exhibit self-renewal ability, *in vitro* multilineage differentiation potential, and capacity for long-term engraftment with context-dependent plasticity after transplantation to injured tissues of immunodeficient mice. In this chapter, I will investigate the capacity of human iMS cells to engraft into and repair injured skeletal muscle of immunodeficient SCID/beige mice in order to understand the specificity of iMS cell plasticity.

6.2 Study design

To evaluate the tissue-specific regeneration potential of reprogrammed human iMS cells, a cardiotoxin (CTX)-induced skeletal muscle injury model in immunodeficient SCID/Beige mice was used. CTX is a peptide isolated from *Naja pallida* (snake) venom. It is a protein kinase-C inhibitor which induces depolarization and contraction of muscle cells with accompanying destruction of cell membranes (C. C. Chang et al., 1972). CTX-mediated injury destroys muscle fibres but preserves the basal lamina, nerves, and blood vessels as well as satellite cells (Harris, 2003). At the histological level, this is evident from distinct muscle fibre necrosis and infiltration of inflammatory components. Marked activation of satellite cells is observed as rapidly as six hours after injury and is accompanied by an increase in muscle fibre length and increased cytoplasmic-to-nuclear ratio (Mahdy et al., 2016).

In our study, skeletal muscle necrosis was induced by injection of 10 µM CTX (Latoxan, France) into the left tibialis anterior (TA) muscles of female immunodeficient SCID/Beige mice as described in **2.2.11.2**. The contralateral TA muscle in each of the mice was kept uninjured as a negative control. After 24 hours, 1 x 10^6 cells were injected into the damaged TA muscle to assess the ability of human cells to survive and participate in host muscle regeneration (Figure 6.1). iMS cells obtained after DCi reprogramming of patient-derived adipocytes, as well as corresponding[25] AdMSCs and treated AdMSCs were used for this *in vivo* study. Three mice received matrigel only (no cells) serving as vehicle controls for host-tissue-mediated regenerative response as mounted by the host's endogenous cells (Refer Table 2.4 for study groups).

[25] All cell populations used for this study were patient and passage matched.

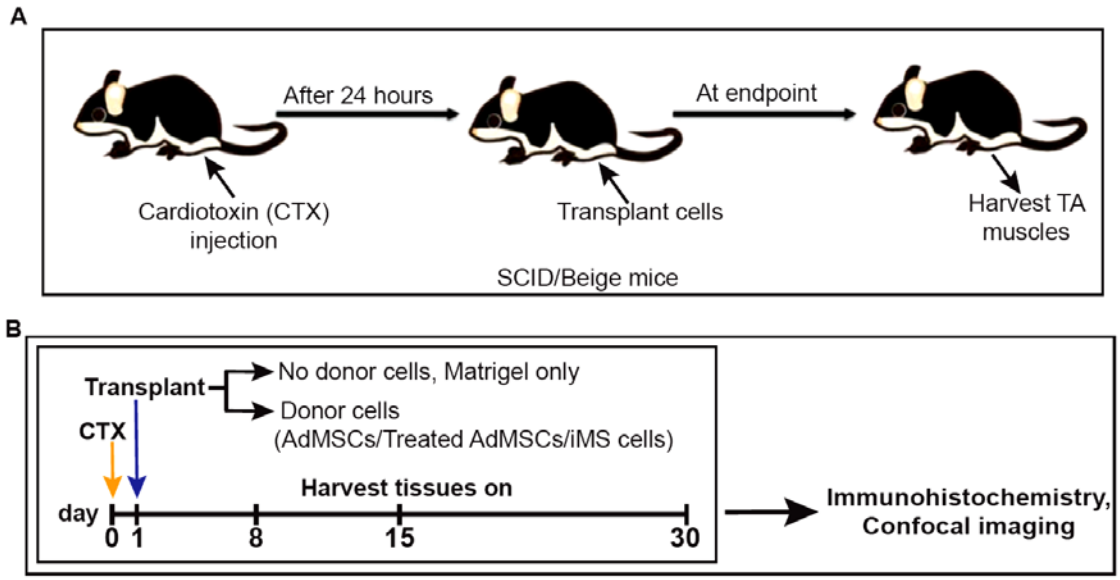

Figure 6. 1 Schematic representation of workflow for CTX-induced skeletal muscle injury model

(A) Schematic showing CTX-mediated TA muscle injury. Human cells (AdMSCs, treated AdMSCs or iMS cells) were transplanted 24 hours post-injury into the damaged muscle of SCID/Beige mice. (B) Schematic showing timeline for CTX injection, cell transplant and study endpoints.

6.3 Results

6.3.1 CTX injury induces severe damage in the injected TA muscle

I first conducted a trial experiment using two animals to evaluate CTX induced myonecrosis by my hand. 10 µM CTX was delivered to the left TA muscle, leaving the contralateral right TA muscle uninjured. On the following day, left and right TA muscles were harvested from both the animals and processed as described in **2.2.11.3.** The tissues were then cryosectioned for analysis by routine Haematoxylin & Eosin (H & E) staining and, immunostaining with anti-laminin antibody and DAPI.

As expected, the uninjured control right TA muscle had intact muscle fibres and did not show intrusion of any inflammatory cells (Figure 6.2, top panel). The myofibres in this uninjured muscle have their post-mitotic nuclei located at the periphery (Figure 6.2, arrows in top panel). In contrast, CTX caused extensive damage of muscle structural architecture as evident from the occurrence of degenerated muscle fibres within the injured muscle sections (Figure 6.2, arrows in bottom panel). Numerous mononucleated cells were seen infiltrating the damaged area (Figure 6.2, circled regions in bottom panel). These cells include satellite cells, myoblasts, interstitial cells, endothelial and inflammatory cells that are activated following injury (Arnold et al., 2007; Saclier et al., 2013).

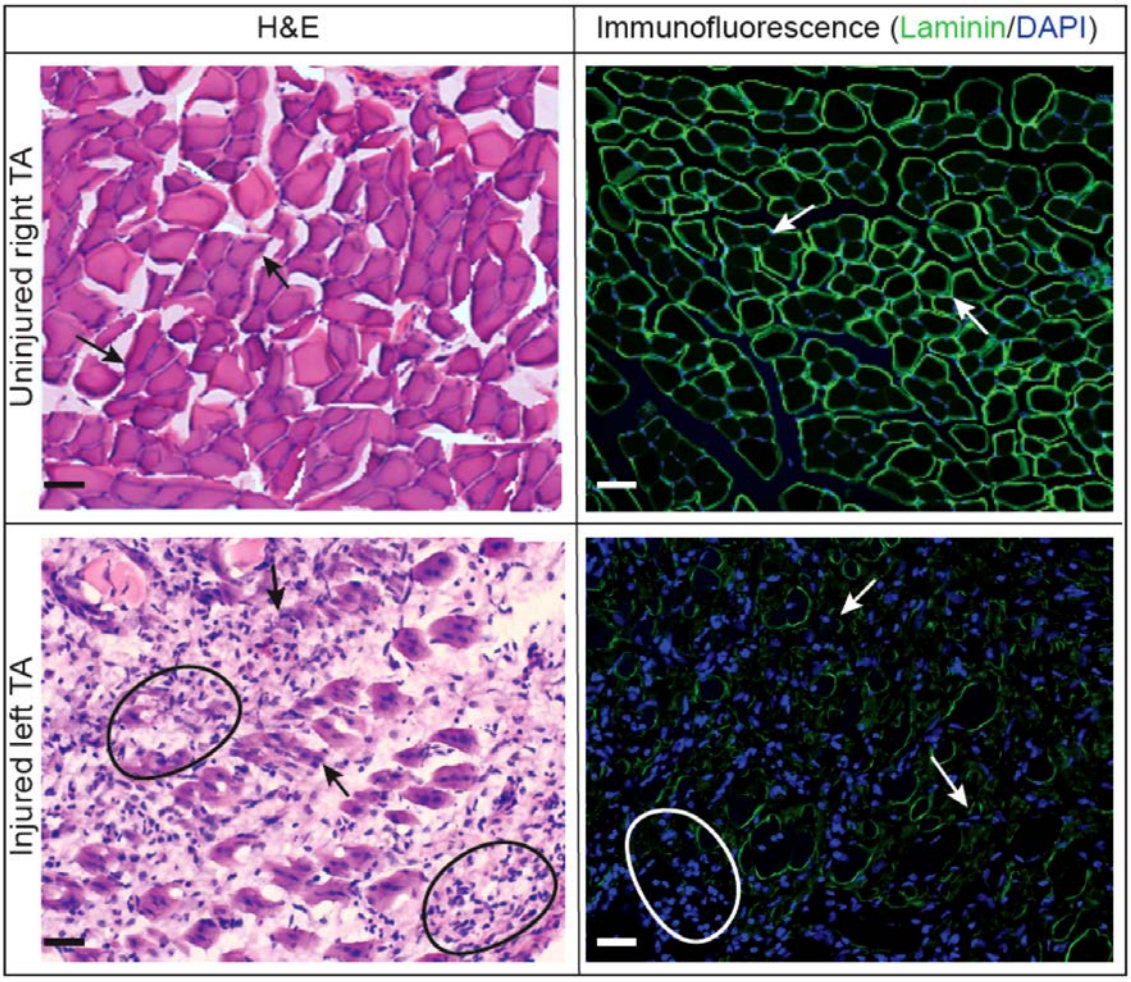

Figure 6. 2 CTX induces damage of muscle fibres

Representative H & E and confocal images of uninjured right TA muscle transverse sections showing laminin-stained intact muscle fibres with peripheral nuclei (arrows in top panel) and extensive muscle fibre necrosis (arrows in bottom panel) induced after CTX injection in left TA muscle of SCID/Beige mice. Circled regions in bottom panel mark areas with infiltrated mononuclear cells. (n=2), (Scale bar, 50 µm).

6.3.2 Donor cells are retained at the site of injury

Once the myodegenerative effect of CTX was confirmed, we then moved on to examine the tissue regenerative potential of human iMS cells transplanted within this environment of damaged muscle fibres in SCID/Beige mice (n=5), as described above in **6.2** and **Figure 6.1**. Animals transplanted with patient and passage matched AdMSCs (n=5) and treated AdMSCs (n=5) in CTX-injured TA muscle were included for comparison. On reaching the study endpoint of either one, two or four weeks post-transplant, the mice were humanely sacrificed, and both the TA muscles were harvested. The collected muscles were processed, cryosectioned and analysed by immunohistochemistry as described in **2.2.11.3.**

We first looked at the muscle tissues harvested one-week post-transplant. To understand whether the donor cells were retained at the site of transplant, muscle sections were stained for human lamin A/C, pan-laminin and DAPI[26]. While the anti-laminin antibody marks muscle fibres of mouse as well as human origin, the anti-human lamin A/C antibody specifically marks human nuclei. This staining strategy allowed us to distinguish between donor human cells and recipient murine cells. Evaluation of gross morphology of muscle sections at this stage revealed the presence of damaged/necrotic muscle fibres (Figure 6.3, white arrows in bottom panel). The presence of small zones with accumulation of multi-nucleated cells within the injured muscles (Figure 6.3, yellow arrows in bottom panel) suggested interaction between different cells to restore tissue integrity. Human cells (co-stained with anti-human lamin A/C and DAPI) were found dispersed throughout the entire left TA muscle section (Figure 6.3, bottom panel), but not in the right uninjected TA. As expected, anti-human lamin A/C stained nuclei were absent

[26] Refer to antibody table in 2.1.2 for exact dilutions.

in injured muscles transplanted with matrigel alone (vehicle control, no donor cells) (Figure 6.3, bottom panel, first image). At this stage, the gross tissue structure was qualitatively similar between the three treatment groups (i.e. AdMSCs, treated AdMSCs or iMS cells) (Figure 6.3, bottom panel).

We next addressed the question of whether the different types of donor cells have differential retention capacity within the injured muscle. Quantification of human nuclei in serial cross-sections was carried out as described earlier in **2.2.11.3.** The abundance of human cells was expressed as the % of total lamin A/C positive nuclei out of the total counted nuclei and plotted for each of the study groups. Differences between experimental groups were analysed by Student's T-test. Although the cells were transplanted in equal numbers[27], iMS cells (18.6±1.4%) and treated AdMSCs (14.7±1.8%) were retained at levels significantly higher than AdMSCs (11.2 ± 1.3%) in this environment of acute skeletal muscle injury (Figure 6.4).

This observation is similar to our previous results where iMS cells displayed comparatively higher retention and eventual plasticity in an injured tissue microenvironment of postero-lateral inter-lumbar vertebral injury model (Chapter 5). As discussed earlier, these findings could be attributed to the ability of DCi reprogrammed cells to better avoid immune cell mediated clearance from injured tissues.

[27] This experiment included a single injection of $1x10^6$ cells/injured muscle.

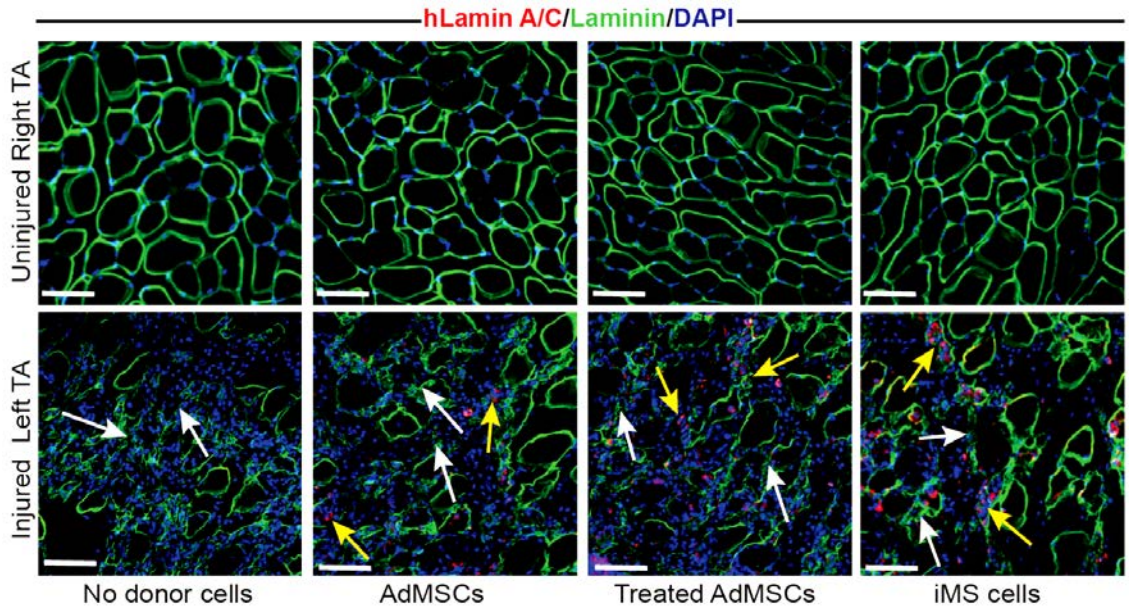

Figure 6. 3 Retention of human cells in CTX-injured TA muscle

Confocal images showing absence of human lamin A/C expressing nuclei in uninjured, uninjected right TA muscles[28] (top panel) and in vehicle control i.e injured left TA muscle not transplanted with any cells (bottom panel, first image), harvested after one week post-surgery. Corresponding muscle sections from animals transplanted with AdMSCs, treated AdMSCs or iMS cells, showing donor human cells in injured TA muscles as detected by anti-human lamin A/C stained[29] nuclei. In the bottom panel, white arrows mark necrotic fibres while yellow arrows mark the accumulation of multi- nucleated cells within CTX injured muscles. (Scale bars, 50 µm).

[28] Right TA muscles of animals in each of the study groups were not injured and served as experimental controls.

[29] All primary and secondary antibodies used here are in routine use and work under identical experimental conditions when the target antigen is present.

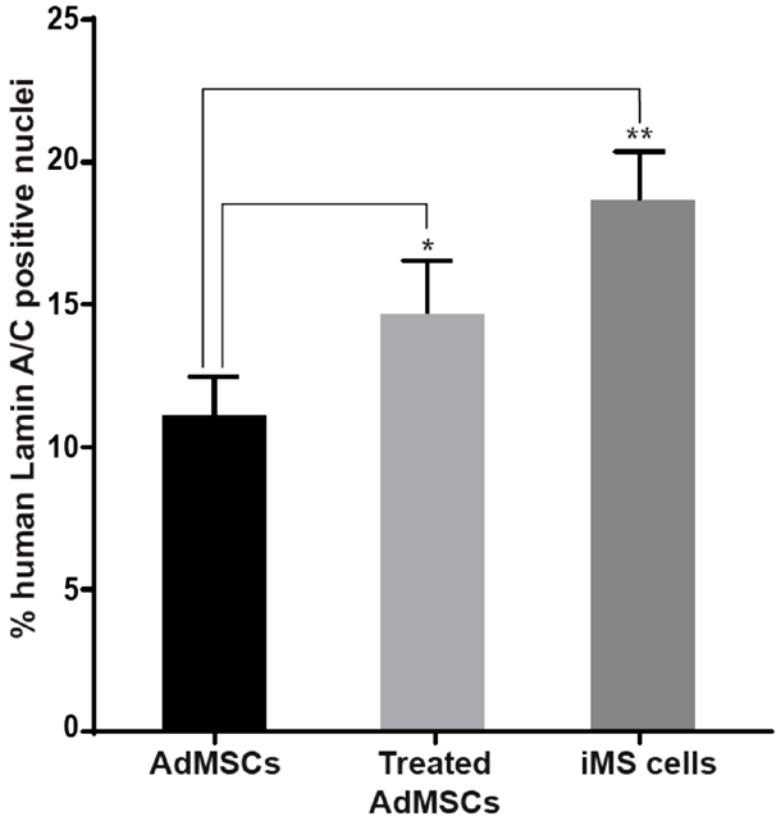

Figure 6. 4 Transplanted iMS cells display better *in vivo* retention at the site of injury

Quantification of engrafted donor cells within injured host tissues one week post-transplant, as detected by % of human lamin A/C positive nuclei. In comparison to AdMSCs, iMS cells and treated AdMSCs showed better retention capacity within the injured muscle. Error bars, SD, (n=3-5). (*P≤0.05, **P≤0.005, Student's T-test).

6.3.3 Donor cells undergo directed differentiation to form satellite cells

Having confirmed the retention of donor human cells in the injected muscles, our next step was to determine the plasticity of transplanted cells in response to local cues within the injured tissue environment. For the transplanted cells to effectively contribute to regeneration, they need to survive within the injured muscle environment and subsequently undergo committed differentiation along the myogenic lineage. Therefore, we looked for the presence of donor-cell-derived satellite cells by staining for human CD56 which is known to specifically mark satellite cells of human origin (Schubert et al., 1989).

In this experiment, animals (n=1 or 2 as per study group) were humanely sacrificed by cervical dislocation at one, two or four weeks post-transplant. Left and right TA muscles were harvested and fixed in 4% PFA. 20 µm serial sections of OCT embedded muscles were used for immunohistochemistry and confocal microscopy as described in **2.2.7.3.1** and **2.2.11.3.** The sections were stained for pan-laminin, hCD56 and DAPI. Immunofluorescence studies on these showed laminin-marked basement membranes (green) and donor-derived hCD56 positive satellite cells (red) distributed across the entire tissue section. At one week post-transplant, mononucleated hCD56 stained cells were seen lodged within the interstitial spaces, in between individual damaged muscle fibres (Figure 6.5, white arrows in top panel).

In sections harvested at two weeks post-transplant, a majority of fibres were found to be centro-nucleated confirming the ongoing regeneration phase at this stage (Figure 6.5, asterisks in middle panel). Distinct zones with aggregation of cells were also evident in regions adjacent to the regenerating myotubes (Figure 6.5, white arrows in middle panel). hCD56 positive satellite cells of human origin had now acquired a morphology

with elongated cell processes which possibly facilitates their spreading across individual regenerating myotubes. These morphological changes suggest that a proportion of donor-derived satellite cells are now prepared to undergo spontaneous fusion with host cells in order to give rise to mature muscle fibres (Figure 6.5, middle panel). Notably, the regenerating myofibres in tissues transplanted with cells were multi nucleated (Figure 6.5, yellow arrows in middle panel). This provides further evidence for fusion occurring in between individual myoblasts, another hallmark of active muscle regeneration.

At the four-week timepoint, the majority of regenerating fibres had progressed towards maturation as indicated by myofibres with nuclei placed at the periphery (Figure 6.5, arrows in bottom panel). The overall architecture of the muscle appeared to be restored to a normal structural organization (Figure S11). Notably, hCD56 stained donor-derived satellite cells were still present at this stage. However, these satellite cells had now taken up a sublaminar position, distinct to that seen at the earlier timepoints (Compare Figure 6.5, bottom panel to Figure 6.5, top panel). Indeed, the observed course of events followed the phases of normal muscle regeneration described earlier. As expected, no donor-derived satellite cells were detected in control muscles at any time point (Figure 6.5).

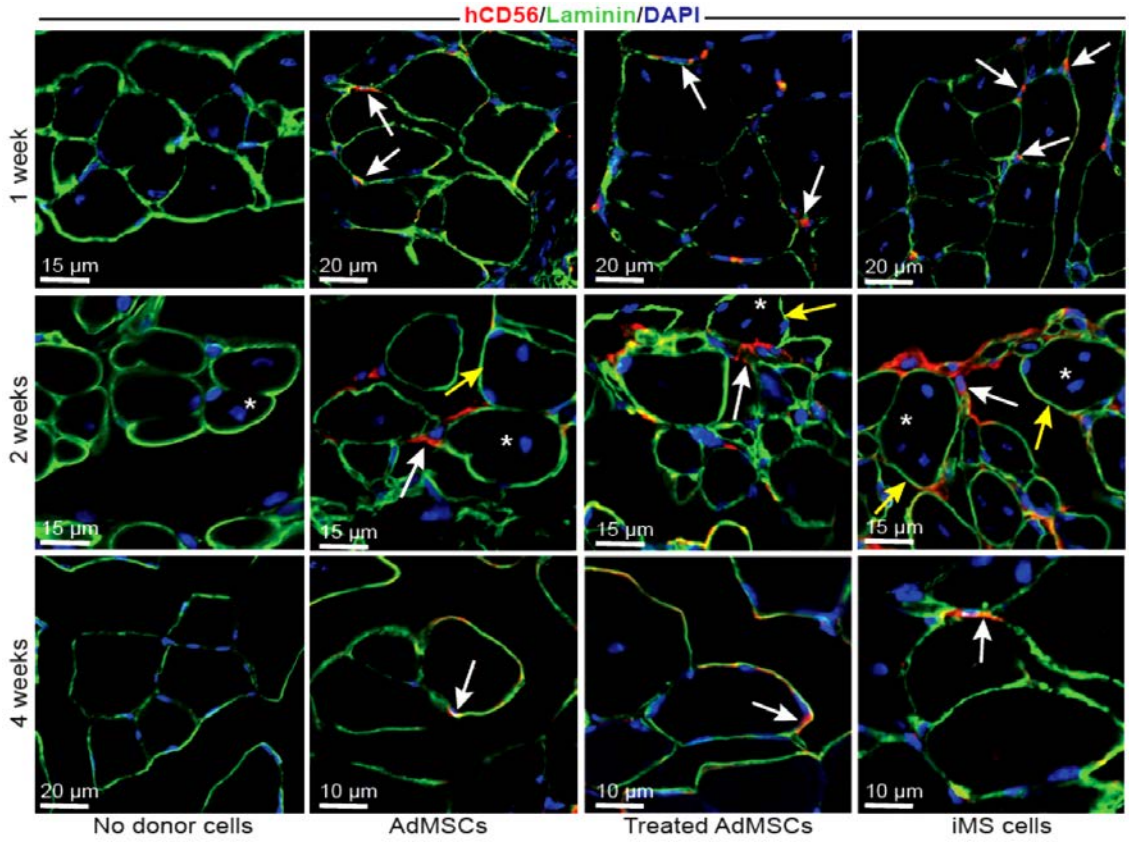

Figure 6. 5 Detection of donor-derived satellite cells within the injured muscle

Representative confocal images of left TA muscle sections harvested at one, two or four weeks from mice (n=1 or 2) transplanted with matrigel alone (vehicle control, no donor cells), AdMSCs, treated AdMSCs or iMS cells. The sections were stained with DAPI (all nuclei), laminin (basal membrane of all muscle fibres) and hCD56 (satellite cells of human origin). The engrafted human cells differentiate to acquire a SC-phenotype as detected by hCD56 staining and are lodged within interstitial spaces at one week after transplant (white arrows in top panel). At two week timepoint, hCD56 stained SCs (white arrows in middle panel) are embedded in between regenerating centro-nucleated myotubes (asterisks in middle panel). Multi-nucleated myofibres are marked with yellow arrows in the middle panel. Finally, at the four-week timepoint, the donor-derived SCs are seen to take up a sub-laminal position (white arrows in bottom panel) within the matured muscle fibres. (Scale bars, 10, 15 or 20 µm as depicted).

6.3.4 DCi reprogrammed cells undergo better myogenic commitment and differentiation than untreated cells

To determine whether donor-derived satellite cell frequency is heterogenous across the different study groups, we next performed a quantitative analysis on the tissue sections. Tile scans of serial 20 µm cryosections, stained for pan-laminin, anti-human CD56 and DAPI, were used to evaluate the number of donor-derived SCs. The percentage of hCD56 positive cells was then calculated on three to five serial sections from each animal (n=1 or n=2, depending on study group), using ImageJ software.

The overall frequency of donor-derived SCs was found to be significantly higher in animals transplanted with iMS cells or treated AdMSCs compared to animals transplanted with AdMSCs at all the time-points studied (Figure 6.6, compare different cell types at each time-point). The difference in frequency of hCD56 stained cells across different cell types was roughly proportional at each of the time-points tested. For example, the proportion of hCD56 stained SCs derived from iMS cells ranged between 2-2.5 times to that derived from AdMSCs, at any of the time-points studied (Figure 6.6, compare AdMSCs v/s iMS cells at one, two and four weeks). However, it is important to note that the initial retention efficiency of transplanted iMS cells and treated AdMSCs was significantly higher than that of AdMSCs, when assessed initially at one-week post-transplant (Refer to Figure 6.4). Further analysis is therefore required to determine if the improved myogenic commitment of iMS cells and treated AdMSCs was due to their better retention at transplant site or as a result of their superior ability to respond to signals within the injured tissue environment.

When compared at different time-points, the frequency of SCs of human origin was found to be higher at two weeks compared to one-week post-transplant. At four

weeks, however, the human SCs showed a decline in their frequency across the tissue section. This trend of change in distribution of SCs was shared across all three study groups (Figure 6.6, compare overall trend at one, two and four weeks).

The acute skeletal muscle injury model used in this study did not include ablation of host SCs. Additionally, xenogeneic transplantation of human cells into mice poses a species barrier which presumably limits the degree of engraftment. The transplanted human cells therefore have to compete with endogenous satellite and other myogenic cells in order to contribute to skeletal muscle regeneration. The presence of donor derived SCs detected as early as one week after transplant indicates the ability of human cells to overcome this species barrier. It also suggests that the transplanted cells could adapt to the competitive and foreign environment of tissue injury. Once the cells had acclimatized, they underwent subsequent proliferation and differentiation as evident from the increase in frequency of donor-derived SCs at the two weeks timepoint (Figure 6.6).

The subsequent decline in frequency of donor-derived SCs at the four-week timepoint could possibly be a result of their asymmetric division giving rise to mature muscle fibres by myogenic differentiation and formation of more SCs, contributing to their ability to self-renew. Against this backdrop, it is important to know whether the donor-derived SCs which are now shown to be committed to the myogenic lineage, indeed give rise to mature muscle fibres. This question will be addressed in the following section.

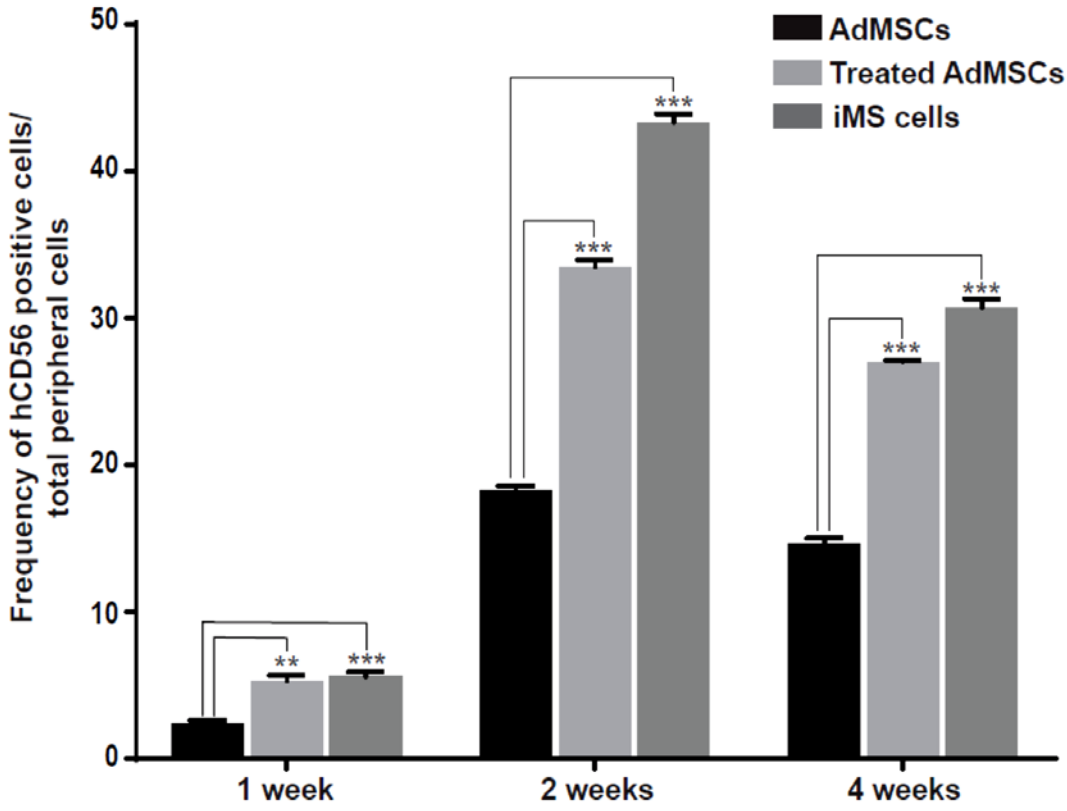

Figure 6. 6 DCi reprogrammed cells exhibit better myogenic commitment and differentiation than untreated cells

Graph showing the frequency (average ± SD) of hCD56 positive SCs identified in three to five serial sections of TA muscles of recipient mice (n=1 at one week and n=2 at two and four-week timepoints) transplanted with AdMSCs, treated AdMSCs or iMS cells. Values calculated using three to five different cryosections of each of the (one or two) samples per experimental group were expressed as mean ± SD. (**P≤0.005, ***P≤0.0005, Student's T-test).

6.3.5 Donor derived satellite cells contribute to formation of mature muscle fibres

In order to address the question of whether donor-derived SCs underwent asymmetric division to maintain an SC pool and to form terminal cell types, we looked for their directed differentiation to form mature muscle fibres. For this experiment, muscle sections harvested at four weeks post-transplant from animals (n=2) of each of the study groups were immunostained with antibodies directed against laminin, hSpectrin and DAPI. hSpectrin has been widely used for detection of muscle fibres of human origin after injection of human cells into damaged muscle of immunodeficient mice (Sacchetti et al., 2016; X. Xu et al., 2015; Zheng et al., 2007). In contrast, the anti-laminin antibody recognizes muscle fibres of both mouse and human origin.

Tissue sections transplanted with human cells formed mosaic muscle fibres i.e. co-staining with anti-laminin and hSpectrin could be observed within a given muscle fibre. As anticipated, tissue sections harvested from animals injected with matrigel alone (vehicle controls, no cells) did not contain of any hSpectrin stained muscle fibres (Figure 6.7, topmost panel). This finding also ruled out the earlier reported non-specific staining associated with hSpectrin antibody (Rozkalne et al., 2014). All the co-stained fibres had continuous staining of laminin throughout their basal membrane whereas the hSpectrin staining in these fibres was seen only on parts of the sarcolemma (Figure 6.7, arrows in right-most ‘merge’ panels). These findings are similar to those previously reported (Cooper et al., 2003) and are indicative of fusion between the donor and host cells leading to formation of a complete, mature fibre derived from both mouse and human cells. We observed no gross qualitative differences in chimeric fibres between animals injected with cells from the three treatment groups.

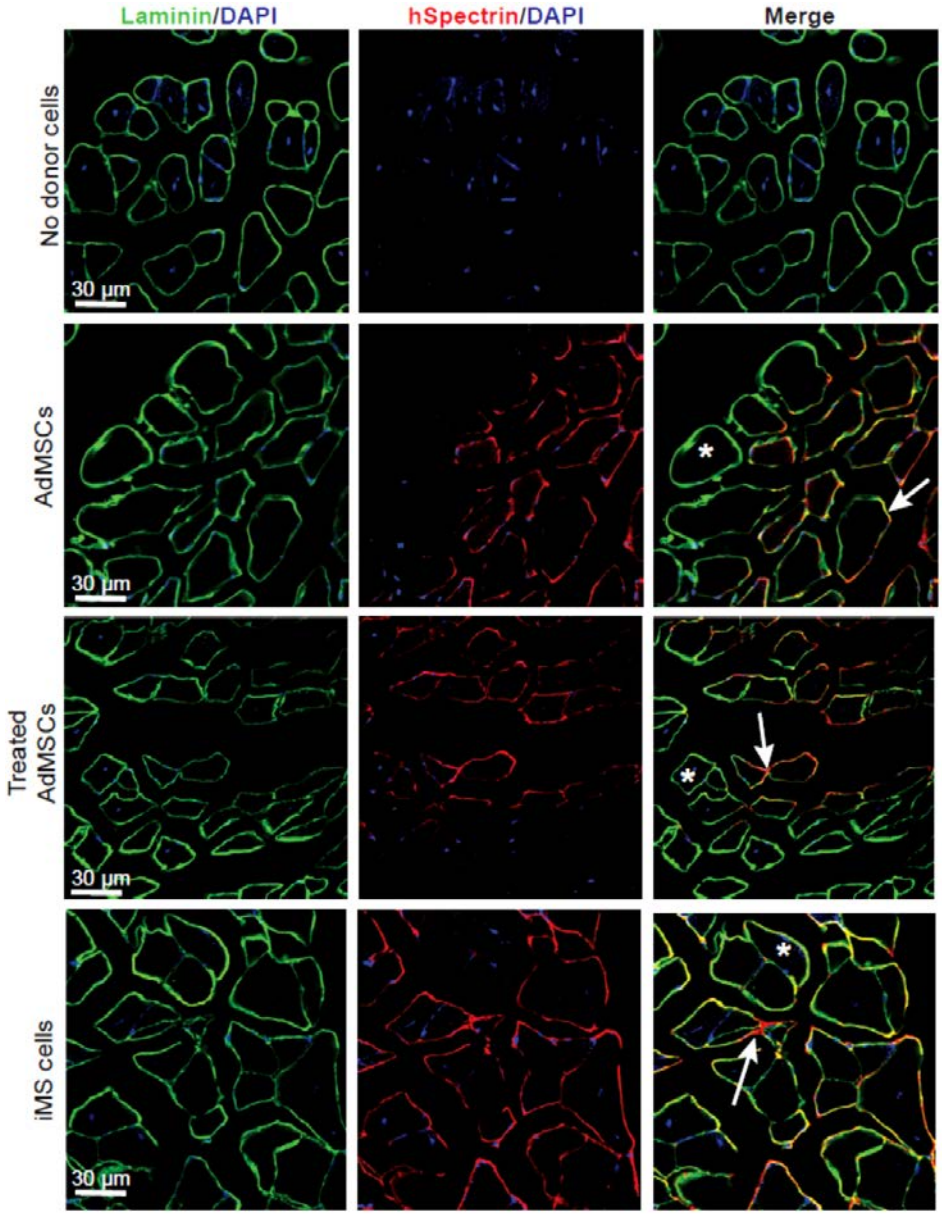

Figure 6. 7 Detection of human spectrin-positive myofibres in animals transplanted with human cells.

Representative confocal images of left TA muscle sections harvested at four weeks from mice (n=2 for each group) transplanted with matrigel alone (vehicle control, no donor cells), AdMSCs, treated AdMSCs or iMS cells. The sections were stained with DAPI (all nuclei), laminin (basal membrane of all muscle fibres) and hSpectrin (muscle fibres of human origin). Arrows in 'Merge' panel represent mosaic human-mouse muscle fibres and asterisks represent mouse muscle fibres. (Scale bar, 30 µm).

We next investigated quantitative differences across different study groups with respect to donor cell contribution to formation of mature, regenerated myofibres. Within a single cross-section, a total of 800-1000 myofibres were scored for laminin and hSpectrin staining. Myofibres stained with laminin alone were deemed to be derived only from endogenous host cells whereas the fibres co-stained with laminin and hSpectrin were deemed to have contribution from transplanted human cells.

Notably, at four weeks post-transplant, human iMS cells (57.6±3.6%) and treated AdMSCs (39.4±2.4%) gave rise to a significantly higher proportion of hSpectrin-positive myofibres than AdMSCs (30.6±3.6%), (Figure 6.8). These data confirm the selective advantage of reprogrammed cells over the untreated AdMSCs with respect to their ability to contribute to repair of damaged murine muscle tissues. Our data demonstrate that this could be because the DCi reprogrammed cells were retained within the injured environment and underwent commitment and differentiation along the myogenic lineage at levels significantly better than untreated AdMSCs. Whether due to superior retention and/or directed differentiation, treatment with AZA and rhPDGF-AB improved tissue repair potential of transplanted cells. Importantly, terminally differentiated adipocytes when subjected to DCi reprogramming, transformed into proliferative cells that responded to resident cues when transplanted into an injured microenvironment.

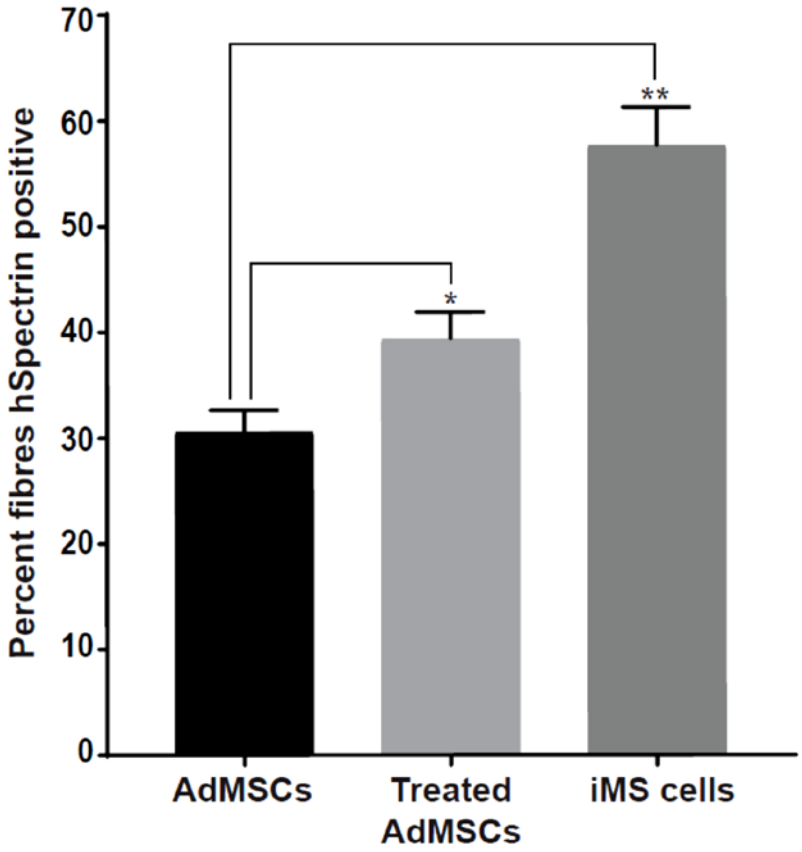

Figure 6. 8 Quantification of donor-derived human fibres in regenerating muscle sections.

Percentage of total myofibres that express hSpectrin at four weeks after transplantation of AdMSCs, treated AdMSCs or iMS cells into the CTX injured TA muscle. Each column represents the (average ± SD) percentage as calculated from three to five successive sections of TA muscles harvested from animals of each study group. n=2 mice for each group. Error bars, SD (n=3-5), (*P≤0.05, **P≤0.005, Student's T-test).

6.4 Chapter summary and discussion

This chapter details the tissue-specific repair potential of DCi reprogrammed human cells in an immunodeficient mouse model of acute skeletal muscle injury. Donor cells transplanted within the injured skeletal muscle underwent directed myogenic differentiation to restore the damaged muscles. The process of myogenesis involves precise co-ordination of diverse cellular events including cell-cell adhesion and cell-cell recognition (Buckingham, 1994). Canonical skeletal muscle regeneration includes fusion between donor cells and host myoblasts to allow progressive restoration of the tissue under the influence of host myogenic factors (Hardy et al., 2016; Sacchetti et al., 2016).

Contribution of donor-derived satellite cells to repair the damaged muscle fibres can occur either by directed differentiation of transplanted cells into muscle-specific cells or by acquisition of a muscle cell-like phenotype after their direct fusion with host cells. Our injury model did not involve ablation of the endogenous host satellite cells or other myogenic precursors. Within this setting wherein the host repair mechanisms to restore tissue damage and homoeostasis are still active, the retained donor cells comprised only a small percentage (<20%) of the total number of cells within the injured tissues (Figure 6.3). This observation could be attributed to the existing species barrier between donor cells and recipient tissues. Additionally, endogenous satellite cells and transient amplifying cells activated post-injury are more competent to participate in damage control. Earlier reports have also demonstrated that incapacitation of endogenous satellite cells can improve donor cell engraftment efficiency (Boldrin et al., 2012). On that background, we believe that the donor-derived satellite cells might have engrafted better within the injured tissues if the endogenous myogenic precursor cells were ablated in our study, however further investigation is required to answer this question.

Collectively, our data suggest that the engrafted donor-derived cells first committed to the myogenic lineage by differentiation into hCD56 stained satellite cells, in response to the resident cues within the injured muscle (Figure 6.5, top panel). These donor-derived SCs then underwent direct fusion with the regenerating myotube which was evident from multinucleated muscle fibres at the two-week timepoint (Figure 6.5, middle panel).

The final repair phase includes maturation of the regenerating myotubes and is expected to be completed within three-four weeks post CTX-mediated injury. In our study, most of the fibres had matured and were assembled into individual bundles, as observed in tissue sections harvested at the four-week time-point. At this stage, a significant proportion of the muscle fibres were co-stained with laminin (marks all muscle fibres) and hSpectrin (specifically marks only human muscle fibres) (Figure 6.7). Notably, within a fibre that was co-stained with hSpectrin and laminin, only a part of the fibre membrane was stained with hSpectrin (Figure 6.7). This is consistent with fusion occurring between the host and donor cells and rules out direct differentiation of the donor-derived satellite cells into myotubes. However, these findings could be further validated by evaluating the expression of species-specific sarcomeric proteins such as myosin heavy chain (MHC) within the regenerated myotubes. With respect to efficiency, DCi reprogrammed iMS cells and treated AdMSCs displayed a significantly higher contribution towards formation of regenerated muscle fibres within the host tissue environment than the corresponding AdMSCs (Figure 6.8).

A subpopulation of hCD56 positive SCs was also retained within tissue sections harvested at the four-week endpoint from each of the study groups. Interestingly, these donor-derived SCs occupied a sub-laminal position, characteristic of dormant SCs in healthy muscles (Figure 6.9). Our data therefore suggests that a proportion of the donor-

derived satellite cells might have undergone fusion and contributed to formation of the chimeric regenerated myofibre; while the other cells underwent self-renewal and were maintained as SCs in the sub-laminal space within the matured myofibres (Figure 6.9). This observation is indicative of reconstitution of a donor-derived SC population within the host niche, that will perhaps be maintained to combat future injuries to the same muscle tissue. However, further analysis is essential to determine the precise extent of fusion v/s self-renewal and the possibility that re-injury can activate this population of human SCs.

Consistent with our previous findings, despite their multipotent nature there was no evidence of ectopic tissue formation within the muscle sections. Although this observation is based on morphological evaluation of tissue sections at the four-week timepoint, further testing with species-specific markers for non-myogenic cells such as endothelial cells (comprising blood vessels within the muscle) or neuronal cells (comprising nerve bundles within the muscle) is required.

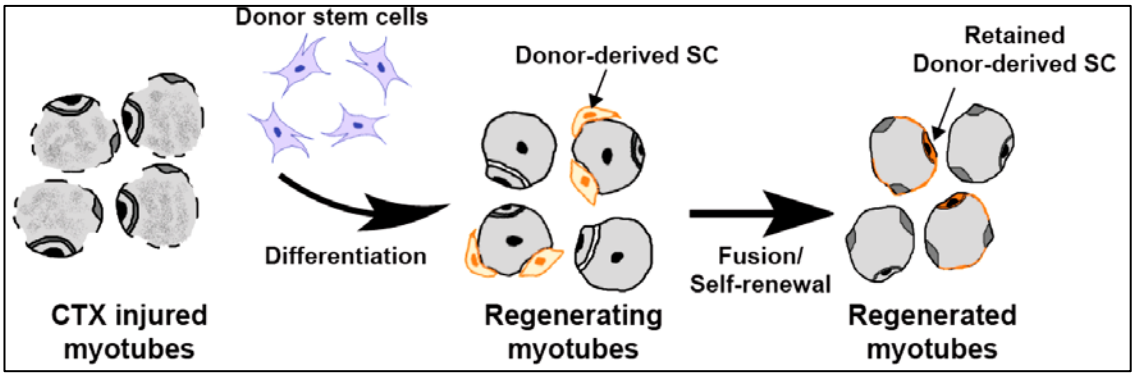

Figure 6. 9 Schematic representation of proposed mechanism for donor cell contribution to myofibre regeneration

Schematic showing course of donor stem cell commitment along the myogenic lineage through initial differentiation into SCs (elongated orange cells) which get lodged onto the centro-nucleated regenerating myotube. Subpopulations of the SCs then undergo fusion with the regenerating myotubes leading to formation of a human-mouse chimeric muscle fibres (fibres marked in gray and orange lamina) whereas the other fraction of SCs undergoes self-renewal to be maintained as SCs (orange cells at sub-laminal position). Adapted from (Garry et al., 2016).

Finally, this study has certain limitations. Firstly, it did not include impairment of the host's endogenous repair capacity. The presence of host satellite cells places the transplanted cells in a competitive environment to bring about tissue repair. Ablation of endogenous host satellite cells prior to transplantation of xenogeneic test stem cell populations will help us better understand the biological response mounted by the host after cell engraftment. Local irradiation of TA muscle prior to injury allows incapacitation of host satellite cells which in turn facilitates better engraftment of transplanted cells. This treatment causes reduction in growth of muscle and surrounding tissues while preserving the post-mitotic fibres. It is important to note that complete ablation of host satellite cells by irradiation with 25 Gy allows almost no donor cell engraftment thereby making it essential to restrict irradiation to the recommended dose of 18 Gy. Hence, controlled incapacitation of endogenous satellite cells combined with retention of a functional niche is required for efficient donor satellite cell-derived muscle regeneration (Boldrin et al., 2012; Morgan et al., 2002). Secondly, our study consisted of acute skeletal muscle injury on immunodeficient mice to alleviate chances of an immune response to the donor cells. However, previous studies have shown that immunodeficient mice have exacerbated muscle pathology, thereby compounding the induced injury state (Boldrin et al., 2009). Nextly, our current study only included one or two animals per time point within a study group. It also focused only on a short time point of four weeks to track the regenerative response and capture acute adverse reactions directly related to transplantation of DCi reprogrammed iMS cells. However, studies examining longer time points after cell injection in the muscle tissues in larger study groups would allow precise interpretation of the response of (now) latent human satellite cells within the host tissues. Lastly, it is not known if re-injury to the mature muscle fibres in mice which retain the donor-derived SCs results in greater quantities of donor-derived mature muscle fibres.

Hence, there is also a need for re-injuring the mature muscle fibres which have the donor derived SCs to help determine if the iMS cells are able to undergo better myogenic differentiation and result in greater quantities of donor-derived mature fibres in comparison to untreated/treated AdMSCs.

Despite these constraints, our pilot study demonstrates the efficacy of DCi reprogrammed iMS cells to repair and regenerate specific tissue within the setting of an injured skeletal muscle. DCi reprogrammed cells can engraft, respond to inherent cues, and undergo controlled, context-dependent differentiation along the myogenic lineage. Along with directly contributing to repair of a tissue-specific injury, the donor cells were also shown to replenish the niche by maintaining their self-renewal property, as evident from reconstitution of the satellite cell pool within the regenerated muscle fibres. In conclusion, terminally differentiated primary adipocytes regained *in vivo* plasticity on exposure to DCi reprogramming factors and this acquired potential could be constructively harnessed to heal damaged tissues without any adverse effects. This study therefore provides preliminary results on the feasibility of DCi reprogrammed cells as viable candidates for cell-based therapeutic approaches in regenerative medicine.

CHAPTER 7 Conclusions and future directions

7.1 DCi reprogramming, a novel technique to generate autologous, multipotent stem cells

Lineage reprogramming is the next frontier in the field of regenerative medicine. Generation of a pool of plastic, autologous stem cells which bear the capacity to contribute directly to repair and regeneration of damaged tissues has significant advantages over using pluripotent stem cells or other off-the-shelf/allogeneic alternatives.

This study describes optimization of a transcription factor-, vector-, and xeno-free method for somatic cell reprogramming using the epigenetic modifier AZA and rhPDGF-AB, a cytokine (**3.2.1-3.2.3**). This novel reprogramming technique (DCi reprogramming) enables generation of patient-specific iMS cells and promises alleviation of many of the challenges associated with allogeneic cell therapy. This study involved use of adipose tissue as the source of somatic cells, selected for its ease of harvest and abundance in the human body. Application of this technique to different tissues might however necessitate case-specific optimization depending on the desired downstream application of reprogrammed cells.

DCi reprogramming for generation of iMS cells from human adipocytes harvested from subjects aged 18-80 years has been optimized with respect to the duration and dose of reprogramming factors. Although we have shown that presence of serum (human/xenogeneic) is indispensable for DCi reprogramming **(3.2.1-3.2.3),** the serum components that facilitate cell fate reversal have not yet been identified. Serum-profiling

using high-throughput protein microarrays (Sharon & Snyder, 2014) could be used to determine components important for *in vitro* induction or maintenance of a specific cell state. Identification of relevant serum components will not only ensure complete avoidance of undefined reprogramming medium but will also help gain a better understanding of the underlying process of cell fate conversion. The current protocol for DCi reprogramming is optimized to efficiently yield iMS cells from primary adipocytes in 25 days. However, certain downstream applications might require quicker cell conversion and/or shorter *ex vivo* culture times, to reduce the risk of contamination or undesirable changes within the cell populations. It would therefore be helpful to improve the efficiency of DCi reprogramming i.e. attaining the same number of reprogrammed cells in a shorter timeframe than the current 25 days. Therefore, in an attempt towards further improving the efficiency of this technique, supplementation of DCi reprogramming factors with other epigenetic modifiers such as Sodium butyrate, Vitamin C, Valproic acid, Trichostatin A, etc. could be tested for their ability to aid cell conversion.

The DCi reprogramming method described in this thesis is also highly amenable to automation. The steps of somatic cell isolation and conversion could potentially be conducted in a closed system, bench-top, FDA approved, cGMP grade machine to generate a patient-specific cell-based therapeutic product for transplantation. Indeed, adapting our procedure to such a system would be highly favourable for use in a clinical setting as minimising the number of manual steps would significantly reduce the risk of contamination and most likely improve reproducibility of the technique. Use of a fully closed, sterile processing system would also ensure sustainability and reduction in clean room requirements. This time-saving, automated system would also permit integrated cell processing thereby allowing simplification of the whole process. Although such work is

well beyond the scope of this thesis, we have already started the process of adapting the DCi process for use in the CliniMACS Prodigy system (Miltenyi).

7.2 *In vitro* characteristics/ insights from molecular work

Although this thesis has included detailed characterisation of the phenotypic characteristics of DCi reprogrammed cells **(3.2.4),** there is still work to be done in understanding the cell conversion process from a more mechanistic point of view. There are several recently developed techniques which will be particularly suitable for such an analysis. Precise quantification of AZA incorporation across the reprogramming time-course (using sophisticated techniques such as AZA-MS (Unnikrishnan et al., 2018)) in cells undergoing conversion would give a better understanding of the mechanism of DCi reprogramming. Epigenomic analysis using techniques such as bisulphite sequencing at different stages of reprogramming or on reprogramming intermediates could reveal details of the temporal dynamics of methylation/demethylation events during cell fate reversal. Emerging technologies such as single-cell RNA-seq or Assay for Transposase-Accessible Chromatin using sequencing (ATAC-seq) (Buenrostro et al., 2015) could also be used to better understand cell fate switching between differentiated cells and DCi reprogrammed cells. Furthermore, use of the comprehensive scM&T-seq that involves parallel single-cell genome-wide methylome and transcriptome sequencing (Angermueller et al., 2016) could help decipher the associations between transcriptional and epigenomic changes induced in cells as a result of exposure to DCi reprogramming factors. The use of such strategies would reveal novel mechanisms and pathways involved in reprogramming, leading to a better understanding of how cell identity can be manipulated and potentially leading to new reprogramming technologies that could be applied to other tissue types.

7.3 Safety, efficacy and specificity of plasticity of iMS cells

Exposure to DCi reprogramming factors resulted in re-expression of pluripotency associated factors in the reprogrammed cells **(4.2.2**). While iMS cells can therefore be deemed pluripotent by this definition, it is still necessary to further validate their pluripotency using gold-standard *in vivo* teratoma assays. As demonstrated from our *in vivo* study in a generic tissue injury model, DCi reprogrammed iMS cells were not only retained at the site of transplantation in an environment of tissue loss **(5.3.1, 5.3.2),** but they also exhibited better context-dependent plasticity in comparison to control cells **(5.3.4).** The specificity of the *in vivo* plasticity of iMS cells was further confirmed in the skeletal muscle injury study where the transplanted human iMS cells contributed to formation of regenerated muscle fibres in response to resident cues **(6.3.3, 6.3.4).** There was no observed cell migration to off-target sites, ectopic tissue formation, or tumorigenicity in any of the studies, further underscoring the *in vivo* safety of transplanted iMS cells. Nevertheless, precise evaluation of their teratogenicity using the gold standard *in vivo* teratoma assays is necessary to rule out any risk of adverse events post transplantation. Moreover, these studies were carried out on a small cohort of immunodeficient mice which lack both T and B cells while most of the individuals being treated would have normal immune function and might present a different environment for the transplanted cells. Evaluation of tissue repair potential in immunocompetent strains of mice can partly address this issue. Using an immunocompetent system is beneficial in that the presence of T and B cells would allow execution of immune-mediated clearance of toxic/dead cells within the damaged tissue through the release of cytokines. However, using this immunocompetent system can also be slightly challenging as it would need to strike the right balance between the effects of tolerance and rejection of transplanted cells for the iMS cells to effectively manifest their tissue repair potential.

Additionally, to better assess the pre-clinical safety and efficacy of human iMS cells, studies with bigger cohorts of large animals like sheep or pigs would be helpful. However, none of these studies can eliminate the species barrier, and the ultimate utility of iMS cells in human tissue repair can only be known through clinical trials conducted in human patients.

In our studies, human somatic cells were first reprogrammed *in vitro*, expanded *ex vivo,* and then transplanted in a tissue injury model. Transplantation of a smaller number of cells and long-term follow-up of their maintenance at the site of transplant, could help understand any time dependent effects on cell engraftment, viability and subsequently the tissue repair potential of iMS cells. In addition, studying the effects of different biomaterials/matrices to assist delivery of cells might improve our understanding of the role of ECM and cell-ECM interactions within the host microenvironment. For example, a recent study demonstrated that slow release of pro-survival peptides from collagen biomaterials improved stem cell engraftment in a mouse model of ischemia (Lee et al. 2018).

Another potential area for improvement of the DCi technique lies in development of in *situ* reprogramming which could potentially be achieved by targeted delivery and controlled release of DCi reprogramming factors into the injured tissues. Such delivery could be achieved with the use of specialised devices such as osmotic minipumps (Doucette et al., 2000) which would also facilitate spatial and temporal control over the *in vivo* effects of administered compounds. Additionally, this would also alleviate the need for isolation of somatic cells and the associated contamination risk of *ex vivo* processing.

On the other hand, using tissue injury models in transgenic mice like the OCT4-GFP line (Lengner et al., 2007) (wherein GFP expression is driven by the Oct4 promoter), would help understand if the endogenous tissue resident progenitor cells adopt a transient de-differentiated state before differentiating into specialised cells required for reconstitution of the damaged tissue. Gain and loss of GFP expression would help delineate the cell fate changes and turn-over of endogenous cells over the course of regeneration. Combining this strategy with *in situ* delivery of DCi reprogramming factors would also help to understand their effects in enhancing tissue repair by quantitative comparison of GFP (OCT4) expression at intermittent stages of tissue healing.

Our skeletal muscle regeneration model elucidated the specificity of *in vivo* plasticity of iMS cells and their ability to directly contribute to tissue repair in a competitive environment containing endogenous host satellite cells. The use of transgenic mice such as Pax7-nGFP line (Sambasivan et al., 2009) (wherein GFP expression is driven by Pax7 promoter) could help delineate the exact timeline of satellite cell activation (through GFP expression) and their subsequent differentiation into muscle fibres (through loss of GFP expression). This would indeed help elucidate the precise contribution of endogenous (GFP positive) or transplanted iMS cells (GFP negative) towards tissue repair or regeneration. However, the behaviour of transplanted cells in an injured tissue environment where the endogenous satellite cells are ablated has not yet been characterised. Exclusion of competing cells might facilitate better engraftment and contribution of the transplanted cells to tissue repair. From our data it was clear that the donor-derived satellite cells participated in reconstituting the satellite cell niche of the regenerated muscle. It would be interesting to know whether these satellite cells could respond to a future episode of acute tissue injury and regenerate the damaged tissue in response to resident cues. Sophisticated techniques such as intravital imaging that allow

live monitoring of the fate of transplanted cells (Pittet & Weissleder, 2011) could also be harnessed to understand cell-cell interactions by monitoring different parameters, for example, calcium ion flux, chemotactic index, etc. These would in turn help in finding ways to further fine tune the reprogramming process. *In situ* regeneration could also be studied for the skeletal muscle injury model, by direct delivery of DCi reprogramming factors within the injured muscle. To further aid the process of scar-free tissue healing, activation of pathways (for example, JAK/STAT-1, mTORC1 signaling) that are involved in tissue repair and regeneration (Doles & Olwin, 2014; Haller et al., 2017; La Fortezza et al., 2016) and inhibition of fibrosis pathways (Zhong et al., 2010) (for example, using TGFβ inhibitors) using specific small molecules can be tested. A recent study on human distal tip regeneration has shown that the dormant regenerative potential in regeneration-incompetent injuries can be stimulated within the regenerative window by targeted treatment with specific morphogenic agents e.g. BMP2 (Dolan et al., 2018). Therefore, the synergistic effect of these molecules and DCi reprogramming factors can be explored in the context of tissue regeneration.

In conclusion, this study demonstrates the generation of therapeutically relevant, autologous, tissue regenerative iMS cells from primary human somatic cells. The DCi reprogramming technique, which is practical, feasible and overcomes most of the limitations associated with other techniques, is an important addition to the toolbox of regenerative medicine approaches. Results in this study optimized the generation of autologous iMS cells, characterized their *in vitro* and *in vivo* features, interrogated their molecular identities, examined their *in vivo* safety and plasticity in the context of tissue injury, and finally established their tissue-specific, context-dependent regenerative potential. Future studies on DCi reprogramming can be directed either towards investigative aspect or translational aspect (Figure 7.1). The investigative aspects involve

understanding the tissue regenerative potential of DCi reprogrammed cells in more severe, debilitating conditions e.g. myocardial infarction or spinal cord injury. Researchers may also direct their efforts in improving the efficiency of DCi reprogramming or elucidating the cell conversion process from a mechanistic point of view by understanding changes induced at the genetic as well as epigenetic level. Finally, on the translational perspective, this study has laid a foundation for demonstrating the safety and efficacy of iMS cells as cell-based therapeutic alternative. These findings provide extensive scope for researchers and clinicians to leverage this data in future clinical trials aimed towards better treatment of acute or chronic tissue injuries.

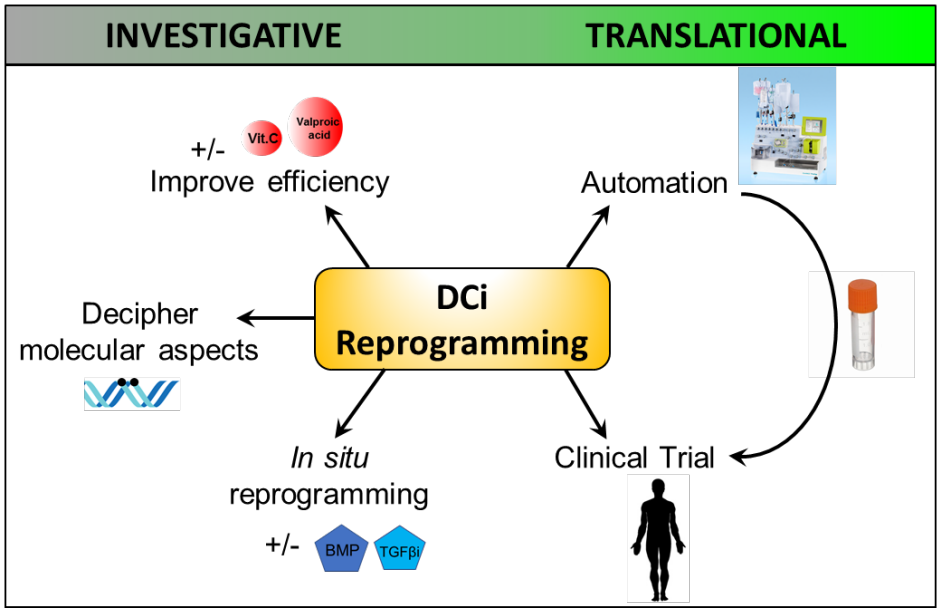

Figure 7. 1 Future directions for DCi reprogramming

Schematic showing possible investigative and translational prospects of DCi reprogramming. (Vit. C: Vitamin C, BMP: Bone Morphogenic Protein, TGFβi: Transforming Growth Factor β inhibitor).

Contributions

Majority of the experiments and data analyses presented herein were completed by A. Yeola. V.Chandrakanthan provided guidance for performing the experiments. For all the experiments, adipose tissue and patient blood was obtained with informed consent from people undergoing surgery and were kindly provided by neurosurgeon R.Mobbs (Neurosurgery unit, Prince of Wales Hospital). Pan-genomic karyotyping described in Chapter 3 was conducted by P.Hardy (Cytolabs).

D.Kang helped with RNA extraction, D.Beck and Y.Huang conducted analysis of transcriptomic data which comprises first section of Chapter 4 in this thesis. D.Ma (St. Vincent's Clinic) and E. Wolvetang (Australian Institute of Bioengineering and Nanotechnology (AIBN)) kindly provided WT C2 iPS cells and P.Fortuna (AIBN) kindly shared the protocol for the *in vitro* teratoma assay which comprises the second section of Chapter 4. M.Tursky, C.Artuz (St. Vincent's Clinic) assisted with setting up *in vitro* teratoma assay experiments. R.A.Oliver (Surgical and Orthopaedic Research Laboratory(SORL)) assisted with sectioning and H&E staining for this experiment and C.Loo (South Eastern Area Laboratory Services) provided guidance with analysing histology results.

J.A.I. Thoms kindly provided guidance and supervision for lentiviral transduction experiments. The LeGO-iG2-Luc2 plasmid was a kind gift from K.Weber. I would like to thank B.Walsh, R.Oliver (SORL) for surgery on the mice and T.Hung, C.Power (Biological Resources Imaging Laboratory) for their help with periodic D-luciferin injections required for bioluminescence imaging, as part of Chapter 5 of this thesis.

I am thankful to M.Kavallaris and J.McCarroll (Children's Cancer Institute Australia) for providing the SCID/Beige mice used in the muscle regeneration study and E.Hardeman and C.Lucas (Neuromuscular and Regenerative Medicine Unit) for their input on technical aspects of surgery on mice, which constitute Chapter 6 of this thesis. J. E. Pimanda and V. Chandrakanthan assisted with data analysis and provided supervision for the entire study.

My sincere thanks to J. A. I. Thoms for her help in proof-reading this thesis. Thanks go to the staff at BMIF UNSW Australia for the use of microscopy facilities, donors and staff of neurosurgery unit at the Prince of Wales Hospital, staff at the BRIL flow cytometry facilities, staff at the BMSF for tissue sectioning, past and present members of the Pimanda laboratory for their assistance throughout.

References

Abdallah, B. M., & Kassem, M. (2008). Human mesenchymal stem cells: from basic biology to clinical applications. *Gene Ther, 15*(2), 109-116. doi:10.1038/sj.gt.3303067

Anders, S., Pyl, P. T., & Huber, W. (2015). HTSeq--a Python framework to work with high-throughput sequencing data. *Bioinformatics, 31*(2), 166-169. doi:10.1093/bioinformatics/btu638

Andrae, J., Gallini, R., & Betsholtz, C. (2008). Role of platelet-derived growth factors in physiology and medicine. *Genes Dev, 22*(10), 1276-1312. doi:10.1101/gad.1653708

Angermueller, C., Clark, S. J., Lee, H. J., et al. (2016). Parallel single-cell sequencing links transcriptional and epigenetic heterogeneity. *Nat Methods, 13*(3), 229-232. doi:10.1038/nmeth.3728

Apostolou, E., & Hochedlinger, K. (2013). Chromatin dynamics during cellular reprogramming. *Nature, 502*(7472), 462-471. doi:10.1038/nature12749

Arnold, L., Henry, A., Poron, F., et al. (2007). Inflammatory monocytes recruited after skeletal muscle injury switch into antiinflammatory macrophages to support myogenesis. *J Exp Med, 204*(5), 1057-1069. doi:10.1084/jem.20070075

Asahara, T., Masuda, H., Takahashi, T., et al. (1999). Bone marrow origin of endothelial progenitor cells responsible for postnatal vasculogenesis in physiological and pathological neovascularization. *Circ Res, 85*(3), 221-228.

Bagheri-Hosseinabadi, Z., Mesbah-Namin, S. A., Salehinejad, P., & Seyedi, F. (2018). Fibrin scaffold could promote survival of the human adipose-derived stem cells during differentiation into cardiomyocyte-like cells. *Cell Tissue Res*. doi:10.1007/s00441-018-2799-9

Baksh, D., Yao, R., & Tuan, R. S. (2007). Comparison of proliferative and multilineage differentiation potential of human mesenchymal stem cells derived from umbilical cord and bone marrow. *Stem Cells, 25*(6), 1384-1392. doi:10.1634/stemcells.2006-0709

Ball, S. G., Shuttleworth, A., & Kielty, C. M. (2012). Inhibition of platelet-derived growth factor receptor signaling regulates Oct4 and Nanog expression, cell shape, and mesenchymal stem cell potency. *Stem Cells, 30*(3), 548-560. doi:10.1002/stem.1015

Ball, S. G., Shuttleworth, C. A., & Kielty, C. M. (2007). Mesenchymal stem cells and neovascularization: role of platelet-derived growth factor receptors. *J Cell Mol Med, 11*(5), 1012-1030. doi:10.1111/j.1582-4934.2007.00120.x

Ball, S. G., Worthington, J. J., Canfield, A. E., Merry, C. L., & Kielty, C. M. (2014). Mesenchymal stromal cells: inhibiting PDGF receptors or depleting fibronectin induces mesodermal progenitors with endothelial potential. *Stem Cells, 32*(3), 694-705. doi:10.1002/stem.1538

Bara, J. J., McCarthy, H. E., Humphrey, E., Johnson, W. E., & Roberts, S. (2014). Bone marrow-derived mesenchymal stem cells become antiangiogenic when chondrogenically or osteogenically differentiated: implications for bone and cartilage tissue engineering. *Tissue Eng Part A, 20*(1-2), 147-159. doi:10.1089/ten.TEA.2013.0196

Barry, F. P., & Murphy, J. M. (2004). Mesenchymal stem cells: clinical applications and biological characterization. *Int J Biochem Cell Biol, 36*(4), 568-584. doi:10.1016/j.biocel.2003.11.001

Ben-David, U., & Benvenisty, N. (2011). The tumorigenicity of human embryonic and induced pluripotent stem cells. *Nat Rev Cancer, 11*(4), 268-277. doi:10.1038/nrc3034

Bergsten, E., Uutela, M., Li, X., et al. (2001). PDGF-D is a specific, protease-activated ligand for the PDGF beta-receptor. *Nat Cell Biol, 3*(5), 512-516. doi:10.1038/35074588

Bianco, P., Cao, X., Frenette, P. S., et al. (2013). The meaning, the sense and the significance: translating the science of mesenchymal stem cells into medicine. *Nat Med, 19*(1), 35-42. doi:10.1038/nm.3028

Bianco, P., Robey, P. G., & Simmons, P. J. (2008). Mesenchymal stem cells: revisiting history, concepts, and assays. *Cell Stem Cell, 2*(4), 313-319. doi:10.1016/j.stem.2008.03.002

Biteau, B., Hochmuth, C. E., & Jasper, H. (2011). Maintaining tissue homeostasis: dynamic control of somatic stem cell activity. *Cell Stem Cell, 9*(5), 402-411. doi:10.1016/j.stem.2011.10.004

Blanchard, J. W., Xie, J., El-Mecharrafie, N., et al. (2017). Replacing reprogramming factors with antibodies selected from combinatorial antibody libraries. *Nat Biotechnol, 35*(10), 960-968. doi:10.1038/nbt.3963

Blau, H. M., Brazelton, T. R., & Weimann, J. M. (2001). The evolving concept of a stem cell: entity or function? *Cell, 105*(7), 829-841.

Blau, H. M., Chiu, C. P., & Webster, C. (1983). Cytoplasmic activation of human nuclear genes in stable heterocaryons. *Cell, 32*(4), 1171-1180.

Bochkov, N. P., Voronina, E. S., Kosyakova, N. V., et al. (2007). Chromosome variability of human multipotent mesenchymal stromal cells. *Bull Exp Biol Med, 143*(1), 122-126.

Boldrin, L., Neal, A., Zammit, P. S., Muntoni, F., & Morgan, J. E. (2012). Donor satellite cell engraftment is significantly augmented when the host niche is preserved and endogenous satellite cells are incapacitated. *Stem Cells, 30*(9), 1971-1984. doi:10.1002/stem.1158

Boldrin, L., Zammit, P. S., Muntoni, F., & Morgan, J. E. (2009). Mature adult dystrophic mouse muscle environment does not impede efficient engrafted satellite cell regeneration and self-renewal. *Stem Cells, 27*(10), 2478-2487. doi:10.1002/stem.162

Bongso, A., Fong, C. Y., & Gauthaman, K. (2008). Taking stem cells to the clinic: Major challenges. *J Cell Biochem, 105*(6), 1352-1360. doi:10.1002/jcb.21957

Boya, P., Codogno, P., & Rodriguez-Muela, N. (2018). Autophagy in stem cells: repair, remodelling and metabolic reprogramming. *Development, 145*(4). doi:10.1242/dev.146506

Boyer, L. A., Lee, T. I., Cole, M. F., et al. (2005). Core transcriptional regulatory circuitry in human embryonic stem cells. *Cell, 122*(6), 947-956. doi:10.1016/j.cell.2005.08.020

Brandenberger, R., Khrebtukova, I., Thies, R. S., et al. (2004). MPSS profiling of human embryonic stem cells. *BMC Dev Biol, 4*, 10. doi:10.1186/1471-213X-4-10

Breitbach, M., Bostani, T., Roell, W., et al. (2007). Potential risks of bone marrow cell transplantation into infarcted hearts. *Blood, 110*(4), 1362-1369. doi:10.1182/blood-2006-12-063412

Briggs, J. A., Sun, J., Shepherd, J., et al. (2013). Integration-free induced pluripotent stem cells model genetic and neural developmental features of down syndrome etiology. *Stem Cells, 31*(3), 467-478. doi:10.1002/stem.1297

Brisby, H., Papadimitriou, N., Brantsing, C., Bergh, P., Lindahl, A., & Barreto Henriksson, H. (2013). The presence of local mesenchymal progenitor cells in human degenerated intervertebral discs and possibilities to influence these in vitro: a descriptive study in humans. *Stem Cells Dev, 22*(5), 804-814. doi:10.1089/scd.2012.0179

Brockes, J. P., & Kumar, A. (2005). Appendage regeneration in adult vertebrates and implications for regenerative medicine. *Science, 310*(5756), 1919-1923. doi:10.1126/science.1115200

Buckingham, M. (1994). Molecular biology of muscle development. *Cell, 78*(1), 15-21.

Buenrostro, J. D., Wu, B., Chang, H. Y., & Greenleaf, W. J. (2015). ATAC-seq: A Method for Assaying Chromatin Accessibility Genome-Wide. *Curr Protoc Mol Biol, 109*, 21 29 21-29. doi:10.1002/0471142727.mb2129s109

Buganim, Y., Faddah, D. A., Cheng, A. W., et al. (2012). Single-cell expression analyses during cellular reprogramming reveal an early stochastic and a late hierarchic phase. *Cell, 150*(6), 1209-1222. doi:10.1016/j.cell.2012.08.023

Caplan, A. I. (2010). Mesenchymal Stem Cells: The Past, the Present, the Future. *Cartilage, 1*(1), 6-9. doi:10.1177/1947603509354992

Caplan, A. I. (2017). Mesenchymal Stem Cells: Time to Change the Name! *Stem Cells Transl Med, 6*(6), 1445-1451. doi:10.1002/sctm.17-0051

Caplan, A. I., & Bruder, S. P. (2001). Mesenchymal stem cells: building blocks for molecular medicine in the 21st century. *Trends Mol Med, 7*(6), 259-264.

Caplan, A. I., & Correa, D. (2011). PDGF in bone formation and regeneration: new insights into a novel mechanism involving MSCs. *J Orthop Res, 29*(12), 1795-1803. doi:10.1002/jor.21462

Carceller, M. C., Guillen, M. I., Ferrandiz, M. L., & Alcaraz, M. J. (2015). Paracrine in vivo inhibitory effects of adipose tissue-derived mesenchymal stromal cells in the early stages of the acute inflammatory response. *Cytotherapy, 17*(9), 1230-1239. doi:10.1016/j.jcyt.2015.06.001

Carey, B. W., Markoulaki, S., Hanna, J. H., et al. (2011). Reprogramming factor stoichiometry influences the epigenetic state and biological properties of induced pluripotent stem cells. *Cell Stem Cell, 9*(6), 588-598. doi:10.1016/j.stem.2011.11.003

Carlson, B. M. (1973). The regeneration of skeletal muscle. A review. *Am J Anat, 137*(2), 119-149. doi:10.1002/aja.1001370202

Carragee, E. J., Hurwitz, E. L., & Weiner, B. K. (2011). A critical review of recombinant human bone morphogenetic protein-2 trials in spinal surgery: emerging safety concerns and lessons learned. *Spine J, 11*(6), 471-491. doi:10.1016/j.spinee.2011.04.023

Centeno, C., Markle, J., Dodson, E., et al. (2017). Treatment of lumbar degenerative disc disease-associated radicular pain with culture-expanded autologous mesenchymal stem cells: a pilot study on safety and efficacy. *J Transl Med, 15*(1), 197. doi:10.1186/s12967-017-1300-y

Chakkalakal, J. V., Jones, K. M., Basson, M. A., & Brack, A. S. (2012). The aged niche disrupts muscle stem cell quiescence. *Nature, 490*(7420), 355-360. doi:10.1038/nature11438

Chandrakanthan, V., Yeola, A., Kwan, J. C., et al. (2016). PDGF-AB and 5-Azacytidine induce conversion of somatic cells into tissue-regenerative multipotent stem cells. *Proc Natl Acad Sci U S A, 113*(16), E2306-2315. doi:10.1073/pnas.1518244113

Chang, C. C., Chuang, S. T., Lee, C. Y., & Wei, J. W. (1972). Role of cardiotoxin and phospholipase A in the blockade of nerve conduction and depolarization of skeletal muscle induced by cobra venom. *Br J Pharmacol, 44*(4), 752-764.

Chang, N. C., & Rudnicki, M. A. (2014). Satellite cells: the architects of skeletal muscle. *Curr Top Dev Biol, 107*, 161-181. doi:10.1016/B978-0-12-416022-4.00006-8

Chang, Y. H., Liu, H. W., Wu, K. C., & Ding, D. C. (2016). Mesenchymal Stem Cells and Their Clinical Applications in Osteoarthritis. *Cell Transplant, 25*(5), 937-950. doi:10.3727/096368915X690288

Charge, S. B., & Rudnicki, M. A. (2004). Cellular and molecular regulation of muscle regeneration. *Physiol Rev, 84*(1), 209-238. doi:10.1152/physrev.00019.2003

Cheloufi, S., Elling, U., Hopfgartner, B., et al. (2015). The histone chaperone CAF-1 safeguards somatic cell identity. *Nature, 528*(7581), 218-224. doi:10.1038/nature15749

Chen, J., Crawford, R., Chen, C., & Xiao, Y. (2013). The key regulatory roles of the PI3K/Akt signaling pathway in the functionalities of mesenchymal stem cells and applications in tissue regeneration. *Tissue Eng Part B Rev, 19*(6), 516-528. doi:10.1089/ten.TEB.2012.0672

Chiche, A., Le Roux, I., von Joest, M., et al. (2017). Injury-Induced Senescence Enables In Vivo Reprogramming in Skeletal Muscle. *Cell Stem Cell, 20*(3), 407-414 e404. doi:10.1016/j.stem.2016.11.020

Chimenti, I., Smith, R. R., Li, T. S., et al. (2010). Relative roles of direct regeneration versus paracrine effects of human cardiosphere-derived cells transplanted into infarcted mice. *Circ Res, 106*(5), 971-980. doi:10.1161/CIRCRESAHA.109.210682

Chong, J. J., Chandrakanthan, V., Xaymardan, M., et al. (2011). Adult cardiac-resident MSC-like stem cells with a proepicardial origin. *Cell Stem Cell, 9*(6), 527-540. doi:10.1016/j.stem.2011.10.002

Christman, J. K. (2002). 5-Azacytidine and 5-aza-2'-deoxycytidine as inhibitors of DNA methylation: mechanistic studies and their implications for cancer therapy. *Oncogene, 21*(35), 5483-5495. doi:10.1038/sj.onc.1205699

ClinicalTrials.gov. (2018). ClinicalTrials.gov. Retrieved from https://clinicaltrials.gov/

Cohen, S., Leshansky, L., Zussman, E., et al. (2010). Repair of full-thickness tendon injury using connective tissue progenitors efficiently derived from human embryonic stem cells and fetal tissues. *Tissue Eng Part A, 16*(10), 3119-3137. doi:10.1089/ten.TEA.2009.0716

Colnot, C. (2011). Cell sources for bone tissue engineering: insights from basic science. *Tissue Eng Part B Rev, 17*(6), 449-457. doi:10.1089/ten.TEB.2011.0243

Cooper, R. N., Thiesson, D., Furling, D., Di Santo, J. P., Butler-Browne, G. S., & Mouly, V. (2003). Extended amplification in vitro and replicative senescence: key factors implicated in the success of human myoblast transplantation. *Hum Gene Ther, 14*(12), 1169-1179. doi:10.1089/104303403322168000

Cornelison, D. D. (2008). Context matters: in vivo and in vitro influences on muscle satellite cell activity. *J Cell Biochem, 105*(3), 663-669. doi:10.1002/jcb.21892

Corson, F., & Siggia, E. D. (2012). Geometry, epistasis, and developmental patterning. *Proc Natl Acad Sci U S A, 109*(15), 5568-5575. doi:10.1073/pnas.1201505109

Cowan, C. A., Atienza, J., Melton, D. A., & Eggan, K. (2005). Nuclear reprogramming of somatic cells after fusion with human embryonic stem cells. *Science, 309*(5739), 1369-1373. doi:10.1126/science.1116447

Crisan, M., Yap, S., Casteilla, L., et al. (2008). A perivascular origin for mesenchymal stem cells in multiple human organs. *Cell Stem Cell, 3*(3), 301-313. doi:10.1016/j.stem.2008.07.003

Currie, J. D., Kawaguchi, A., Traspas, R. M., Schuez, M., Chara, O., & Tanaka, E. M. (2016). Live Imaging of Axolotl Digit Regeneration Reveals Spatiotemporal Choreography of Diverse Connective Tissue Progenitor Pools. *Dev Cell, 39*(4), 411-423. doi:10.1016/j.devcel.2016.10.013

Dale, T. P., Mazher, S., Webb, W. R., et al. (2018). Tenogenic Differentiation of Human Embryonic Stem Cells. *Tissue Eng Part A, 24*(5-6), 361-368. doi:10.1089/ten.TEA.2017.0017

Daley, G. Q., Lensch, M. W., Jaenisch, R., Meissner, A., Plath, K., & Yamanaka, S. (2009). Broader implications of defining standards for the pluripotency of iPSCs. *Cell Stem Cell, 4*(3), 200-201; author reply 202. doi:10.1016/j.stem.2009.02.009

Daley, G. Q., & Scadden, D. T. (2008). Prospects for stem cell-based therapy. *Cell, 132*(4), 544-548. doi:10.1016/j.cell.2008.02.009

Dave, M., Mehta, K., Luther, J., Baruah, A., Dietz, A. B., & Faubion, W. A., Jr. (2015). Mesenchymal Stem Cell Therapy for Inflammatory Bowel Disease: A Systematic Review and Meta-analysis. *Inflamm Bowel Dis, 21*(11), 2696-2707. doi:10.1097/MIB.0000000000000543

Davis, R. L., Weintraub, H., & Lassar, A. B. (1987). Expression of a single transfected cDNA converts fibroblasts to myoblasts. *Cell, 51*(6), 987-1000.

Day, K., Shefer, G., Shearer, A., & Yablonka-Reuveni, Z. (2010). The depletion of skeletal muscle satellite cells with age is concomitant with reduced capacity of single progenitors to produce reserve progeny. *Dev Biol, 340*(2), 330-343. doi:10.1016/j.ydbio.2010.01.006

De Carvalho, D. D., You, J. S., & Jones, P. A. (2010). DNA methylation and cellular reprogramming. *Trends Cell Biol, 20*(10), 609-617. doi:10.1016/j.tcb.2010.08.003

De Los Angeles, A., Ferrari, F., Xi, R., et al. (2015). Hallmarks of pluripotency. *Nature, 525*(7570), 469-478. doi:10.1038/nature15515

de Lucas, B., Perez, L. M., & Galvez, B. G. (2018). Importance and regulation of adult stem cell migration. *J Cell Mol Med, 22*(2), 746-754. doi:10.1111/jcmm.13422

Demoulin, J. B., & Essaghir, A. (2014). PDGF receptor signaling networks in normal and cancer cells. *Cytokine Growth Factor Rev, 25*(3), 273-283. doi:10.1016/j.cytogfr.2014.03.003

Dennis, J. E., Carbillet, J. P., Caplan, A. I., & Charbord, P. (2002). The STRO-1+ marrow cell population is multipotential. *Cells Tissues Organs, 170*(2-3), 73-82. doi:10.1159/000046182

Diffner, E., Beck, D., Gudgin, E., et al. (2013). Activity of a heptad of transcription factors is associated with stem cell programs and clinical outcome in acute myeloid leukemia. *Blood, 121*(12), 2289-2300. doi:10.1182/blood-2012-07-446120

DiStefano, T., Chen, H. Y., Panebianco, C., et al. (2018). Accelerated and Improved Differentiation of Retinal Organoids from Pluripotent Stem Cells in Rotating-Wall Vessel Bioreactors. *Stem Cell Reports, 10*(1), 300-313. doi:10.1016/j.stemcr.2017.11.001

Do, J. T., & Scholer, H. R. (2004). Nuclei of embryonic stem cells reprogram somatic cells. *Stem Cells, 22*(6), 941-949. doi:10.1634/stemcells.22-6-941

Dobin, A., Davis, C. A., Schlesinger, F., et al. (2013). STAR: ultrafast universal RNA-seq aligner. *Bioinformatics, 29*(1), 15-21. doi:10.1093/bioinformatics/bts635

Dolan, C. P., Dawson, L. A., & Muneoka, K. (2018). Digit Tip Regeneration: Merging Regeneration Biology with Regenerative Medicine. *Stem Cells Transl Med, 7*(3), 262-270. doi:10.1002/sctm.17-0236

Doles, J. D., & Olwin, B. B. (2014). The impact of JAK-STAT signaling on muscle regeneration. *Nat Med, 20*(10), 1094-1095. doi:10.1038/nm.3720

Dominici, M., Le Blanc, K., Mueller, I., et al. (2006). Minimal criteria for defining multipotent mesenchymal stromal cells. The International Society for Cellular Therapy position statement. *Cytotherapy, 8*(4), 315-317. doi:10.1080/14653240600855905

Dor, Y., Brown, J., Martinez, O. I., & Melton, D. A. (2004). Adult pancreatic beta-cells are formed by self-duplication rather than stem-cell differentiation. *Nature, 429*(6987), 41-46. doi:10.1038/nature02520

Doucette, T. A., Ryan, C. L., & Tasker, R. A. (2000). Use of osmotic minipumps for sustained drug delivery in rat pups: effects on physical and neurobehavioural development. *Physiol Behav, 71*(1-2), 207-212.

Draper, J. S., Smith, K., Gokhale, P., et al. (2004). Recurrent gain of chromosomes 17q and 12 in cultured human embryonic stem cells. *Nat Biotechnol, 22*(1), 53-54. doi:10.1038/nbt922

Egli, D., Birkhoff, G., & Eggan, K. (2008). Mediators of reprogramming: transcription factors and transitions through mitosis. *Nat Rev Mol Cell Biol, 9*(7), 505-516. doi:10.1038/nrm2439

El Agha, E., Kramann, R., Schneider, R. K., et al. (2017). Mesenchymal Stem Cells in Fibrotic Disease. *Cell Stem Cell, 21*(2), 166-177. doi:10.1016/j.stem.2017.07.011

El Kharroubi, A., Piras, G., & Stewart, C. L. (2001). DNA demethylation reactivates a subset of imprinted genes in uniparental mouse embryonic fibroblasts. *J Biol Chem, 276*(12), 8674-8680. doi:10.1074/jbc.M009392200

Escobedo-Lucea, C., Bellver, C., Gandia, C., et al. (2013). A xenogeneic-free protocol for isolation and expansion of human adipose stem cells for clinical uses. *PLoS One, 8*(7), e67870. doi:10.1371/journal.pone.0067870

Evans, M. J., & Kaufman, M. H. (1981). Establishment in culture of pluripotential cells from mouse embryos. *Nature, 292*(5819), 154-156.

Fairbank, J. C., & Pynsent, P. B. (2000). The Oswestry Disability Index. *Spine (Phila Pa 1976), 25*(22), 2940-2952; discussion 2952.

Falanga, V. (2005). Wound healing and its impairment in the diabetic foot. *Lancet, 366*(9498), 1736-1743. doi:10.1016/S0140-6736(05)67700-8

Falanga, V. (2012). Stem cells in tissue repair and regeneration. *J Invest Dermatol, 132*(6), 1538-1541. doi:10.1038/jid.2012.77

Fernyhough, M. E., Vierck, J. L., Hausman, G. J., Mir, P. S., Okine, E. K., & Dodson, M. V. (2004). Primary adipocyte culture: adipocyte purification methods may lead to a new understanding of adipose tissue growth and development. *Cytotechnology, 46*(2-3), 163-172. doi:10.1007/s10616-005-2602-0

Fishman, J. A. (2007). Infection in solid-organ transplant recipients. *N Engl J Med, 357*(25), 2601-2614. doi:10.1056/NEJMra064928

Fitter, S., Gronthos, S., Ooi, S. S., & Zannettino, A. C. (2017). The Mesenchymal Precursor Cell Marker Antibody STRO-1 Binds to Cell Surface Heat Shock Cognate 70. *Stem Cells, 35*(4), 940-951. doi:10.1002/stem.2560

Freiman, A., Shandalov, Y., Rozenfeld, D., et al. (2016). Adipose-derived endothelial and mesenchymal stem cells enhance vascular network formation on three-dimensional constructs in vitro. *Stem Cell Res Ther, 7*, 5. doi:10.1186/s13287-015-0251-6

Friedenstein, A. J., Chailakhjan, R. K., & Lalykina, K. S. (1970). The development of fibroblast colonies in monolayer cultures of guinea-pig bone marrow and spleen cells. *Cell Tissue Kinet, 3*(4), 393-403.

Friedenstein, A. J., Gorskaja, J. F., & Kulagina, N. N. (1976). Fibroblast precursors in normal and irradiated mouse hematopoietic organs. *Exp Hematol, 4*(5), 267-274.

Fu, J. D., Stone, N. R., Liu, L., et al. (2013). Direct reprogramming of human fibroblasts toward a cardiomyocyte-like state. *Stem Cell Reports, 1*(3), 235-247. doi:10.1016/j.stemcr.2013.07.005

Fukuda, K. (2002). Reprogramming of bone marrow mesenchymal stem cells into cardiomyocytes. *C R Biol, 325*(10), 1027-1038.

Fukushima, K., Badlani, N., Usas, A., Riano, F., Fu, F., & Huard, J. (2001). The use of an antifibrosis agent to improve muscle recovery after laceration. *Am J Sports Med, 29*(4), 394-402. doi:10.1177/03635465010290040201

Fusaki, N., Ban, H., Nishiyama, A., Saeki, K., & Hasegawa, M. (2009). Efficient induction of transgene-free human pluripotent stem cells using a vector based on Sendai virus, an RNA virus that does not integrate into the host genome. *Proc Jpn Acad Ser B Phys Biol Sci, 85*(8), 348-362.

Gafni, O., Weinberger, L., Mansour, A. A., et al. (2013). Derivation of novel human ground state naive pluripotent stem cells. *Nature, 504*(7479), 282-286. doi:10.1038/nature12745

Garcia-Prat, L., Sousa-Victor, P., & Munoz-Canoves, P. (2017). Proteostatic and Metabolic Control of Stemness. *Cell Stem Cell, 20*(5), 593-608. doi:10.1016/j.stem.2017.04.011

Garry, G. A., Antony, M. L., & Garry, D. J. (2016). Cardiotoxin Induced Injury and Skeletal Muscle Regeneration. *Methods Mol Biol, 1460*, 61-71. doi:10.1007/978-1-4939-3810-0_6

Gehmert, S., Gehmert, S., Hidayat, M., et al. (2011). Angiogenesis: the role of PDGF-BB on adipose-tissue derived stem cells (ASCs). *Clin Hemorheol Microcirc, 48*(1), 5-13. doi:10.3233/CH-2011-1397

Gerstenfeld, L. C., Cullinane, D. M., Barnes, G. L., Graves, D. T., & Einhorn, T. A. (2003). Fracture healing as a post-natal developmental process: molecular, spatial, and temporal aspects of its regulation. *J Cell Biochem, 88*(5), 873-884. doi:10.1002/jcb.10435

Giordani, L., Parisi, A., & Le Grand, F. (2018). Satellite Cell Self-Renewal. *Curr Top Dev Biol, 126*, 177-203. doi:10.1016/bs.ctdb.2017.08.001

Glowacki, J., & Mizuno, S. (2008). Collagen scaffolds for tissue engineering. *Biopolymers, 89*(5), 338-344. doi:10.1002/bip.20871

Gonzalez, M. E., Martin, E. E., Anwar, T., et al. (2017). Mesenchymal Stem Cell-Induced DDR2 Mediates Stromal-Breast Cancer Interactions and Metastasis Growth. *Cell Rep, 18*(5), 1215-1228. doi:10.1016/j.celrep.2016.12.079

Gronthos, S., & Simmons, P. J. (1996). The biology and application of human bone marrow stromal cell precursors. *J Hematother, 5*(1), 15-23. doi:10.1089/scd.1.1996.5.15

Gronthos, S., & Zannettino, A. C. (2008). A method to isolate and purify human bone marrow stromal stem cells. *Methods Mol Biol, 449*, 45-57. doi:10.1007/978-1-60327-169-1_3

Gronthos, S., Zannettino, A. C., Graves, S. E., Ohta, S., Hay, S. J., & Simmons, P. J. (1999). Differential cell surface expression of the STRO-1 and alkaline phosphatase antigens on discrete developmental stages in primary cultures of human bone cells. *J Bone Miner Res, 14*(1), 47-56. doi:10.1359/jbmr.1999.14.1.47

Gupta, S. (2016). Animal models: Unlock your inner salamander. *Nature, 540*(7632), S58-S59. doi:10.1038/540S58a

Gurdon, J. B. (1962). The developmental capacity of nuclei taken from intestinal epithelium cells of feeding tadpoles. *J Embryol Exp Morphol, 10*, 622-640.

Haller, S., Kapuria, S., Riley, R. R., et al. (2017). mTORC1 Activation during Repeated Regeneration Impairs Somatic Stem Cell Maintenance. *Cell Stem Cell, 21*(6), 806-818 e805. doi:10.1016/j.stem.2017.11.008

Halloran, P. F. (2004). Immunosuppressive drugs for kidney transplantation. *N Engl J Med, 351*(26), 2715-2729. doi:10.1056/NEJMra033540

Han, C., Nie, Y., Lian, H., et al. (2015). Acute inflammation stimulates a regenerative response in the neonatal mouse heart. *Cell Res, 25*(10), 1137-1151. doi:10.1038/cr.2015.110

Han, J., Sachdev, P. S., & Sidhu, K. S. (2010). A combined epigenetic and non-genetic approach for reprogramming human somatic cells. *PLoS One, 5*(8), e12297. doi:10.1371/journal.pone.0012297

Han, J., & Sidhu, K. (2011). Embryonic stem cell extracts: use in differentiation and reprogramming. *Regen Med, 6*(2), 215-227. doi:10.2217/rme.11.8

Hanawa, H., Kelly, P. F., Nathwani, A. C., et al. (2002). Comparison of various envelope proteins for their ability to pseudotype lentiviral vectors and transduce primitive hematopoietic cells from human blood. *Mol Ther, 5*(3), 242-251. doi:10.1006/mthe.2002.0549

Hanawa, H., Persons, D. A., & Nienhuis, A. W. (2005). Mobilization and mechanism of transcription of integrated self-inactivating lentiviral vectors. *J Virol, 79*(13), 8410-8421. doi:10.1128/JVI.79.13.8410-8421.2005

Hardy, D., Besnard, A., Latil, M., et al. (2016). Comparative Study of Injury Models for Studying Muscle Regeneration in Mice. *PLoS One, 11*(1), e0147198. doi:10.1371/journal.pone.0147198

Harris, J. B. (2003). Myotoxic phospholipases A2 and the regeneration of skeletal muscles. *Toxicon, 42*(8), 933-945. doi:10.1016/j.toxicon.2003.11.011

Hass, R., Kasper, C., Bohm, S., & Jacobs, R. (2011). Different populations and sources of human mesenchymal stem cells (MSC): A comparison of adult and neonatal tissue-derived MSC. *Cell Commun Signal, 9*, 12. doi:10.1186/1478-811X-9-12

Hatzistergos, K. E., Quevedo, H., Oskouei, B. N., et al. (2010). Bone marrow mesenchymal stem cells stimulate cardiac stem cell proliferation and differentiation. *Circ Res, 107*(7), 913-922. doi:10.1161/CIRCRESAHA.110.222703

Heldin, C. H., Betsholtz, C., Johnsson, A., et al. (1985). Platelet-derived growth factor: mechanism of action and relation to oncogenes. *J Cell Sci Suppl, 3*, 65-76.

Heldin, C. H., Wasteson, A., & Westermark, B. (1985). Platelet-derived growth factor. *Mol Cell Endocrinol, 39*(3), 169-187.

Heldin, C. H., & Westermark, B. (1990). Platelet-derived growth factor: mechanism of action and possible in vivo function. *Cell Regul, 1*(8), 555-566.

Hemberger, M., Dean, W., & Reik, W. (2009). Epigenetic dynamics of stem cells and cell lineage commitment: digging Waddington's canal. *Nat Rev Mol Cell Biol, 10*(8), 526-537. doi:10.1038/nrm2727

Heng, J. C., Orlov, Y. L., & Ng, H. H. (2010). Transcription factors for the modulation of pluripotency and reprogramming. *Cold Spring Harb Symp Quant Biol, 75*, 237-244. doi:10.1101/sqb.2010.75.003

Herberts, C. A., Kwa, M. S., & Hermsen, H. P. (2011). Risk factors in the development of stem cell therapy. *J Transl Med, 9*, 29. doi:10.1186/1479-5876-9-29

Heredia, J. E., Mukundan, L., Chen, F. M., et al. (2013). Type 2 innate signals stimulate fibro/adipogenic progenitors to facilitate muscle regeneration. *Cell, 153*(2), 376-388. doi:10.1016/j.cell.2013.02.053

Hoch, R. V., & Soriano, P. (2003). Roles of PDGF in animal development. *Development, 130*(20), 4769-4784. doi:10.1242/dev.00721

Hochedlinger, K., Yamada, Y., Beard, C., & Jaenisch, R. (2005). Ectopic expression of Oct-4 blocks progenitor-cell differentiation and causes dysplasia in epithelial tissues. *Cell, 121*(3), 465-477. doi:10.1016/j.cell.2005.02.018

Horie, M., Choi, H., Lee, R. H., et al. (2012). Intra-articular injection of human mesenchymal stem cells (MSCs) promote rat meniscal regeneration by being activated to express Indian hedgehog that enhances expression of type II collagen. *Osteoarthritis Cartilage, 20*(10), 1197-1207. doi:10.1016/j.joca.2012.06.002

Hou, P., Li, Y., Zhang, X., et al. (2013). Pluripotent stem cells induced from mouse somatic cells by small-molecule compounds. *Science, 341*(6146), 651-654. doi:10.1126/science.1239278

Huang, P., He, Z., Ji, S., et al. (2011). Induction of functional hepatocyte-like cells from mouse fibroblasts by defined factors. *Nature, 475*(7356), 386-389. doi:10.1038/nature10116

Huard, J., Verreault, S., Roy, R., Tremblay, M., & Tremblay, J. P. (1994). High efficiency of muscle regeneration after human myoblast clone transplantation in SCID mice. *J Clin Invest, 93*(2), 586-599. doi:10.1172/JCI117011

Hussein, S. M., Puri, M. C., Tonge, P. D., et al. (2014). Genome-wide characterization of the routes to pluripotency. *Nature, 516*(7530), 198-206. doi:10.1038/nature14046

Hutton, D. L., Moore, E. M., Gimble, J. M., & Grayson, W. L. (2013). Platelet-derived growth factor and spatiotemporal cues induce development of vascularized bone tissue by adipose-derived stem cells. *Tissue Eng Part A, 19*(17-18), 2076-2086. doi:10.1089/ten.TEA.2012.0752

Hwang, N. S., Zhang, C., Hwang, Y. S., & Varghese, S. (2009). Mesenchymal stem cell differentiation and roles in regenerative medicine. *Wiley Interdiscip Rev Syst Biol Med, 1*(1), 97-106. doi:10.1002/wsbm.26

Ichida, J. K., Blanchard, J., Lam, K., et al. (2009). A small-molecule inhibitor of tgf-Beta signaling replaces sox2 in reprogramming by inducing nanog. *Cell Stem Cell, 5*(5), 491-503. doi:10.1016/j.stem.2009.09.012

Ieda, M., Fu, J. D., Delgado-Olguin, P., et al. (2010). Direct reprogramming of fibroblasts into functional cardiomyocytes by defined factors. *Cell, 142*(3), 375-386. doi:10.1016/j.cell.2010.07.002

Issa, J. P., & Kantarjian, H. M. (2009). Targeting DNA methylation. *Clin Cancer Res, 15*(12), 3938-3946. doi:10.1158/1078-0432.CCR-08-2783

Jin, H. J., Bae, Y. K., Kim, M., et al. (2013). Comparative analysis of human mesenchymal stem cells from bone marrow, adipose tissue, and umbilical cord blood as sources of cell therapy. *Int J Mol Sci, 14*(9), 17986-18001. doi:10.3390/ijms140917986

Johnston, A. P., Yuzwa, S. A., Carr, M. J., et al. (2016). Dedifferentiated Schwann Cell Precursors Secreting Paracrine Factors Are Required for Regeneration of the

Mammalian Digit Tip. *Cell Stem Cell, 19*(4), 433-448. doi:10.1016/j.stem.2016.06.002

Jones, I., Novikova, L. N., Novikov, L. N., et al. (2018). Regenerative effects of human embryonic stem cell-derived neural crest cells for treatment of peripheral nerve injury. *J Tissue Eng Regen Med*. doi:10.1002/term.2642

Jones, P. A., & Taylor, S. M. (1980). Cellular differentiation, cytidine analogs and DNA methylation. *Cell, 20*(1), 85-93.

Jopling, C., Boue, S., & Izpisua Belmonte, J. C. (2011). Dedifferentiation, transdifferentiation and reprogramming: three routes to regeneration. *Nat Rev Mol Cell Biol, 12*(2), 79-89. doi:10.1038/nrm3043

Jopling, C., Sleep, E., Raya, M., Marti, M., Raya, A., & Izpisua Belmonte, J. C. (2010). Zebrafish heart regeneration occurs by cardiomyocyte dedifferentiation and proliferation. *Nature, 464*(7288), 606-609. doi:10.1038/nature08899

Julier, Z., Park, A. J., Briquez, P. S., & Martino, M. M. (2017). Promoting tissue regeneration by modulating the immune system. *Acta Biomater, 53*, 13-28. doi:10.1016/j.actbio.2017.01.056

Kagey, M. H., Newman, J. J., Bilodeau, S., et al. (2010). Mediator and cohesin connect gene expression and chromatin architecture. *Nature, 467*(7314), 430-435. doi:10.1038/nature09380

Kang, Y. J., & Zheng, L. (2013). Rejuvenation: an integrated approach to regenerative medicine. *Regen Med Res, 1*(1), 7. doi:10.1186/2050-490X-1-7

Karp, J. M., & Leng Teo, G. S. (2009). Mesenchymal stem cell homing: the devil is in the details. *Cell Stem Cell, 4*(3), 206-216. doi:10.1016/j.stem.2009.02.001

Kasap, S., Barutcu, A., Guc, H., Yazgan, S., Kivanc, M., & Vatansever, H. S. (2017). Effects of Keratinocytes Differentiated from Embryonic and Adipogenic Stem Cells on Wound Healing in a Diabetic Mouse Model. *Wounds, 29*(11), 297-305.

Katz, L. S., Geras-Raaka, E., & Gershengorn, M. C. (2013). Reprogramming adult human dermal fibroblasts to islet-like cells by epigenetic modification coupled to transcription factor modulation. *Stem Cells Dev, 22*(18), 2551-2560. doi:10.1089/scd.2013.0134

Kaur, K., Yang, J., Eisenberg, C. A., & Eisenberg, L. M. (2014). 5-azacytidine promotes the transdifferentiation of cardiac cells to skeletal myocytes. *Cell Reprogram, 16*(5), 324-330. doi:10.1089/cell.2014.0021

Keating, A. (2012). Mesenchymal stromal cells: new directions. *Cell Stem Cell, 10*(6), 709-716. doi:10.1016/j.stem.2012.05.015

Keefer, C. L. (2015). Artificial cloning of domestic animals. *Proc Natl Acad Sci U S A, 112*(29), 8874-8878. doi:10.1073/pnas.1501718112

Kern, S., Eichler, H., Stoeve, J., Kluter, H., & Bieback, K. (2006). Comparative analysis of mesenchymal stem cells from bone marrow, umbilical cord blood, or adipose tissue. *Stem Cells, 24*(5), 1294-1301. doi:10.1634/stemcells.2005-0342

Kim, D., Kim, C. H., Moon, J. I., et al. (2009). Generation of human induced pluripotent stem cells by direct delivery of reprogramming proteins. *Cell Stem Cell, 4*(6), 472-476. doi:10.1016/j.stem.2009.05.005

Kim, J., Wu, Q., Zhang, Y., et al. (2010). PDGF signaling is required for epicardial function and blood vessel formation in regenerating zebrafish hearts. *Proc Natl Acad Sci U S A, 107*(40), 17206-17210. doi:10.1073/pnas.0915016107

Kim, J. B., Zaehres, H., Wu, G., et al. (2008). Pluripotent stem cells induced from adult neural stem cells by reprogramming with two factors. *Nature, 454*(7204), 646-650. doi:10.1038/nature07061

Koga, M., Matsuda, M., Kawamura, T., et al. (2014). Foxd1 is a mediator and indicator of the cell reprogramming process. *Nat Commun, 5*, 3197. doi:10.1038/ncomms4197

Kogut, I., McCarthy, S. M., Pavlova, M., et al. (2018). High-efficiency RNA-based reprogramming of human primary fibroblasts. *Nat Commun, 9*(1), 745. doi:10.1038/s41467-018-03190-3

Koo, T., Popplewell, L., Athanasopoulos, T., & Dickson, G. (2014). Triple trans-splicing adeno-associated virus vectors capable of transferring the coding sequence for full-length dystrophin protein into dystrophic mice. *Hum Gene Ther, 25*(2), 98-108. doi:10.1089/hum.2013.164

Korbling, M., & Estrov, Z. (2003). Adult stem cells for tissue repair - a new therapeutic concept? *N Engl J Med, 349*(6), 570-582. doi:10.1056/NEJMra022361

Kramann, R., Schneider, R. K., DiRocco, D. P., et al. (2015). Perivascular Gli1+ progenitors are key contributors to injury-induced organ fibrosis. *Cell Stem Cell, 16*(1), 51-66. doi:10.1016/j.stem.2014.11.004

Krawczyk, J., Keane, N., Freeman, C. L., Swords, R., O'Dwyer, M., & Giles, F. J. (2013). 5-Azacytidine for the treatment of myelodysplastic syndromes. *Expert Opin Pharmacother, 14*(9), 1255-1268. doi:10.1517/14656566.2013.794222

Kuah, D., Sivell, S., Longworth, T., et al. (2018). Safety, tolerability and efficacy of intra-articular Progenza in knee osteoarthritis: a randomized double-blind placebo-controlled single ascending dose study. *J Transl Med, 16*(1), 49. doi:10.1186/s12967-018-1420-z

Kubin, T., Poling, J., Kostin, S., et al. (2011). Oncostatin M is a major mediator of cardiomyocyte dedifferentiation and remodeling. *Cell Stem Cell, 9*(5), 420-432. doi:10.1016/j.stem.2011.08.013

Kumar, A., Godwin, J. W., Gates, P. B., Garza-Garcia, A. A., & Brockes, J. P. (2007). Molecular basis for the nerve dependence of limb regeneration in an adult vertebrate. *Science, 318*(5851), 772-777. doi:10.1126/science.1147710

Kumar, H., Ha, D. H., Lee, E. J., et al. (2017). Safety and tolerability of intradiscal implantation of combined autologous adipose-derived mesenchymal stem cells and hyaluronic acid in patients with chronic discogenic low back pain: 1-year follow-up of a phase I study. *Stem Cell Res Ther, 8*(1), 262. doi:10.1186/s13287-017-0710-3

Kume, T., Taguchi, R., Katsuki, H., et al. (2006). Serofendic acid, a neuroprotective substance derived from fetal calf serum, inhibits mitochondrial membrane depolarization and caspase-3 activation. *Eur J Pharmacol, 542*(1-3), 69-76. doi:10.1016/j.ejphar.2006.04.038

Kunitz, M. (1950). Crystalline desoxyribonuclease; isolation and general properties; spectrophotometric method for the measurement of desoxyribonuclease activity. *J Gen Physiol, 33*(4), 349-362.

La Fortezza, M., Schenk, M., Cosolo, A., Kolybaba, A., Grass, I., & Classen, A. K. (2016). JAK/STAT signalling mediates cell survival in response to tissue stress. *Development, 143*(16), 2907-2919. doi:10.1242/dev.132340

LaRochelle, W. J., Jeffers, M., McDonald, W. F., et al. (2001). PDGF-D, a new protease-activated growth factor. *Nat Cell Biol, 3*(5), 517-521. doi:10.1038/35074593

Lavine, K. J., Epelman, S., Uchida, K., et al. (2014). Distinct macrophage lineages contribute to disparate patterns of cardiac recovery and remodeling in the neonatal and adult heart. *Proc Natl Acad Sci U S A, 111*(45), 16029-16034. doi:10.1073/pnas.1406508111

Le Blanc, K., Frassoni, F., Ball, L., et al. (2008). Mesenchymal stem cells for treatment of steroid-resistant, severe, acute graft-versus-host disease: a phase II study. *Lancet, 371*(9624), 1579-1586. doi:10.1016/S0140-6736(08)60690-X

Le Blanc, K., Samuelsson, H., Lonnies, L., Sundin, M., & Ringden, O. (2007). Generation of immunosuppressive mesenchymal stem cells in allogeneic human serum. *Transplantation, 84*(8), 1055-1059. doi:10.1097/01.tp.0000285088.44901.ea

Le Grand, F., Jones, A. E., Seale, V., Scime, A., & Rudnicki, M. A. (2009). Wnt7a activates the planar cell polarity pathway to drive the symmetric expansion of satellite stem cells. *Cell Stem Cell, 4*(6), 535-547. doi:10.1016/j.stem.2009.03.013

Lee, H. Y., & Hong, I. S. (2017). Double-edged sword of mesenchymal stem cells: Cancer-promoting versus therapeutic potential. *Cancer Sci, 108*(10), 1939-1946. doi:10.1111/cas.13334

Lee, M., Jeong, S. Y., Ha, J., et al. (2014). Low immunogenicity of allogeneic human umbilical cord blood-derived mesenchymal stem cells in vitro and in vivo. *Biochem Biophys Res Commun, 446*(4), 983-989. doi:10.1016/j.bbrc.2014.03.051

Lee, N. K., Na, D. L., & Chang, J. W. (2017). Killing two birds with one stone: The multifunctional roles of mesenchymal stem cells in the treatment of neurodegenerative and muscle diseases. *Histol Histopathol*, 11951. doi:10.14670/HH-11-951

Lee, S., Kim, H. S., Roh, K. H., et al. (2015). DNA methyltransferase inhibition accelerates the immunomodulation and migration of human mesenchymal stem cells. *Sci Rep, 5*, 8020. doi:10.1038/srep08020

Lee, S. B., Han, S. H., Kim, M. J., et al. (2017). Post-irradiation promotes susceptibility to reprogramming to pluripotent state in human fibroblasts. *Cell Cycle, 16*(21), 2119-2127. doi:10.1080/15384101.2017.1371887

Lengner, C. J., Camargo, F. D., Hochedlinger, K., et al. (2007). Oct4 expression is not required for mouse somatic stem cell self-renewal. *Cell Stem Cell, 1*(4), 403-415. doi:10.1016/j.stem.2007.07.020

Lenoir, N. (2000). Europe confronts the embryonic stem cell research challenge. *Science, 287*(5457), 1425-1427.

Leo, A. J., & Grande, D. A. (2006). Mesenchymal stem cells in tissue engineering. *Cells Tissues Organs, 183*(3), 112-122. doi:10.1159/000095985

Lerou, P. H., & Daley, G. Q. (2005). Therapeutic potential of embryonic stem cells. *Blood Rev, 19*(6), 321-331. doi:10.1016/j.blre.2005.01.005

Leung, V. Y., Aladin, D. M., Lv, F., et al. (2014). Mesenchymal stem cells reduce intervertebral disc fibrosis and facilitate repair. *Stem Cells, 32*(8), 2164-2177. doi:10.1002/stem.1717

Li, A., Xia, X., Yeh, J., et al. (2014). PDGF-AA promotes osteogenic differentiation and migration of mesenchymal stem cell by down-regulating PDGFRalpha and derepressing BMP-Smad1/5/8 signaling. *PLoS One, 9*(12), e113785. doi:10.1371/journal.pone.0113785

Li, J. Y., Christophersen, N. S., Hall, V., Soulet, D., & Brundin, P. (2008). Critical issues of clinical human embryonic stem cell therapy for brain repair. *Trends Neurosci, 31*(3), 146-153. doi:10.1016/j.tins.2007.12.001

Li, J. Y., Ke, H. H., He, Y., et al. (2018). Transplantation of mesenchymal stem cells modulated Cx43 and Cx45 expression in rats with myocardial infarction. *Cytotechnology, 70*(1), 225-234. doi:10.1007/s10616-017-0136-x

Li, W., Li, K., Wei, W., & Ding, S. (2013). Chemical approaches to stem cell biology and therapeutics. *Cell Stem Cell, 13*(3), 270-283. doi:10.1016/j.stem.2013.08.002

Li, X., Zuo, X., Jing, J., et al. (2015). Small-Molecule-Driven Direct Reprogramming of Mouse Fibroblasts into Functional Neurons. *Cell Stem Cell, 17*(2), 195-203. doi:10.1016/j.stem.2015.06.003

Lim, M. H., Ong, W. K., & Sugii, S. (2014). The current landscape of adipose-derived stem cells in clinical applications. *Expert Rev Mol Med, 16*, e8. doi:10.1017/erm.2014.8

Lin, H. (2002). The stem-cell niche theory: lessons from flies. *Nat Rev Genet, 3*(12), 931-940. doi:10.1038/nrg952

Lissenberg-Thunnissen, S. N., de Gorter, D. J., Sier, C. F., & Schipper, I. B. (2011). Use and efficacy of bone morphogenetic proteins in fracture healing. *Int Orthop, 35*(9), 1271-1280. doi:10.1007/s00264-011-1301-z

Liu, Y., Zhao, J., Liu, J., Zhang, H., Liu, M., & Xiao, X. (2008). Upregulation of the constitutively expressed HSC70 by KLF4. *Cell Stress Chaperones, 13*(3), 337-345. doi:10.1007/s12192-008-0033-5

Lo, B., & Parham, L. (2009). Ethical issues in stem cell research. *Endocr Rev, 30*(3), 204-213. doi:10.1210/er.2008-0031

Locklin, R. M., Oreffo, R. O., & Triffitt, J. T. (1998). Modulation of osteogenic differentiation in human skeletal cells in Vitro by 5-azacytidine. *Cell Biol Int, 22*(3), 207-215. doi:10.1006/cbir.1998.0240

Loewer, S., Cabili, M. N., Guttman, M., et al. (2010). Large intergenic non-coding RNA-RoR modulates reprogramming of human induced pluripotent stem cells. *Nat Genet, 42*(12), 1113-1117. doi:10.1038/ng.710

Loi, P., Boyazoglu, S., Gallus, M., et al. (1997). Embryo cloning in sheep: work in progress. *Theriogenology, 48*(1), 1-10. doi:10.1016/S0093-691X(97)00187-8

Loi, P., Czernik, M., Zacchini, F., Iuso, D., Scapolo, P. A., & Ptak, G. (2013). Sheep: the first large animal model in nuclear transfer research. *Cell Reprogram, 15*(5), 367-373. doi:10.1089/cell.2013.0032

Luni, C., Giulitti, S., Serena, E., et al. (2016). High-efficiency cellular reprogramming with microfluidics. *Nat Methods, 13*(5), 446-452. doi:10.1038/nmeth.3832

Maddaluno, L., Urwyler, C., & Werner, S. (2017). Fibroblast growth factors: key players in regeneration and tissue repair. *Development, 144*(22), 4047-4060. doi:10.1242/dev.152587

Madhurakkat Perikamana, S. K., Lee, J., Ahmad, T., et al. (2018). Harnessing biochemical and structural cues for tenogenic differentiation of adipose derived stem cells (ADSCs) and development of an in vitro tissue interface mimicking tendon-bone insertion graft. *Biomaterials, 165*, 79-93. doi:10.1016/j.biomaterials.2018.02.046

Maehr, R., Chen, S., Snitow, M., et al. (2009). Generation of pluripotent stem cells from patients with type 1 diabetes. *Proc Natl Acad Sci U S A, 106*(37), 15768-15773. doi:10.1073/pnas.0906894106

Magli, A., Incitti, T., & Perlingeiro, R. C. (2016). Myogenic Progenitors from Mouse Pluripotent Stem Cells for Muscle Regeneration. *Methods Mol Biol, 1460*, 191-208. doi:10.1007/978-1-4939-3810-0_14

Mahdy, M. A., Warita, K., & Hosaka, Y. Z. (2016). Early ultrastructural events of skeletal muscle damage following cardiotoxin-induced injury and glycerol-induced injury. *Micron, 91*, 29-40. doi:10.1016/j.micron.2016.09.009

Maherali, N., Sridharan, R., Xie, W., et al. (2007). Directly reprogrammed fibroblasts show global epigenetic remodeling and widespread tissue contribution. *Cell Stem Cell, 1*(1), 55-70. doi:10.1016/j.stem.2007.05.014

Makino, S., Fukuda, K., Miyoshi, S., et al. (1999). Cardiomyocytes can be generated from marrow stromal cells in vitro. *J Clin Invest, 103*(5), 697-705. doi:10.1172/JCI5298

Mandai, M., Watanabe, A., Kurimoto, Y., et al. (2017). Autologous Induced Stem-Cell-Derived Retinal Cells for Macular Degeneration. *N Engl J Med, 376*(11), 1038-1046. doi:10.1056/NEJMoa1608368

Mannello, F. (2006). Multipotent mesenchymal stromal cell recruitment, migration, and differentiation: what have matrix metalloproteinases got to do with it? *Stem Cells, 24*(8), 1904-1907. doi:10.1634/stemcells.2005-0608

Mannello, F., & Tonti, G. A. (2007). Concise review: no breakthroughs for human mesenchymal and embryonic stem cell culture: conditioned medium, feeder layer, or feeder-free; medium with fetal calf serum, human serum, or enriched plasma; serum-free, serum replacement nonconditioned medium, or ad hoc formula? All that glitters is not gold! *Stem Cells, 25*(7), 1603-1609. doi:10.1634/stemcells.2007-0127

Manzoni, E. F., Pennarossa, G., deEguileor, M., Tettamanti, G., Gandolfi, F., & Brevini, T. A. (2016). 5-azacytidine affects TET2 and histone transcription and reshapes morphology of human skin fibroblasts. *Sci Rep, 6*, 37017. doi:10.1038/srep37017

Mao, A. S., & Mooney, D. J. (2015). Regenerative medicine: Current therapies and future directions. *Proc Natl Acad Sci U S A, 112*(47), 14452-14459. doi:10.1073/pnas.1508520112

Marti, M., Mulero, L., Pardo, C., et al. (2013). Characterization of pluripotent stem cells. *Nat Protoc, 8*(2), 223-253. doi:10.1038/nprot.2012.154

Martin, G. R. (1981). Isolation of a pluripotent cell line from early mouse embryos cultured in medium conditioned by teratocarcinoma stem cells. *Proc Natl Acad Sci U S A, 78*(12), 7634-7638.

Masuda, S., Yokoo, T., Sugimoto, N., et al. (2012). A Simplified In Vitro Teratoma Assay for Pluripotent Stem Cells Injected Into Rodent Fetal Organs. *Cell Med, 3*(1-3), 103-112. doi:10.3727/215517912X639351

McCarthy, D. J., Chen, Y., & Smyth, G. K. (2012). Differential expression analysis of multifactor RNA-Seq experiments with respect to biological variation. *Nucleic Acids Res, 40*(10), 4288-4297. doi:10.1093/nar/gks042

McConnell, S., Kolopack, P., & Davis, A. M. (2001). The Western Ontario and McMaster Universities Osteoarthritis Index (WOMAC): a review of its utility and measurement properties. *Arthritis Rheum, 45*(5), 453-461.

McCusker, C., Bryant, S. V., & Gardiner, D. M. (2015). The axolotl limb blastema: cellular and molecular mechanisms driving blastema formation and limb regeneration in tetrapods. *Regeneration (Oxf), 2*(2), 54-71. doi:10.1002/reg2.32

McCusker, C. D., & Gardiner, D. M. (2013). Positional information is reprogrammed in blastema cells of the regenerating limb of the axolotl (Ambystoma mexicanum). *PLoS One, 8*(9), e77064. doi:10.1371/journal.pone.0077064

Medvinsky, A., Taoudi, S., Mendes, S., & Dzierzak, E. (2008). Analysis and manipulation of hematopoietic progenitor and stem cells from murine embryonic tissues. *Curr Protoc Stem Cell Biol, Chapter 2*, Unit 2A 6. doi:10.1002/9780470151808.sc02a06s4

Meng, X. M., Nikolic-Paterson, D. J., & Lan, H. Y. (2016). TGF-beta: the master regulator of fibrosis. *Nat Rev Nephrol, 12*(6), 325-338. doi:10.1038/nrneph.2016.48

MesoblastNews. (2017). Mesoblast Report on MPC-06-ID Phase 2 Clinical Trial. Retrieved from http://www.mesoblast.com/clinical-trial-results/mpc-06-id-phase-2).

Miguelez-Rivera, L., Perez-Castrillo, S., Gonzalez-Fernandez, M. L., et al. (2017). Immunomodulation of mesenchymal stem cells in discogenic pain. *Spine J*. doi:10.1016/j.spinee.2017.09.002

Miki, T., Yasuda, S. Y., & Kahn, M. (2011). Wnt/beta-catenin signaling in embryonic stem cell self-renewal and somatic cell reprogramming. *Stem Cell Rev, 7*(4), 836-846. doi:10.1007/s12015-011-9275-1

Mikkelsen, T. S., Hanna, J., Zhang, X., et al. (2008). Dissecting direct reprogramming through integrative genomic analysis. *Nature, 454*(7200), 49-55. doi:10.1038/nature07056

Missinato, M. A., Saydmohammed, M., Zuppo, D. A., et al. (2018). Dusp6 attenuates Ras/MAPK signaling to limit zebrafish heart regeneration. *Development, 145*(5). doi:10.1242/dev.157206

Mitalipova, M. M., Rao, R. R., Hoyer, D. M., et al. (2005). Preserving the genetic integrity of human embryonic stem cells. *Nat Biotechnol, 23*(1), 19-20. doi:10.1038/nbt0105-19

Montarras, D., Morgan, J., Collins, C., et al. (2005). Direct isolation of satellite cells for skeletal muscle regeneration. *Science, 309*(5743), 2064-2067. doi:10.1126/science.1114758

Morgan, J. E., Gross, J. G., Pagel, C. N., et al. (2002). Myogenic cell proliferation and generation of a reversible tumorigenic phenotype are triggered by preirradiation of the recipient site. *J Cell Biol, 157*(4), 693-702. doi:10.1083/jcb.200108047

Mueller, A. A., van Velthoven, C. T., Fukumoto, K. D., Cheung, T. H., & Rando, T. A. (2016). Intronic polyadenylation of PDGFRalpha in resident stem cells attenuates muscle fibrosis. *Nature, 540*(7632), 276-279. doi:10.1038/nature20160

Muller, F. J., Goldmann, J., Loser, P., & Loring, J. F. (2010). A call to standardize teratoma assays used to define human pluripotent cell lines. *Cell Stem Cell, 6*(5), 412-414. doi:10.1016/j.stem.2010.04.009

Muller, I., Kordowich, S., Holzwarth, C., et al. (2006). Animal serum-free culture conditions for isolation and expansion of multipotent mesenchymal stromal cells from human BM. *Cytotherapy, 8*(5), 437-444. doi:10.1080/14653240600920782

Murphy, M. B., Moncivais, K., & Caplan, A. I. (2013). Mesenchymal stem cells: environmentally responsive therapeutics for regenerative medicine. *Exp Mol Med, 45*, e54. doi:10.1038/emm.2013.94

Nakagawa, M., Koyanagi, M., Tanabe, K., et al. (2008). Generation of induced pluripotent stem cells without Myc from mouse and human fibroblasts. *Nat Biotechnol, 26*(1), 101-106. doi:10.1038/nbt1374

Nelakanti, R. V., Kooreman, N. G., & Wu, J. C. (2015). Teratoma formation: a tool for monitoring pluripotency in stem cell research. *Curr Protoc Stem Cell Biol, 32*, 4A 8 1-17. doi:10.1002/9780470151808.sc04a08s32

Ng, F., Boucher, S., Koh, S., et al. (2008). PDGF, TGF-beta, and FGF signaling is important for differentiation and growth of mesenchymal stem cells (MSCs): transcriptional profiling can identify markers and signaling pathways important in differentiation of MSCs into adipogenic, chondrogenic, and osteogenic lineages. *Blood, 112*(2), 295-307. doi:10.1182/blood-2007-07-103697

Nixon, B. T., & Green, H. (1984). Growth hormone promotes the differentiation of myoblasts and preadipocytes generated by azacytidine treatment of 10T1/2 cells. *Proc Natl Acad Sci U S A, 81*(11), 3429-3432.

Odorico, J. S., Kaufman, D. S., & Thomson, J. A. (2001). Multilineage differentiation from human embryonic stem cell lines. *Stem Cells, 19*(3), 193-204. doi:10.1634/stemcells.19-3-193

Olee, T., Grogan, S. P., Lotz, M. K., Colwell, C. W., Jr., D'Lima, D. D., & Snyder, E. Y. (2014). Repair of cartilage defects in arthritic tissue with differentiated human embryonic stem cells. *Tissue Eng Part A, 20*(3-4), 683-692. doi:10.1089/ten.TEA.2012.0751

Orozco, L., Soler, R., Morera, C., Alberca, M., Sanchez, A., & Garcia-Sancho, J. (2011). Intervertebral disc repair by autologous mesenchymal bone marrow cells: a pilot study. *Transplantation, 92*(7), 822-828. doi:10.1097/TP.0b013e3182298a15

Pasque, V., Tchieu, J., Karnik, R., et al. (2014). X chromosome reactivation dynamics reveal stages of reprogramming to pluripotency. *Cell, 159*(7), 1681-1697. doi:10.1016/j.cell.2014.11.040

Passier, R., & Mummery, C. (2003). Origin and use of embryonic and adult stem cells in differentiation and tissue repair. *Cardiovasc Res, 58*(2), 324-335.

Payer, B., Rosenberg, M., Yamaji, M., et al. (2013). Tsix RNA and the germline factor, PRDM14, link X reactivation and stem cell reprogramming. *Mol Cell, 52*(6), 805-818. doi:10.1016/j.molcel.2013.10.023

Peault, B., Rudnicki, M., Torrente, Y., et al. (2007). Stem and progenitor cells in skeletal muscle development, maintenance, and therapy. *Mol Ther, 15*(5), 867-877. doi:10.1038/mt.sj.6300145

Peiris, T. H., Ramirez, D., Barghouth, P. G., & Oviedo, N. J. (2016). The Akt signaling pathway is required for tissue maintenance and regeneration in planarians. *BMC Dev Biol, 16*, 7. doi:10.1186/s12861-016-0107-z

Pennarossa, G., Maffei, S., Campagnol, M., Tarantini, L., Gandolfi, F., & Brevini, T. A. (2013). Brief demethylation step allows the conversion of adult human skin fibroblasts into insulin-secreting cells. *Proc Natl Acad Sci U S A, 110*(22), 8948-8953. doi:10.1073/pnas.1220637110

Pereira, C. F., Chang, B., Qiu, J., et al. (2013). Induction of a hemogenic program in mouse fibroblasts. *Cell Stem Cell, 13*(2), 205-218. doi:10.1016/j.stem.2013.05.024

Pereira, C. L., Teixeira, G. Q., Ribeiro-Machado, C., et al. (2016). Mesenchymal Stem/Stromal Cells seeded on cartilaginous endplates promote Intervertebral Disc Regeneration through Extracellular Matrix Remodeling. *Sci Rep, 6*, 33836. doi:10.1038/srep33836

Phillips, T. J., Manzoor, J., Rojas, A., et al. (2002). The longevity of a bilayered skin substitute after application to venous ulcers. *Arch Dermatol, 138*(8), 1079-1081.

Pinol-Jurado, P., Gallardo, E., de Luna, N., et al. (2017). Platelet-Derived Growth Factor BB Influences Muscle Regeneration in Duchenne Muscle Dystrophy. *Am J Pathol, 187*(8), 1814-1827. doi:10.1016/j.ajpath.2017.04.011

Pittenger, M. F., Mackay, A. M., Beck, S. C., et al. (1999). Multilineage potential of adult human mesenchymal stem cells. *Science, 284*(5411), 143-147.

Pittet, M. J., & Weissleder, R. (2011). Intravital imaging. *Cell, 147*(5), 983-991. doi:10.1016/j.cell.2011.11.004

Polo, J. M., Anderssen, E., Walsh, R. M., et al. (2012). A molecular roadmap of reprogramming somatic cells into iPS cells. *Cell, 151*(7), 1617-1632. doi:10.1016/j.cell.2012.11.039

Ponte, A. L., Marais, E., Gallay, N., et al. (2007). The in vitro migration capacity of human bone marrow mesenchymal stem cells: comparison of chemokine and

growth factor chemotactic activities. *Stem Cells, 25*(7), 1737-1745. doi:10.1634/stemcells.2007-0054

Raggatt, L. J., & Partridge, N. C. (2010). Cellular and molecular mechanisms of bone remodeling. *J Biol Chem, 285*(33), 25103-25108. doi:10.1074/jbc.R109.041087

Raghavan, S. S., Woon, C. Y., Kraus, A., Megerle, K., Pham, H., & Chang, J. (2012). Optimization of human tendon tissue engineering: synergistic effects of growth factors for use in tendon scaffold repopulation. *Plast Reconstr Surg, 129*(2), 479-489. doi:10.1097/PRS.0b013e31823aeb94

Rajasingh, J., Lambers, E., Hamada, H., et al. (2008). Cell-free embryonic stem cell extract-mediated derivation of multipotent stem cells from NIH3T3 fibroblasts for functional and anatomical ischemic tissue repair. *Circ Res, 102*(11), e107-117. doi:10.1161/CIRCRESAHA.108.176115

Rajasingh, J., Thangavel, J., Siddiqui, M. R., et al. (2011). Improvement of cardiac function in mouse myocardial infarction after transplantation of epigenetically-modified bone marrow progenitor cells. *PLoS One, 6*(7), e22550. doi:10.1371/journal.pone.0022550

Rao, R. D., Bagaria, V. B., & Cooley, B. C. (2007). Posterolateral intertransverse lumbar fusion in a mouse model: surgical anatomy and operative technique. *Spine J, 7*(1), 61-67. doi:10.1016/j.spinee.2006.03.004

Reisman, M., & Adams, K. T. (2014). Stem cell therapy: a look at current research, regulations, and remaining hurdles. *P T, 39*(12), 846-857.

Riddell, J., Gazit, R., Garrison, B. S., et al. (2014). Reprogramming committed murine blood cells to induced hematopoietic stem cells with defined factors. *Cell, 157*(3), 549-564. doi:10.1016/j.cell.2014.04.006

Ringner, M. (2008). What is principal component analysis? *Nat Biotechnol, 26*(3), 303-304. doi:10.1038/nbt0308-303

Rinn, J. L., Bondre, C., Gladstone, H. B., Brown, P. O., & Chang, H. Y. (2006). Anatomic demarcation by positional variation in fibroblast gene expression programs. *PLoS Genet, 2*(7), e119. doi:10.1371/journal.pgen.0020119

Risbud, M. V., Guttapalli, A., Tsai, T. T., et al. (2007). Evidence for skeletal progenitor cells in the degenerate human intervertebral disc. *Spine (Phila Pa 1976), 32*(23), 2537-2544. doi:10.1097/BRS.0b013e318158dea6

Ritschka, B., Storer, M., Mas, A., et al. (2017). The senescence-associated secretory phenotype induces cellular plasticity and tissue regeneration. *Genes Dev, 31*(2), 172-183. doi:10.1101/gad.290635.116

Robinson, M. D., McCarthy, D. J., & Smyth, G. K. (2010). edgeR: a Bioconductor package for differential expression analysis of digital gene expression data. *Bioinformatics, 26*(1), 139-140. doi:10.1093/bioinformatics/btp616

Rosca, A. M., & Burlacu, A. (2011). Effect of 5-azacytidine: evidence for alteration of the multipotent ability of mesenchymal stem cells. *Stem Cells Dev, 20*(7), 1213-1221. doi:10.1089/scd.2010.0433

Rozkalne, A., Adkin, C., Meng, J., Lapan, A., Morgan, J. E., & Gussoni, E. (2014). Mouse regenerating myofibers detected as false-positive donor myofibers with anti-human spectrin. *Hum Gene Ther, 25*(1), 73-81. doi:10.1089/hum.2013.126

Ryan, J. M., Barry, F. P., Murphy, J. M., & Mahon, B. P. (2005). Mesenchymal stem cells avoid allogeneic rejection. *J Inflamm (Lond), 2*, 8. doi:10.1186/1476-9255-2-8

Sacchetti, B., Funari, A., Remoli, C., et al. (2016). No Identical "Mesenchymal Stem Cells" at Different Times and Sites: Human Committed Progenitors of Distinct Origin and Differentiation Potential Are Incorporated as Adventitial Cells in

Microvessels. *Stem Cell Reports, 6*(6), 897-913. doi:10.1016/j.stemcr.2016.05.011

Saclier, M., Yacoub-Youssef, H., Mackey, A. L., et al. (2013). Differentially activated macrophages orchestrate myogenic precursor cell fate during human skeletal muscle regeneration. *Stem Cells, 31*(2), 384-396. doi:10.1002/stem.1288

Sakai, D., Mochida, J., Iwashina, T., et al. (2006). Regenerative effects of transplanting mesenchymal stem cells embedded in atelocollagen to the degenerated intervertebral disc. *Biomaterials, 27*(3), 335-345. doi:10.1016/j.biomaterials.2005.06.038

Salazar, V. S., Gamer, L. W., & Rosen, V. (2016). BMP signalling in skeletal development, disease and repair. *Nat Rev Endocrinol, 12*(4), 203-221. doi:10.1038/nrendo.2016.12

Sambasivan, R., Gayraud-Morel, B., Dumas, G., et al. (2009). Distinct regulatory cascades govern extraocular and pharyngeal arch muscle progenitor cell fates. *Dev Cell, 16*(6), 810-821. doi:10.1016/j.devcel.2009.05.008

Sanchez Alvarado, A., & Tsonis, P. A. (2006). Bridging the regeneration gap: genetic insights from diverse animal models. *Nat Rev Genet, 7*(11), 873-884. doi:10.1038/nrg1923

Sandler, V. M., Lis, R., Liu, Y., et al. (2014). Reprogramming human endothelial cells to haematopoietic cells requires vascular induction. *Nature, 511*(7509), 312-318. doi:10.1038/nature13547

Saunders, L. R., & McClay, D. R. (2014). Sub-circuits of a gene regulatory network control a developmental epithelial-mesenchymal transition. *Development, 141*(7), 1503-1513. doi:10.1242/dev.101436

Schubert, W., Zimmermann, K., Cramer, M., & Starzinski-Powitz, A. (1989). Lymphocyte antigen Leu-19 as a molecular marker of regeneration in human skeletal muscle. *Proc Natl Acad Sci U S A, 86*(1), 307-311.

Seifert, R. A., Hart, C. E., Phillips, P. E., et al. (1989). Two different subunits associate to create isoform-specific platelet-derived growth factor receptors. *J Biol Chem, 264*(15), 8771-8778.

Sekiya, S., & Suzuki, A. (2011). Direct conversion of mouse fibroblasts to hepatocyte-like cells by defined factors. *Nature, 475*(7356), 390-393. doi:10.1038/nature10263

Selvaraj, V., Plane, J. M., Williams, A. J., & Deng, W. (2010). Switching cell fate: the remarkable rise of induced pluripotent stem cells and lineage reprogramming technologies. *Trends Biotechnol, 28*(4), 214-223. doi:10.1016/j.tibtech.2010.01.002

Senyo, S. E., Steinhauser, M. L., Pizzimenti, C. L., et al. (2013). Mammalian heart renewal by pre-existing cardiomyocytes. *Nature, 493*(7432), 433-436. doi:10.1038/nature11682

Shah, P., Keppler, L., & Rutkowski, J. (2014). A review of platelet derived growth factor playing pivotal role in bone regeneration. *J Oral Implantol, 40*(3), 330-340. doi:10.1563/AAID-JOI-D-11-00173

Sharon, D., & Snyder, M. (2014). Serum profiling using protein microarrays to identify disease related antigens. *Methods Mol Biol, 1176*, 169-178. doi:10.1007/978-1-4939-0992-6_14

Silva, J., Nichols, J., Theunissen, T. W., et al. (2009). Nanog is the gateway to the pluripotent ground state. *Cell, 138*(4), 722-737. doi:10.1016/j.cell.2009.07.039

Silverman, L. R., & Mufti, G. J. (2005). Methylation inhibitor therapy in the treatment of myelodysplastic syndrome. *Nat Clin Pract Oncol, 2 Suppl 1*, S12-23. doi:10.1038/ncponc0347

Simard, A. R., & Rivest, S. (2004). Bone marrow stem cells have the ability to populate the entire central nervous system into fully differentiated parenchymal microglia. *FASEB J, 18*(9), 998-1000. doi:10.1096/fj.04-1517fje

Simonson, O. E., Domogatskaya, A., Volchkov, P., & Rodin, S. (2015). The safety of human pluripotent stem cells in clinical treatment. *Ann Med, 47*(5), 370-380. doi:10.3109/07853890.2015.1051579

Sivanathan, K. N., Rojas-Canales, D. M., Hope, C. M., et al. (2015). Interleukin-17A-Induced Human Mesenchymal Stem Cells Are Superior Modulators of Immunological Function. *Stem Cells, 33*(9), 2850-2863. doi:10.1002/stem.2075

Skrypek, N., Goossens, S., De Smedt, E., Vandamme, N., & Berx, G. (2017). Epithelial-to-Mesenchymal Transition: Epigenetic Reprogramming Driving Cellular Plasticity. *Trends Genet, 33*(12), 943-959. doi:10.1016/j.tig.2017.08.004

Song, G., Ouyang, G., & Bao, S. (2005). The activation of Akt/PKB signaling pathway and cell survival. *J Cell Mol Med, 9*(1), 59-71.

Song, W. K., Park, K. M., Kim, H. J., et al. (2015). Treatment of macular degeneration using embryonic stem cell-derived retinal pigment epithelium: preliminary results in Asian patients. *Stem Cell Reports, 4*(5), 860-872. doi:10.1016/j.stemcr.2015.04.005

Spaeth, E., Klopp, A., Dembinski, J., Andreeff, M., & Marini, F. (2008). Inflammation and tumor microenvironments: defining the migratory itinerary of mesenchymal stem cells. *Gene Ther, 15*(10), 730-738. doi:10.1038/gt.2008.39

Stadtfeld, M., Maherali, N., Breault, D. T., & Hochedlinger, K. (2008). Defining molecular cornerstones during fibroblast to iPS cell reprogramming in mouse. *Cell Stem Cell, 2*(3), 230-240. doi:10.1016/j.stem.2008.02.001

Stone, R. M. (2009). How I treat patients with myelodysplastic syndromes. *Blood, 113*(25), 6296-6303. doi:10.1182/blood-2008-09-038935

Stresemann, C., & Lyko, F. (2008). Modes of action of the DNA methyltransferase inhibitors azacytidine and decitabine. *Int J Cancer, 123*(1), 8-13. doi:10.1002/ijc.23607

Strober, W. (2001). Trypan blue exclusion test of cell viability. *Curr Protoc Immunol, Appendix 3*, Appendix 3B. doi:10.1002/0471142735.ima03bs21

Stute, N., Holtz, K., Bubenheim, M., Lange, C., Blake, F., & Zander, A. R. (2004). Autologous serum for isolation and expansion of human mesenchymal stem cells for clinical use. *Exp Hematol, 32*(12), 1212-1225. doi:10.1016/j.exphem.2004.09.003

Su, X., Paris, M., Gi, Y. J., et al. (2009). TAp63 prevents premature aging by promoting adult stem cell maintenance. *Cell Stem Cell, 5*(1), 64-75. doi:10.1016/j.stem.2009.04.003

Sul, J. Y., Kim, T. K., Lee, J. H., & Eberwine, J. (2012). Perspectives on cell reprogramming with RNA. *Trends Biotechnol, 30*(5), 243-249. doi:10.1016/j.tibtech.2012.02.004

Sun, Z., Zhang, M., Zhao, X. H., et al. (2013). Immune cascades in human intervertebral disc: the pros and cons. *Int J Clin Exp Pathol, 6*(6), 1009-1014.

Tada, M., Takahama, Y., Abe, K., Nakatsuji, N., & Tada, T. (2001). Nuclear reprogramming of somatic cells by in vitro hybridization with ES cells. *Curr Biol, 11*(19), 1553-1558.

Takahashi, K., Tanabe, K., Ohnuki, M., et al. (2007). Induction of pluripotent stem cells from adult human fibroblasts by defined factors. *Cell, 131*(5), 861-872. doi:10.1016/j.cell.2007.11.019

Takahashi, K., & Yamanaka, S. (2006). Induction of pluripotent stem cells from mouse embryonic and adult fibroblast cultures by defined factors. *Cell, 126*(4), 663-676. doi:10.1016/j.cell.2006.07.024

Takahashi, K., & Yamanaka, S. (2013). Induced pluripotent stem cells in medicine and biology. *Development, 140*(12), 2457-2461. doi:10.1242/dev.092551

Talele, N. P., Fradette, J., Davies, J. E., Kapus, A., & Hinz, B. (2015). Expression of alpha-Smooth Muscle Actin Determines the Fate of Mesenchymal Stromal Cells. *Stem Cell Reports, 4*(6), 1016-1030. doi:10.1016/j.stemcr.2015.05.004

Talman, V., & Ruskoaho, H. (2016). Cardiac fibrosis in myocardial infarction-from repair and remodeling to regeneration. *Cell Tissue Res, 365*(3), 563-581. doi:10.1007/s00441-016-2431-9

Tan, S. J., Fang, J. Y., Wu, Y., Yang, Z., Liang, G., & Han, B. (2015). Muscle tissue engineering and regeneration through epigenetic reprogramming and scaffold manipulation. *Sci Rep, 5*, 16333. doi:10.1038/srep16333

Tanaka, E. M. (2003). Cell differentiation and cell fate during urodele tail and limb regeneration. *Curr Opin Genet Dev, 13*(5), 497-501.

Taub, R. (2004). Liver regeneration: from myth to mechanism. *Nat Rev Mol Cell Biol, 5*(10), 836-847. doi:10.1038/nrm1489

Taylor, S. M., & Jones, P. A. (1979). Multiple new phenotypes induced in 10T1/2 and 3T3 cells treated with 5-azacytidine. *Cell, 17*(4), 771-779.

Teixeira, G. Q., Pereira, C. L., Ferreira, J. R., et al. (2017). Immunomodulation of human mesenchymal stem/stromal cells in intervertebral disc degeneration: insights from a proinflammatory/degenerative ex vivo model. *Spine (Phila Pa 1976).* doi:10.1097/BRS.0000000000002494

Thal, M. A., Krishnamurthy, P., Mackie, A. R., et al. (2012). Enhanced angiogenic and cardiomyocyte differentiation capacity of epigenetically reprogrammed mouse and human endothelial progenitor cells augments their efficacy for ischemic myocardial repair. *Circ Res, 111*(2), 180-190. doi:10.1161/CIRCRESAHA.112.270462

TheJapanTimes. (2018). First serious adverse reaction to iPS-derived retinal cell transplant reported.

Thomson, J. A., Itskovitz-Eldor, J., Shapiro, S. S., et al. (1998). Embryonic stem cell lines derived from human blastocysts. *Science, 282*(5391), 1145-1147.

Tonge, P. D., Corso, A. J., Monetti, C., et al. (2014). Divergent reprogramming routes lead to alternative stem-cell states. *Nature, 516*(7530), 192-197. doi:10.1038/nature14047

Tuan, R. S., Boland, G., & Tuli, R. (2003). Adult mesenchymal stem cells and cell-based tissue engineering. *Arthritis Res Ther, 5*(1), 32-45.

Uccelli, A., Mancardi, G., & Chiesa, S. (2008). Is there a role for mesenchymal stem cells in autoimmune diseases? *Autoimmunity, 41*(8), 592-595. doi:10.1080/08916930802200166

Unnikrishnan, A., Vo, A. N. Q., Pickford, R., et al. (2018). AZA-MS: a novel multiparameter mass spectrometry method to determine the intracellular dynamics of azacitidine therapy in vivo. *Leukemia, 32*(4), 900-910. doi:10.1038/leu.2017.340

Vadala, G., Sowa, G., Hubert, M., Gilbertson, L. G., Denaro, V., & Kang, J. D. (2012). Mesenchymal stem cells injection in degenerated intervertebral disc: cell leakage

may induce osteophyte formation. *J Tissue Eng Regen Med, 6*(5), 348-355. doi:10.1002/term.433

Vidal, S. E., Stadtfeld, M., & Apostolou, E. (2015). F-class cells: new routes and destinations for induced pluripotency. *Cell Stem Cell, 16*(1), 9-10. doi:10.1016/j.stem.2014.12.007

Vierbuchen, T., Ostermeier, A., Pang, Z. P., Kokubu, Y., Sudhof, T. C., & Wernig, M. (2010). Direct conversion of fibroblasts to functional neurons by defined factors. *Nature, 463*(7284), 1035-1041. doi:10.1038/nature08797

Vierbuchen, T., & Wernig, M. (2012). Molecular roadblocks for cellular reprogramming. *Mol Cell, 47*(6), 827-838. doi:10.1016/j.molcel.2012.09.008

Vogelin, E., Jones, N. F., Huang, J. I., Brekke, J. H., & Toth, J. M. (2000). Practical illustrations in tissue engineering: surgical considerations relevant to the implantation of osteoinductive devices. *Tissue Eng, 6*(4), 449-460. doi:10.1089/107632700418155

Vu, M. Q., Der Sarkissian, S., Borie, M., Bessette, P. O., & Noiseux, N. (2016). Optimization of Mesenchymal Stem Cells to Increase Their Therapeutic Potential. *Methods Mol Biol, 1416*, 275-288. doi:10.1007/978-1-4939-3584-0_16

Wada, N., Gronthos, S., & Bartold, P. M. (2013). Immunomodulatory effects of stem cells. *Periodontol 2000, 63*(1), 198-216. doi:10.1111/prd.12024

Waddington, C. H. (1957). The strategy of the genes. In.

Wagers, A. J. (2012). The stem cell niche in regenerative medicine. *Cell Stem Cell, 10*(4), 362-369. doi:10.1016/j.stem.2012.02.018

Wallace, H., Watson, A., & Egar, M. (1981). Regeneration of subnormally innervated axolotl arms. *J Embryol Exp Morphol, 62*, 1-11.

Wang, S., Mo, M., Wang, J., et al. (2018). Platelet-derived growth factor receptor beta identifies mesenchymal stem cells with enhanced engraftment to tissue injury and pro-angiogenic property. *Cell Mol Life Sci, 75*(3), 547-561. doi:10.1007/s00018-017-2641-7

Warren, L., Manos, P. D., Ahfeldt, T., et al. (2010). Highly efficient reprogramming to pluripotency and directed differentiation of human cells with synthetic modified mRNA. *Cell Stem Cell, 7*(5), 618-630. doi:10.1016/j.stem.2010.08.012

Weber, K., Bartsch, U., Stocking, C., & Fehse, B. (2008). A multicolor panel of novel lentiviral "gene ontology" (LeGO) vectors for functional gene analysis. *Mol Ther, 16*(4), 698-706. doi:10.1038/mt.2008.6

Weissman, I. L. (2000). Stem cells: units of development, units of regeneration, and units in evolution. *Cell, 100*(1), 157-168.

Whited, J. L., & Tabin, C. J. (2009). Limb regeneration revisited. *J Biol, 8*(1), 5. doi:10.1186/jbiol105

Whitworth, D. J., Frith, J. E., Frith, T. J., Ovchinnikov, D. A., Cooper-White, J. J., & Wolvetang, E. J. (2014). Derivation of mesenchymal stromal cells from canine induced pluripotent stem cells by inhibition of the TGFbeta/activin signaling pathway. *Stem Cells Dev, 23*(24), 3021-3033. doi:10.1089/scd.2013.0634

Whitworth, D. J., Ovchinnikov, D. A., Sun, J., Fortuna, P. R., & Wolvetang, E. J. (2014). Generation and characterization of leukemia inhibitory factor-dependent equine induced pluripotent stem cells from adult dermal fibroblasts. *Stem Cells Dev, 23*(13), 1515-1523. doi:10.1089/scd.2013.0461

Wilmut, I., Schnieke, A. E., McWhir, J., Kind, A. J., & Campbell, K. H. (1997). Viable offspring derived from fetal and adult mammalian cells. *Nature, 385*(6619), 810-813. doi:10.1038/385810a0

Wilson, A., Laurenti, E., Oser, G., et al. (2008). Hematopoietic stem cells reversibly switch from dormancy to self-renewal during homeostasis and repair. *Cell, 135*(6), 1118-1129. doi:10.1016/j.cell.2008.10.048

Wong, D. J., Liu, H., Ridky, T. W., Cassarino, D., Segal, E., & Chang, H. Y. (2008). Module map of stem cell genes guides creation of epithelial cancer stem cells. *Cell Stem Cell, 2*(4), 333-344. doi:10.1016/j.stem.2008.02.009

Xu, J., Du, Y., & Deng, H. (2015). Direct lineage reprogramming: strategies, mechanisms, and applications. *Cell Stem Cell, 16*(2), 119-134. doi:10.1016/j.stem.2015.01.013

Xu, X., Wilschut, K. J., Kouklis, G., et al. (2015). Human Satellite Cell Transplantation and Regeneration from Diverse Skeletal Muscles. *Stem Cell Reports, 5*(3), 419-434. doi:10.1016/j.stemcr.2015.07.016

Xu, Y., Wei, X., Wang, M., et al. (2013). Proliferation rate of somatic cells affects reprogramming efficiency. *J Biol Chem, 288*(14), 9767-9778. doi:10.1074/jbc.M112.403881

Yagi, H., Soto-Gutierrez, A., Parekkadan, B., et al. (2010). Mesenchymal stem cells: Mechanisms of immunomodulation and homing. *Cell Transplant, 19*(6), 667-679. doi:10.3727/096368910X508762

Yamanaka, S. (2009). Elite and stochastic models for induced pluripotent stem cell generation. *Nature, 460*(7251), 49-52. doi:10.1038/nature08180

Yamanaka, S., & Blau, H. M. (2010). Nuclear reprogramming to a pluripotent state by three approaches. *Nature, 465*(7299), 704-712. doi:10.1038/nature09229

Yao, B., Huang, S., Gao, D., Xie, J., Liu, N., & Fu, X. (2016). Age-associated changes in regenerative capabilities of mesenchymal stem cell: impact on chronic wounds repair. *Int Wound J, 13*(6), 1252-1259. doi:10.1111/iwj.12491

Yokoo, T., Fukui, A., Ohashi, T., et al. (2006). Xenobiotic kidney organogenesis from human mesenchymal stem cells using a growing rodent embryo. *J Am Soc Nephrol, 17*(4), 1026-1034. doi:10.1681/ASN.2005101043

Young, F. E. (2000). A time for restraint. *Science, 287*(5457), 1424.

Yun, I. S., Jeon, Y. R., Lee, W. J., et al. (2012). Effect of human adipose derived stem cells on scar formation and remodeling in a pig model: a pilot study. *Dermatol Surg, 38*(10), 1678-1688. doi:10.1111/j.1524-4725.2012.02495.x

Zannettino, A. C., Paton, S., Arthur, A., et al. (2008). Multipotential human adipose-derived stromal stem cells exhibit a perivascular phenotype in vitro and in vivo. *J Cell Physiol, 214*(2), 413-421. doi:10.1002/jcp.21210

Zhang, F., Wang, L., Li, Y., et al. (2017). Optimizing mesoderm progenitor selection and three-dimensional microniche culture allows highly efficient endothelial differentiation and ischemic tissue repair from human pluripotent stem cells. *Stem Cell Res Ther, 8*(1), 6. doi:10.1186/s13287-016-0455-4

Zhao, J., Ross, J. W., Hao, Y., et al. (2009). Significant improvement in cloning efficiency of an inbred miniature pig by histone deacetylase inhibitor treatment after somatic cell nuclear transfer. *Biol Reprod, 81*(3), 525-530. doi:10.1095/biolreprod.109.077016

Zheng, B., Cao, B., Crisan, M., et al. (2007). Prospective identification of myogenic endothelial cells in human skeletal muscle. *Nat Biotechnol, 25*(9), 1025-1034. doi:10.1038/nbt1334

Zhong, Z., Tsukada, S., Rehman, H., et al. (2010). Inhibition of transforming growth factor-beta/Smad signaling improves regeneration of small-for-size rat liver grafts. *Liver Transpl, 16*(2), 181-190. doi:10.1002/lt.21966

Zhou, Q., Brown, J., Kanarek, A., Rajagopal, J., & Melton, D. A. (2008). In vivo reprogramming of adult pancreatic exocrine cells to beta-cells. *Nature, 455*(7213), 627-632. doi:10.1038/nature07314

Zhou, W., & Freed, C. R. (2009). Adenoviral gene delivery can reprogram human fibroblasts to induced pluripotent stem cells. *Stem Cells, 27*(11), 2667-2674. doi:10.1002/stem.201

Zhu, H., Mitsuhashi, N., Klein, A., et al. (2006). The role of the hyaluronan receptor CD44 in mesenchymal stem cell migration in the extracellular matrix. *Stem Cells, 24*(4), 928-935. doi:10.1634/stemcells.2005-0186

Zuk, P. A., Zhu, M., Ashjian, P., et al. (2002). Human adipose tissue is a source of multipotent stem cells. *Mol Biol Cell, 13*(12), 4279-4295. doi:10.1091/mbc.E02-02-0105

Appendix: Supplementary data

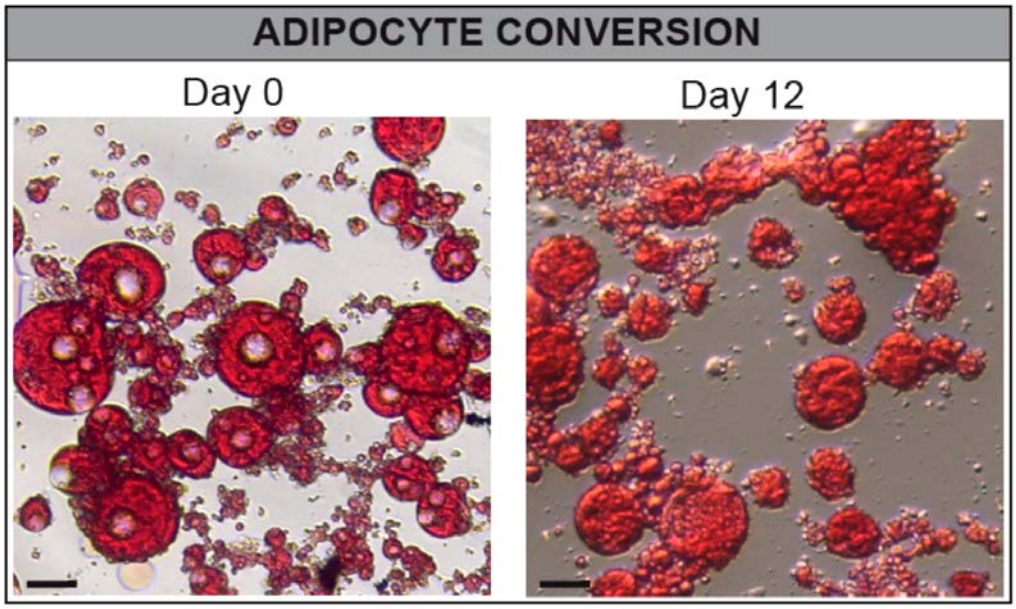

Figure S1. Primary adipocytes subjected to DCi reprogramming in FCS-supplemented medium do not undergo cell conversion by day 12 in culture (n=5, Scale bar = 30µm).

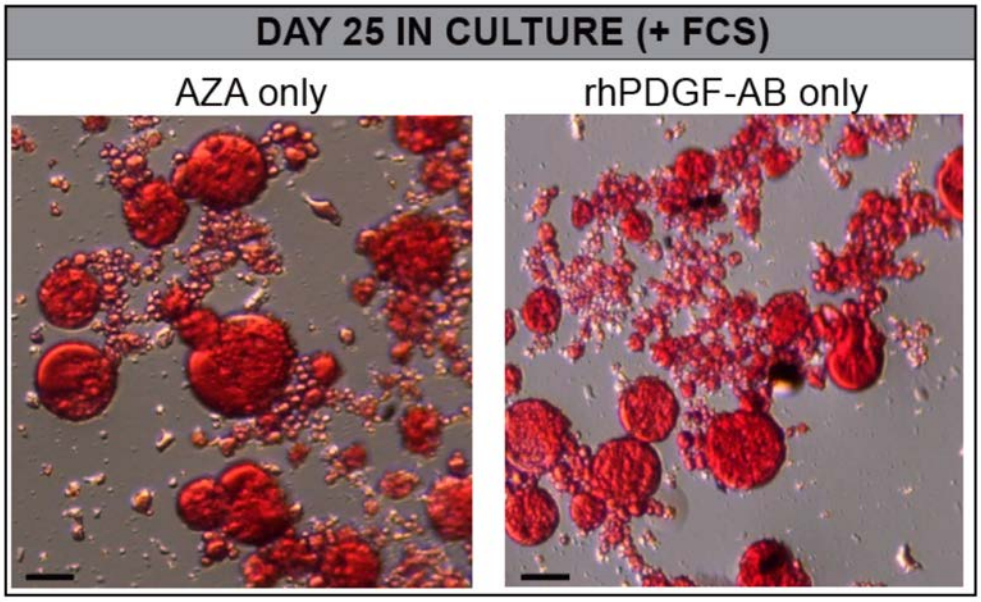

Figure S2. Primary adipocytes exposed to FCS-supplemented medium containing AZA or rhPDGF-AB alone, do not undergo cell conversion and are maintained as dormant cells in culture (n=3, Scale bar = 30µm).

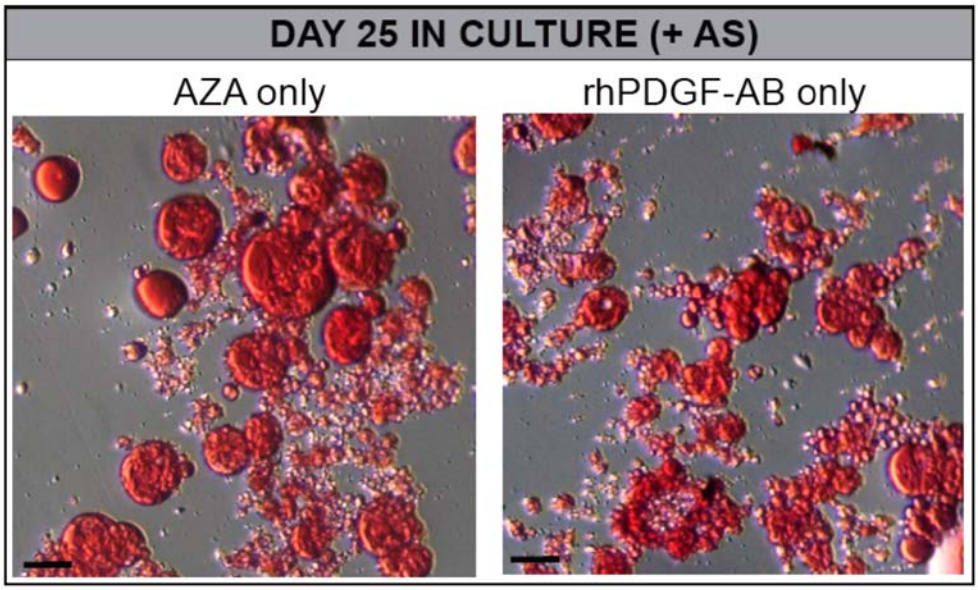

Figure S3. Primary adipocytes exposed to AS-supplemented medium containing AZA or rhPDGF-AB alone, do not undergo cell conversion and are maintained as dormant cells in culture (n=5, Scale bar = 30µm).

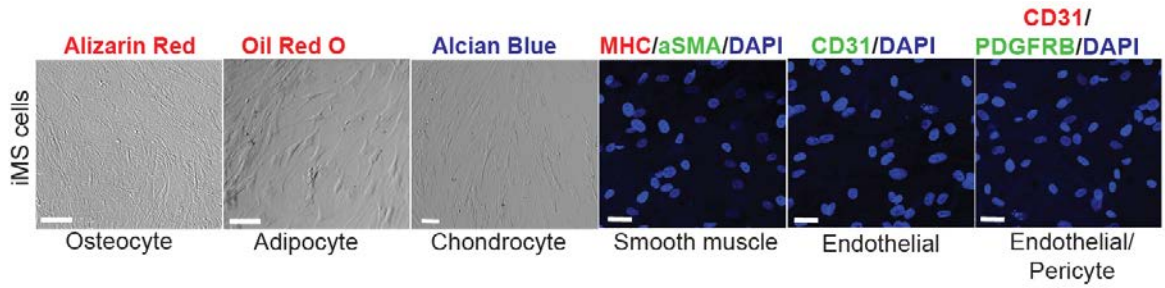

Figure S4. DCi reprogrammed iMS cells not induced for mesenchymal lineage differentiations, stain negative for the respective differentiation markers (n=3, Scale bar = 20µm).

Sample ID	Sample type	Conc. (ng/µL)	260/280	260/230
AY1	Primary Adipo 1	210.72	1.98	1.53
AY2	AdMSC1	616.11	2.11	2.01
AY3	Treated AdMSC1	2589.15	2.08	2.17
AY4	iMS 1	921.8	2.12	1.98
AY5	Primary Adipo 2	143.53	1.89	0.98
AY6	AdMSC2	502.54	2.08	1.78
AY7	Treated AdMSC2	2948.67	2.07	2.08
AY8	iMS 2	956.95	2.11	1.91
AY9	Primary Adipo 3	749.46	2.11	2.10
AY10	AdMSC3	303.94	2.05	1.75
AY11	Treated AdMSC3	2203.43	2.10	2.16
AY12	iMS3	3814.67	1.91	1.99

Table S1: The quality and integrity of extracted mRNA of each of the triplicate samples of primary adipocytes, AdMSCs, treated AdMSCs and iMS cells were assessed using the Nanodrop spectrophotometer.

Sample ID	Sample type	Total Reads	Mapped Reads	% Mapping
AY1	Primary Adipo 1	30174198	29235908	96.9%
AY2	AdMSC1	33513230	32899698	98.2%
AY3	Treated AdMSC1	30564218	29981108	98.1%
AY4	iMS 1	25732810	25293322	98.3%
AY5	Primary Adipo 2	23802312	22733044	95.5%
AY6	AdMSC2	26635578	26160170	98.2%
AY7	Treated AdMSC2	32703468	32157856	98.3%
AY8	iMS 2	27211976	26768232	98.4%
AY9	Primary Adipo 3	32214206	31290512	97.1%
AY10	AdMSC3	29859976	29345238	98.3%
AY11	Treated AdMSC3	34308962	33705510	98.2%
AY12	iMS3	31501710	30715744	97.5%

Table S2: Table depicting % Mapping of the sequenced tracks aligned to human genome (UCSC genome assembly hg19).

A. PPAR signaling

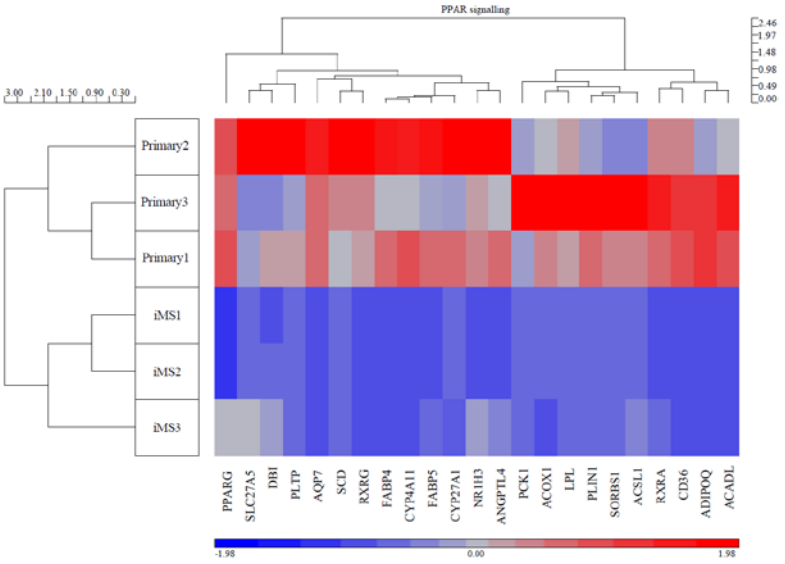

B. TGFβ signaling

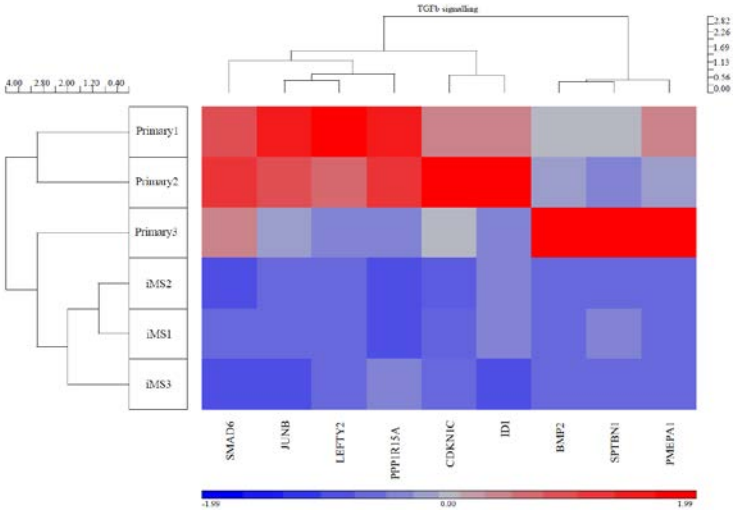

C. Allograft rejection mechanism

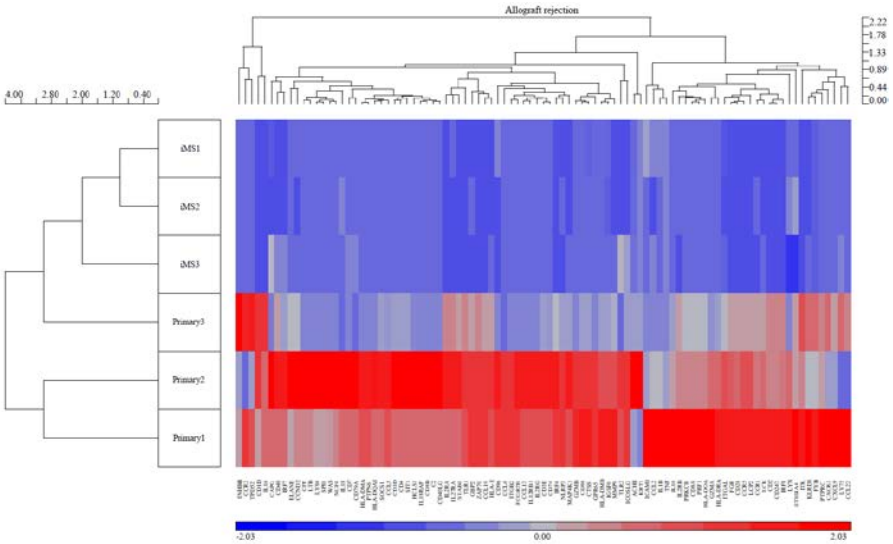

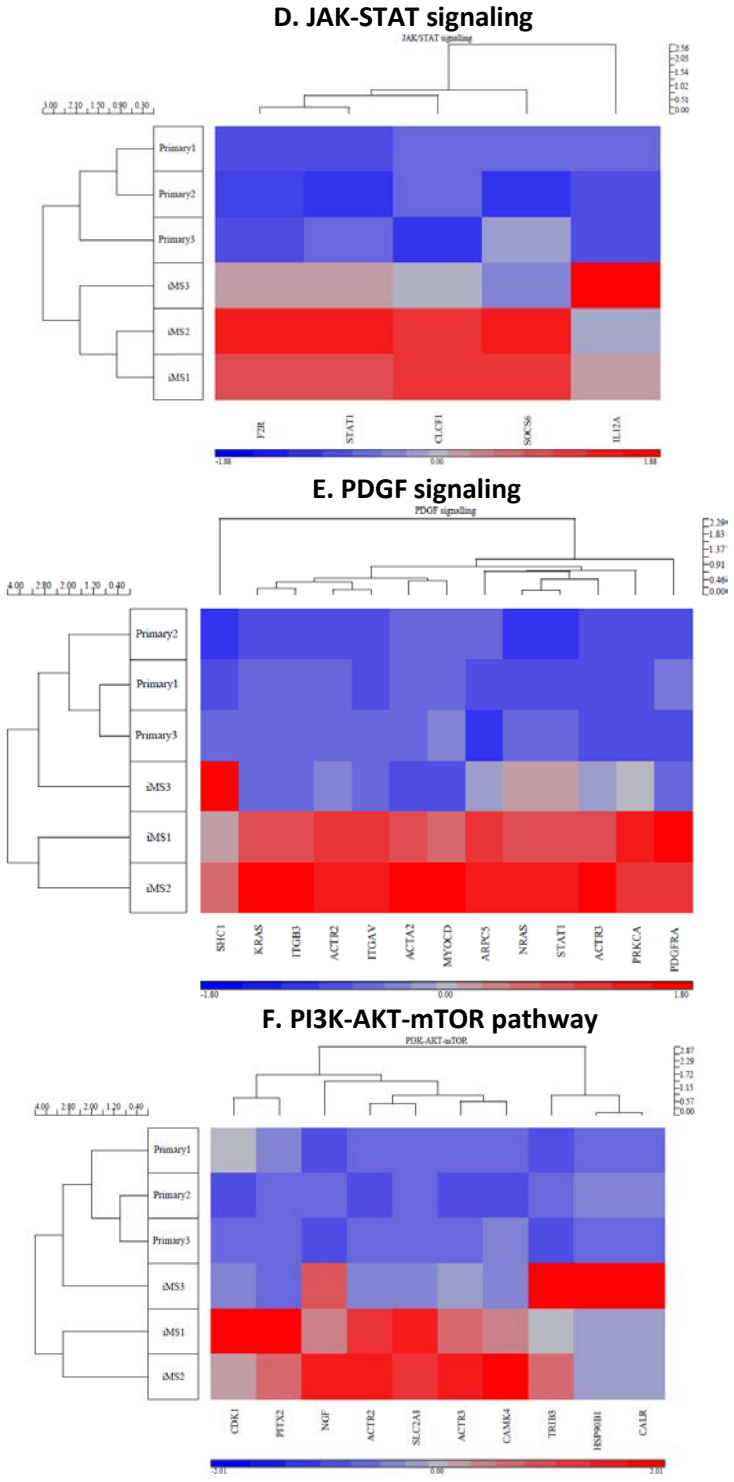

Figure S5: Unsupervised hierarchical clustering of DE genes across 'primary adipocytes v/s iMS cells' comparison, filtered for transcriptional regulators and matched for different pathways. In this comparison, iMS cells showed downregulation of genes associated with (A) PPAR signaling, (B) TGFb signaling, (C) Allograft rejection mechanism; and upregulation of genes associated with (D) JAK-STAT signaling, (E) PDGF signaling and (F) PI3K-AKT-mTOR pathway.

Ingenuity Canonical Pathways	p value	Molecules
Wnt/β-catenin Signaling	1.17E-08	CDKN2A,SOX7,SOX10,TLE1,MDM2,SOX11,SOX13,SOX17,JUN,SOX6,SOX8,LEF1,SOX18,SOX15,SOX5
Adipogenesis pathway	3.24E-08	ZNF423,FOXC2,ARNTL,EGR2,FOXO1,SREBF1,EZH2,CEBPA,CEBPD,HIF1A,CEBPB,STAT5B,PER2
Th2 Pathway	1.10E-07	STAT5A,RUNX3,IKZF1,MAF,TBX21,SPI1,NOTCH4,JUN,NFATC2,VAV1,GATA3,STAT5B,NOTCH1
Th1 and Th2 Activation Pathway	1.91E-07	STAT5A,RUNX3,IKZF1,MAF,TBX21,SPI1,NOTCH4,JUN,NFATC2,VAV1,STAT5B,GATA3,STAT1,NOTCH1
TGF-β Signaling	3.02E-07	RUNX3,ZNF423,FOS,IRF7,GSC,JUN,RUNX2,SMAD6,VDR,PITX2
Notch Signaling	5.89E-07	NOTCH4,DTX1,HES5,HES1,HEY2,NOTCH1,HEY1
IL-17A Signaling in Fibroblasts	7.08E-06	NFKBID,FOS,NFKBIA,JUN,CEBPD,CEBPB
IL-7 Signaling Pathway	2.29E-05	PAX5,FOXO4,STAT5A,JUN,FOXO6,FOXO1,STAT5B,STAT1
iNOS Signaling	2.82E-05	NFKBID,FOS,NFKBIA,JUN,HMGA1,STAT1
VDR/RXR Activation	8.71E-05	FOXO1,RUNX2,CEBPA,HES1,VDR,CEBPB,KLF4
Unfolded protein response	9.12E-05	CALR,SREBF1,CEBPA,CEBPD,CEBPB,CEBPE
Osteoarthritis Pathway	1.32E-04	GLI2,RUNX2,DLX5,SMAD6,MEF2C,LEF1,HES1,HIF1A,CEBPB,NOTCH1,NKX3-2
April Mediated Signaling	1.82E-04	NFKBID,FOS,NFKBIA,JUN,NFATC2
B Cell Activating Factor Signaling	2.29E-04	NFKBID,FOS,NFKBIA,JUN,NFATC2
Cell Cycle: G1/S Checkpoint Regulation	2.57E-04	CDKN2A,FOXO1,E2F7,CDKN2C,MDM2,E2F3
PPAR Signaling	2.69E-04	NFKBID,STAT5A,FOS,NFKBIA,JUN,STAT5B,SCAND1
PI3K Signaling	3.39E-04	NFKBID,FOS,ATF3,NFKBIA,JUN,ATF5,NFATC2,VAV1
Th1 Pathway	4.27E-04	RUNX3,NOTCH4,NFATC2,VAV1,TBX21,STAT1,GATA3,NOTCH1
BMP signaling pathway	5.25E-04	ZNF423,MAGED1,JUN,RUNX2,SMAD6,PITX2
Chronic Myeloid Leukemia Signaling	6.03E-04	CDKN2A,STAT5A,MECOM,E2F7,MDM2,E2F3,STAT5B
TNFR2 Signaling	6.17E-04	NFKBID,FOS,NFKBIA,JUN
Regulation of IL-2 Expression in Activated and Anergic T Lymphocytes	7.41E-04	NFKBID,FOS,NFKBIA,JUN,NFATC2,VAV1

p53 Signaling	8.32E-04	CDKN2A,SNAI2,JUN,PLAGL1,MDM2,HIF1A,TRIM29
Erythropoietin Signaling	8.51E-04	NFKBID,STAT5A,FOS,NFKBIA,JUN,STAT5B
Molecular Mechanisms of Cancer	9.55E-04	CDKN2A,SMAD6,CDKN2C,MDM2,HIF1A,E2F3,NFKBID,FOS,JUN,NFKBIA,FOXO1,E2F7,LEF1,NOTCH1
IL-3 Signaling	9.55E-04	STAT5A,FOS,JUN,FOXO1,STAT5B,STAT1
Prolactin Signaling	9.55E-04	STAT5A,FOS,JUN,CEBPB,STAT5B,STAT1
JAK/Stat Signaling	9.55E-04	STAT5A,FOS,JUN,CEBPB,STAT5B,STAT1
B Cell Receptor Signaling	1.15E-03	PAX5,NFKBID,NFKBIA,JUN,FOXO1,EGR1,NFATC2,MEF2C,VAV1
Role of Osteoblasts, Osteoclasts and Chondrocytes in Rheumatoid Arthritis	1.20E-03	NFKBID,FOS,NFKBIA,JUN,FOXO1,RUNX2,DLX5,SMAD6,NFATC2,LEF1
Pancreatic Adenocarcinoma Signaling	1.32E-03	CDKN2A,E2F7,BRCA2,MDM2,E2F3,STAT1,NOTCH1
Activation of IRF by Cytosolic Pattern Recognition Receptors	1.45E-03	NFKBID,IRF7,NFKBIA,JUN,STAT1
Acute Myeloid Leukemia Signaling	1.66E-03	RUNX1,STAT5A,CEBPA,LEF1,STAT5B,SPI1
Thrombopoietin Signaling	1.95E-03	STAT5A,FOS,JUN,STAT5B,STAT1
ErbB2-ErbB3 Signaling	2.34E-03	STAT5A,JUN,FOXO1,ETV4,STAT5B
MIF Regulation of Innate Immunity	2.75E-03	NFKBID,FOS,NFKBIA,JUN
Hypoxia Signaling in the Cardiovascular System	3.24E-03	NFKBID,NFKBIA,JUN,MDM2,HIF1A
IL-12 Signaling and Production in Macrophages	3.72E-03	FOS,JUN,MAF,CEBPB,IRF8,STAT1,SPI1
Angiopoietin Signaling	4.07E-03	NFKBID,STAT5A,NFKBIA,FOXO1,STAT5B
IL-22 Signaling	4.17E-03	STAT5A,STAT5B,STAT1
TNFR1 Signaling	4.17E-03	NFKBID,FOS,NFKBIA,JUN
RAR Activation	4.27E-03	STAT5A,FOS,JUN,NRIP2,SMAD6,STAT5B,ZBTB16,SCAND1
Regulation of the Epithelial-Mesenchymal Transition Pathway	4.27E-03	FOXC2,NOTCH4,GSC,SNAI2,EGR1,LEF1,HIF1A,NOTCH1
Cancer Drug Resistance By Drug Efflux	4.47E-03	FOXO4,FOXO6,FOXO1,MDM2
Role of JAK family kinases in IL-6-type Cytokine Signaling	4.68E-03	STAT5A,STAT5B,STAT1
NRF2-mediated Oxidative Stress Response	4.68E-03	FOS,JUN,MAF,JUND,JUNB,DNAJB1,MAFF,BACH1
CD27 Signaling in Lymphocytes	5.50E-03	NFKBID,FOS,NFKBIA,JUN
Growth Hormone Signaling	6.17E-03	STAT5A,FOS,CEBPA,STAT5B,STAT1

Transcriptional Regulatory Network in Embryonic Stem Cells	6.31E-03	GATA6,SKIL,EOMES,FOXC1
Glucocorticoid Receptor Signaling	6.76E-03	NFKBID,STAT5A,FOS,NFKBIA,JUN,CEBPA, NFATC2,CEBPB,STAT5B,STAT1,TSC22D3
CD28 Signaling in T Helper Cells	7.94E-03	NFKBID,FOS,NFKBIA,JUN,NFATC2,VAV1
Role of Macrophages, Fibroblasts and Endothelial Cells in Rheumatoid Arthritis	9.12E-03	NFKBID,FOS,NFKBIA,JUN,CEBPA,CEBPD, NFATC2,LEF1,CEBPB,CEBPE
4-1BB Signaling in T Lymphocytes	9.33E-03	NFKBID,NFKBIA,JUN
Role of JAK2 in Hormone-like Cytokine Signaling	9.33E-03	STAT5A,STAT5B,STAT1
Prostate Cancer Signaling	9.77E-03	NFKBID,NFKBIA,FOXO1,MDM2,LEF1
Sumoylation Pathway	1.02E-02	FOS,NFKBIA,JUN,CEBPA,MDM2
ATM Signaling	1.07E-02	NFKBIA,JUN,H2AFX,TP53BP1,MDM2
Circadian Rhythm Signaling	1.10E-02	PER1,ARNTL,PER2
Oncostatin M Signaling	1.10E-02	STAT5A,STAT5B,STAT1
IL-2 Signaling	1.15E-02	STAT5A,FOS,JUN,STAT5B
RANK Signaling in Osteoclasts	1.20E-02	NFKBID,FOS,NFKBIA,JUN,NFATC2
Cell Cycle Regulation by BTG Family Proteins	1.38E-02	E2F7,BTG2,E2F3
IL-10 Signaling	1.48E-02	NFKBID,FOS,NFKBIA,JUN
T Cell Receptor Signaling	1.62E-02	FOS,NFKBIA,JUN,NFATC2,VAV1
Production of Nitric Oxide and Reactive Oxygen Species in Macrophages	1.70E-02	NFKBID,FOS,NFKBIA,JUN,IRF8,STAT1,SPI1
Role of PKR in Interferon Induction and Antiviral Response	1.82E-02	NFKBID,NFKBIA,STAT1
PKCÎ¸ Signaling in T Lymphocytes	1.95E-02	NFKBID,FOS,NFKBIA,JUN,NFATC2,VAV1
Glioma Signaling	1.95E-02	CDKN2A,E2F7,CDKN2C,MDM2,E2F3
Role of RIG1-like Receptors in Antiviral Innate Immunity	1.95E-02	NFKBID,IRF7,NFKBIA
CD40 Signaling	2.19E-02	NFKBID,FOS,NFKBIA,JUN
Estrogen-Dependent Breast Cancer Signaling	2.29E-02	STAT5A,FOS,JUN,STAT5B
Cyclins and Cell Cycle Regulation	2.29E-02	CDKN2A,E2F7,CDKN2C,E2F3
Glioblastoma Multiforme Signaling	2.34E-02	CDKN2A,FOXO1,E2F7,MDM2,LEF1,E2F3
IL-9 Signaling	2.34E-02	STAT5A,STAT5B,STAT1

Role of Oct4 in Mammalian Embryonic Stem Cell Pluripotency	2.34E-02	KDM5B,UTF1,SALL4
Role of BRCA1 in DNA Damage Response	2.40E-02	E2F7,BRCA2,E2F3,STAT1
Cardiomyocyte Differentiation via BMP Receptors	2.75E-02	SMAD6,MEF2C
IL-6 Signaling	3.09E-02	NFKBID,FOS,NFKBIA,JUN,CEBPB
LPS-stimulated MAPK Signaling	3.16E-02	NFKBID,FOS,NFKBIA,JUN
IL-1 Signaling	3.72E-02	NFKBID,FOS,NFKBIA,JUN
Corticotropin Releasing Hormone Signaling	3.80E-02	FOS,GLI2,JUN,MEF2C,JUND
GÎ±12/13 Signaling	3.80E-02	NFKBID,NFKBIA,JUN,MEF2C,VAV1
Role of NFAT in Regulation of the Immune Response	3.80E-02	NFKBID,FOS,NFKBIA,JUN,NFATC2,MEF2C
Aryl Hydrocarbon Receptor Signaling	3.89E-02	CDKN2A,FOS,JUN,NFIA,MDM2
OX40 Signaling Pathway	4.07E-02	NFKBID,NFKBIA,JUN
Human Embryonic Stem Cell Pluripotency	4.37E-02	FOXO1,UTF1,SMAD6,LEF1,SALL4
IL-17A Signaling in Gastric Cells	4.57E-02	FOS,JUN
Epithelial Adherens Junction Signaling	4.68E-02	NOTCH4,SNAI2,LEF1,NOTCH1,ACTN1
Estrogen-mediated S-phase Entry	4.90E-02	E2F7,E2F3
PCP pathway	4.90E-02	JUN,JUND,JUNB
Diseases and Functions	**p value**	**Molecules**
Cell Cycle	2.38E-11	AJUBA,ARNTL2,ATF3,BRCA2,CALR,CDKN2A,CDKN2C,CEBPB,E2F3,EBF4,EZH2,FHL2,FOS,FOXC1,FOXM1,FOXO4,GAS7,GATA2,GATA3,HIF1A,IRF5,IRF7,IRX1,KLF4,MDM2,MECOM,MEIS2,MLXIPL,NFATC2,NOTCH1,PAWR,PER1,PLAGL1,PTTG1,RUNX1,RUNX2,RUNX3,SERTAD1,STAT1,TAL1,VAV1,ZFP36
Cellular Movement	2.69E-07	ACTN1,ATF3,ATOH8,BTG2,CALR,CDKN2A,CEBPB,CREB3L1,DACH1,DTX1,EGR1,EGR3,ERG,ETV4,EZH2,FHL2,FOS,FOSB,FOXC1,FOXM1,FOXO1,GATA1,GATA3,GATA6,HES6,HEY1,HHEX,HIF1A,HMGA1,IER2,IKZF1,JUN,JUND,KLF2,KLF4,KLF8,LEF1,MDM2,NFATC2,NFKBIA,NOTCH1,NOTCH4,PAX5,PITX2,PTTG1,RUNX1,RUNX2,RUNX3,SNAI2,STAT1,STAT5A,TFAP2C,TSC22D3,ZBTB16

Cellular Development	6.30E-07	DTX1,EZH2,FOXO4,GATA2,HES1,JUN,LMX1A,MDM2,NOTCH1,RUNX1
Embryonic Development, Organismal Development	3.52E-06	ANKRD1,EZH2,FOXC1,FOXC2,FOXL1,KLF11,NOTCH1,NOTCH4,RUNX1,RUNX3,SALL1,SOX17,TBX1
Cellular Development	3.93E-06	ERG,FOXC2,FOXM1,FOXO1,GATA3,GSC,HIF1A,KLF4,KLF8,LEF1,PTTG1,SNAI2,STAT5A
Cellular Development, Embryonic Development, Organismal Development	1.35E-05	EZH2,GAS7,HOPX,JUN,LMX1A,MDM2,MEF2C,RUNX1
Cell Death and Survival	2.91E-05	ATF3,BCL6B,BRCA2,BTG2,CALR,CDKN2A,CEBPB,CEBPD,ERCC6,EZH2,FOXM1,FOXO1,GATA2,GATA6,HES1,HEY1,HHEX,HIF1A,HMGA1,ID4,JUN,KLF4,LEF1,MDM2,MECOM,NFKBIA,NOTCH1,RUNX2,SNAI2,SOX10,STAT5B,TAL1,TFEB,TP53BP1,TRIM29,UHRF1,VDR,ZBTB16,ZFP36
Embryonic Development, Organismal Development, Tissue Development	4.13E-05	IKZF1,IKZF3,TBX6,TCF15
Cellular Development, Cellular Growth and Proliferation	3.54E-03	CDKN2A,CEBPD,HES1,RUNX1
Cell-mediated Immune Response, Cellular Development, Cellular Function and Maintenance, Cellular Growth and Proliferation, Embryonic Development, Hematological System Development and Function, Hematopoiesis, Lymphoid Tissue Structure and Development, Organ Development, Organismal Development, Tissue Development	3.73E-03	GATA3,VAV1
Cell Cycle, Cellular Development, Connective Tissue Development and Function	3.85E-03	3.85E-03

Table S3 List of canonical pathways and categories of diseases and functions from IPA of differentially expressed transcriptional regulators across ‘primary adipocytes v/s iMS cells’, ($P < 0.05$).

Ingenuity Canonical Pathways	p value	Molecules
Agranulocyte Adhesion and Diapedesis	5.12861E-08	AOC3,SELE,MMP3,CXCR4,PF4,PPBP,MYH11,CXCL6,CDH5,PECAM1,MYL4,PODXL,ACTG2,CD34,MMP9,MYL3
Atherosclerosis Signaling	1.1749E-06	SELE,LYZ,MMP3,CXCR4,CD36,RARRES3,PLA2G7,PLA2G2A,PDGFB,MMP9,RBP4,APOD
Th2 Pathway	3.63078E-05	FGFR3,NOTCH4,PTGDR2,HLA-DRB1,CXCR4,CD4,HLA-DRA,MAF,HLA-DMB,PIK3R5,JAG1
Neuroinflammation Signaling Pathway	5.24807E-05	GRIN3B,MMP3,TYROBP,PIK3R5,CREB5,PLA2G2A,FGFR3,HLA-DRB1,SYK,HLA-DMB,IL34,HLA-DRA,CYBB,TGFB3,SLC1A2,MMP9
Th1 and Th2 Activation Pathway	5.37032E-05	FGFR3,NOTCH4,PTGDR2,HLA-DRB1,CXCR4,CD4,HLA-DRA,MAF,HLA-DMB,PIK3R5,JAG1,DLL4
Hepatic Fibrosis / Hepatic Stellate Cell Activation	6.30957E-05	EDN1,NGFR,TGFB3,MYL4,LBP,MYH11,KDR,PDGFB,MYL3,MMP9,COL6A6,PGF
G-Protein Coupled Receptor Signaling	6.60693E-05	ADRA2B,APLNR,PTGER3,NPY1R,CNR1,PIK3R5,RGS16,CREB5,AVPR1A,FGFR3,ADRA2A,GNAO1,PDE1B,PTH1R,ADRA2C
Granulocyte Adhesion and Diapedesis	6.60693E-05	FPR3,SELE,CDH5,MMP3,CXCR4,PPBP,NGFR,PF4,PECAM1,MMP9,CXCL6
LXR/RXR Activation	6.60693E-05	MLXIPL,LYZ,NGFR,CD36,NR1H3,LBP,MMP9,RBP4,APOD
Complement System	6.60693E-05	CFD,C7,C1QA,C1QC,ITGAX
Signaling by Rho Family GTPases	6.60693E-05	ARHGEF15,PIK3R5,CDH6,CDH15,DES,FGFR3,CDH5,GNAO1,CYBB,CDH8,MYL4,ACTG2,MYL3
Notch Signaling	6.60693E-05	NOTCH4,CNTN1,HEY2,JAG1,DLL4
Axonal Guidance Signaling	6.60693E-05	PLXNC1,MMP3,NTN4,CXCR4,ARHGEF15,PIK3R5,WNT16,PDGFB,PGF,FGFR3,EPHB6,NTRK2,NGFR,GNAO1,WNT4,MYL4,MYL3,MMP9
RhoGDI Signaling	6.60693E-05	CDH5,ARHGEF15,GNAO1,CDH8,CDH6,MYL4,ACTG2,CDH15,ARHGDIB,MYL3
cAMP-mediated signaling	6.60693E-05	ADRA2B,APLNR,ADRA2A,PTGER3,NPY1R,CNR1,PDE1B,GNAO1,PTH1R,ADRA2C,CREB5
Th1 Pathway	6.60693E-05	FGFR3,NOTCH4,HLA-DRB1,CD4,HLA-DRA,HLA-DMB,PIK3R5,DLL4
Melatonin Degradation II	6.60693E-05	MAOB,MAOA
Inhibition of Angiogenesis by TSP1	6.60693E-05	GUCY1A1,CD36,KDR,MMP9

GÎ±12/13 Signaling	6.60693E-05	FGFR3,CDH5,CDH8,PIK3R5,CDH6,MYL4,CDH15,MYL3
Nitric Oxide Signaling in the Cardiovascular System	6.60693E-05	FGFR3,PLN,GUCY1A1,PDE1B,PIK3R5,KDR,PGF
Osteoarthritis Pathway	6.60693E-05	FGFR3,H19,MMP3,PTH1R,WNT16,JAG1,CREB5,MMP9,RBP4,PGF
Ephrin Receptor Signaling	6.60693E-05	EPHB6,GRIN3B,SORBS1,CXCR4,ARHGEF15,GNAO1,CREB5,PDGFB,PGF
IL-4 Signaling	6.60693E-05	FGFR3,HLA-DRB1,HLA-DRA,HLA-DMB,PIK3R5,HMGA1
Putrescine Degradation III	6.60693E-05	MAOB,ALDH3A1,MAOA
GÎ±i Signaling	6.60693E-05	ADRA2B,APLNR,ADRA2A,PTGER3,NPY1R,CNR1,ADRA2C
Endothelin-1 Signaling	6.60693E-05	FGFR3,GUCY1A1,EDN1,GNAO1,PIK3R5,RARRES3,PLA2G7,SHE,PLA2G2A
Tryptophan Degradation X (Mammalian, via Tryptamine)	6.60693E-05	MAOB,ALDH3A1,MAOA
Regulation of the Epithelial-Mesenchymal Transition Pathway	6.60693E-05	FGFR3,NOTCH4,PIK3R5,TGFB3,WNT16,WNT4,JAG1,MMP9,FGF13
Eicosanoid Signaling	6.60693E-05	AKR1C3,PTGER3,RARRES3,PLA2G7,PLA2G2A
Role of Macrophages, Fibroblasts and Endothelial Cells in Rheumatoid Arthritis	6.60693E-05	FGFR3,SELE,SFRP2,MMP3,NGFR,GNAO1,PIK3R5,WNT16,WNT4,CREB5,PDGFB,PGF
ILK Signaling	6.60693E-05	FGFR3,PIK3R5,MYL4,ACTG2,MYH11,CREB5,MYL3,MMP9,PGF
CD28 Signaling in T Helper Cells	6.60693E-05	FGFR3,HLA-DRB1,CD4,SYK,HLA-DRA,HLA-DMB,PIK3R5
STAT3 Pathway	6.60693E-05	FGFR3,CSF2RB,NTRK2,NGFR,KDR,PDGFB
Calcium Signaling	6.60693E-05	GRIN3B,TNNT3,CACNA1H,MYL4,TRPC6,MYH11,CREB5,MYL3,CASQ2
Corticotropin Releasing Hormone Signaling	6.60693E-05	CRHR2,GUCY1A1,CNR1,UCN,GNAO1,CACNA1H,CREB5
Wnt/β-catenin Signaling	6.60693E-05	SOX17,SFRP2,CDH5,GNAO1,TGFB3,WNT16,WNT4,SOX18
Leukocyte Extravasation Signaling	6.60693E-05	FGFR3,CDH5,MMP3,CXCR4,CYBB,PIK3R5,PECAM1,ACTG2,MMP9
Clathrin-mediated Endocytosis Signaling	6.60693E-05	FGFR3,LYZ,PIK3R5,ACTG2,PDGFB,RBP4,FGF13,PGF,APOD
LPS/IL-1 Mediated Inhibition of RXR Function	6.60693E-05	CHST2,CHST1,MAOB,NGFR,ABCC2,NR1H3,LBP,ALDH3A1,MAOA
Human Embryonic Stem Cell Pluripotency	6.60693E-05	FGFR3,NTRK2,PIK3R5,TGFB3,WNT16,WNT4,PDGFB

Neurotrophin/TRK Signaling	6.60693E-05	FGFR3,NTRK2,NGFR,PIK3R5,CREB5
Ovarian Cancer Signaling	6.60693E-05	FGFR3,EDN1,PIK3R5,WNT16,WNT4,MMP9,PGF
Paxillin Signaling	6.60693E-05	FGFR3,ITGA9,ITGA8,PIK3R5,ACTG2,ITGAX
IL-12 Signaling and Production in Macrophages	6.60693E-05	FGFR3,LYZ,MAF,PIK3R5,TGFB3,RBP4,APOD
Role of NFAT in Regulation of the Immune Response	6.60693E-05	FGFR3,HLA-DRB1,CD4,SYK,HLA-DRA,HLA-DMB,GNAO1,PIK3R5
B Cell Development	6.60693E-05	HLA-DRB1,HLA-DRA,HLA-DMB
Actin Cytoskeleton Signaling	6.60693E-05	FGFR3,PIK3R5,MYL4,ACTG2,LBP,MYH11,PDGFB,MYL3,FGF13
Dendritic Cell Maturation	6.60693E-05	FGFR3,HLA-DRB1,TYROBP,NGFR,HLA-DRA,HLA-DMB,PIK3R5,CREB5
HIFα Signaling	6.60693E-05	FGFR3,EDN1,MMP3,PIK3R5,MMP9,PGF
Dopamine Degradation	6.60693E-05	MAOB,ALDH3A1,MAOA
OX40 Signaling Pathway	6.60693E-05	HLA-DRB1,CD4,HLA-DRA,HLA-DMB
iCOS-iCOSL Signaling in T Helper Cells	6.60693E-05	FGFR3,HLA-DRB1,CD4,HLA-DRA,HLA-DMB,PIK3R5
PTEN Signaling	6.60693E-05	FGFR3,NTRK2,NGFR,PIK3R5,PREX2,KDR
PKCÎ¸ Signaling in T Lymphocytes	6.60693E-05	FGFR3,HLA-DRB1,CD4,HLA-DRA,HLA-DMB,CACNA1H,PIK3R5
Bladder Cancer Signaling	6.60693E-05	FGFR3,MMP3,MMP9,FGF13,PGF
Sperm Motility	6.60693E-05	GUCY1A1,PDE1B,CACNA1H,RARRES3,PLA2G7,PLA2G2A
VEGF Family Ligand-Receptor Interactions	6.60693E-05	FGFR3,PIK3R5,KDR,PLA2G2A,PGF
Cardiac Hypertrophy Signaling	6.60693E-05	ADRA2B,FGFR3,ADRA2A,GNAO1,PIK3R5,TGFB3,MYL4,ADRA2C,MYL3
Crosstalk between Dendritic Cells and Natural Killer Cells	6.60693E-05	CSF2RB,HLA-DRB1,TYROBP,HLA-DRA,ACTG2
Phospholipases	6.60693E-05	RARRES3,LIPG,PLA2G7,PLA2G2A
Xenobiotic Metabolism Signaling	6.60693E-05	CHST2,FGFR3,CHST1,MAOB,CYP1A1,ABCC2,MAF,PIK3R5,ALDH3A1,MAOA
IL-8 Signaling	6.60693E-05	FGFR3,ANGPT2,CYBB,PIK3R5,KDR,MMP9,ITGAX,PGF
Calcium-induced T Lymphocyte Apoptosis	6.60693E-05	HLA-DRB1,CD4,HLA-DRA,HLA-DMB

Bile Acid Biosynthesis, Neutral Pathway	6.60693E-05	AKR1C1/AKR1C2,AKR1C3
Cellular Effects of Sildenafil (Viagra)	6.60693E-05	GUCY1A1,PDE1B,MYL4,ACTG2,MYH11,MYL3
Coagulation System	6.60693E-05	VWF,F13A1,THBD
Noradrenaline and Adrenaline Degradation	6.60693E-05	MAOB,ALDH3A1,MAOA
CXCR4 Signaling	6.60693E-05	FGFR3,CXCR4,CD4,GNAO1,PIK3R5,MYL4,MYL3
IL-6 Signaling	6.60693E-05	HSPB3,FGFR3,NGFR,PIK3R5,HSPB7,LBP
Colorectal Cancer Metastasis Signaling	6.60693E-05	FGFR3,MMP3,PTGER3,PIK3R5,TGFB3,WNT16,WNT4,MMP9,PGF
Phenylalanine Degradation IV (Mammalian, via Side Chain)	6.60693E-05	MAOB,MAOA
Methylglyoxal Degradation III	6.60693E-05	AKR1C1/AKR1C2,AKR1C3
Role of Pattern Recognition Receptors in Recognition of Bacteria and Viruses	6.60693E-05	FGFR3,SYK,PIK3R5,TGFB3,C1QA,C1QC
Antigen Presentation Pathway	6.60693E-05	HLA-DRB1,HLA-DRA,HLA-DMB
PAK Signaling	6.60693E-05	FGFR3,PIK3R5,MYL4,PDGFB,MYL3
VEGF Signaling	6.60693E-05	FGFR3,PIK3R5,ACTG2,KDR,PGF
T Helper Cell Differentiation	6.60693E-05	HLA-DRB1,NGFR,HLA-DRA,HLA-DMB
Caveolar-mediated Endocytosis Signaling	6.60693E-05	ITGA9,ITGA8,ACTG2,ITGAX
MSP-RON Signaling Pathway	6.60693E-05	FGFR3,CSF2RB,PIK3R5,ACTG2
Autoimmune Thyroid Disease Signaling	6.60693E-05	HLA-DRB1,HLA-DRA,HLA-DMB
Epithelial Adherens Junction Signaling	6.60693E-05	NOTCH4,SORBS1,MYL4,ACTG2,MYH11,MYL3
Antiproliferative Role of Somatostatin Receptor 2	6.60693E-05	FGFR3,SSTR2,GUCY1A1,PIK3R5
Graft-versus-Host Disease Signaling	6.60693E-05	HLA-DRB1,HLA-DRA,HLA-DMB
Amyotrophic Lateral Sclerosis Signaling	6.60693E-05	FGFR3,GRIN3B,PIK3R5,SLC1A2,PGF
Role of Osteoblasts, Osteoclasts and Chondrocytes in Rheumatoid Arthritis	6.60693E-05	FGFR3,SFRP2,MMP3,NGFR,PIK3R5,WNT16,WNT4,ACP5

Angiopoietin Signaling	6.60693E-05	FGFR3,ANGPT2,PIK3R5,TIE1
NRF2-mediated Oxidative Stress Response	6.60693E-05	FGFR3,ABCC2,MAF,PIK3R5,ACTG2,FKBP5,EPHX1
Gap Junction Signaling	6.60693E-05	FGFR3,NOV,GUCY1A1,PIK3R5,ACTG2,GJA5,GJA4
Fcγ RIIB Signaling in B Lymphocytes	6.60693E-05	FGFR3,SYK,CACNA1H,PIK3R5
Allograft Rejection Signaling	6.60693E-05	HLA-DRB1,HLA-DRA,HLA-DMB
Relaxin Signaling	6.60693E-05	FGFR3,GUCY1A1,PDE1B,GNAO1,PIK3R5,MMP9
Proline Degradation	6.60693E-05	LOC102724788/PRODH
Diseases and Functions	**p value**	**Molecules**
Cell Morphology	3.59E-12	ZG16B,CRYAB,EDN1,CXCR4,ARHGEF15,MGP,PECAM1,PLXDC1,KDR
Cell Death and Survival	7.71E-09	CD36,MMP9,PDGFB
Cellular Growth and Proliferation	8.35E-09	ANGPT2,CXCR4,PF4,CD36,TAL1,RGCC,HMGA1,PDGFB,EPHB6,FGFR3,ZG16B,CASZ1,NTRK2,MERTK,EDN1,CYBB,MGP,RET,KDR,DLL4,CD34
Cellular Function and Maintenance	4.6E-07	ANGPT2,PF4,CD36,TAL1,RGCC,PDGFB,FGFR3,ZG16B,MERTK,EDN1,CYBB,MGP,KDR,DLL4,CD34
Cellular Development	0.000106	ANGPT2,CXCR4,PF4,CD36,TAL1,RGCC,HMGA1,PDGFB,EPHB6,FGFR3,ZG16B,CASZ1,NTRK2,MERTK,EDN1,CYBB,MGP,RET,KDR,DLL4,CD34
Tissue Development	0.000155	CRYAB,ANGPT2,SFRP2,CXCR4,NPY1R,ARHGEF15,PF4,CD36,TAL1,RGCC,WNT16,GJA5,PDGFB,FGFR3,ZG16B,MERTK,EDN1,CYBB,MGP,PECAM1,PLXDC1,SOX18,KDR,EREG,DLL4,CD34
Cell-To-Cell Signaling and Interaction	0.000168	MRC1,ADRA2B,CRYAB,AKR1C3,CD36,CD4,MAF,CACNA1H,MARK1,C1QA,CD163,PGR,RSPO3,MERTK,STAB1,ADGRD1,CD84,RET,RIPOR2,SELE,PTGDR2,APLNR,PPBP,PF4,CD93,PREX2,THBD,PDGFB,TIE1,CRHBP,ADRA2A,CDH5,SYK,PECAM1,JAG1,EREG,CD34,AOC3,FPR3,ANGPT2,PTGER3,RAB27B,CHL1,PGF,FGF13,EDN1,NGFR,UCN,KIT,LIPG,NPW,LBP,CD7,GJA4,AKR1C1/AKR1C2,CXCR4,TYROBP,VWF,ITPKA,GJA5,HUNK,PLA2G2A,CXCL6,ZG16B,SSTR2,DOCK8,ADRA2C,KDR,DLL4,ITGAX
Organismal Development	0.000168	ANGPT2,CRYAB,SFRP2,CD36,TAL1,RGCC,PGF,FGFR3,EDN1,MERTK,MGP,CYBB,

		STAB1,SOX18,SELE,APLNR,NPY1R,CXCR4,PF4,ARHGEF15,VWF,TRPC6,GJA5,PDGFB,ZG16B,NOTCH4,NOV,CDH5,PECAM1,PLXDC1,KDR,CD34,DLL4,MMP9
Skeletal and Muscular System Development and Function	0.000168	CRYAB,TNNT3,GNAO1,CACNA1H,MYL4,ANO1,GJA5,DES,CASQ2,MYL3
Developmental Disorder	0.000245	ADRA2B,AOC3,CFD,COL14A1,ANGPT2,MMP3,EXOC3L2,ITGA8,C1QC,C1QA,FGF13,C7,WNT4,RET,ZBTB16,PLN,MLXIPL,AKR1C1/AKR1C2,ADGRL3,NR0B1,CRELD1,PLA2G2A,SSTR2,ADRA2A,ADRA2C,KDR,KCNMB1,MMP9
Cellular Movement	0.000366	CRYAB,MMP3,CD4,CD36,IGF2BP3,RGCC,TMEFF2,GMFG,PLA2G7,PGR,FGFR3,CHST2,ADGRF5,TPPP,MERTK,ITGA9,AJAP1,MGP,STAB1,LYVE1,RET,ZBTB16,RIPOR2,CARMIL2,ELN,PTGDR2,SELE,APLNR,CNR1,PF4,PPBP,HMGA1,SMOC2,THBD,ARHGDIB,PDGFB,SPARCL1,ADRA2A,CDH5,SYK,GNAO1,TGFB3,PECAM1,JAG1,EREG,AOC3,PCDH10,ANGPT2,SFRP2,NTN4,OSGIN1,EXOC3L2,PIK3R5,CHL1,PGF,EPHB6,MGAT3,EDN1,CMTM8,IL34,KIT,PODXL,EGFL6,ACKR1,CXCR4,VWF,CXCL6,ZG16B,CHST1,NOTCH4,NTRK2,NOV,KDR,DLL4,MMP9,ITGAX

Table S4 List of canonical pathways and categories of diseases and functions from IPA of differentially expressed genes across 'AdMSCs v/s iMS cells', ($P < 0.05$).

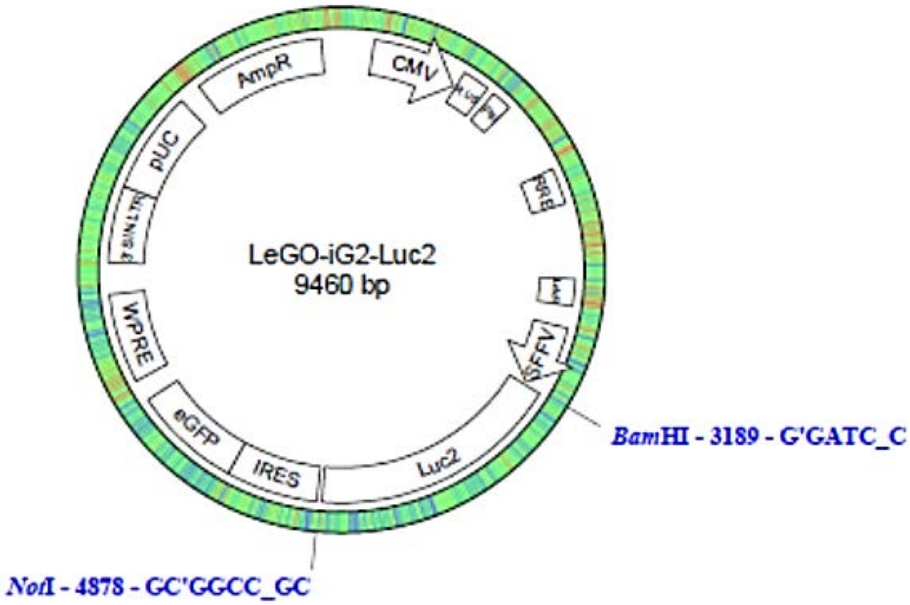

Figure S6: Vector map of LeGO-iG2-Luc2 lentiviral vector (obtained from http://www.LentiGO-Vectors.de)

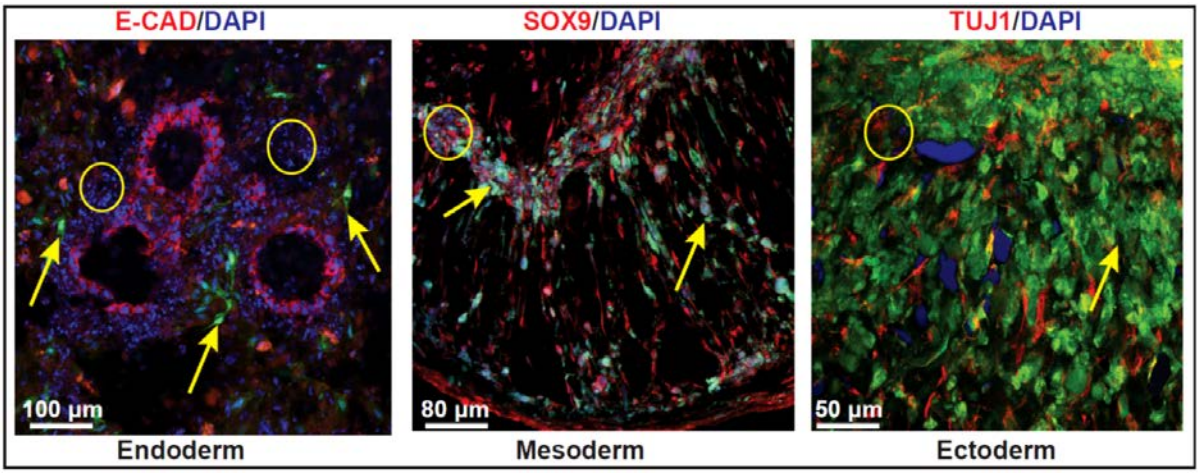

Figure S7: Immunofluorescence staining of cell aggregates from co-culture of iMS cells and WT C2 iPS cells (1:1). Representative confocal images of sections stained for detection of differentiation into endoderm (E-CAD in red), mesoderm (SOX9 in red), ectoderm (TUJ1 in red) and DAPI in blue for each of the images. Arrows point to GFP positive iMS cells which do not form differentiated cells as shown by absence of staining with respective lineage specific marker. Circled regions mark patches of necrotic cells with disintegrated nuclei. All images were taken on the Confocal Microscope Zeiss LSM 780. (Scale bars, as indicated).

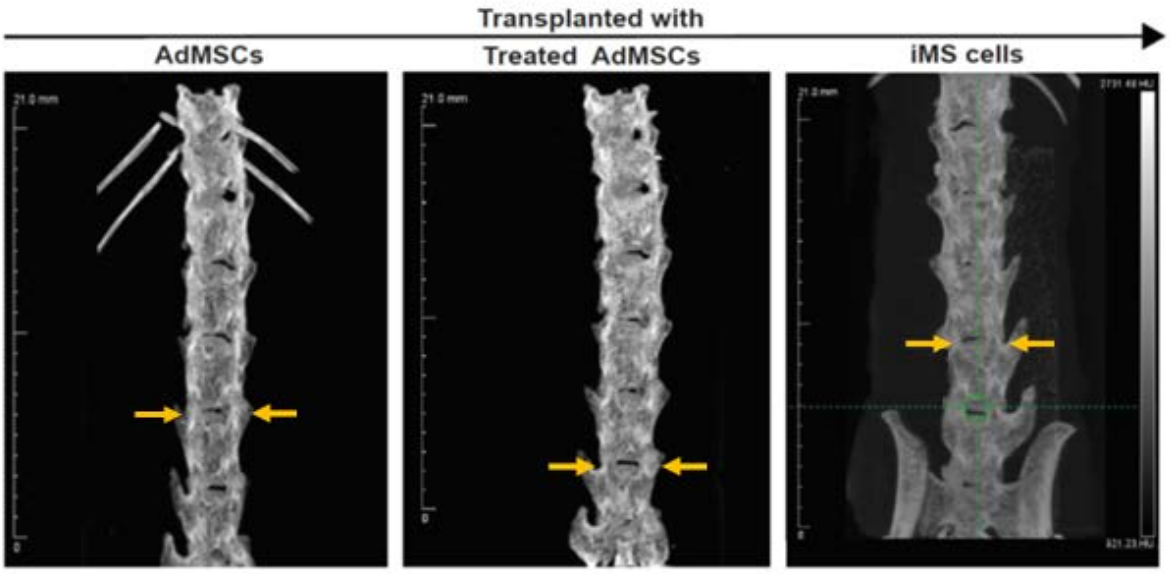

Figure S8: Representative microCT images of spines implanted with untreated AdMSCs, treated AdMSCs or iMS cells, harvested at 6 months post-transplant (n=3). Arrows indicate site of transplant. No incidence of new tissue or ectopic bone formation could be seen in any of the harvested spines.

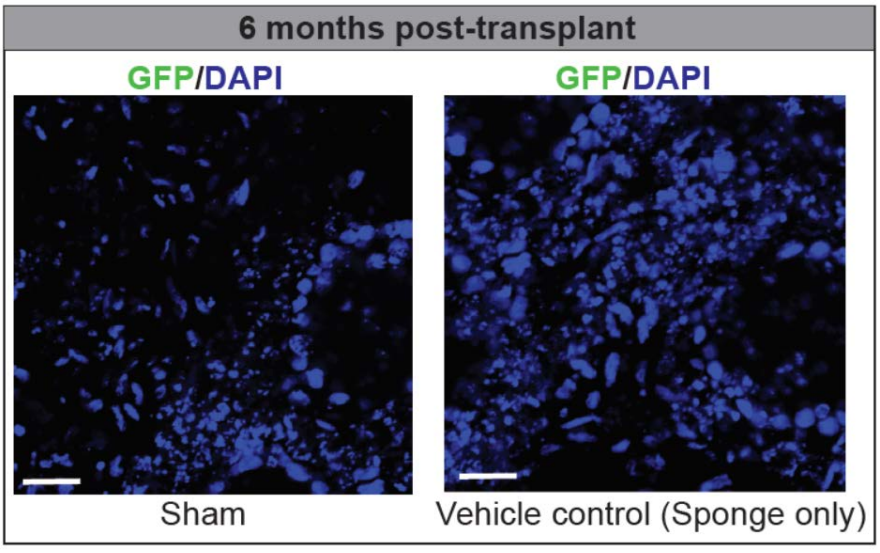

Figure S9: Representative confocal images of spine sections harvested at 6 months from animals that served as sham and vehicle controls, showing absence of GFP positive human cells (Scale bars, 50 µm).

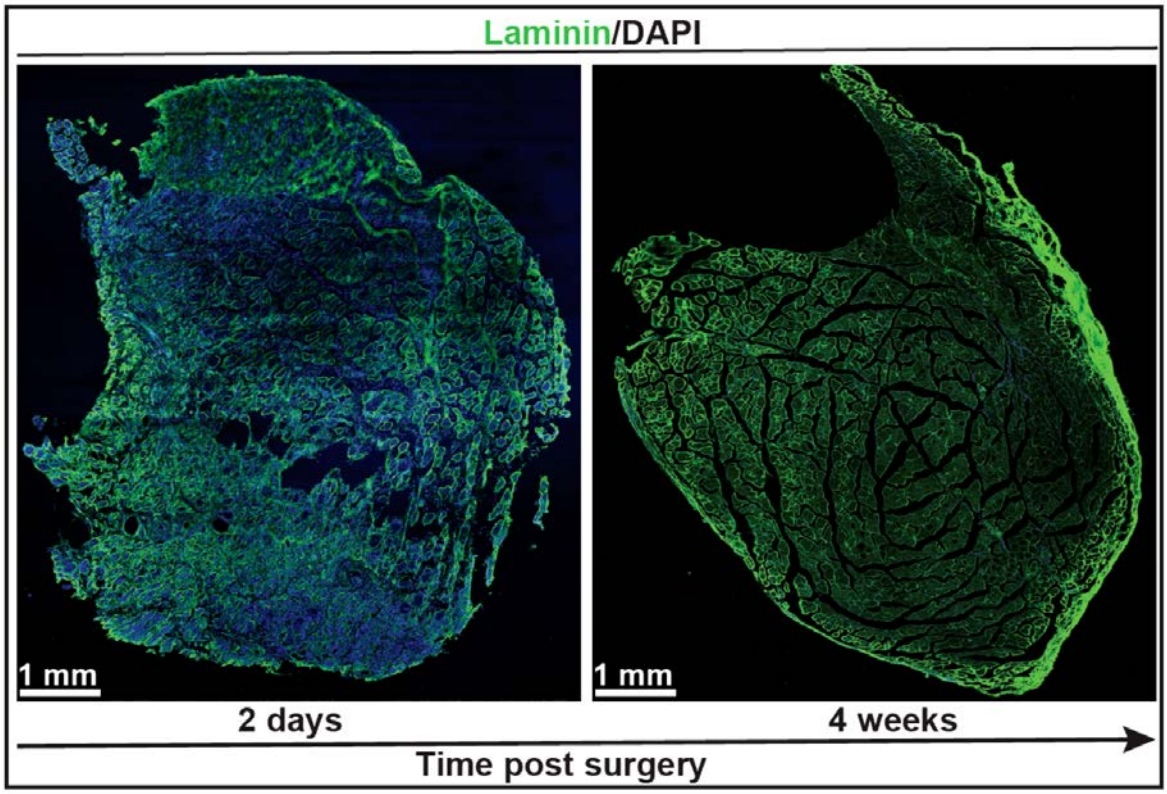

Figure S10: Representative confocal images of CTX injured TA sections transplanted with iMS cells after two days and four weeks post-surgery (n=2 for each time point). At two days after injection, the muscle fibres are disintegrated and necrotic. As the muscle fibres regenerate, the overall architecture of the muscle appeared to regain its structural organization as observed at four weeks. The sections were stained with DAPI (nuclei) and laminin (basal membrane of muscle fibres).